AN ABSTRACT OF THE THESIS OF

RONALD DAVID TASKEY for the DOCTOR OF PHILOSOPHY degree in SOIL SCIENCE presented on September 12, 1977

Title: RELATIONSHIPS OF CLAY MINERALOGY TO LANDSCAPE STABILITY IN WESTERN OREGON

Abstract approved: _____

Soil erosion by mass wasting is the major problem on forest lands of the Pacific Northwest. The clay fractions of soils from a large number of sites in Oregon's Western Cascades were characterized in order to determine the relationships of various clay materials to mass movements. Each site was either designated as stable or assigned to one or more of the following categories: debris avalanche, debris flow, slump, earthflow, creep. All clay samples were analyzed by X-ray diffraction, and certain selected samples were analyzed by differential thermal analysis and/or electron microscopy.

The most significant findings related amorphous gel and hydrated halloysite to flowage-type failures. These occurred in deposits of weathered basaltic colluvium and volcanic ash which overlie highly weathered, smectite-rich pyroclastic tuffs and breccias. These conditions are most notable near the contacts of the Sardine Formation and the Little Butte Volcanic Series. The smectite clays, which are highly cohesive and slowly permeable, support perched water tables which keep much of the overlying soil saturated, or nearly saturated, throughout the year. Furthermore, the amorphous clays and hydrated halloysite help to maintain the saturated conditions due to their very high water holding capacities. The amorphous gels are thought to form microscopic "water balloons" which release their contents upon disturbance.

Smectites, primarily montmorillonite, formed in pyroclastic tuffs and breccias are the most important clays of the well defined rotational slumps and of the areas of deep seated soil creep--in which the soil mass undergoes gradual deformation rather than abrupt

failure. Contrastingly, the shallow cohesionless soils which are prone to failure by debris avalanche tend to have clay materials which are typically of large size, low charge and low water holding capacity. These include chloritic intergrades or hydroxy interlayered smectites, and microaggregates of halloysite and other materials bound by amorphous films and strands (i.e., imogolite). Associations of gibbsite, zeolite, mica, and kaolinite are also common.

The more stable sites occur either at high elevations, with poorly formed soils having minimal clay development; or at low elevations, with relatively well drained soils containing kaolinite, dehydrated halloysite, chloritic intergrades, and microaggregates bound by amorphous materials.

Relationships of Clay Mineralogy to Landscape Stability in Western Oregon

by

Ronald David Taskey

A THESIS

submitted to

Oregon State University

in partial fulfillment of
the requirements for the
degree of

Doctor of Philosophy

Completed September 1977

Commencement June 1978

APPROVED:

Redacted for Privacy

Professor of soils in charge of major

Redacted for Privacy

Head of Department of Soil Science

Redacted for Privacy

Dean of Graduate School

Date thesis is presented Sept. 12, 1977

ACKNOWLEDGEMENTS

I wish to express sincere gratitude to Dr. M. E. Harward for the many hours of consultation, and for the true encouragement which he provided during the course of the study. Thanks go to Dr. C. T. Youngberg for serving as my graduate committee chairman and for securing funds for my support. Dr. D. N. Swanston deserves much credit and thanks for his timely advice and comment on several key points during the study. Thanks also to Dr. H. E. Enlows and Dr. D. O. Chilcote for serving on my graduate committee.

Much of the electron microscope work was conducted in the U. S. Forest Service's Forestry Sciences Laboratory, Corvallis. The use of equipment and facilities, and the assistance of Mr. Bo Addison, USFS, FSL, are gratefully acknowledged.

Finally, Teris, my wife, rates kudos for many hours of assisting in the laboratory, tracing X-ray diffraction patterns, typing, and putting up with too many lonely weekends.

TABLE OF CONTENTS

LIST OF FIGURES

LIST OF PLATES

LIST OF TABLES

RELATIONSHIPS OF CLAY MINERALOGY TO LANDSCAPE STABILITY IN WESTERN OREGON

I. INTRODUCTION

Massive slope failures constitute the dominant form of erosion in the mountains of the Pacific Coast states. The failures are common on undisturbed land, and their occurrence and severity are greatly increased by activities such as timber harvesting and road building. Each year mass movements cause an unmeasurable amount of damage in the form of degraded stream quality and soil losses, and they contribute heavily to the costs of maintaining roads and other property.

Although most soil properties and conditions which contribute to instability are well known from a mechanical standpoint, the underlying reasons for differences in stability from one site to another are not well known. Therefore, the overall problem with which this study is concerned is to adequately characterize unstable sites, and distinguish them from sites which are relatively stable. The characterization must include an evaluation of the nature of those constituents in the clay fraction which may have a controlling influence on slope stability.

Previous research and general field observations suggest that certain clay materials, or assemblages thereof, are common to particular types of land failures within a given physiographic unit. These materials often can be contrasted, to varying degrees, to the clay fractions of relatively stable landforms. For example, chlorite and mica are the major components of the notorious quick clays of Norway, eastern Canada and Alaska (Rosenqvist, 1966; Berry and Jorgensen, 1971; Crawford, 1968; Kerr and Drew, 1968). Similar clay minerals (although they have not been termed "quick") are critical in parts of northern California (Winzler and Kelly, 1975).

Smectites, the materials most frequently associated with the unstable landscapes, are common to earthflows in New Zealand (Crozier, 1969), deep creep and landslides in California (Fleming and

Johnson, 1975; Borchardt, 1976), and landslides in Colorado (Wahlstrom and Nichols, 1969), Wyoming (Beey and Kerr, 1973) and Montana (Klages and Hsieh, 1975). The type of landslide in the West Indies varies with the clay mineralogy, with montmorillenite being common in the complex and the simple rotational land failures which result in the greatest distortion and destruction of structure. The displaced material tends to break up less and become less distorted, however, when kaolinite is present with the montmorillonite (Prior and Ho, 1972). In California and the Western Cascades of Oregon, kaolinite tends to be found in the more stable soils (Borchardt, 1976, Paeth et al., 1971). Furthermore, kaolinite exhibits more favorable engineering properties than do most other clays (Gillott, 1968; Grim, 1962).

Numerous field observations in the volcanic mountain regions of the West have suggested that relationships of clay mineralogy and landscape stability are more complex than simple associations of smectite with unstable soils and kaolinite with stable soils. A question of the importance of amorphous clay components in Oregon's Western Cascades was raised, but not resolved, by Paeth et al. (1971) and by Youngberg et al. (1971). In addition, my preliminary work suggested that the role of halloysite as well as amorphous materials might be significant, and that the type of failure might vary with the type of clay minerals involved.

The primary objective, then, was to determine whether or not there are certain clay materials which are commonly associated with mass soil movements in the Western Cascades, and if so, whether they contrast consistently to the clay materials of relatively stable portions of the landscape.

There were three secondary objectives, all of which presupposed positive affirmation of the primary objective. These were to (1) determine the physiographic and environmental conditions under which the critical clay materials exist, (2) identify significant properties of these materials, (3) postulate cause-effect relationships for the influence of the clay materials on landscape stability.

Hence, the study was more analytical than predictive, and was an attempt to develop an integrated picture of the macroscopic events which shape the landscape and the microscopic particles which regulate those events. This is not to suggest that clay mineralogy is the only or even the most important factor controlling slope stability; however, it must be recognized that knowledge of the soil's clay fraction might be used as an additional tool in solving problems of slope stability.

The approach was intended to be broad scale. Multiple samples were collected from sites representing a wide range of lithologies and degrees of alteration in the mountains of western Oregon, but with emphasis on the central portion of the Western Cascades. (Discussions of sites outside the Western Cascades are presented in Appendix I.) Areas were delineated on the basis of their geology as determined from geologic maps, and specific sampling sites within these areas were selected to represent differing weathering environments and degrees of stability.

The clay fractions of all samples were analyzed by X-ray diffraction and those of selected samples by differential thermal analysis and electron microscopy. Emphasis was placed on the role played by the phyllosilicate and noncrystalline clay components at each site, with respect, not only to relative stability, but also to the type of failure if the site had failed.

II. BACKGROUND INFORMATION

Types of Mass Movements

In order to develop the relationships between landscape stability and clay mineralogy, it is helpful to begin at the macroscale--that is, landscape development by mass failure processes--and gradually work down to the microscale, so as to suggest underlying controlling factors. Therefore, the various idealized categories of mass failures will be reviewed briefly along with generalizations of the nature of their materials.

Although slope failures may be distinguished according to many criteria, they are often classified geometrically, such that they may be described and analyzed by a relatively simple mathematical model. Thus, there are two basic catergories of soil mass movements: (1) translational or planar and (2) rotational.

Translational or planar failures are those in which the longitudinal dimension far exceeds the depth. They consist of a simple downslope sliding of cohesionless soil, or blocks of cohesive soil, along a relatively flat plane of weakness. The failure plane commonly occurs at a lithic or hydraulic discontinuity which roughly parallels the soil surface. Hillslopes composed of heterogeneous layers of materials typically suffer the translational type failures. In the Pacific Northwest, translational failures are best exemplified by the debris avalanche, which is a rapid downslope sliding of shallow, cohesionless soil (Figure 1). Debris avalanches are the most common type of mass failure in western Oregon and usually occur during or immediately following a period of intense rainfall (Dyrness, 1967; Swanston, 1969, 1970, 1976).

Rotational failures have lengths and depths of comparable magnitude. They involve deep homogenous masses of wet cohesive soil, and are characterized by a failure surface which is concave upward in an elliptical arc (Figure 2). The failure surface does not

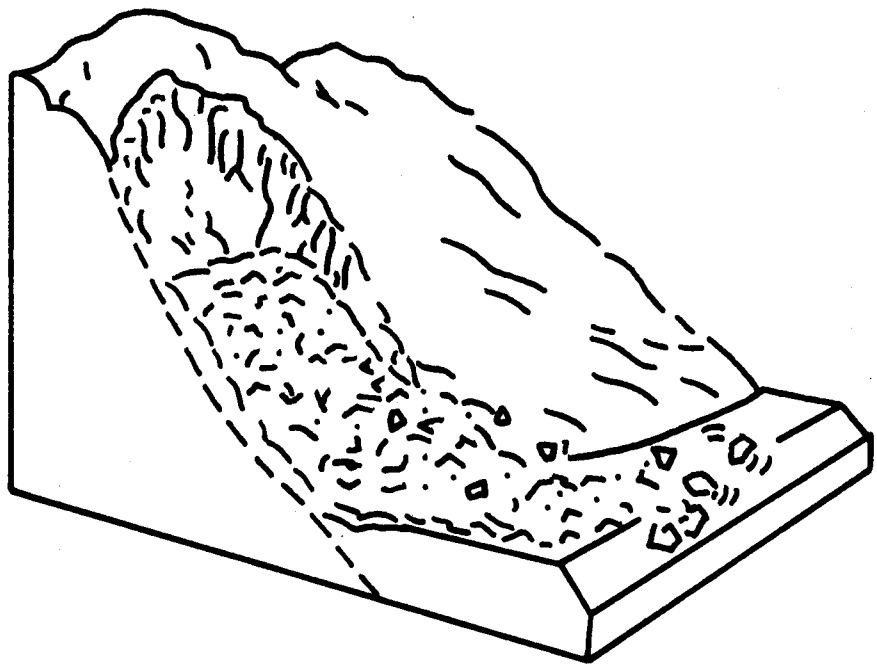

Figure 1. Debris avalanche of noncohesive material overlying a subsurface discontinuity (after Varnes, 1958).

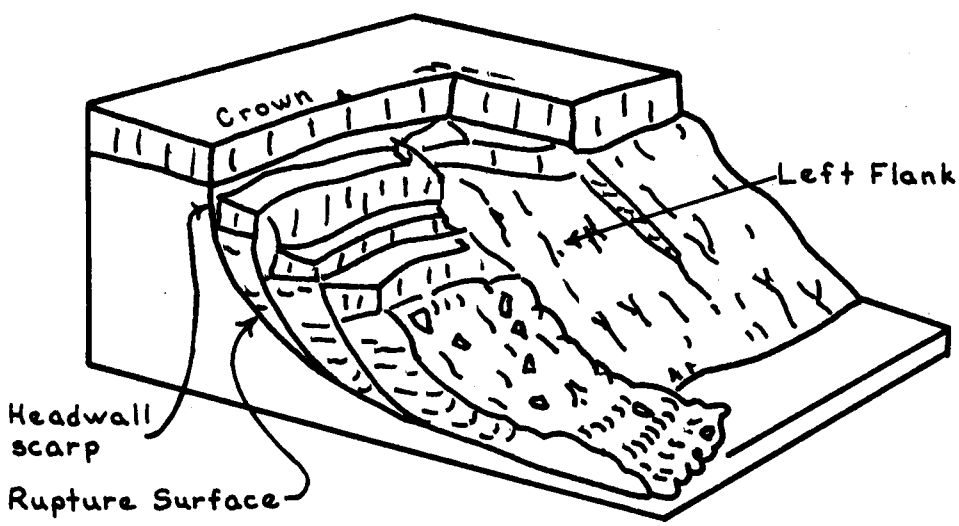

Figure 2. Slump-earthflow of homogeneous soil with overburden of hard volcanic rock (after Varnes, 1958).

necessarily coincide with a subsurface discontinuity; instead it is controlled by the moments of forces acting upon the center of gravity of the soil mass (Terzaghi and Peck, 1967; Wu, 1976).

The material of a rotational slump may disintegrate into a viscous mass of floating blocks or into a virtual slurry which flows downslope at a rate dependent upon the fluidity of the material and the steepness of the slope. Hence, rotational failures in soils often initiate earthflow movements, which are considered as translational. The fluidity, which partially determines the rate and distance of travel as well as the overall magnitude of the earthflow, is controlled not only by the water content but also by the degree of cohesiveness of the material. Thus, at a given water content, clayey materials with greater cohesive strength will develop less significant earthflows than will clayey materials with lesser cohesive strength. The soil may lose much of its cohesive character and become somewhat cohesionless during the slumping process; however, after a period of time the cohesive forces may be somewhat restored. Even so, the material may continue to move slowly downslope either by flowage or by creep processes.

Deep seated soil creep, another type of mass movement common in the Northwest, refers to a time dependent (i.e., progressive) deformation of a plastic soil volume, involving local translational or rotational rearrangements. It is distinguished from other mass failure processes by the absence of a distinct failure plane and by the almost imperceptibly slow rate of movement. Although there is no distinct plane of failure, there is a transitional boundary between the stationary material below and the straining mass above. The rate of movement--and hence the degree of deformation--is normally greater nearer the slope surface than at depth, primarily because of the increased viscous resistance of soil structural units with depth.

In addition to the geometric classification, failures may be distinguished according to several other criteria, including: specific controlling processes, the relative speed of movement, the

type of materials involved and their wetness, the depth of failure, and even the stage of development. Detailed discussions of the various failure types and modeling procedures are given in a number of references (Carson and Kirkby, 1972; Ladd, 1935; Sharpe, 1938; Swanston, 1970, 1976; Terzaghi, 1929, 1950; Terzaghi and Peck, 1967; Varnes, 1958; Wu, 1976; Zaruba and Mencl, 1969).

Physiography and Geology of the Western Cascades

The landscape of the Western Cascades is characterized by adolescent, rapidly developing stream drainage systems and an overall appearance which is hummocky and violently uneven. Steep slopes, high annual precipitation and a history of seismic activity are combined with clayey soils, formed from low-strength pyroclastic tuffs and breccias to make the mountains highly susceptible to land failures. Although surficial erosion is common along roadways and on other sites which are unprotected by vegetation, massive soil movements are the dominant erosional processes. The mass movements occur as landslides (slumps, debris avalanches, etc.), earthflows, and deep seated soil creep.

The distinctive features of instability include fresh failure surfaces, ancient slump blocks, jackstrawed trees, pressure ridges, tension cracks, and numerous sink ponds and small lakes which have formed behind debris dams and in failure depressions. The tension cracks, which vary in width from a few centimeters to several meters, often have live roots stretched taut across the gap from one soil mass to another. A dramatic example of a stress boundary and of the importance of vegetation in holding soil masses together occurs near a recent road failure in the Middle Santiam drainage. Here, a sliding soil mass has split a tree vertically to a height of about three meters leaving the two halves of its trunk bridging a crack two meters wide.

The deep rotational slumps and subsequent earthflows, which may continue to creep downslope, have occurred throughout most of

the Western Cascades for thousands of years. Specific failures are recognized by the very steep headwall scarps and bench-like surfaces below. A number of the scarps are several hundred meters high. A few of the most notable of these are the infamous "Tiller Slide", on Dompier Creek in the South Umpqua drainage, and the cliffs of Knob Rock, Gordan Peak, and Trappers Butte, which mark the contact of the Sardine and Little Butte deposits in the Middle Santiam drainage.

The debris avalanches commonly occur along stream banks and on the steeper side slopes. They range in size from only a few cubic meters to several thousand cubic meters of displaced material, most of which ends up in the stream channels. Although failures of these types are common throughout the Western Cascades, they are most often associated with logging roads and clearcuts. On the H. J. Andrews Experimental Forest, 78% of all mass movements following a heavy storm occurred on sites which had been roaded and/or logged (Dyrness, 1967). Clearcutting can accelerate erosion by debris avalanches by two to four times over that on forested sites. Road building on the same lands can lead to an erosional increase by avalanche of 49 times if the roads are relatively well designed and contructed, and 344 times if they are not (Swanston and Swanson, 1976).

To a great extent, the geology of western Oregon controls the distribution, frequency of occurrence and types of massive slope failures. The materials of certain geologic formations are notorious for their susceptibility to mass movement (Burroughs et al., 1976; Dyrness, 1967; Paeth et al., 1971; Pope and Anderson, 1960; Swanson and James, 1975); furthermore, major land failures have frequently occurred near the contact of two differing geologic materials. A brief review of the geology of western Oregon, and especially of the Western Cascades, will provide some of the perspective needed to appreciate the clay mineral relationships to be presented later.

A geologic outline (Figure 3) of those portions of western Oregon included in this study shows that the southern half of the Coast Range is dominated by Cenozoic sedimentary rocks; the Klamath Range is a composite of mesozoic sedimentary, igneous and metamorphic

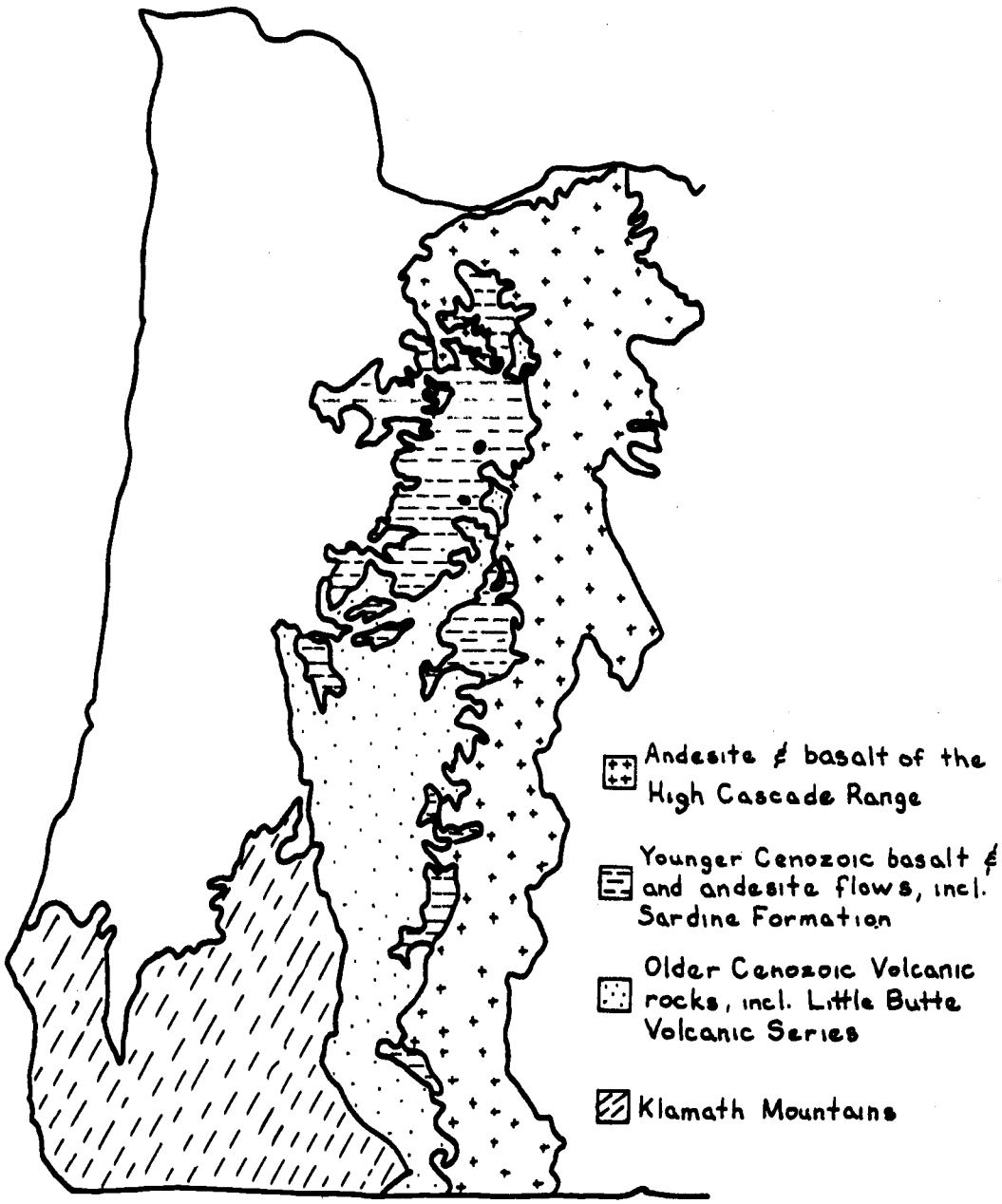

Figure 3. Geologic outline of those portions of western Oregon included in study (Walker and King, 1969).

lithologies; and the Cascade Range is composed of Cenozoic volcanic materials.

The Cascade Range is divided into two adjacent chains of volcanic mountains which are aligned in the north-south direction. The rocks of the Western Cascades, the older of the two chains, were formed during the Tertiary period, and range in age from about 5 to 40 million years. The High Cascades are composed of much younger rocks, which formed from lava and ash, most of which was ejected within the last million years.

During the late Eocene to early Miocene epochs of the Tertiary period (about 40 to 25 million years ago) volcanic vents and fissures discharged enough ash and lava to create deposits which were about five miles thick. The rock fragments and fine debris from the exploding volcanoes fused to form new, fairly soft pyroclastic rocks. Erosion processes immediately began shaping this new landscape, and today the remnants of these deposits constitute the Little Butte Volcanic Series (Baldwin, 1976; Beaulieu, 1971; Peck et al., 1964). Sometime after the eruptions, tremendous forces within the earth buckled, folded and lifted a portion of these deposits, thus creating a long uplift and an adjacent depression running in roughly the northeast-southwest direction. In the central portions of the range these are known as the Breitenbush anticline and Sardine syncline, respectively. This volcanic activity and subsequent upheaval initiated the formation of the Western Cascades.

Millions of years later, during the late Miocene (perhaps 15 million years ago) more eruptions filled the valleys with new lava which solidified into hard volcanic rock (basalt and andesite), which comprises the Sardine formation, north of the McKenzie River. As more millions of years passed erosion continued to remove the older, softer pyroclastic materials, but the younger rock in the valleys was, for the most part, hard and more resistant to erosion. The result was a landscape reversal, that is, the ridge tops became valley bottoms, and vice versa (Figure 4).

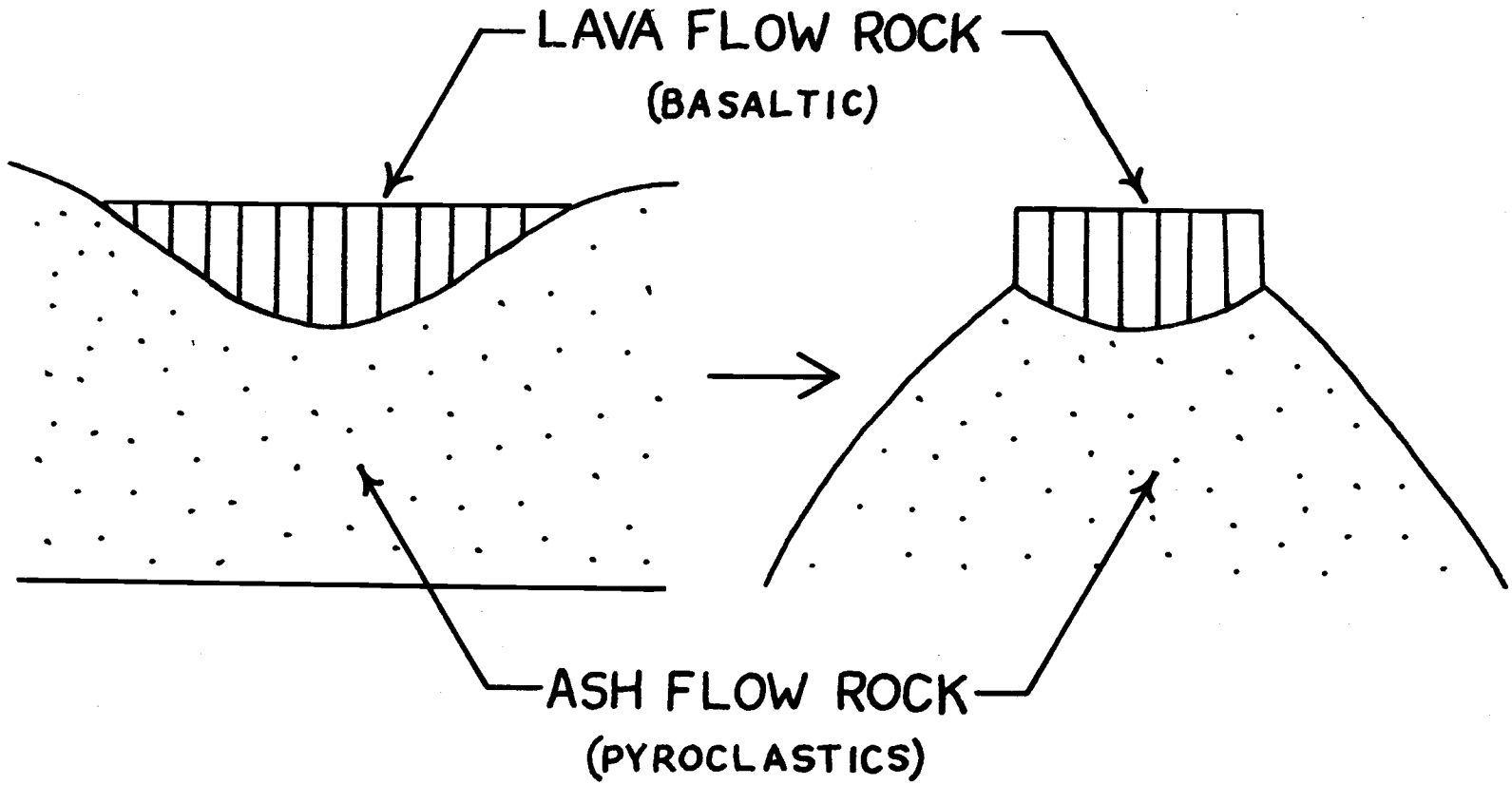

Figure 4. Landscape reversal due to differential weathering and erosion of contrasting materials in the Western Cascades (adapted from McKee, 1972).

Then about a million years ago, a new age of volcanic activity began on the eastern flanks of the mountains. These eruptions spilled new, High Cascade, lava over the eastern portion of the Western Cascades, and eventually created the High Cascade peaks. These materials are relatively stable and have little clay development. They are included in this study to only a very minor extent.

III. METHODS

Field Methods

A total of 160 soil samples were collected from 59 sites which were selected to represent a broad range of geologic, soil and stability conditions in western Oregon, but with emphasis on the central portion of the Western Cascades. Sites were selected according to broadly defined parameters of scope, rather than on the basis of specific criteria. Thus, the study sites included:

a. the mountainous regions of western Oregon;
b. sites with fresh evidence of regolith failure, or sites which were judged as prone to failure on the basis of other factors, including: steepness of slope, close proximity to a known unstable region, evidence of ancient failures, tension cracks, pressure ridges, small road cut failures;
c. sites judged to be relatively stable;
d. nearly all types of soil slope failures--translational rotational--including debris avalanche, debris flow, slump, earthflow and deep creep;
e. logged and unlogged areas;
f. roaded and unroaded areas.

General study areas were outlined on the basis of their geology, and were delineated to coincide with geologic formations and mapping units as indicated in Geologic Map of Oregon West of the 121st Meridian (Wells and Peck, 1961) and other sources (Peck et al., 1964; Ramp, 1972). Specific sampling sites (Figure 5) representing differing weathering environments, degrees of stability and failure processes were selected within these areas. Published soil surveys and inventories, aerial photographs, topographic maps, field reconnaissance, and interviews with knowledgeable individuals facilitated the selections. The various sites were designated according to the major and tributary drainages in which they are located (Table 1). (For

Figures 5a, b, c, d. Locations of sites in the Western Cascades (U. S. Geol. Survey 1:250,000 maps).

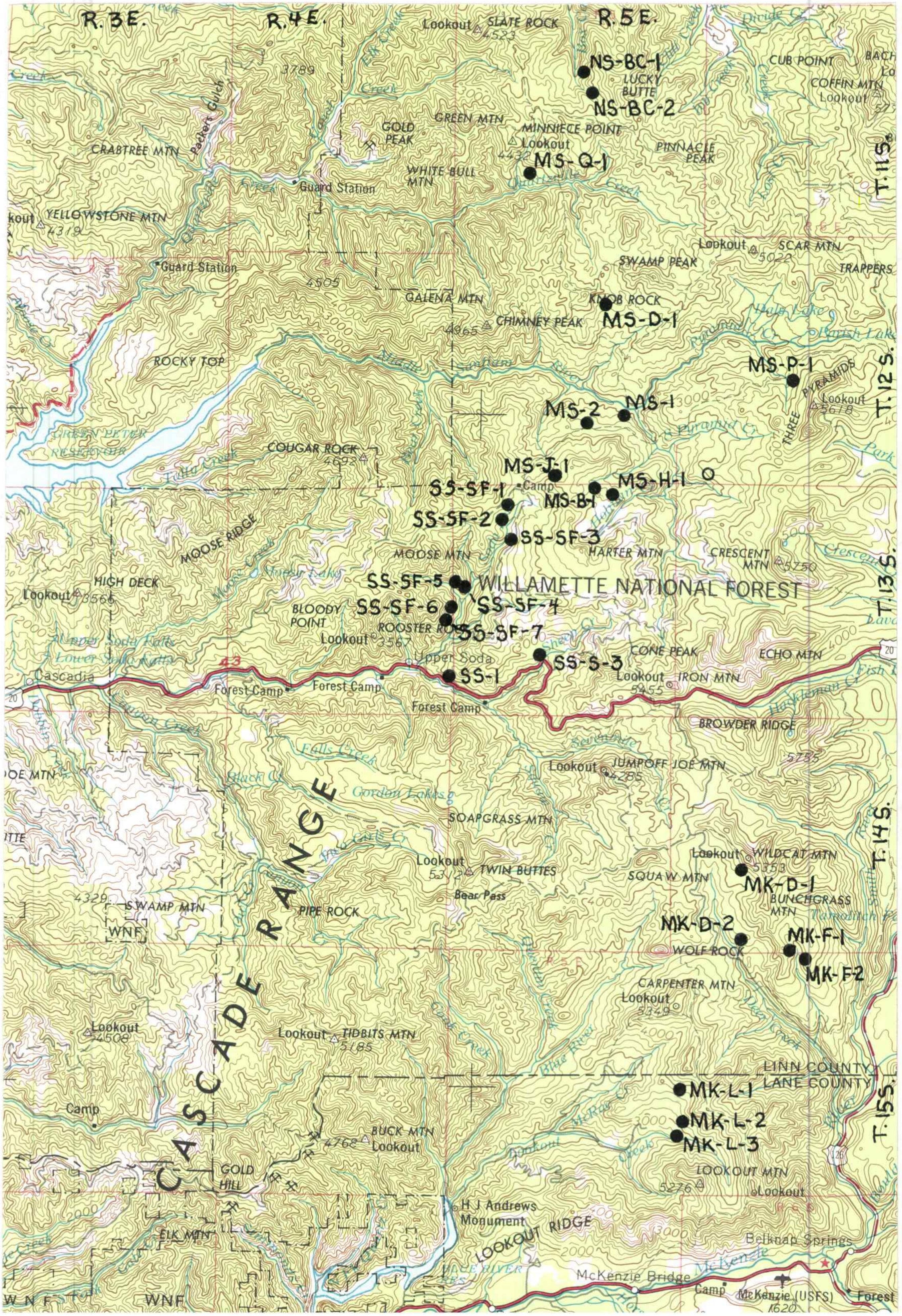
R.3E.
R.4E.
R.5E.
T.11S.
T.12S.
T.13S.
T.14S.
T.15S.
NS-BC-1
NS-BC-2
MS-Q-1
MS-D-1
MS-P-1
MS-2
MS-1
MS-J-1
MS-H-1
MS-B-1
SS-SF-1
SS-SF-2
SS-SF-3
SS-SF-5
SS-SF-4
SS-SF-6
SS-SF-7
SS-S-3
SS-1
MK-D-1
MK-D-2
MK-F-1
MK-F2
MK-L-1
MK-L-2
MK-L-3
WILLAMETTE NATIONAL FOREST
CASCADE RANGE
LINN COUNTY
LANE COUNTY
SLATE ROCK
LUCKY BUTTE
CUB POINT
COFFIN MTN
GREEN MTN
MINNIECE POINT
GOLD PEAK
CRABTREE MTN
WHITE BULL MTN
PINNACLE PEAK
Guard Station
YELLOWSTONE MTN
SCAR MTN
SWAMP PEAK
TRAPPERS
GALENA MTN
KNOB ROCK
CHIMNEY PEAK
ROCKY TOP
THREE PYRAMIDS
GREEN PETER RESERVOIR
COUGAR ROCK
MOOSE RIDGE
HARTER MTN
CRESCENT MTN
MOOSE MTN
HIGH DECK
BLOODY POINT
ROOSTER ROCK
CONE PEAK
ECHO MTN
IRON MTN
Upper Soda
Cascadia
Forest Camp
BROWDER RIDGE
JUMPOFF JOE MTN
SOAPGRASS MTN
TWIN BUTTES
Bear Pass
WILDCAT MTN
SQUAW MTN
BUNCHGRASS MTN
SWAMP MTN
WNF
PIPE ROCK
WOLF ROCK
CARPENTER MTN
TIDBITS MTN
BUCK MTN
LOOKOUT MTN
GOLD HILL
H J Andrews Monument
LOOKOUT RIDGE
ELK MTN
Belknap Springs
McKenzie Bridge
McKenzie (USFS)
Lookout


R.2E.
R.3E.
R.4E.
Vida
Blue River
Rainbow
Forest Camp
Lookout
WILLAMETTE NA
Lookout
JIMBO MTN
MT HAGAN
3330
THORS HAMMER
DEATHBALL ROCK
Frog Rock
Nimrod
WNF
DEATHBALL MTN
KATSUK BUTTE
HARVEY MTN
SFMK-8-1
SAWTOOTH RIDGE
Lookout
TIPSOO BUTTE
T.17S.
GOAT POINT
PERNOT MTN
Lookout
FAWN ROCK
NIMROD BUTTE
Lookout
LITTLE COWHORN MTN
SYMBOL ROCK
Lookout
HEHE MTN
4066
INDIAN RIDGE
Hidden Lake
3597
GIBRALTAR MTN
WILLAMETTE NATIONAL FOREST
Lookout
5406
HARDY RIDGE
T.18S.
7
1118
SARDINE BUTTE
5214
NFMFW-C-1
5075
LOWELL MTN
SINKER MTN
MIYU RIDGE
ALPINE RIDGE
Cabin
BATTLE PEAK
GRASSHOPPER MTN
T.19S.
4969
SADDLEBLANKET MTN
6
WINBERRY MTN
SOURGRASS MOUNTAIN
Guard station
HUCKLEBERRY MOUNTAIN
Lookout tower
5549
TIRE MTN
MULE MTN
BUCKHEAD MOUNTAIN


R.3E.
R.4E.
T.21S.
T.22S.
T.23S.
Landax
High Prairie
DEAD MTN
3852
Westfir
Oakridge
AUBREY MTN
SQUAW BUTTE
WILLAMETTE
NATIONAL FOREST
Oakridge State
Willamette City
DECEPTION BUTTE
DECEPTION ROCK
LARISON ROCK
KITSON RIDGE
COUGAR MTN
SOUTHERN PACIFIC
BUNCHGRASS RIDGE
KOCH
MFW-H-1
TUFTI MTN
MFW-1
BEACH MTN
MFW-L-1
COYOTE MTN
SALT CREEK
Ranch
SLAPJACK BUTTE
MFW-8W-1
TIMBERED KNOLL
MC FARLAND PT
4562
WOLF MTN
6461
GAME REFUGE
PINTO MTN
GRASS MTN
MFW-CP-1
MFW-B-1
6170
JUNIPER RIDGE
WARNER MTN
Lookout tower
LOGGER BUTTE
4910
BEARBONES MOUNTAIN
Lookout tower
BUSTER BUTTE
4610
BEAR MOUNTAIN
Pioneer Gulch
DIAMOND ROCK PILE
LIGHTHOUSE ROCK
MFW-D-1
DOME ROCK
5740
LANE CO
6137
EMIGRANT BUTTE

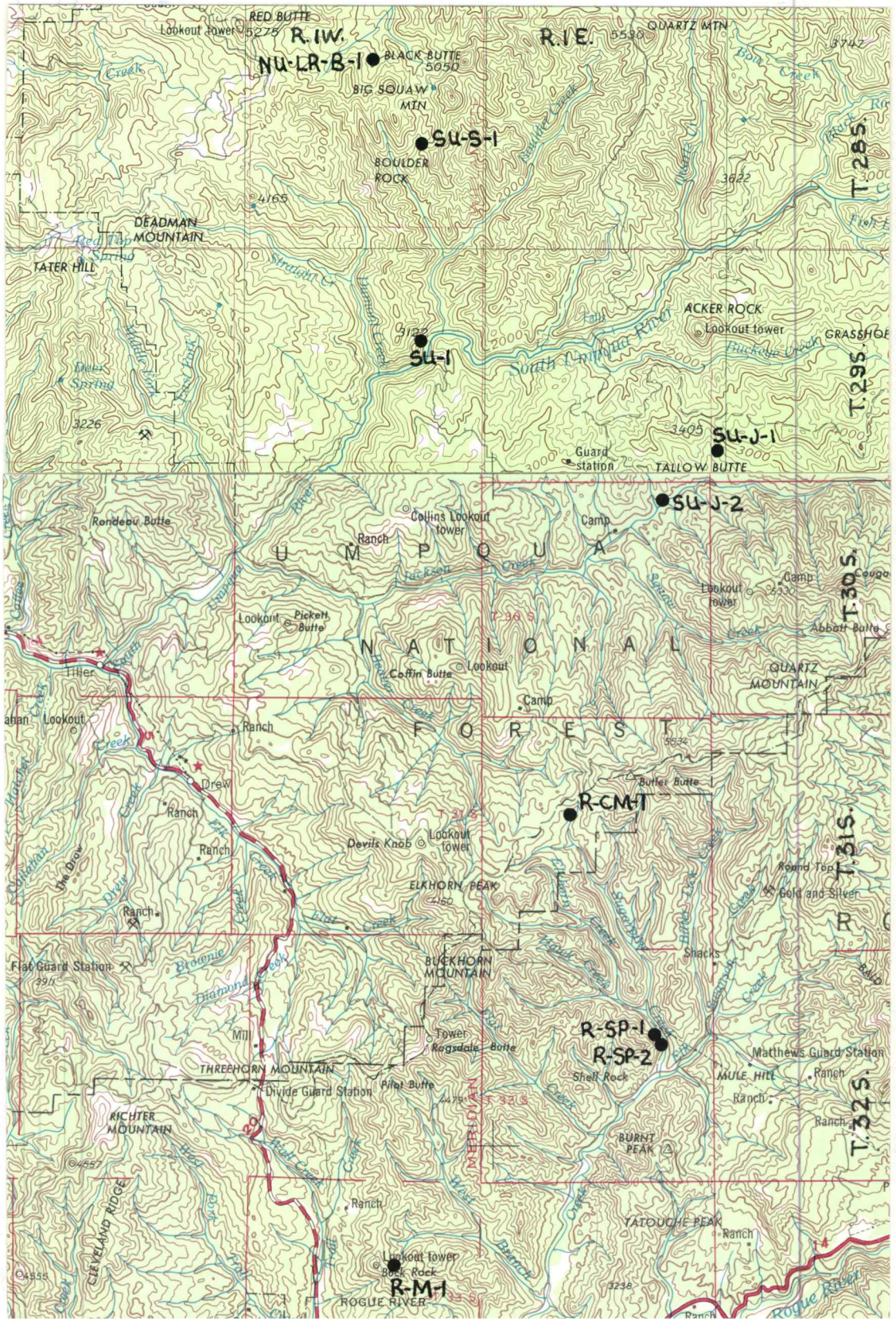
R.1W.
R.1E.
NU-LR-B-1
SU-S-1
SU-1
SU-J-1
SU-J-2
R-CM-1
R-SP-1
R-SP-2
R-M-1
RED BUTTE
BLACK BUTTE
5050
BIG SQUAW MTN
BOULDER ROCK
DEADMAN MOUNTAIN
TATER HILL
ACKER ROCK
Lookout tower
TALLOW BUTTE
Guard station
Collins Lookout tower
Rondeau Butte
Pickett Butte
Coffin Butte
Tiller
Drew
Ranch
Devils Knob
ELKHORN PEAK
BUCKHORN MOUNTAIN
Flat Guard Station
THREEHORN MOUNTAIN
Divide Guard Station
Pilot Butte
Ragsdale Butte
RICHTER MOUNTAIN
CLEVELAND RIDGE
Butler Butte
QUARTZ MOUNTAIN
Abbott Butte
Round Top
Gold and Silver
Matthews Guard Station
MULE HILL
BURNT PEAK
TATOUCHE PEAK
Rogue River
South Umpqua River
Camp
Lookout tower
Shell Rock
Snacks
T.29S.
T.30S.
T.31S.
T.32S.
UMPQUA NATIONAL FOREST

Table 1. Key to site designation abbreviations, including those outside of the Western Cascades.

Drainage Designation	Major Drainage	Minor Drainage
NS-BC	North Santiam	Box Canyon Creek
MS-Q	Middle Santiam	Quartzville Creek
MS-D	Middle Santiam	Donaca Creek
MS-P	Middle Santiam	Pyramid Creek
MS-J	Middle Santiam	Jude Creek
MS-B	Middle Santiam	Bachelor Creek
MS-H	Middle Santiam	Holman Creek
SS-SF	South Santiam	Soda Fork
SS-S	South Santiam	Sheep Creek
MK-D	McKenzie	Deer Creek
MK-F	McKenzie	Fritz Creek
MK-L	McKenzie	Lookout Creek
SFMK-B	South Fork McKenzie	Boone Creek
NFMFW-C	North Fork Middle Fork Willamette	Christy Creek
MFW-H	Middle Fork Willamette	Hills Creek
MFW-L	Middle Fork Willamette	Landes Creek
MFW-BW	Middle Fork Willamette	Big Willow Creek
MFW-CP	Middle Fork Willamette	Coffeepot Creek
MFW-B	Middle Fork Willamette	Buck Creek
MFW-D	Middle Fork Willamette	Dome Creek
NU-LR-B	North Umpqua	Little River, Black Creek
SU-S	South Umpqua	Slick Creek
SU-J	South Umpqua	Jackson Creek
SU-C	South Umpqua	Canyon Creek
R-CM	Rogue River	Coal Mine Creek
R-SP	Rogue River	Sugar Pine Creek
R-M	Rogue River	Morine Creek
R-WUR	Rogue River	Wake Up Rilea Creek
A-S	Applegate River	Squaw Creek
A-B	Applegate River	Bigelow Creek
S	Sixes River	

example, SS-SF-1 refers to the site nearest the head of the Soda Fork of the South Santiam River.)

Site descriptions and variables of greatest interest, including specific locations, drainage basins, geologic formations, and elevations were recorded on Field Data Forms (Appendix II). The geologic formations were identified simply by locating the sites on published geologic maps (referenced above); thus, the accuracy of formational designations is limited by the accuracy, scale and other limitations of the available maps. The most frequently sampled geologic units were the Little Butte Volcanic Series and the Sardine Formation.

One of the major problems to be solved during the course of the study involved soil sampling procedures. A paired sampling technique was initially attempted whereby it was hoped that the general mineralogy of an unstable site could be compared with that of a more stable site of similar topography. This approach proved to be unfeasible, because comparable sites for pairing could not be found without introducing a large number of other variables which would confound the interpretations.

It was decided to sample several arbitrarily selected locations within an unstable area in order to identify possible mineralogical trends or patterns. These were then compared with samples collected from arbitrarily chosen sites in generally stable areas. This approach ultimately led to the use of variable sample selection procedures which made allowances for the several different types of slope failures encountered in the field. These procedures were physically limited by the fact that samples from all but one site were collected using a shovel, pick and hand auger, because mechanized drilling and coring equipment was unavailable. Thus, the guidelines for selecting a specific sample location at a site varied with the type of failure (if any) and with site conditions. In all cases, however, special attention was given to the materials associated with profile discontinuities and perched water tables.

Translational failures normally were sampled so as to determine the nature of the clay above, below and within the zone of

failure. Debris avalanches and flows were sampled on the failure surface and at the head or flank in the remaining overlying material, with an occasional random sample from the debris pile.

It was rarely possible to collect totally reliable samples from above and below failure surfaces in rotational slumps due to the obscurity of the surfaces caused by the great thickness or disintegration of the slump block. In the case of relatively fresh failures, samples were collected from the failure surface, scarps and debris pile; whereas, ancient slumps were more randomly or subjectively sampled.

Large, ancient, earthflows and sites of deep creep were sampled by digging and augering into roadcuts or stream sides at several locations within the mass. Normally, if a number of pits were opened only the soils from a few of these were analyzed because of apparent uniformity of soils among pits. Although this procedure provided reliable information about the nature of the moving mass, it allowed only limited interpretation of the materials at the bottom of the failure.

Laboratory Methods

The laboratory investigation was limited to the phyllosilicate and noncrystalline clay (< 2 μm esd) materials which are identifiable by means of X-ray diffraction (XRD), differential thermal analysis (DTA) or transmission electron microscopy (TEM). The clay fraction of each sample was characterized by XRD on a Phillips Norelco X-ray diffractometer operated at 35 kv and 25 ma, utlising CuKα radiation and fitted with a focusing monochrometer. Appendix IV gives detailed sample preparation methods and criteria for identification of phyllosilicates by XRD.

Selected samples were subjected to DTA on a Dupont Model 900 analyzer equipped with a high temperature (1200°C) furnace, and operated at a heating rate of 20°C per minute in an N_2 atmosphere, and using Al_2O_3 as the reference material. Clay samples which had

been Mg-saturated and equilibrated to 54% RH for XRD were used for DTA. Interpretations were made according to Mackenzie (1957, 1970).

The clay fractions of certain samples were further observed by TEM. Dilute suspensions of the samples were applied by the drop method to copper grids coated with Formvar (Gard, 1971). These were viewed with either a Phillips EM 200 operated at 60 kv or a Phillips EM 300 operated at 80 kv and 15 to 20μa beam current.[1]

Particle size analyses were conducted on selected samples by the Bouyoucos hydrometer method and spot samples were double checked by the ASTM hydrometer method (Ullery, C. H. undated. The hydrometer method. Unpubs. Ms. Dept. of Soil Science, Oregon State Univ., Corvallis). These data are presented in Appendix IV.

1/ Microscope time donated by USFS Forestry Sciences Laboratory, Corvallis, and assistance provided by Bo Addison (FSL), Al Soeldner and Jane Knopper (Botany Dept., OSU), and Gody Spycher (Soil Science Dept., OSU) are greatfully acknowledged.

IV. CLAY MINERALOGY OF VARIOUS TYPES OF FAILURES

Several different mass erosion processes, as well as stable conditions, are represented by the numerous study sites. In order to interpret the role of clay minerals in controlling landscape stability, it is necessary to consider the mineralogy of various sites with respect to particular erosional processes and stability conditions. In most cases, site data from physiographic regions other than the Western Cascades are too limited to receive adequate evaluation. Therefore, a number of representative sites from the Western Cascades were selected to demonstrate each of the following categories: 1) debris avalanche, 2) debris flow, 3) rotational slump, 4) large earthflow, 5) deep seated creep, 6) stable. (Additional site information and clay analyses are given in Appendices II and III.)

Debris Avalanche

A common situation is one in which coarse textured, cohesionless, relatively dry soil with little clay development overlies a steeply sloping surface of bedrock or cohesive clay. The soil mantle of these kinds of sites is subject to avalanching whenever the shear stress acting on it exceeds its shear strength--as may happen when support is removed by undercutting or when the soil is rapidly saturated by intense rainfall.

The debris avalanche is best exemplified by sites SS-SF-5, SS-1 R-SP-1, NS-BC-1, and MFW-B-1. Sites SS-SF-5 and SS-1, in the South Santiam drainage, and R-SP-1, in the Rogue drainage, involve shallow cohesionless soil which failed over bedrock; whereas the soil of sites NS-BC-1 in the North Santiam drainage, and MFW-B-1 in the Middle Fork Willamette drainage, failed over heavy, plastic montmorillonite clay which has weathered from greenish breccia.

The clay fractions of the failure materials at these sites were usually found to consist of amorphous material and low charge,

nonexpanding minerals which have relatively large size and low specific surface. These usually included some form of volcanic glass, chlorite, and chloritic intergrade, although crystalline components were not always detected. Various combinations of gibbsite, zeolite, mica, dehydrated halloysite or kaolinite were often present. Expandable minerals or those with high charge or high water holding capacity such as smectite and hydrated halloysite were not found to be major constituents, unless they were associated with the underlying support material. The smectite in these cases had weathered from the underlying breccia; whereas most of the hydrated halloysite probably formed from lava and amorphous material along the discontinuity, where water is most plentiful. (See Dudas and Harward, 1975 for somewhat similar conditions of halloysite formation.)

There is little mineralogical difference between the overlying soil mantle and the underlying weathered bedrock surface upon which failure occurred at site SS-SF-5 (Figure 6). Samples of both materials show strong evidence of chlorite and chloritic intergrade minerals as indicated in the XRD patterns by nonexpanding 14 Å peaks which partially resist collapse upon heating. Vermiculite becomes discernible with K-saturation as the moderately strong 10 Å peaks, although there may be traces of smectite and mica as well. Halloysite in various stages of hydration is revealed in the broad 7.5-10 Å region which disappears with heating at 550°C. Kaolinite is probably present as the sharp 7.1-7.2 Å peaks, although its identification is uncertain in the presence of chlorite (Brindley, 1961). (Kaolinite giving similar XRD patterns was identified by TEM at site SS-SF-7 which is nearby and has somewhat similar soil.) Iron oxide components were indicated in the 3.2-3.6 Å region (not shown), and a trace of amorphous material appeared as a weak band in the XRD pattern from about 17 to 30 2θ.

XRD patterns of failed soils from sites SS-1 and R-SP-1 show the presence of chloritic intergrade mineral in both soils (Figure 7) The underlying rock surface is different at the two sites, however, in that the rock of site SS-1 consists of moderately weathered

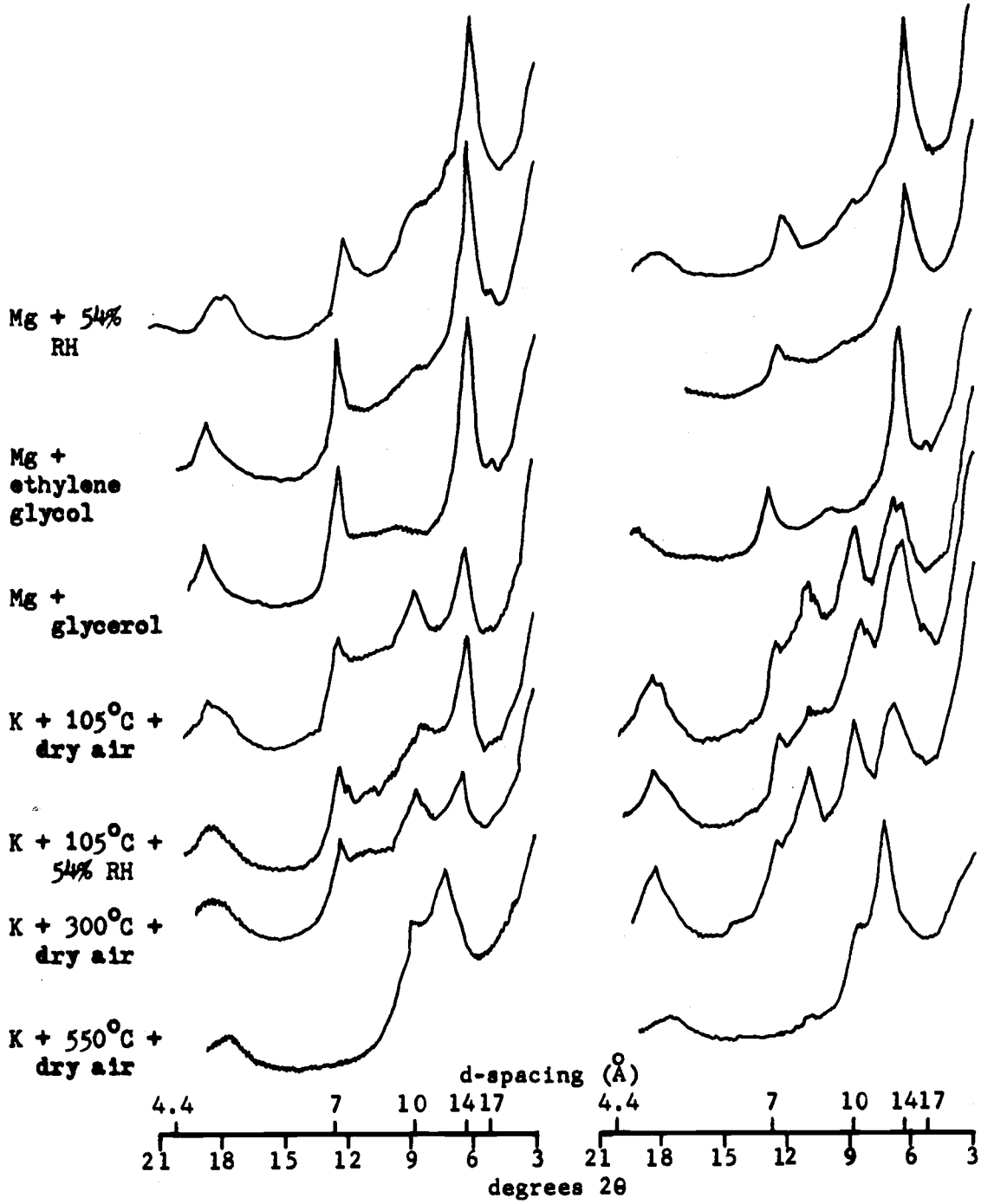

Figure 6. Site SS-SF-5 XRD patterns. Sample b (left), from left flank, 75 cm depth. Sample c (right), from midslope slip plane in altered rock outcrop.

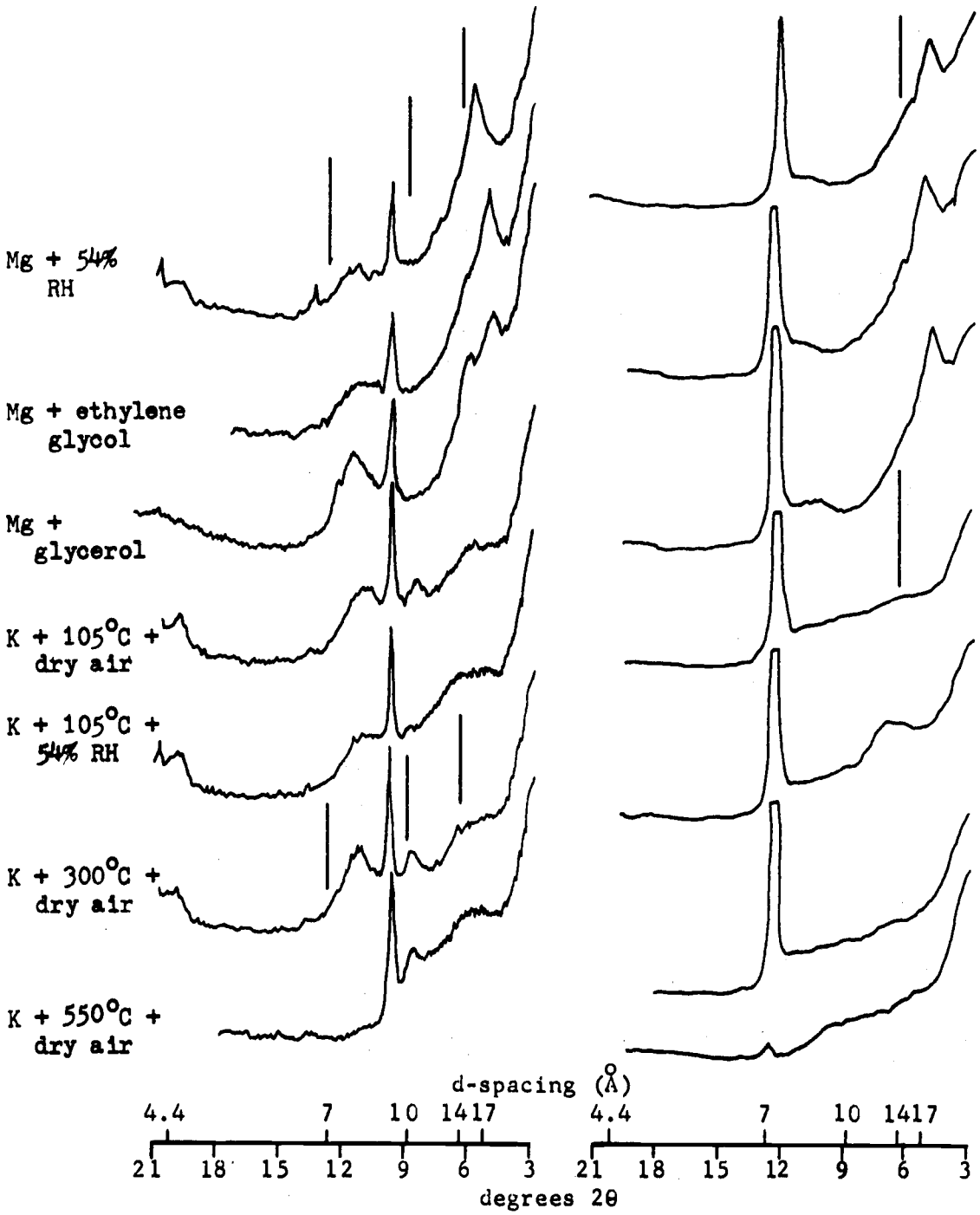

Figure 7. XRD patterns of shallow, relatively dry soils which failed as debris avalanches over bedrock at sites SS-1 (left) and R-SP-1 (right).

greenish pyroclastic rock of the Little Butte Series and that of site R-SP-1 is less weathered, less mafic and appears to be a rhyolitic breccia. Site SS-1, the wetter of the two sites, represents an area which is less stable. These differences are reflected mineralogically by the presence of zeolite, halloysite and hydroxy interlayered smectite at site SS-1, and by the strong presence of kaolinite at site R-SP-1. In the SS-1 patterns the zeolite appears as the sharp 9 Å peak; the halloysite as the broad 7.5-8 Å peak which disappears with heating at 550°C; and the hydroxy interlayered smectite as the 15 Å peak which partially expands with solvation, and collapses to 10 Å with some difficulty with K-saturation. Kaolinite in the R-SP-1 patterns is indicated by the distinctive 7.1 Å peaks.

Sites NS-BC-1 and MFW-B-1 are examples of debris avalanches involving soil mantles similar to those just discussed, but which overlie steep, smooth layers of cohesive clay instead of bedrock. The soil mantle of site NS-BC-1 has little clay development; the XRD patterns (Figure 8, sample b) show that the clay consists of amorphous material, poorly crystalline, slightly expandable chloritic intergrade, well developed gibbsite (sharp, strong 4.8 Å peaks) and perhaps a hint of halloysite. Electron microscope observations revealed tubular and spheroidal halloysite in the sample, as well as microaggregates of these and other clay sized particles held together by strands and films of amorphous components. (Although micrographs of this sample are not presented due to the very low quality of pictures obtained, similar clays and aggregates found at other sites are shown later.) The underlying sliding surface (sample d) consists of a highly contrasting zone of montmorillonite, with some halloysite and probably zeolite.

These components are also indicated by DTA patterns (Figure 9), of which the one for sample b shows a low temperature (150°C) dehydration endotherm, a strong 350°C gibbsite endotherm, a small 540°C endotherm probably due to halloysite dehydroxylation and a high temperature (950°C) exotherm due to halloysite or chloritic intergrade (Mackenzie, 1970). The pattern for sample d shows a somewhat broader low temperature

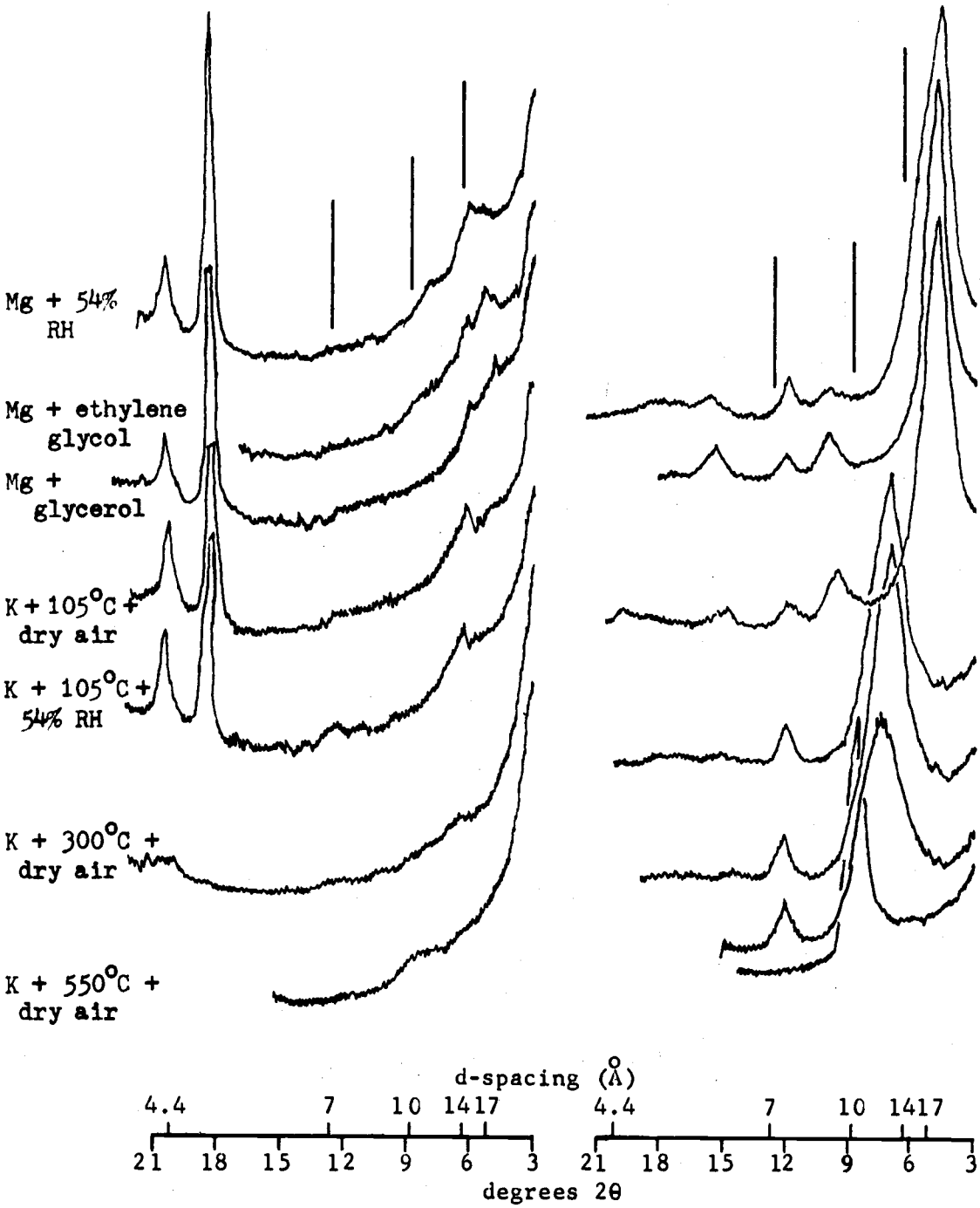

Figure 8. Site NS-BC-1 XRD patterns. Sample b (left), from head of slide, surface material above failure plane, 45 cm from crown. Sample d (right), from failure plane, reddish clay.

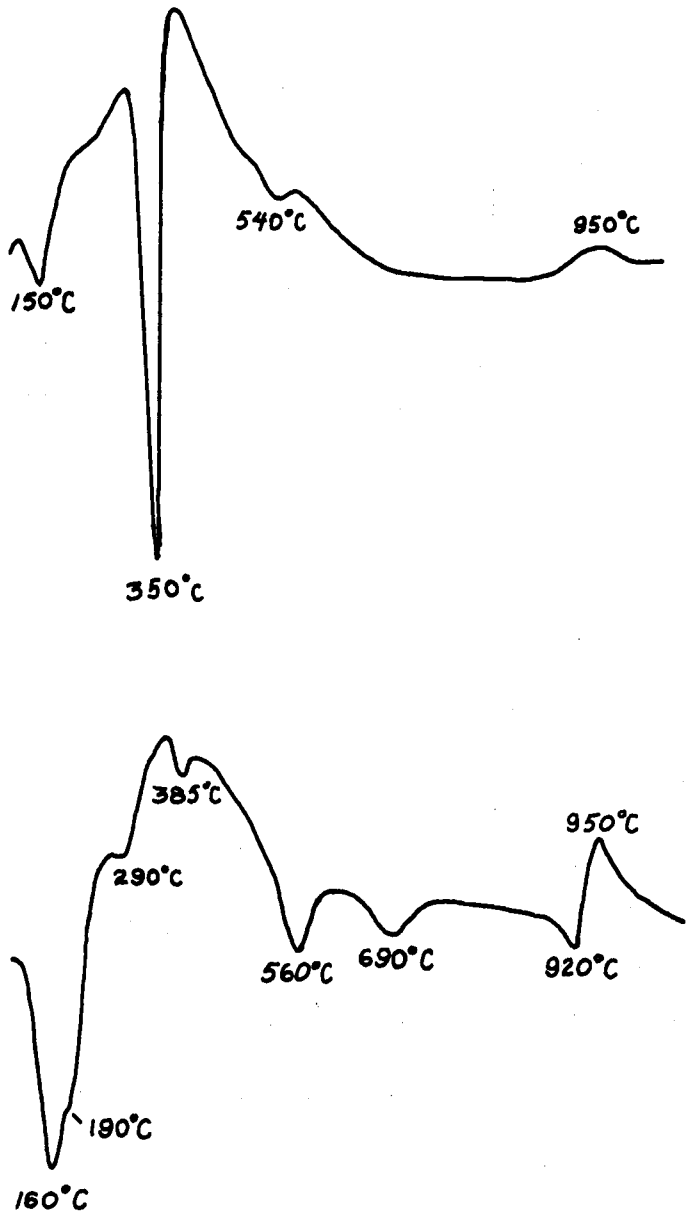

Figure 9. DTA patterns of failing soil, NS-BC-1b, at head of avalanche (top) and of reddish plastic clay, NS-BC-1d, over which failure occurred.

dehydration endotherm at 160°C, a halloysite dehydroxylation endotherm, a smectite dehydroxylation endotherm at 690°C and an endothermic-exothermic smectite inversion in the range of 920 to 950°C which is probably combined with the high temperature halloysite exotherm.

In the case of the Buck Creek slide area (MFW-B-1), upstream from the Hills Creek Reservoir, the relatively dry soil mantle formed in basaltic colluvium shows little clay development; the XRD patterns reveal only amorphous material and some poorly defined chloritic intergrade (Figure 10). However, the zone of the failure plane, which is saturated year around, consists primarily of well developed montmorillonite with some accessory halloysite, zeolite and perhaps mica (Figure 11).

It is notable that the evidence of halloysite in the failure zone is stronger in the wetter sample c than in the slightly drier sample a. Information collected from a large number of sites under similar conditions suggests that further examination of this site, especially on a less steep portion of the slope, would reveal even stronger evidence of hydrated halloysite in a perched water table just above the montmorillonite.

Electron micrographs (Plates 1 and 2) of sample c, which is a blue colored clay, show what is thought to be thin sheets of montmorillonite (Beutelspacher and Van Der Marel, 1968; Gard, 1971), many of which are covered with a gel-like coating which gives rise to small (< 0,04 μm) hollow speres. The true identity of the spheres is unknown, but it is proposed that they might be specimens of the spheroidal form of halloysite in a very early stage of formation. Unfortunately, no additional micrographs of samples from site MFW-B-1 were made, nor were electron diffraction analyses conducted.

Debris Flow

Debris flows are similar in many respects to debris avalanches in that they involve sudden and rapid downslope movement of relatively shallow cohesionless soil along a planar subsurface discontinuity.

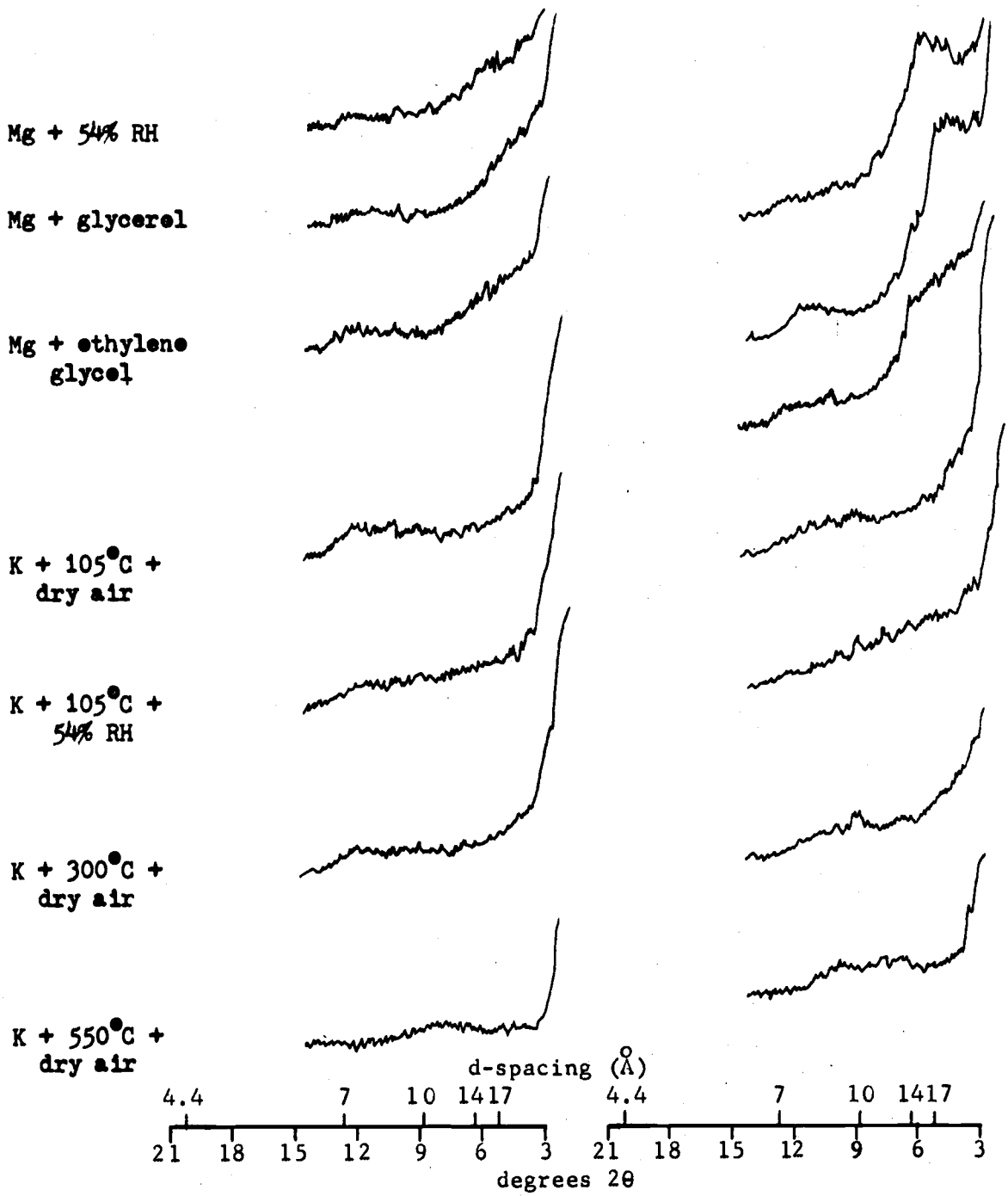

Figure 10. Site MFW-B-1 XRD patterns of dry soil mantle (taken from Youngberg et al., 1971).

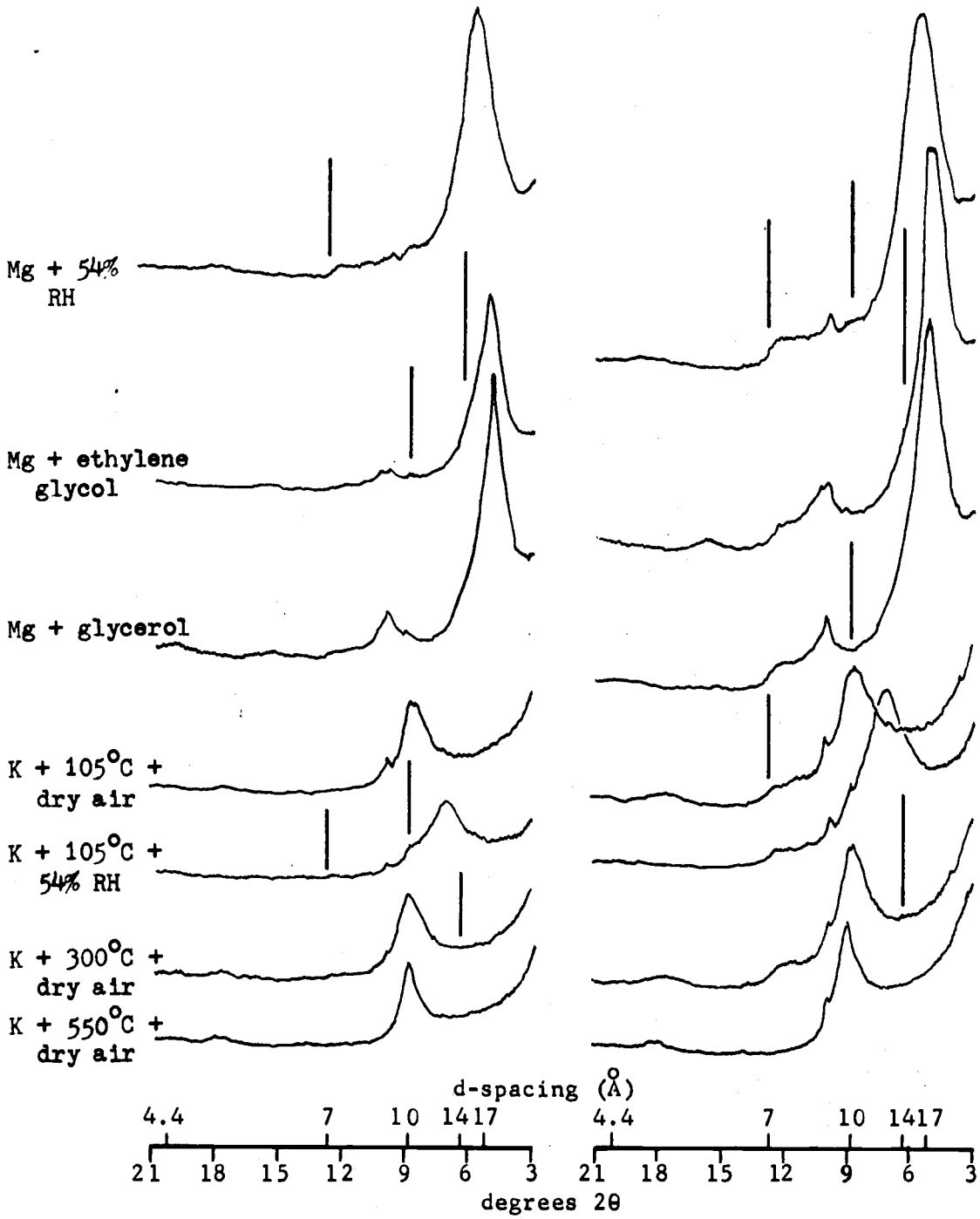

Figure 11. Site MFW-B-1 XRD patterns. Sample a (left), near top of failure plane 10 cm below surface. Sample c (right), just below failure plane 30-50 cm below surface.

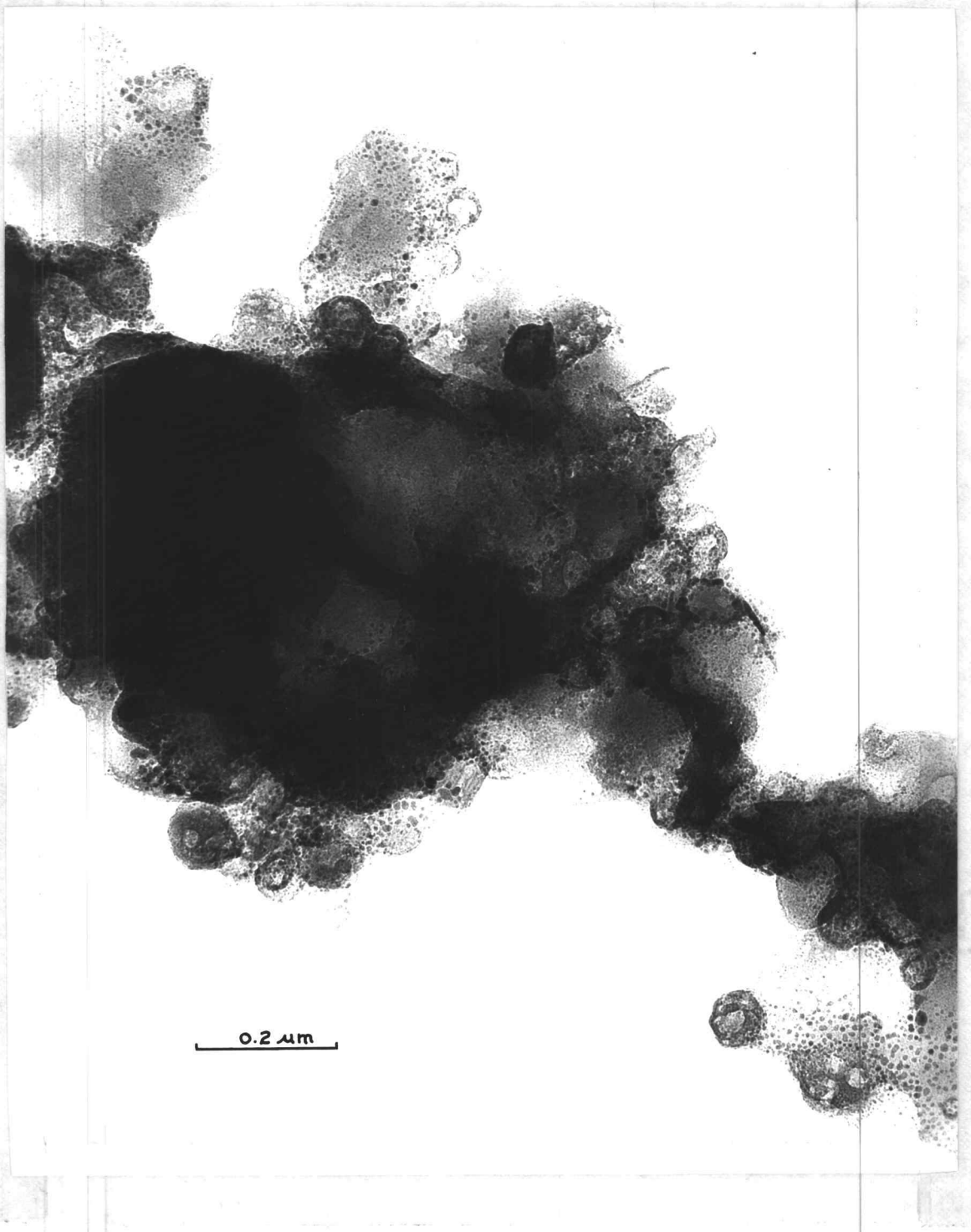

Plate 1. Electron micrograph of clay, sample MFW-B-1c, showing growths of small hollow spheres.

Plate 2. Electron micrograph of clay, sample MFW-B-1c, showing growth of small hollow spheres.

Definitively, they are distinguished from debris avalanches primarily on the basis of their high water content which causes them to exhibit more distinct flowage characteristics. In practice, debris flows frequently are not distinguished from other forms of translational landslides (Burroughs et al., 1976; Swanston and Swanson, 1976). However, for purposes of this investigation it is appropriate to consider them separately, as they represent a transition between the debris avalanche and the earthflow, and because they tend to involve soils with differing mineralogies.

Debris flows in the Western Cascades not only have a higher water content than do debris avalanches, but they also involve materials with a higher affinity for water, and they may occur on gentler slopes. The clay materials also are likely to exhibit a relatively high sensitivity (i.e., loss of shear strength with disturbance, Mitchell, 1976). Those sites involving failure by debris flow and which best exemplify the process are: MS-P-1, MS-1, MS-2, R-CM-1, SS-SF-1, SS-SF-3, MK-D-1, MFW-D-1, and MS-Q-1. Several of these sites also have experienced rotational slumping at depths greater than the debris flow events.

The road-related failure at site MS-P-1 is quite complex in that it involves an ancient, progressive rotational slump in clayey, decomposed pyroclastic material which is overlain by wet, highly unstable soil in basaltic colluvium. The ancient slump is composed of several units, which support a stand of large, mature Douglas-fir. Water emerges from just below the crown of the ancient slump block, several tens of meters upslope from the road. The colluvial soil holds water very well, and much of it is saturated throughout the year. Road construction activities apparently triggered a debris flow of the overlying saturated colluvial soil by cutting through the slump below the perched water table.

The XRD patterns reveal the nature of the clay constituents at various locations at the site. Sample b was taken from relatively dry, stable soil upslope from the crown of the ancient slump; sample f , which is somewhat similar in macroscopic appearance but is

saturated and flows readily when disturbed, was taken from downslope of the crown in the unstable colluvial soil lying just above the recent road-caused disturbance (Figure 12). A major difference between the two samples, both of which contain amorphous material and chloritic intergrade, is that the saturated sample f contains considerably more hydrated halloysite than does sample b. This is indicated in f by the 10.8 Å peak in the unsolvated Mg-saturated treatment which shifts to 7.5-8 Å upon drying and K-saturation, and disappears with heating at 550°C; and in sample b by the subtle indication in the region of 7.3 Å.

DTA patterns (Figure 13) indicate the presence of halloysite in the two samples by the low temperature dehydration endotherm, the dehydroxylation endotherm and the high temperature exotherm. Amorphous material cannot be separated from halloysite in the patterns because of the congruity of their low temperature endotherms and high temperature exotherms. The large exotherms in the vicinity of 310°C are unexplained, but are probably a function of the particular furnace, as a significant rise in the reference material pattern also commenced immediately after the start of heating. Furthermore, the exotherm did not appear nearly as dramatically in the pattern of another sample, e, which is comparable to sample f, and was heated in another furnace. Plant opal, which was seen in the samples under the electron microscope, could also contribute to these exotherms (Wilding, 1976 and personal communication). It is doubtful that the exotherms were caused by organic matter oxidation because the samples were first subjected to a vacuum and then heated in an N_2 atmosphere. One effect of these large peaks is to decrease the apparent intensity of the dehydration endotherms.

Although the XRD patterns indicate a much stronger presence of halloysite in sample f, electron micrographs clearly show the presence of some spheroidal and tubular halloysite in sample b (Plate 3). Additionally, the amorphous component of the drier sample, b, tends to form microaggregates, the components of which are bound together by a network of amorphous films and strands which resemble imogolite

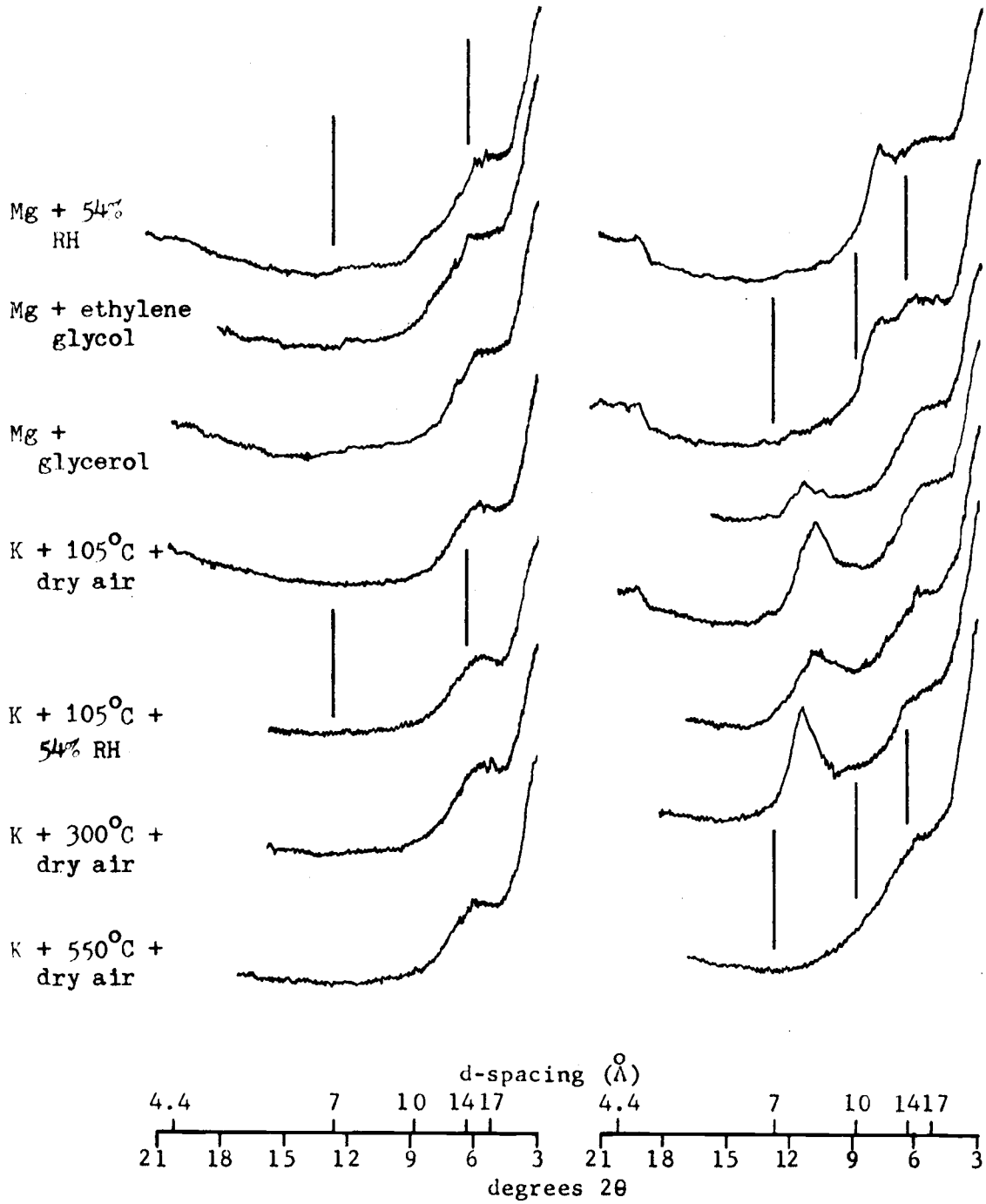

Figure 12. Site MS-P-1 XRD patterns. Sample b (left): dry, stable soil upslope from failure, 75 cm depth. Sample f (right): wet, flowing soil in failure, 75 cm depth.

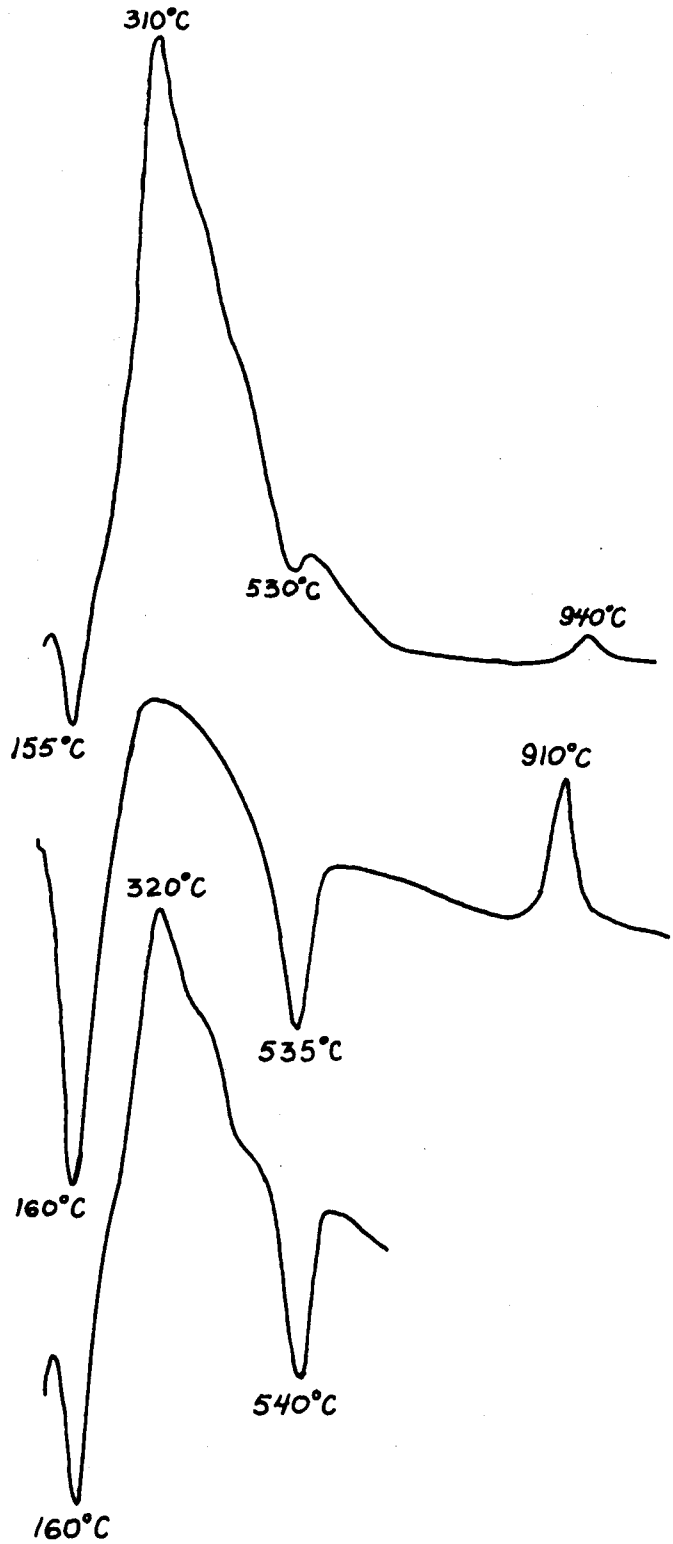

Figure 13. DTA patterns for samples MS-P-1b, MS-P-1e, and MS-P-1f.

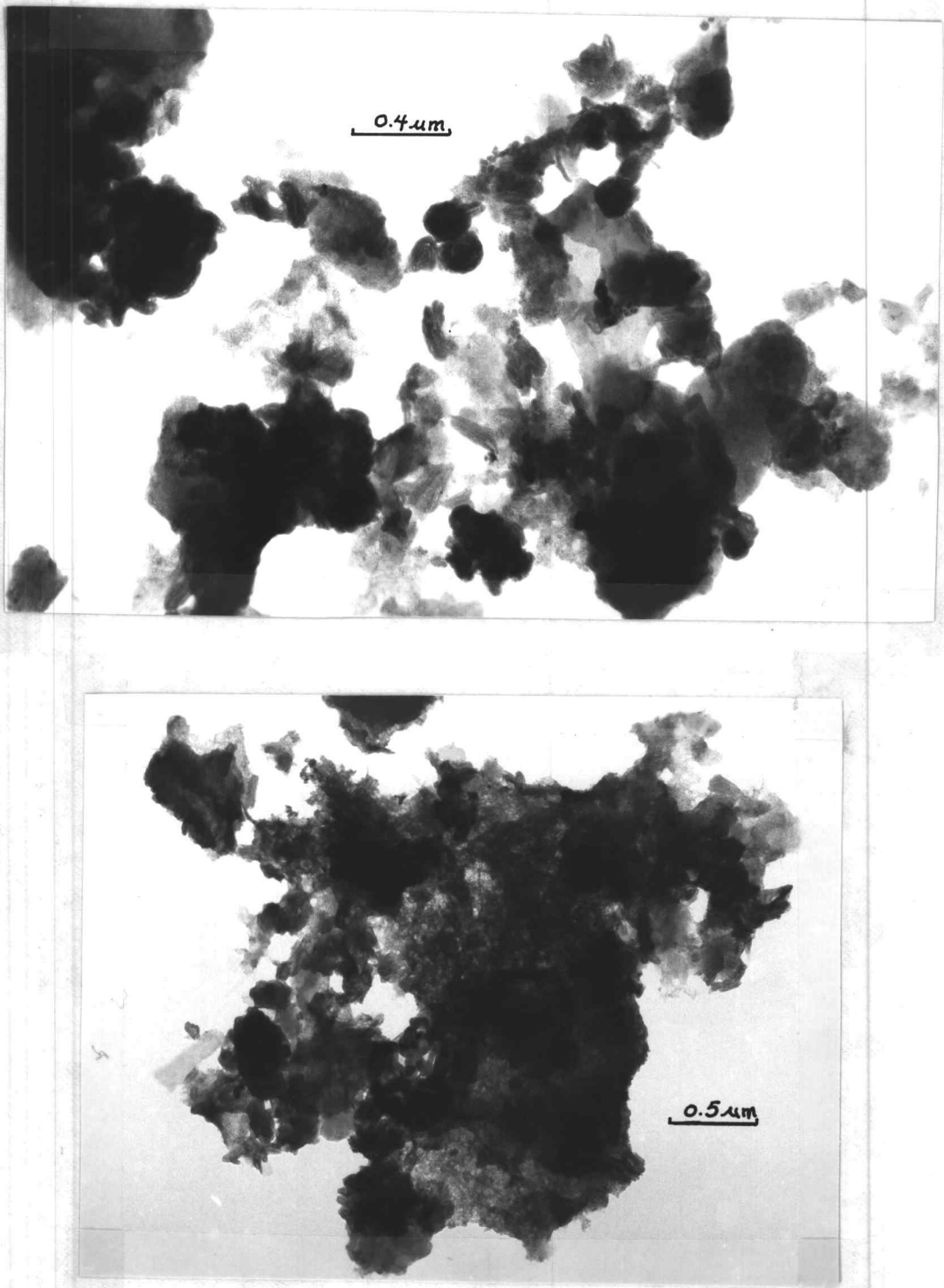

Plate 3. Electron micrographs of clay sample MS-P-1b.

(Plate 3). (The microaggregate shown is similar to that described previously for the debris avalanche sample NS-BC-1b.) The saturated sample, f, clearly contains a greater abundance of tubular and spheroidal halloysite (Plate 4). The amorphous component of sample f generally appears more gel-like, and has a tendency to occur in relatively large bulbous masses (not shown) which are more susceptible to disintegration under the electron beam (Jones and Uehara, 1973). The greater abundance of halloysite in the saturated, less stable soil, and the different forms of amorphous material noted in the two samples most likely play a key role in the water holding characteristics and shear strength characteristics of the two soils.

Samples i and h (Figure 14) were collected a short distance downslope from sample f in the area where the failure was cut through during road construction. The presence of montmorillonite is quite strong in these samples, and the hydrated halloysite in sample i is sharper and stronger than in the other samples, indicating a better developed mineral at this location. Halloysite is also indicated in sample h, but its presence is not nearly as strong. Careful observation of the site suggests that sample i originated from near the debris flow failure plane in the perched water zone at the contact of the colluvium and the weathered pyroclastic rock, whereas sample h originated in the weathered pyroclastic material beneath the failure plane and upon which the water table is perched. However, sampling difficulties caused by the saturated conditions of the soil and by the natural and man-caused disturbances made it impossible to determine the precise relationships of these samples to each other and to others collected at the site.

The slopes bordering the failure area are relatively stable. This is especially true of the left slope (considered as the failure's left), the soil of which is dry, coarse textured and generally poorly developed. The XRD pattern for this sample indicates the presence of chloritic intergrade, zeolite and possible traces of halloysite and amorphous material (Figure 15).

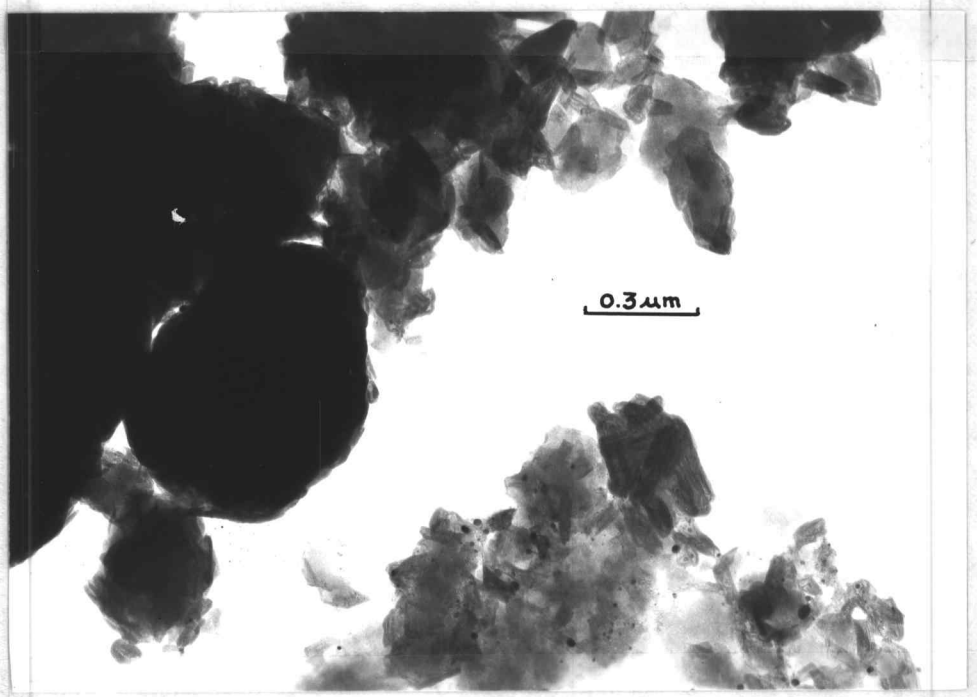

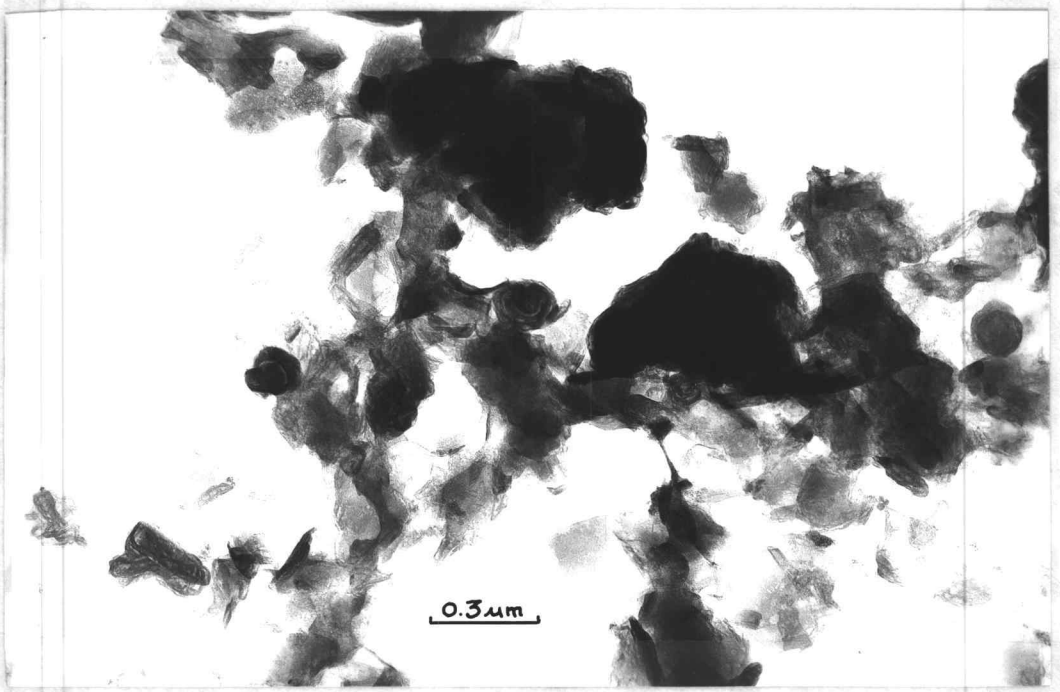

Plate 4. Electron micrographs of clay sample MS-P-1f.

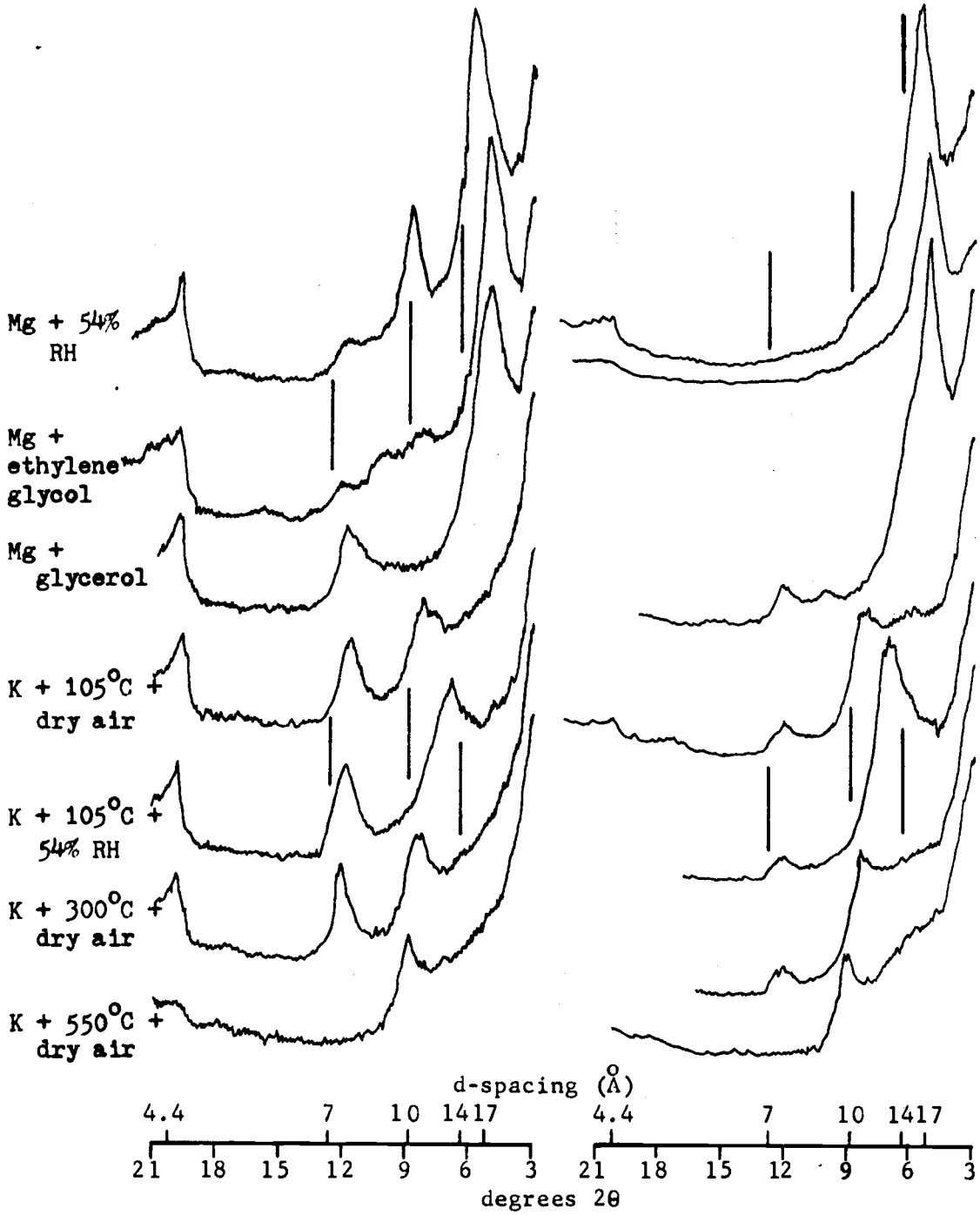

Figure 14. Site MS-P-1 XRD patterns. Sample i (left), random sample of mixed, failed material. Sample h (right), plastic clay underlying flowing soil and which supports perched water table.

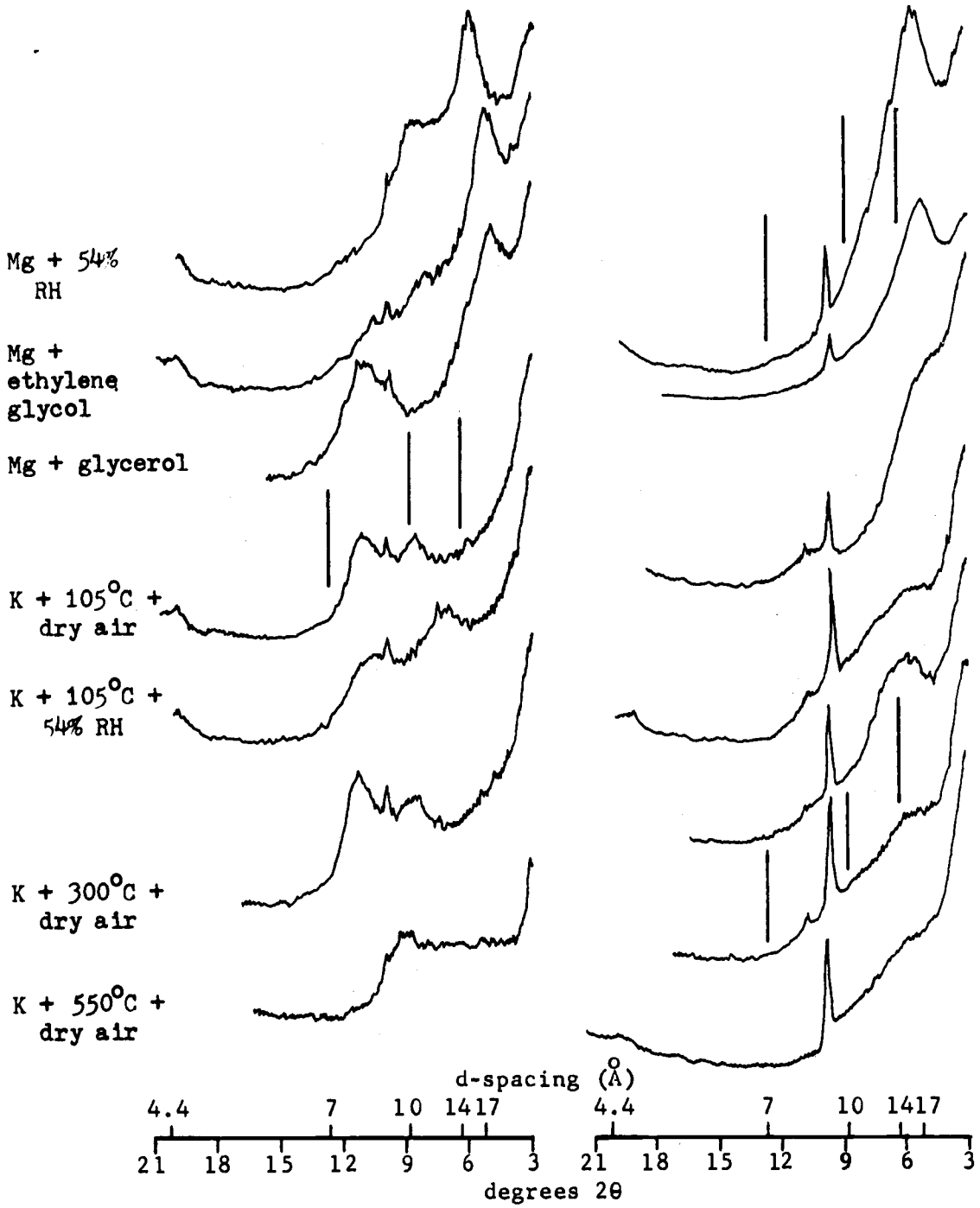

Figure 15. Site MS-P-1 XRD patterns. Sample j (left), somewhat drier, more stable (?) cutbank at the right edge of failure area. Sample g (right), dry, stable cutbank to left of failure area.

The failure site MS-1 is a fairly large debris flow, again involving soil with a high water holding capacity, and which is slippery but only slightly sticky. XRD analyses (Figure 16) and DTA (Figure 17) show the very strong presence of hydrated and dehydrated halloysite and amorphous material, with some smectite and chloritic intergrade. These materials are also shown in the electron micrographs (Plate 5).

Figure 16 also gives the strong montmorillonite patterns of the soil from site MS-2 which was collected from an area of deep soil creep and rotational slumping located about a mile from MS-1 in the same drainage. Field observations suggest that the clay of site MS-2 is probably similar to that underlying the deposit at MS-1.

Similar relationships of saturated soil containing halloysite, amorphous material and chloritic intergrade failing as a debris flow over montmorillonite are shown by the clay fractions at site R-CM-1. Samples a and c (Figure 18) represent different depths in the material which is subject to flowage. Sample b, which was collected from saturated soil at the failure plane, generally shows greater evidence of hydrated halloysite and stronger smectite than does sample a, which was collected from moist soil approximately one meter above the current perched water table. (The strengthening of the 7.6 Å peak and concurrent diminishing of the plateau in the vicinity of 10 Å with glycerol solvation of the Mg-saturated treatment is due to dehydration of the halloysite, caused by heating the sample during vapor solvation.) The small sharp peak at 6.4 Å is probably due to plagioclase.

The soils represented by samples d and f (Figure 19), which give strong montmorillonite peaks and weak halloysite peaks, are stable as compared to the overlying saturated soil, but nonetheless have undergone rotational slumping at greater depths. Surprisingly, the plastic clay samples d and f also exhibit small but distinct 7.16 Å peaks which may be indicative of kaolinite. The presence of kaolinite in this sample may indicate additional erosion of better drained soil from further up the slope, as it is highly unlikely that

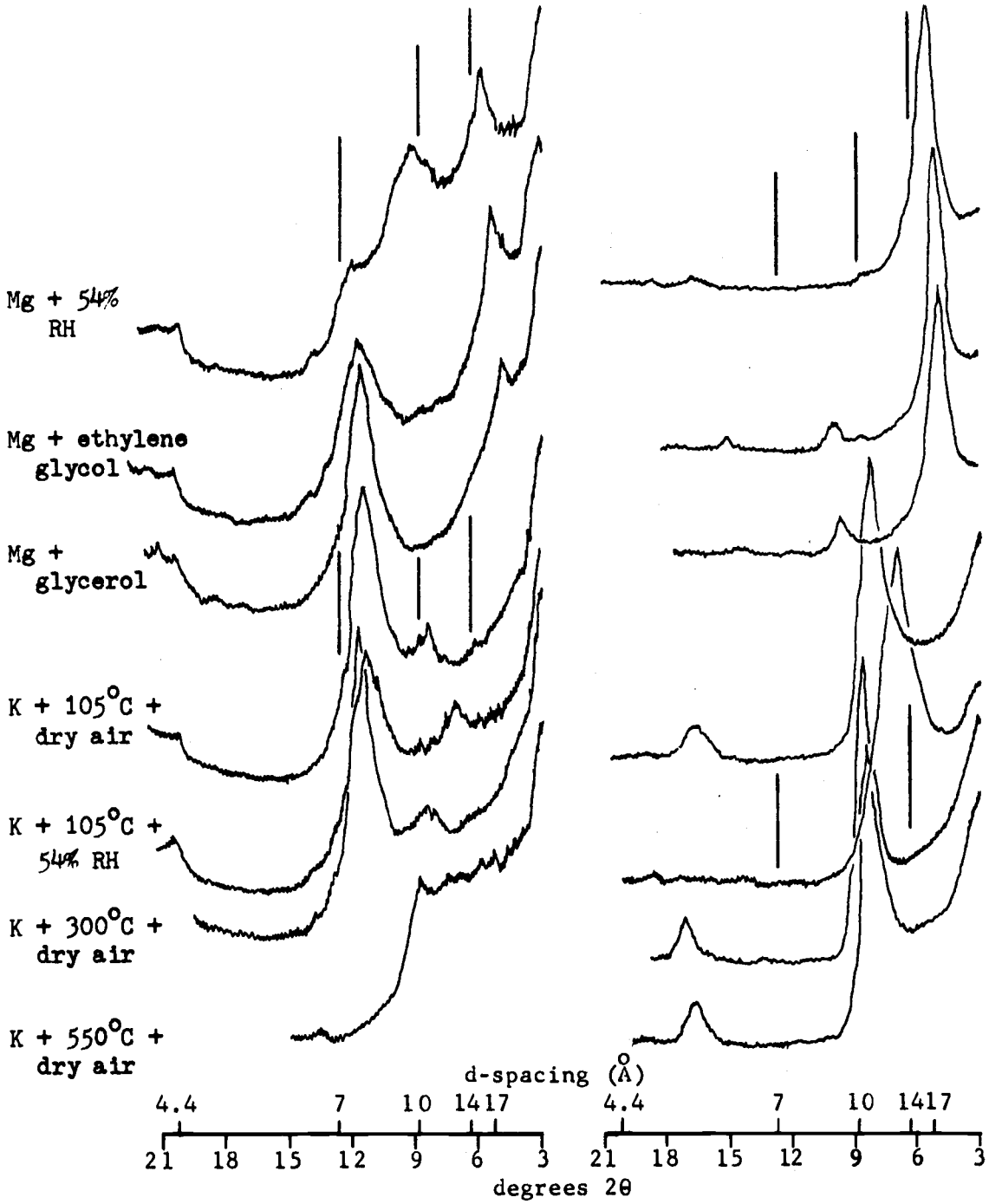

Figure 16. Site MS-1 (left) XRD patterns, 20 cm deep into remaining bank of large debris flow road failure. Site MS-2 (right) XRD patterns of material similar to that underlying MS-1

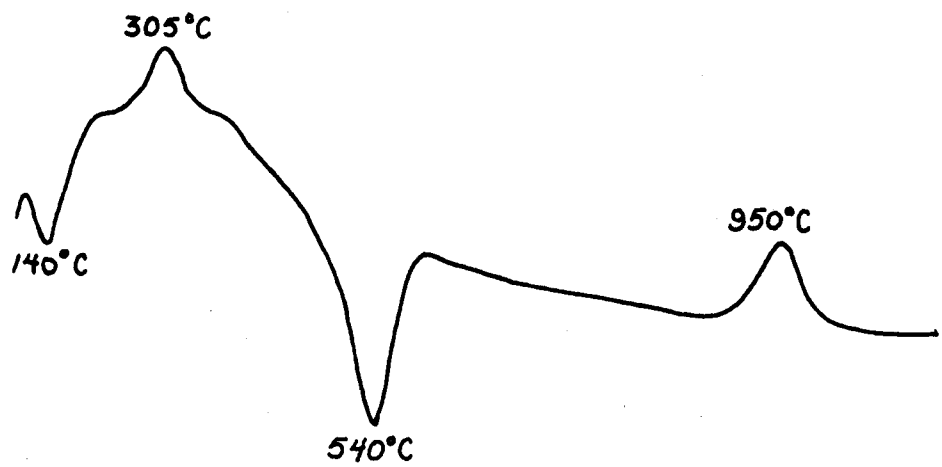

Figure 17. DTA pattern for sample MS-1.

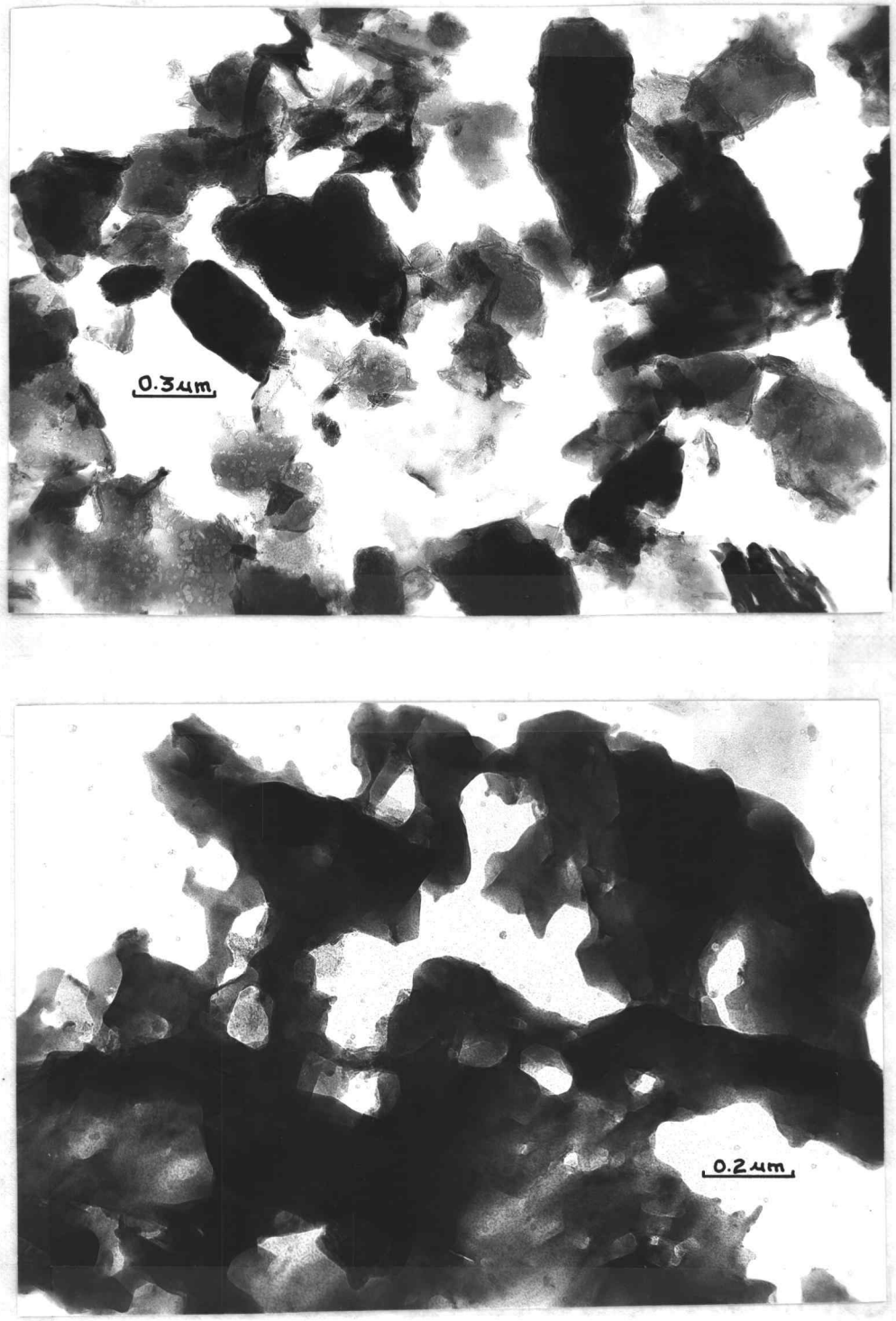

Plate 5. Electron micrographs of site MS-1 clay.

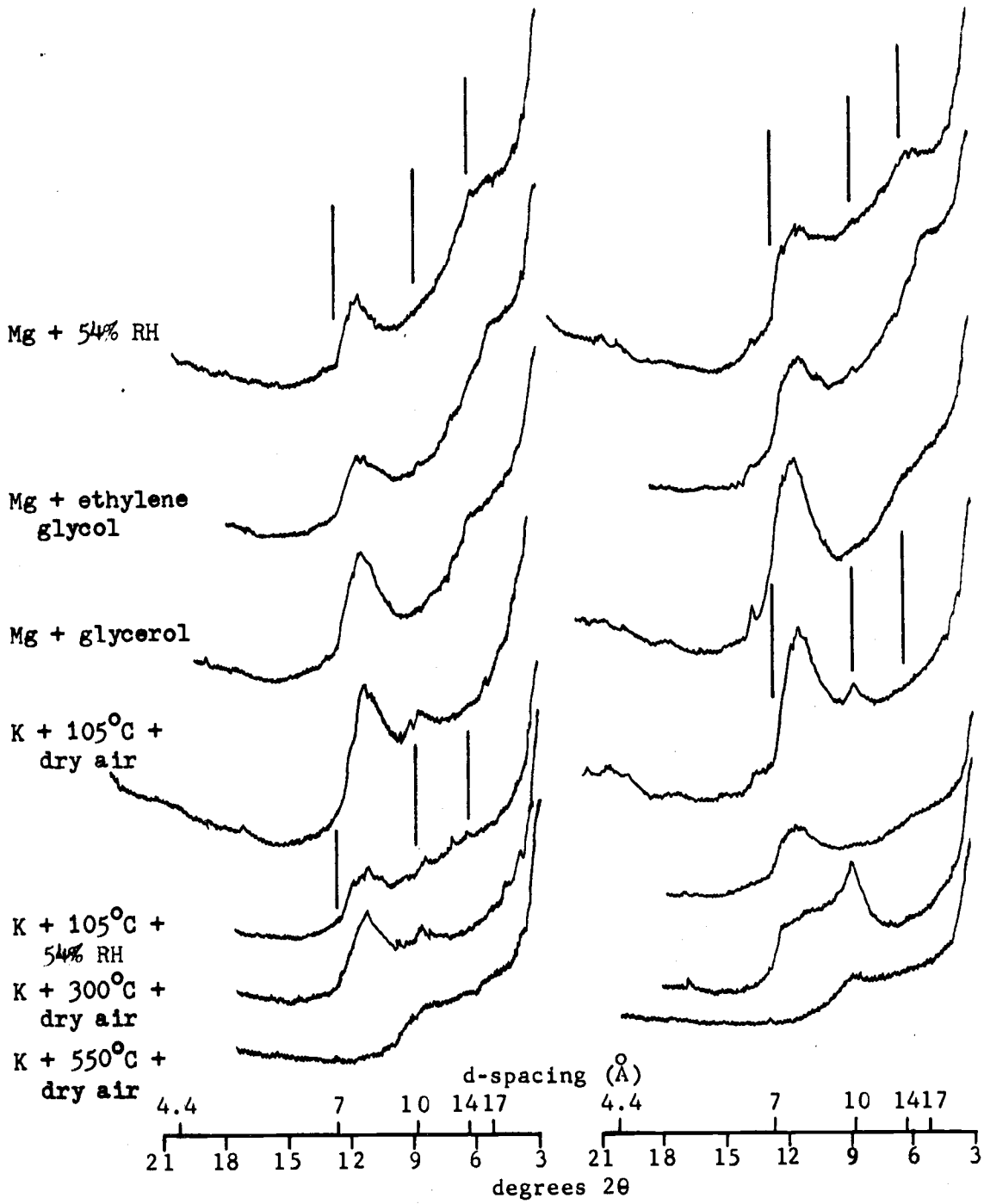

Figure 18. Site R-CM-1 XRD patterns. Sample a (left), headwall region of failure, 1 m from crown. Sample c (right), failure surface at level of emerging water, 2½ m from crown.

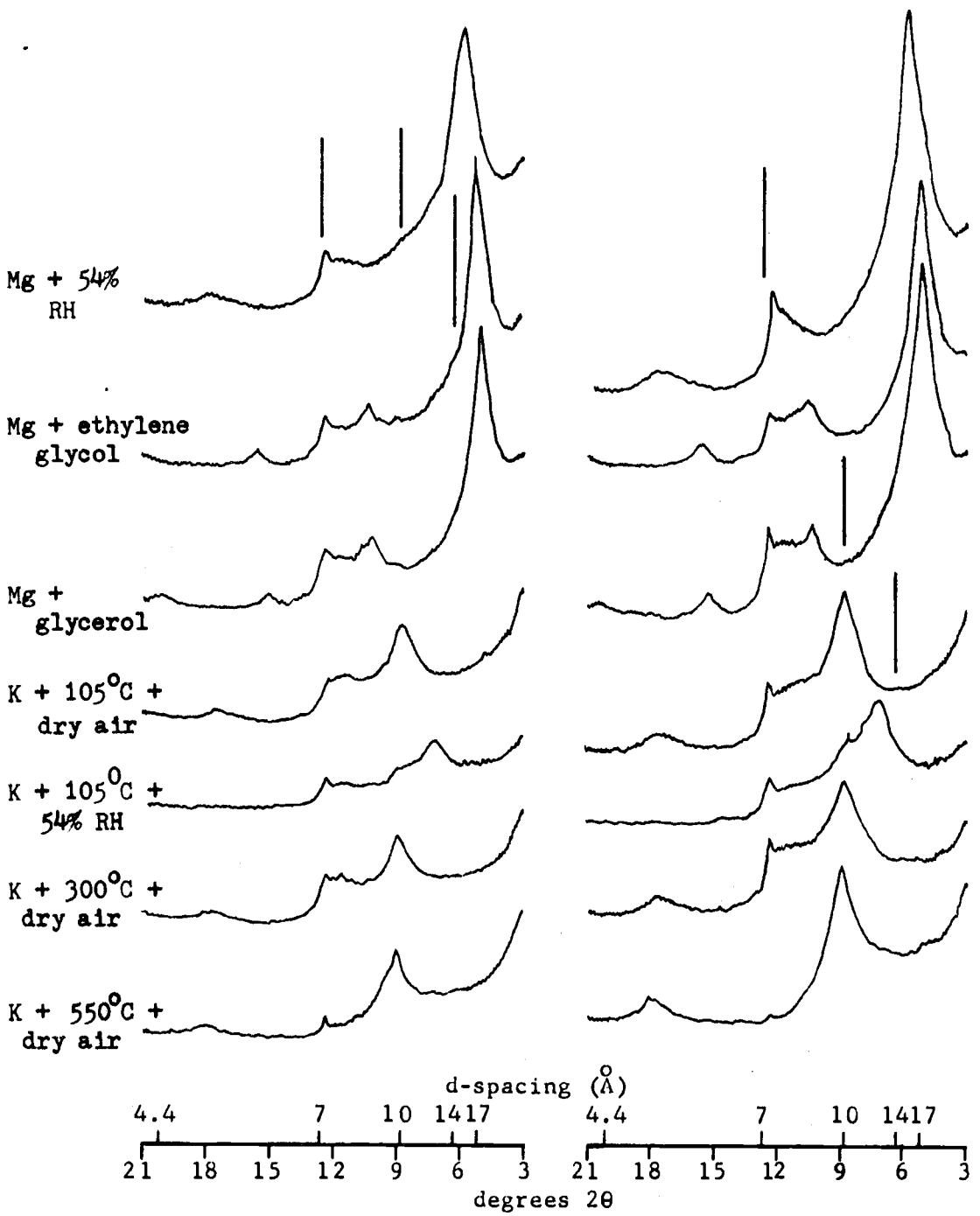

Figure 19. Site R-CM-1 XRD patterns. Sample d (left), plastic clay below failure plane. Sample f (right), gleyed, sample of plastic clay adjacent to failure.

kaolinite would form under the environmental conditions of this site. These may, however, be nothing more than unusually sharp peaks of dehydrated halloysite.

The clay of sample e, site SS-SF-1 was collected from a layer containing basaltic colluvium and volcanic ash, and consists of halloysite, amorphous material, some gibbsite and chloritic intergrade with indications of smectite (Figure 20). This material which is approximately two meters in depth, has failed by the flowage process on a 30% slope underlain by montmorillonite (Figure 20, sample h).

These trends are also shown in the DTA patterns (Figure 21) for samples f, g, and h. Sample f, which is comparable to sample e, gives a typical halloysite pattern with the large dehydration endotherm, strong dehydroxylation endotherm and high temperature exotherm. The endotherm at 335°C is due to gibbsite. Sample g, which was collected from near the top of the saprolite and transitional between f and h, shows weaker halloysite peaks and definite signs of montmorillonite, with a shallow endotherm at approximately 675°C and a high temperature exotherm. The pattern of sample f, collected at approximately one and one-half meters deep into the saprolite, indicates much stronger montmorillonite, XRD patterns for samples f and g are given in Appendix III.

Electron micrographs (Plate 6) of the clay fraction of the soil from above the failure plane show bulbous masses of amorphous gel, which appear similar to those described earlier for sample MS-P-1f. These gel masses are highly unstable under the electron beam, and upon disintegration reveal numerous individual clay particles as well as amorphous material which is more stable under the beam. Thus, it appears that these kinds of masses are analagous to microscopic balloons consisting of a gel-like membrane and filled with clay particles with a high affinity for water. It seems reasonable to suggest that in the field these "balloons" are also filled with water which would be released upon rupture of the membrane. This hypothesis could explain in part the unusual sensitivity of these soils. Unfortunately, the "water balloons" were difficult to photograph due

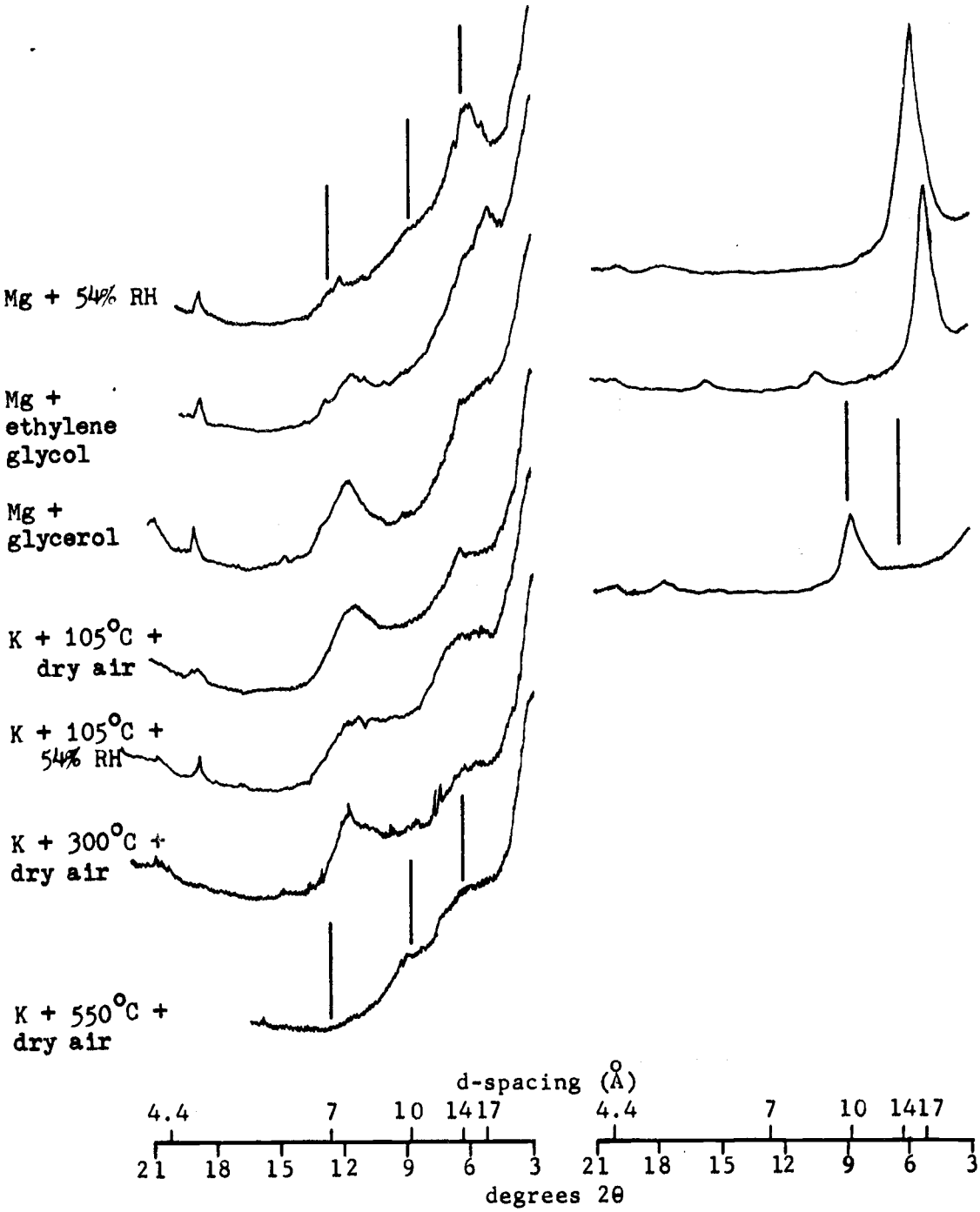

Figure 20. Site SS-SF-1 XRD patterns. Sample e (left), flowing soil neartop of perched water table, 1 m depth. Sample h (right), gleyed plastic clay beneath perched water table, 4 m depth.

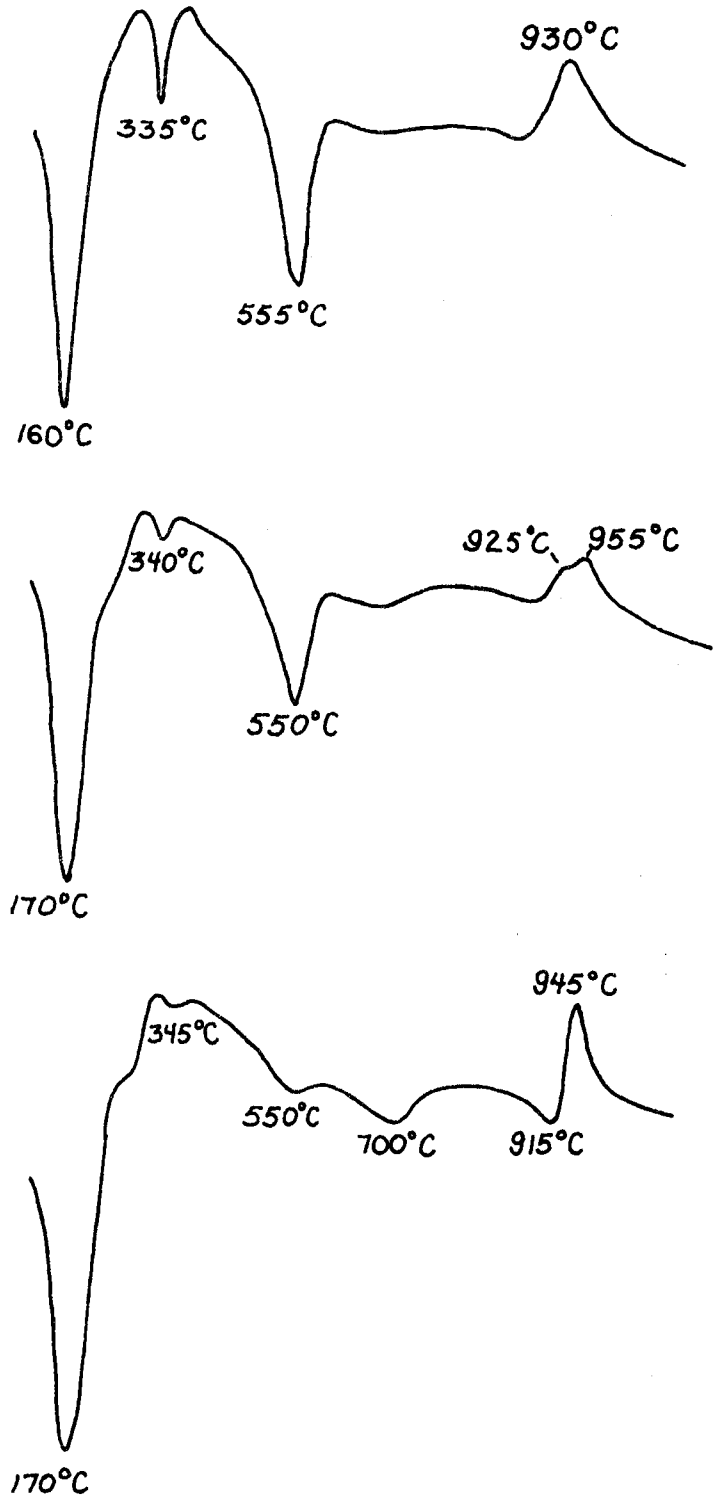

Figure 21. DTA patterns for samples SS-SF-1f, SS-SF-1g, and SS-SF-1h.

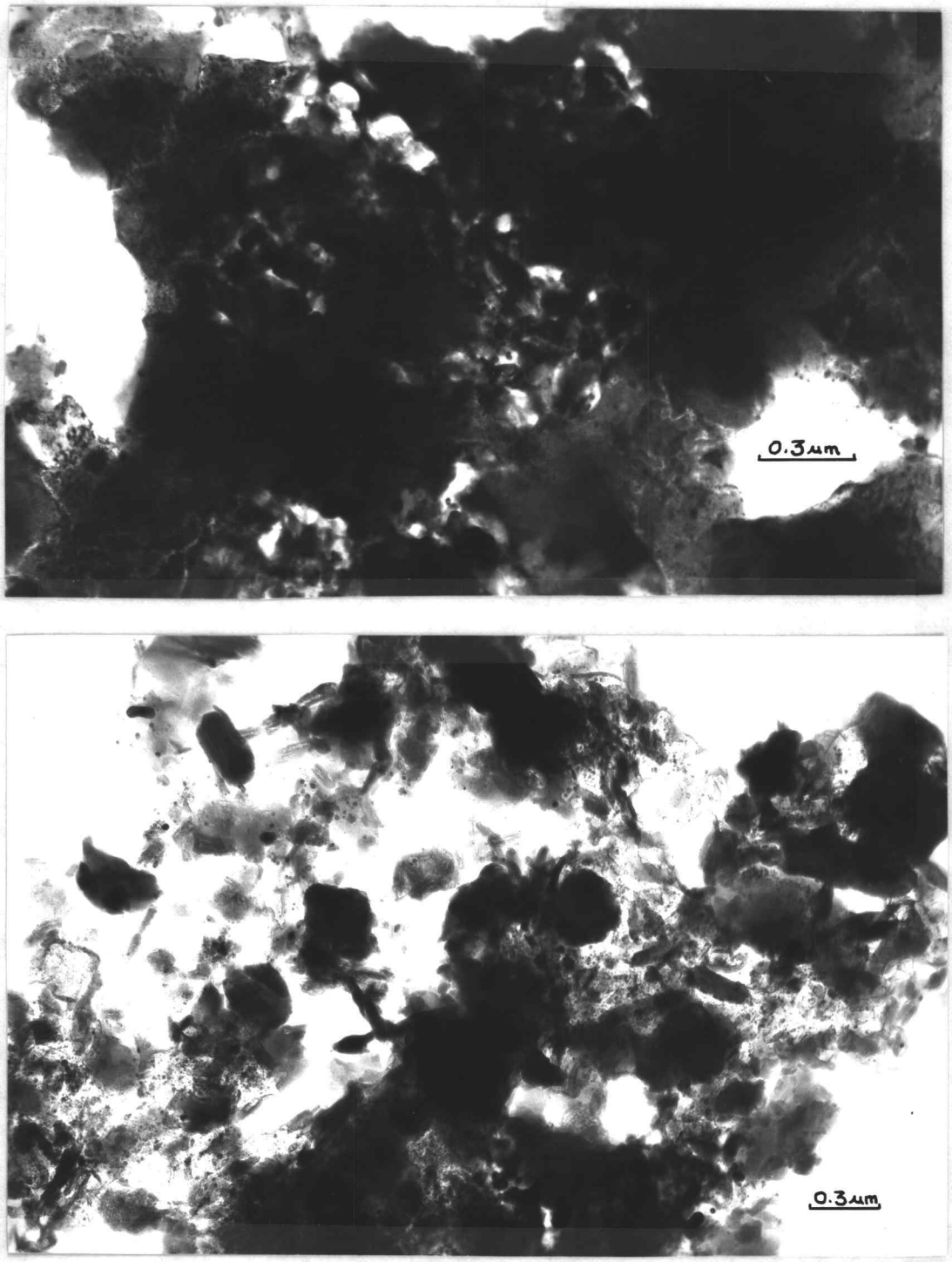

Plate 6. Electron micrographs of clay sample SS-SF-1j from above the debris flow failure plane, before (above) and after (below) disintegration of amorphous gel under the electron beam (different areas of the sample holding grid).

to their massive, nondescript nature and to their instability under the electron beam. However, they were seen quite commonly in samples of those soils which are most subject to sudden flowage following disturbance.

An additional micrograph of the same sample shows halloysite, amorphous material and chloritic intergrade which are not coated with the gel (Plate 7). Montmorillonite with some halloysite and amorphous material from below the plane of failure, and which supports the perched water table, is also shown (Plate 8).

The liquid limit and natural water content of soil from site SS-SF-1 after failure were 54.3% and 56.7%, respectively (McNabb, D. H. 1977. Correlation of soil plasticity with amorphous clay constituents. Unpubs. Ms.). (Natural water content as a soils engineering parameter is on the weight basis of total soil solids.) Although the liquid limits of highly sensitive clays rarely exceed 50% (Mitchell, 1976), an important characteristic of sensitive clays is that the natural water content exceeds the liquid limit. The differences in values might have been greater if the analyses had been conducted on soil which had not yet flowed in the field. Flowage of the soil typically tends to separate particle sizes by carrying smaller and lower density particles greater distances than the larger, heavier particles. Therefore, it would be expected that the liquid limit would be lower, and the natural water content higher, on the unfailed soil.

The soil-stability relationships exemplified by site SS-SF-1 are quite common in the upper reaches of the Soda Fork drainage, and are repeated at site SS-SF-3, but with less distinction and more variation due to greater disruption of the landscape. Once again, the soil subject to flowage is reddish brown in color, wet, slippery but not sticky, and appears to have developed mostly from basaltic colluvium. This overlies yellowish, somewhat plastic saprolitic material.

Mineralogically, however, the soil at the plane of flowage differs from that at failure planes discussed previously. The XRD

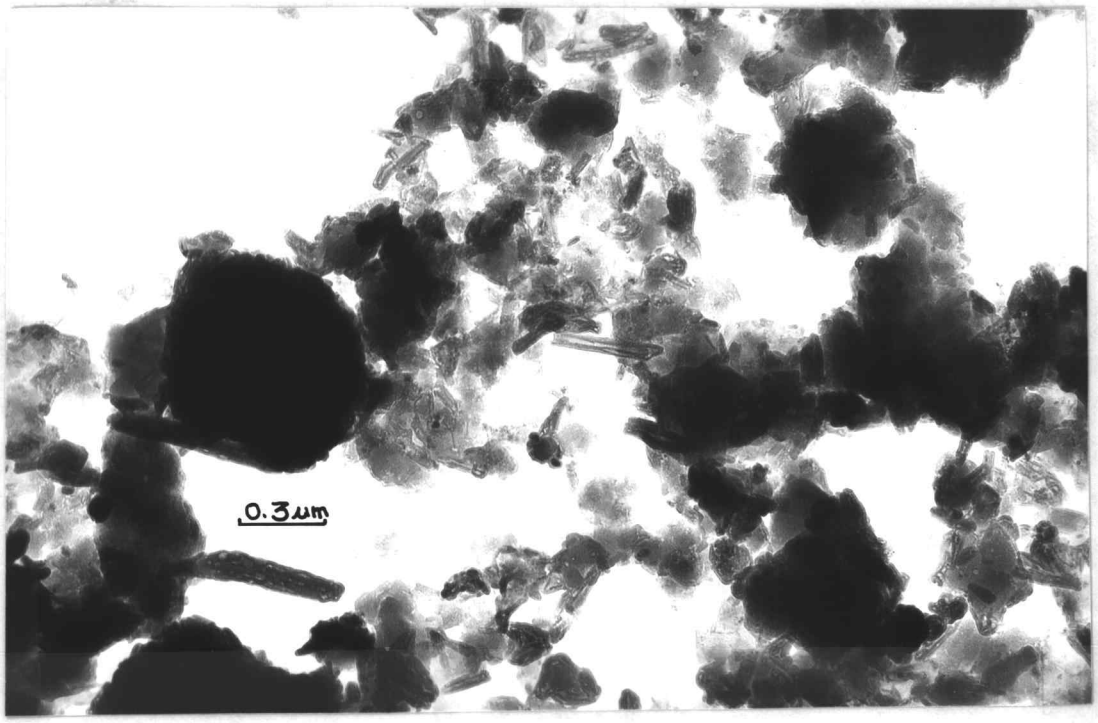

Plate 7. Electron micrograph of clay from above the plane of failure at site SS-SF-1 (sample j).

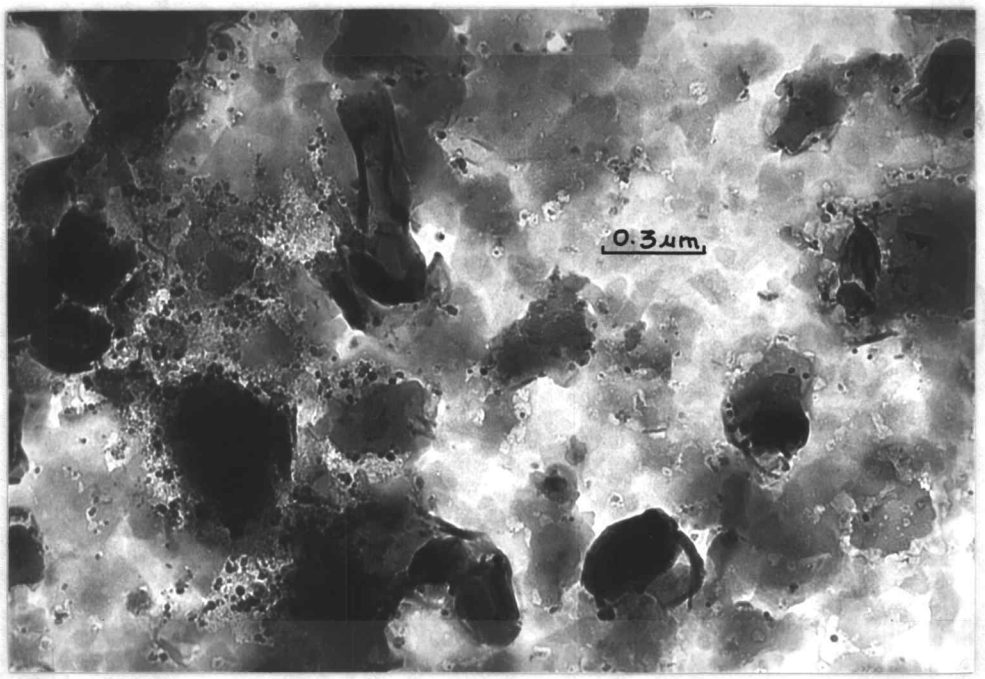

Plate 8. Electron micrograph of clay from below the plane of failure at site SS-SF-1 (sample g).

patterns (Figure 22) show the presence of amorphous material, halloysite, chloritic intergrade, and gibbsite (4.8 Å) in the failing soil (sample a), but they do not show the strong smectite peaks in the underlying clay (sample b) as seen at other failure sites. Instead, the patterns of the underlying and overlying clays are strikingly similar--except for the significant presence of strong, sharp, hydrated halloysite peaks in the yellowish material below the flowage plane. This mineralogical change with depth appears to coincide with a hydraulic discontinuity on the site. However, these relationships are indistinct due to the disturbance which has occurred.

The apparent mineralogical anomaly may be explained by the possibility that samples a and b do not actually represent soil from above and below the plane of failure. The combined presence of well developed hydrated halloysite and gibbsite in sample b suggests that there has been considerable mixing of the profile, as the conditions of formation are very different for these two minerals (Rai and Lindsay, 1975). This suggestion is supported by the fact that the basaltic colluvium is well mixed into the underlying saprolite. Deeper into the slope the soil gradually exhibits stronger characteristics of cohesive, smectite clay, which on previously mentioned sites has marked a sharp boundary at the base of the perched water table. (Laboratory analyses were not conducted on this cohesive clay.) It is interpreted that the failure processes at this site, which are quite complex, involve flowage of surficial material which was undercut by road construction; soil creep, and perhaps slow flow, extending to some greater depth into cohesive clay; and ancient, deep seated progressive rotational failure at even greater depths.

Although the mineralogy presented for site SS-SF-3 appears anomalous, further evidence of an association between the debris flow process, a mineralogical transition with depth involving halloysite and amorphous material, and a hydraulic discontinuity is given by the findings at sites MK-D-1, MFW-D-1 and MS-Q-1. Debris flows at each of these sites involved soil that was relatively dry at the time of sampling, and whose clay fraction is mostly amorphous, as indicated

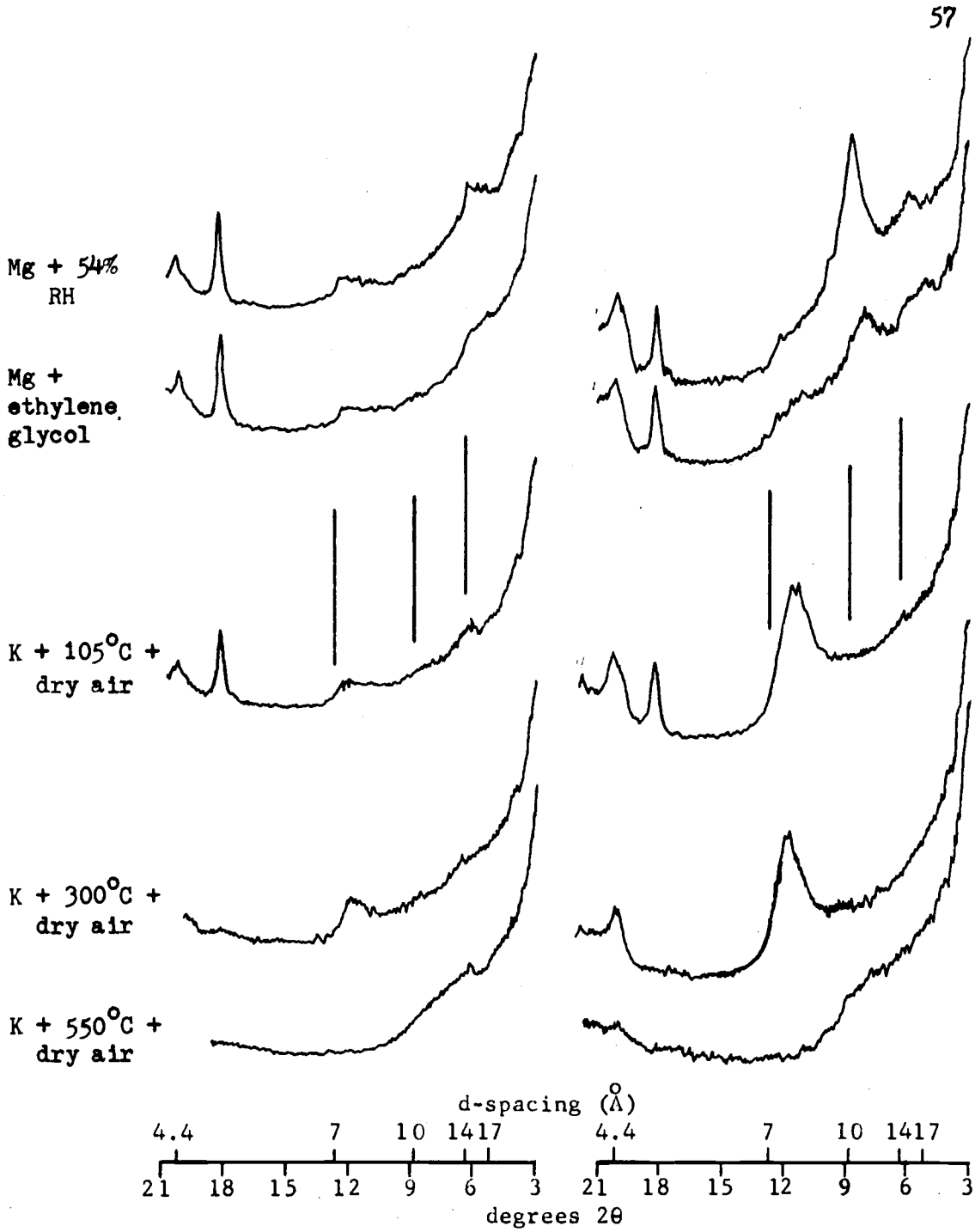

Figure 22. Site SS-SF-3 XRD patterns. Sample a (left), moist, failing soil at failure plane. Sample b (right), wet, mixed soil beneath failure plane.

by the left-hand sets of diffractograms in Figures 23, 24, and 25. In each case, the soil remaining on the failure is saturated at only a few centimeters beneath the surface at some point about midway down the failure. This soil contains amorphous material and well developed hydrated halloysite, as indicated by the right-hand sets of patterns. DTA patterns for the two samples at site MK-D-1 and for sample d, site MS-Q-1 show similar results (Figure 26).

These findings also appear anomalous to the situations described previously in which saturated soil with amorphous material and halloysite failed over a montmorillonitic deposit. However, later investigation at site MK-D-1 revealed the presence of plastic, smectite clay at greater depth, but at a different (more accessible) location within the failure. It is suggested that the smectite supports the perched water layer, and that deeper sampling at sites MFW-D-1 and MS-Q-1 would yield similar results.

Electron micrographs of sample MK-D-1a reveal fragments of devitrified glass linked by imogolite strands, as well as occasional unidentified spherical bodies which appear to be growing from a particle edge (Plate 9). The devitrified glass and imogolite are similar to that found in Mazama ash (Dingus, 1973). Sample MK-D-1b (Plate 10) contains a considerable amount of tubular and some spheroidal halloysite with coatings and attachments of amorphous gel. Careful examination suggests that the tubular forms are forming by the rolling of the gel and by peeling off of the spheroids. A relatively large, unidentified lath-like particle and silica bodies (?) are also present.

The micrograph of sample MFW-D-1a (Plate 11), from the relatively dry soil of the failure headwall at Dome Creek, shows several features, including the gelatinous nature of the amorphous material; several rough surfaced, broken spheroidal particles which appear similar, but smaller in size, to those noted in sample MK-D-1a; and a particle of tubular halloysite which may have formed, at least partially, in the vacuum of the microscope, as suggested by the low density appearance of the surrounding support film.

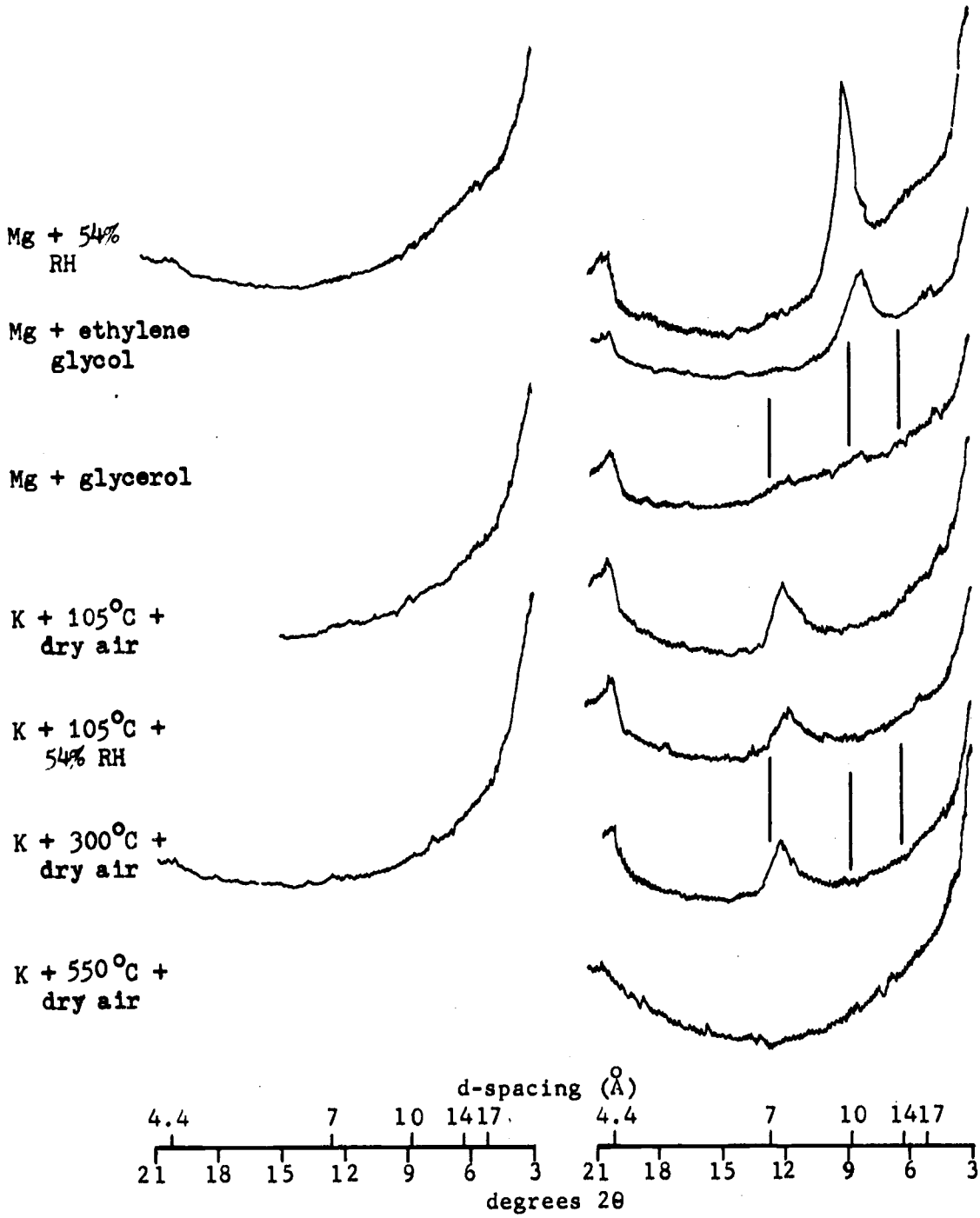

Figure 23. Site MK-D-1 XRD patterns. Sample a (left), failing soil of lateral failure plane. Sample b (right), wetter soil beneath failure plane.

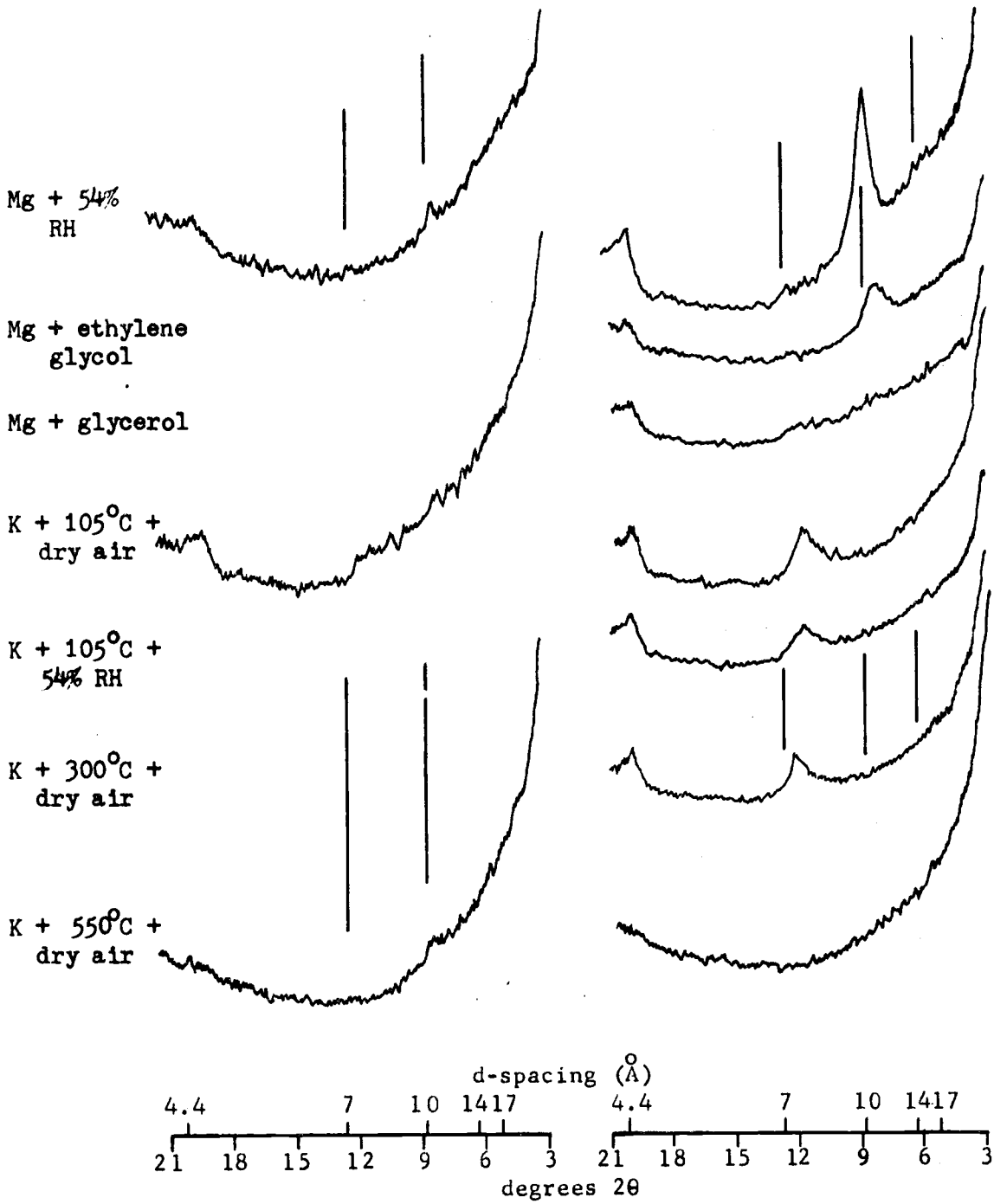

Figure 24. Site MFW-D-1 XRD patterns. Sample a (left), relatively soil of failure headwall. Sample b (right), wet soil remaining on failure surface.

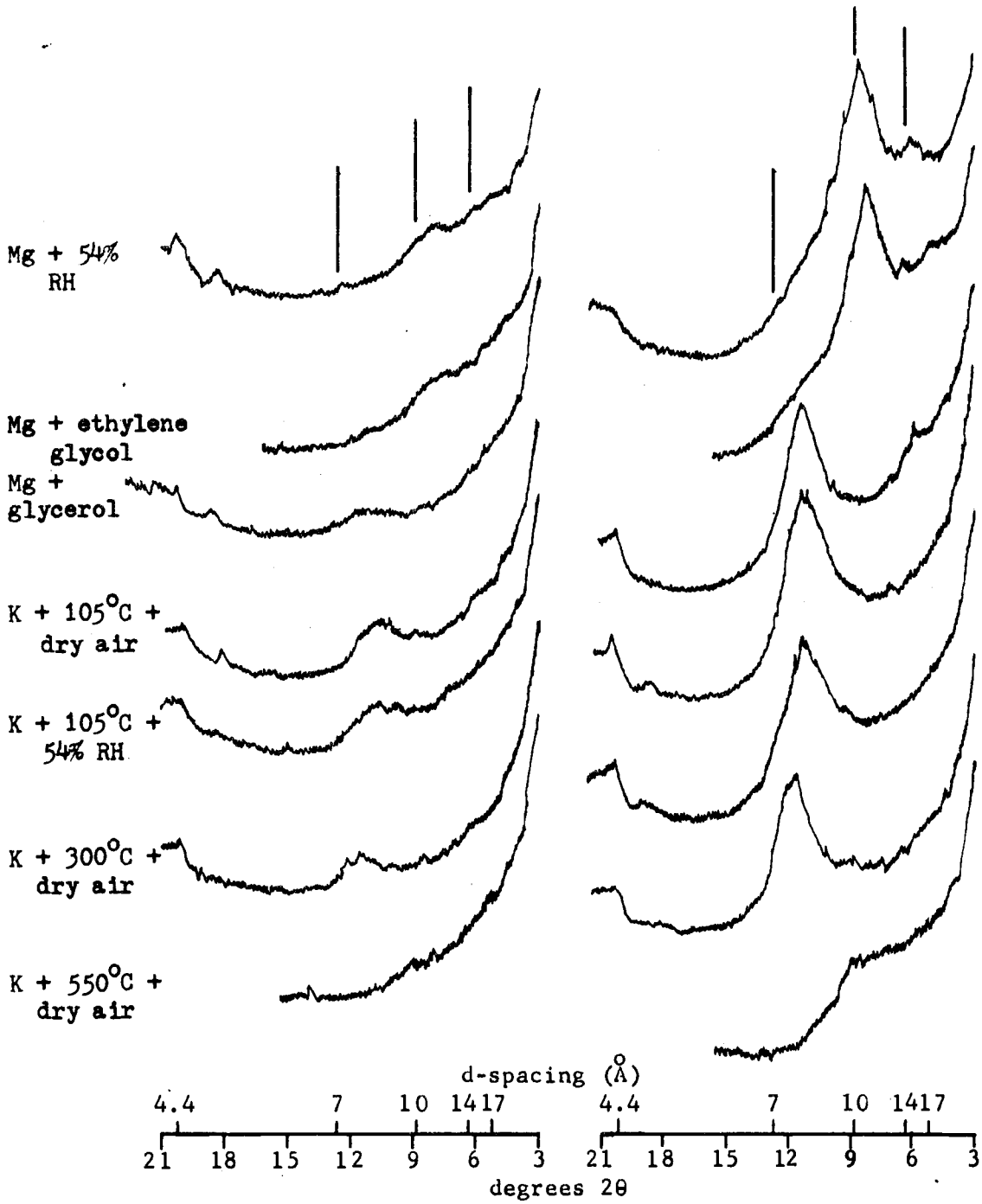

Figure 25. Site MS-Q-1 XRD patterns. Sample c (left), relatively dry soil 30 cm beneath fresh failure surface. Sample d (right), wet soil 75 cm beneath fresh failure surface.

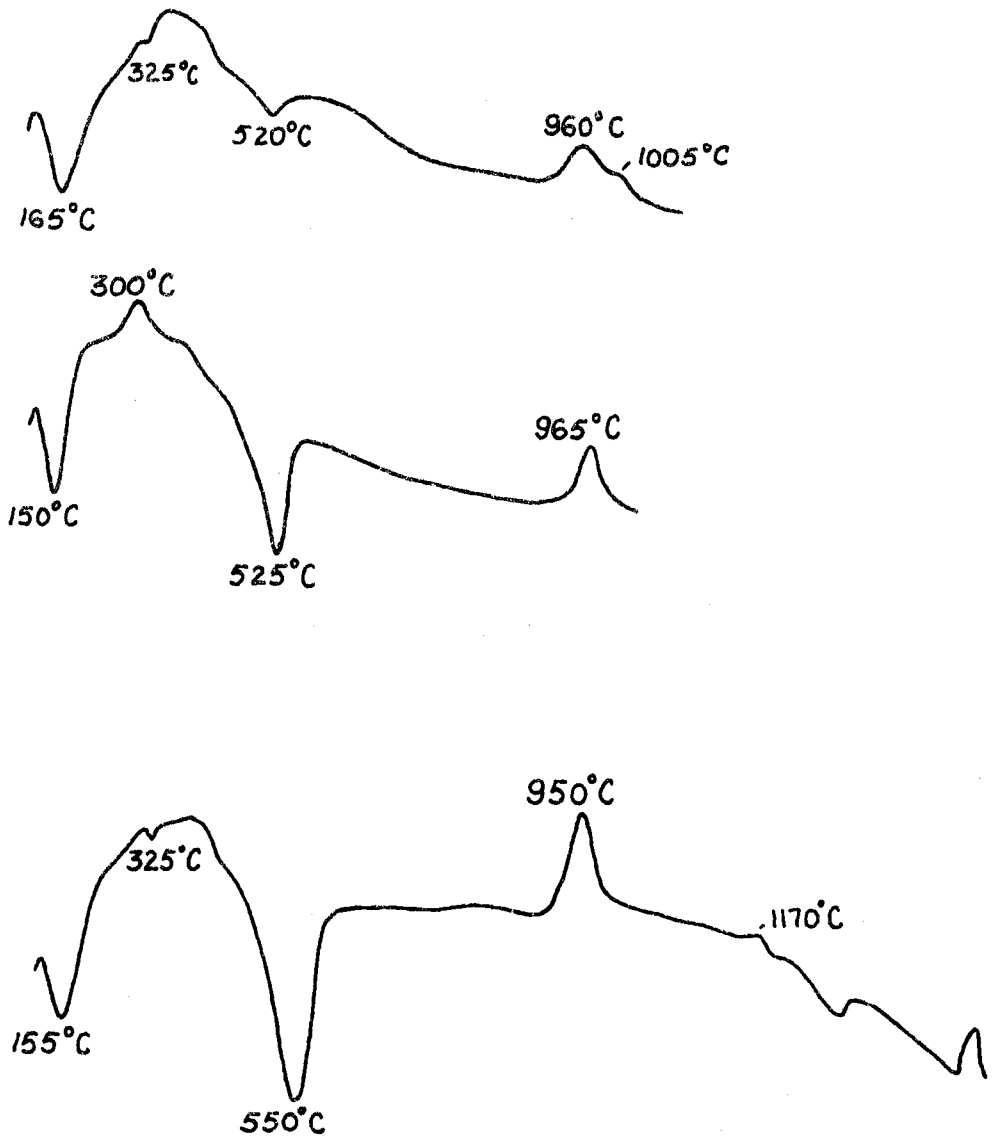

Figure 26. DTA patterns for samples MK-D-1a, MK-D-1b, and MS-Q-1d.

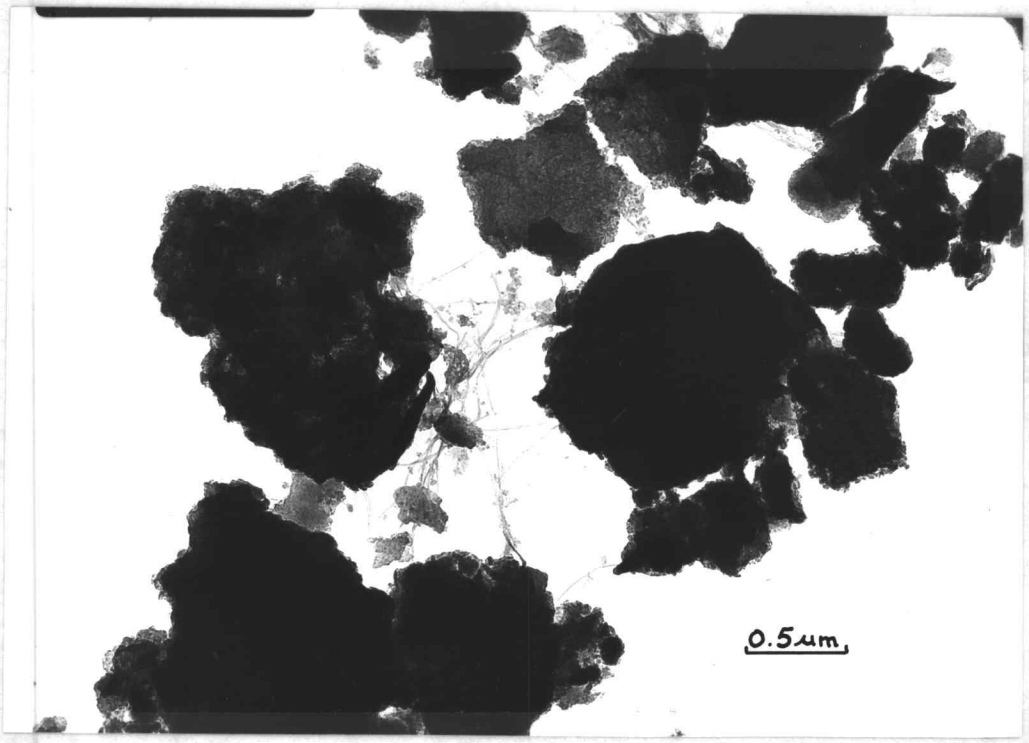

Plate 9. Electron micrographs of clay sample MK-D-1a.

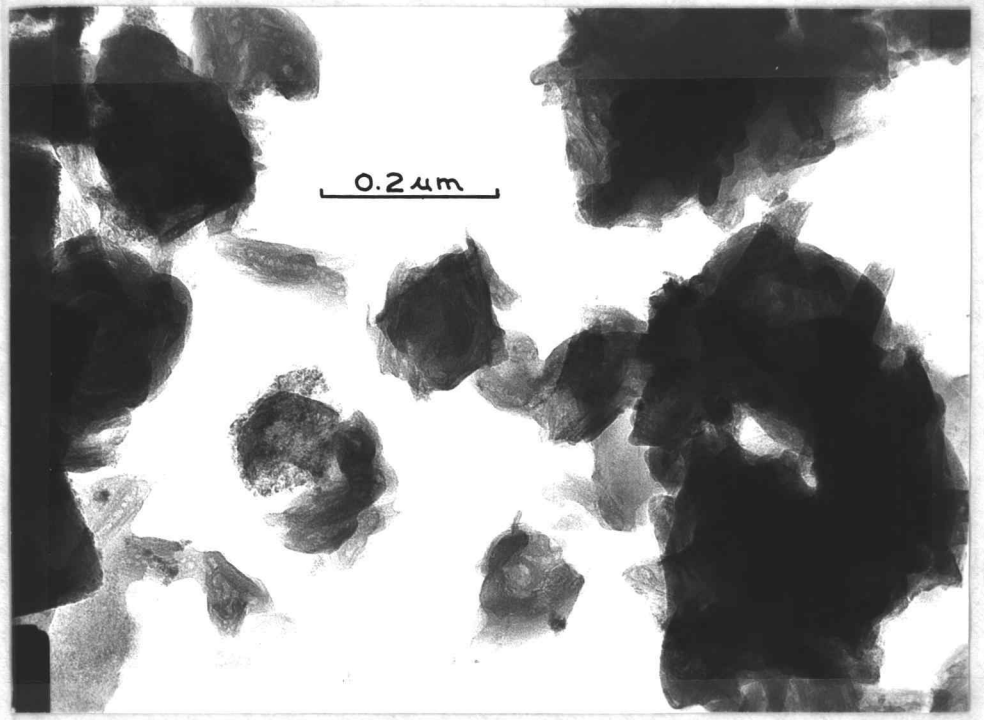

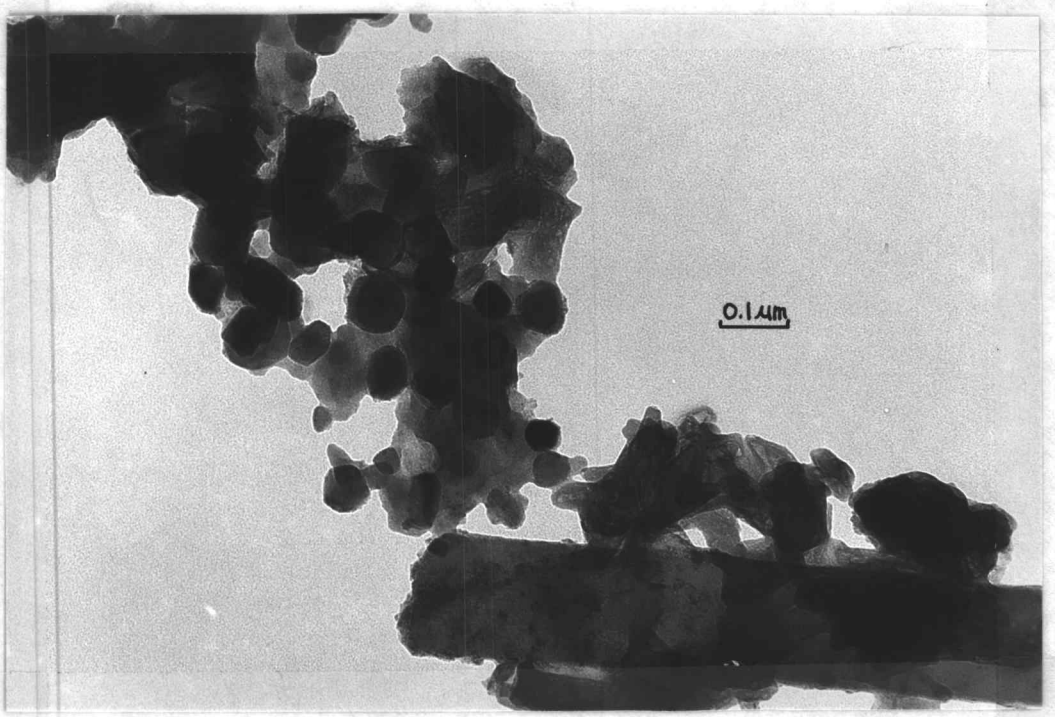

Plate 10. Electron micrographs of clay sample MK-D-1b.

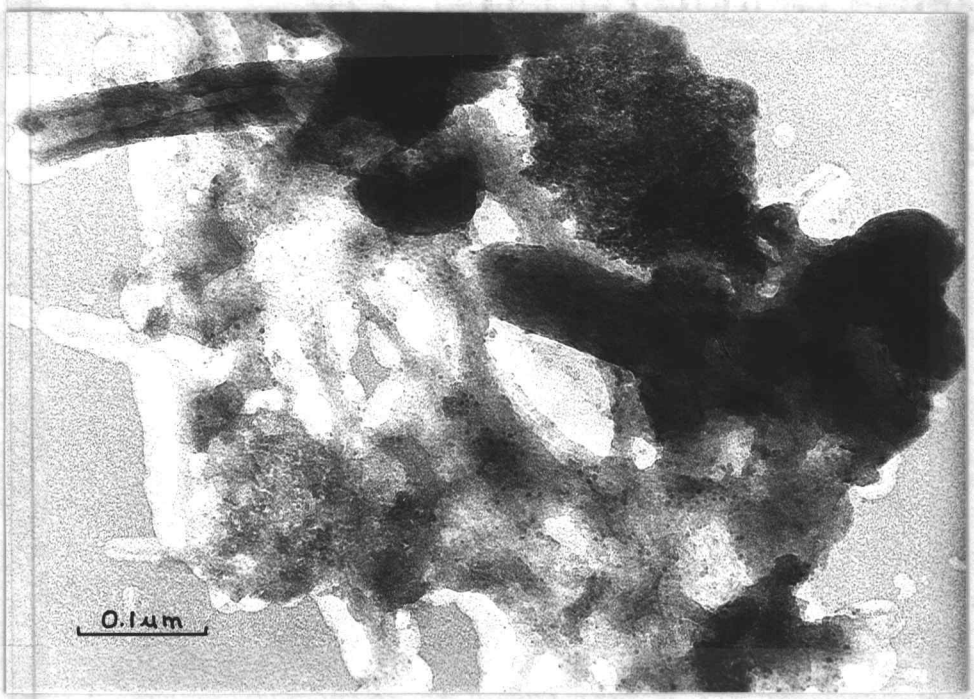

Plate 11. Electron micrograph of clay sample MFW-D-1a.

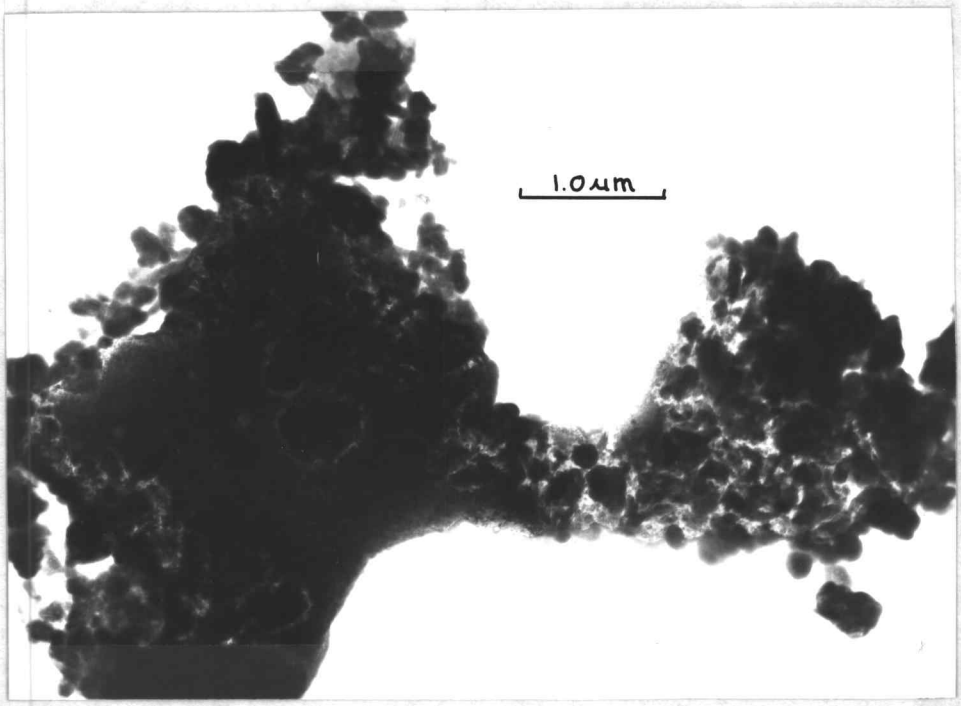

Plate 12. Electron micrograph of clay sample MFW-D-1b.

Sample b (Plate 12), from a more moist area at the same site, shows an aggregate which before exposure to the electron beam was entirely covered by a bulbous mass of gel-like material--similar to the "water balloons" described at sites MS-P-1 and SS-SF-1. This mass is highly unstable under the beam; and at the time of exposure of the micrograph negative, the coating on the left portion of the aggregate had disintegrated, while that on the right was still largely intact. As the gel disintegrated it revealed a myriad of distinguishable clay particles--including spheroidal and tubular halloysite--which appear to be supported on a translucent sheet of glass (?) which gives the aggregate its irregular shape.

Additional micrographs of portions of sample MFW-D-1b which had been air dried for several weeks and then heated at 105°C for one hour on the support grid show aggregates similar to that shown in sample MS-P-1b (Plate 13) and described for sample NS-BC-1b. These aggregates are composed of halloysite and other particles and are bound together by an intricate web of amorphous strands, as shown in the blow-up of a portion of the aggregate. These kinds of aggregates were noted most frequently in those portions of failure soils which were drier and appeared to have the greatest strength. Unaggregated spheroidal and tubular halloysite and amorphous material from the same sample are also shown (Plate 14).

The sample from saturated soil MFW-D-1c (Plate 15) shows more of the rough textured, solid surfaced, multilayered spheroids that were noted in other samples. One of these spheroids has split partially and appears to be generating tubular halloysite. A cluster of spheroidal halloysite particles is also shown. Sample MS-Q-1d (Plate 16) shows many particles of tubular halloysite and amorphous films which appear to be generating bubbles similar to those noted previously.

Based on observations under the electron microscope it is suggested that spheroidal halloysite may form directly from amorphous material as solid surfaced, hollow bubbles which gradually build up into larger spherical bodies. These particles may then begin to deform

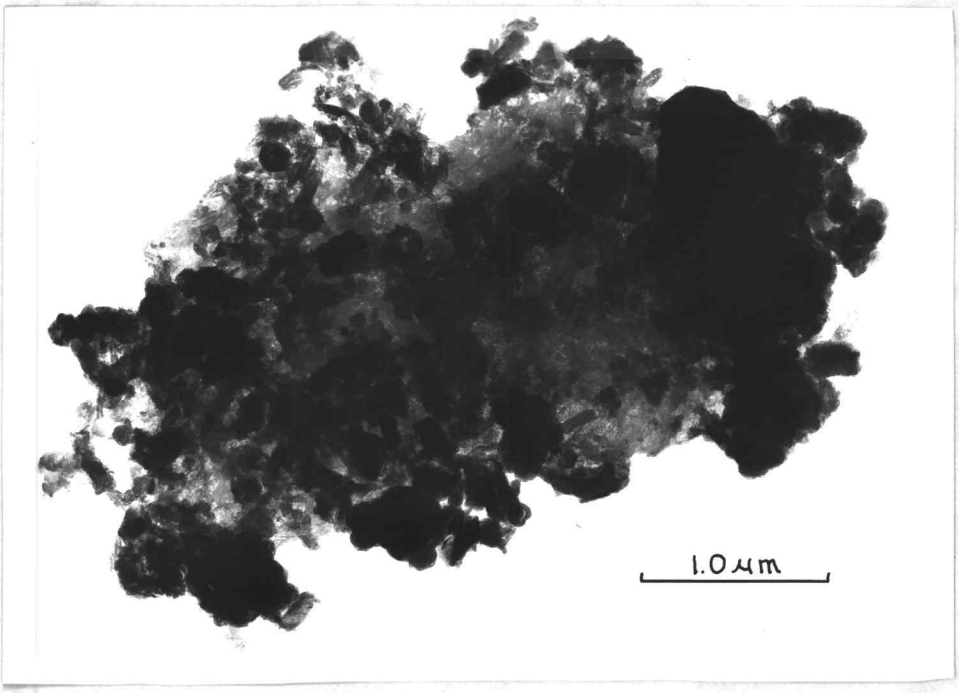

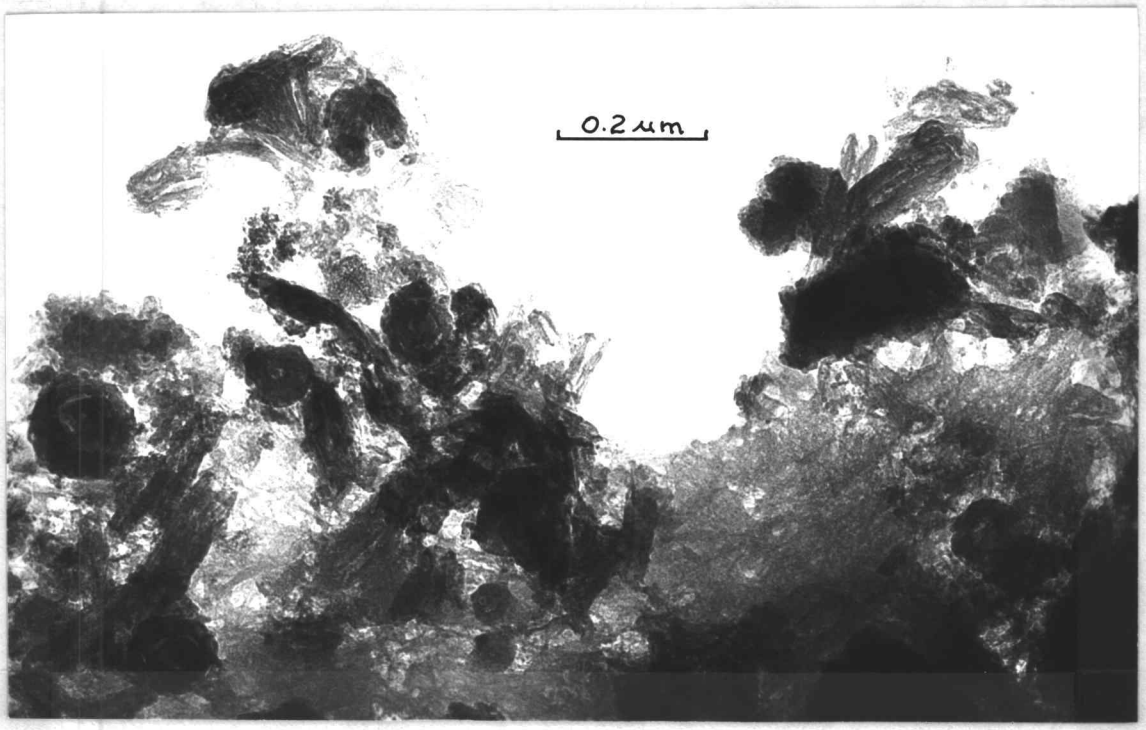

Plate 13. Electron micrographs of clay sample MFW-D-1b. Bottom photograph is a blow-up of the top one.

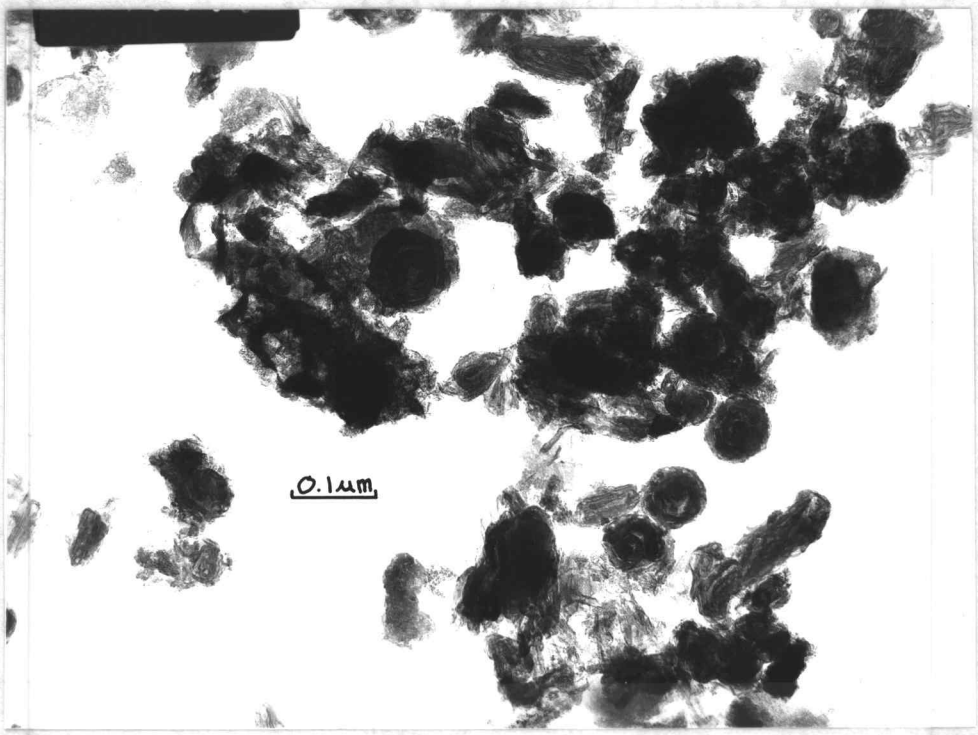

Plate 14. Electron micrograph of clay sample MFW-D-1b.

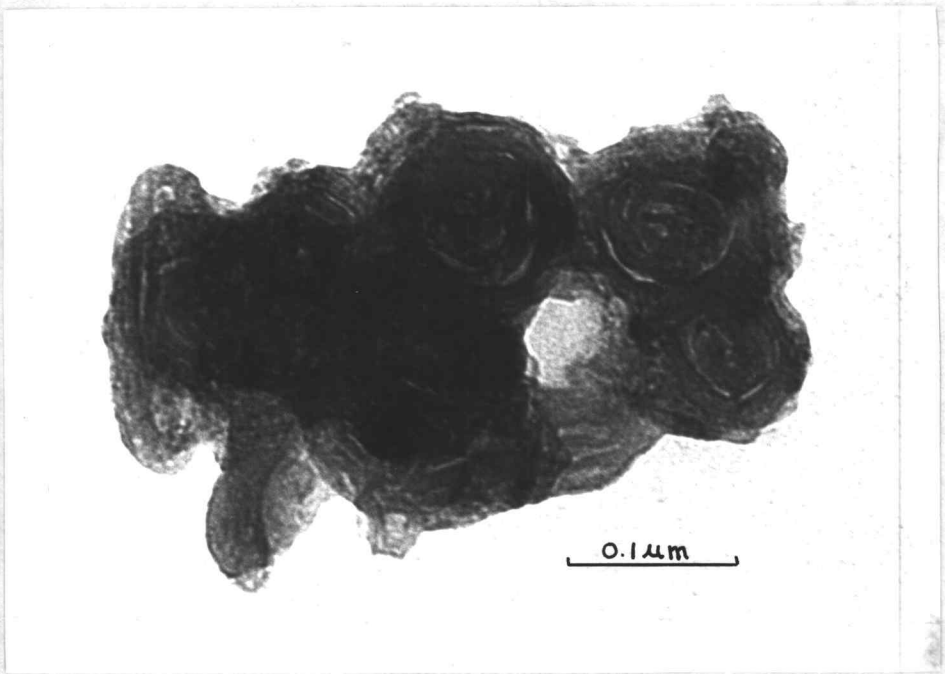

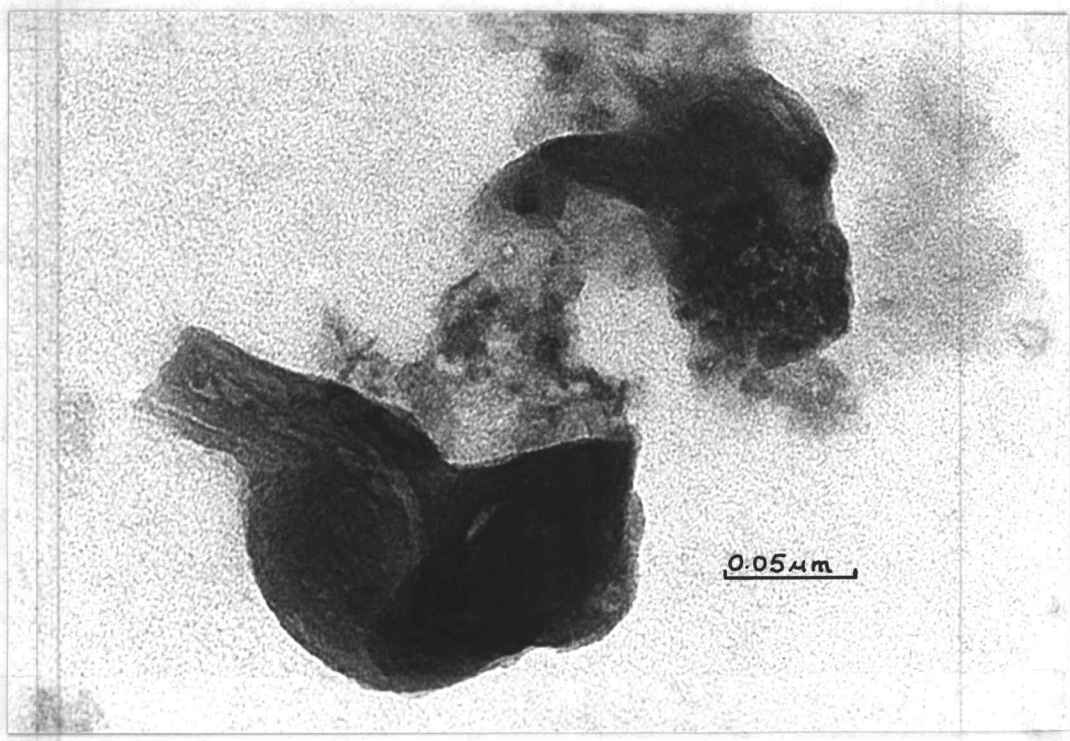

Plate 15. Electron micrographs of clay sample MFW-D-1c.

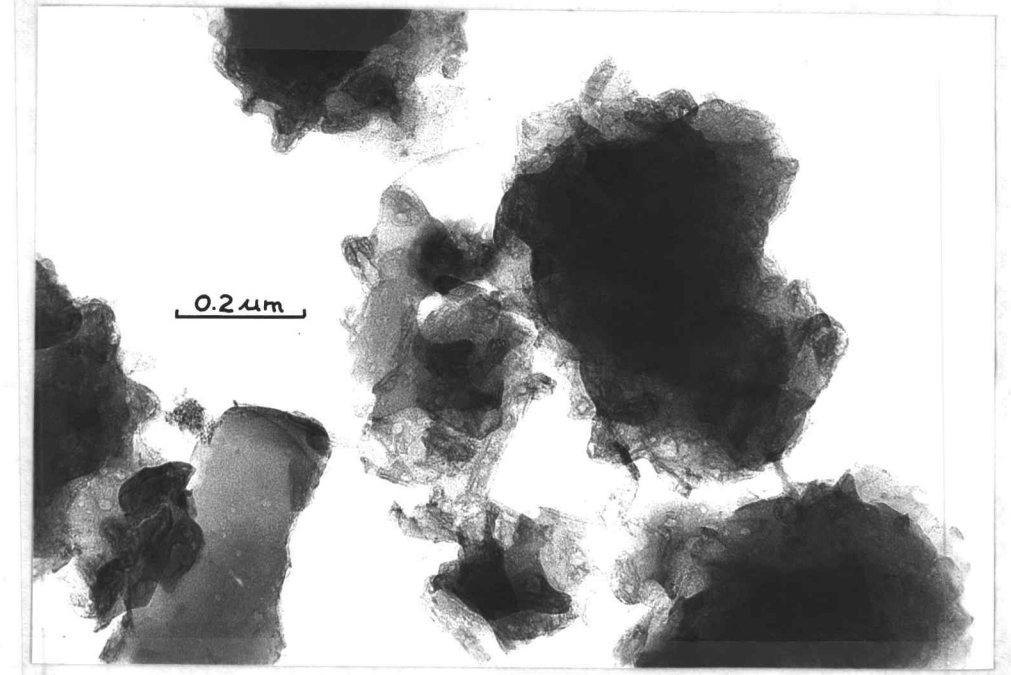

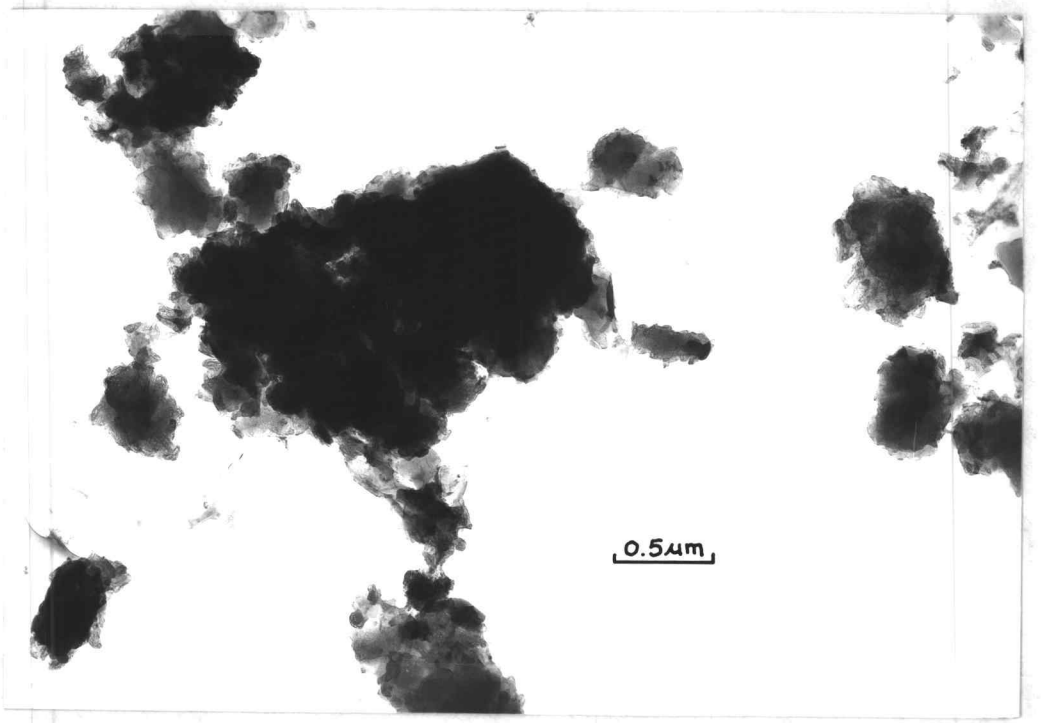

Plate 16. Electron micrographs of clay sample MS-Q-1d.

and break open in a fashion somewhat similar in appearance to that of a blooming rose, yielding the "typical" form of spheroidal halloysite most often seen in TEM. This "blooming" could conceivably occur in response to drying in the field or laboratory, or in response to the vacuum of the microscope. Further, the layers of these spheroids may be subject to peeling to form tubular halloysite as shown in Plate 12 and recently by Sudo and Yotsumoto (1977). It seems clear that the tubular halloysite may also form directly by the rolling of amorphous films in the field and occasionally in the microscope vacuum. (See Parham, 1969 for the rolling of halloysite tubes directly from plagioclase surfaces.) Further work utilizing electron diffraction in conjunction with transmission and scanning electron microscopy could lead to a more defensible model of halloysite formation and alteration.

A failure involving a planar slide with a significant rotational component in the headwall exists at the Sheep Creek bridge along Hwy. 20 at site SS-S-3. The most important components at the site are a thick deposit of basaltic colluvial soil overlying compacted glacial drift which served as the planar failure surface. Water emerges in the failure at the contact of the two deposits.

Clay samples a, c, and d (Figures 27 and 28) were collected from various depths in the left flank, and sample f (Figure 28) was collected from the glacial material at the base of the headwall. The surficial soil (sample a), which is quite dry, has little relevance to the failure itself, but helps to show a progression of mineralogy with depth. It is composed of chloritic intergrade, halloysite, amorphous material, and gibbsite. Sample c, taken from greater depth at the flank and still above the failure surface, perhaps best represents the colluvial overburden which slid; the chloritic intergrade shows some smectite character; the halloysite is strong and hydrated; the amorphous band is strong; and there is evidence of zeolite.

Sample d, which originated from very near the failure plane in the left flank, shows only a questionable trace of halloysite and no

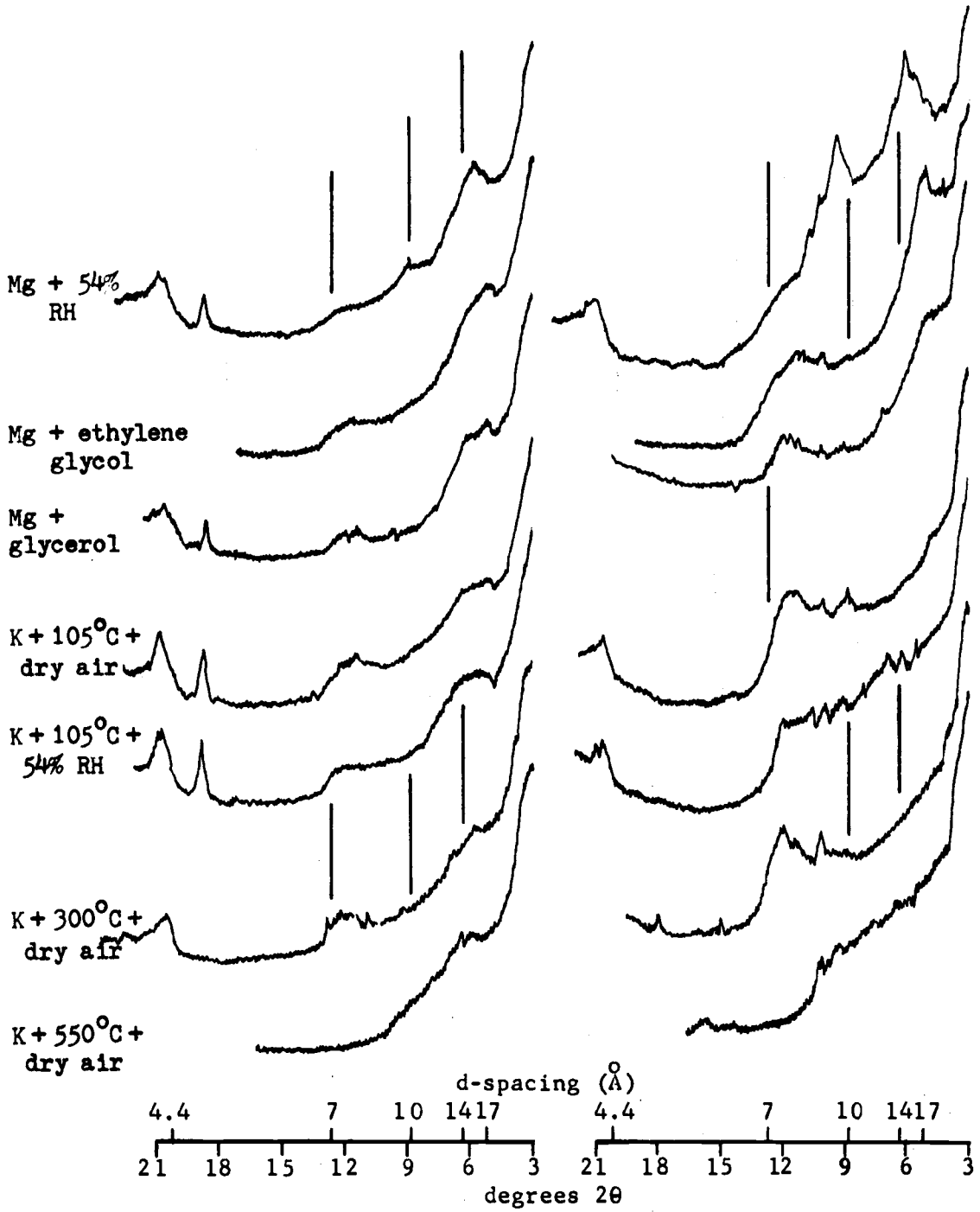

Figure 27. Site SS-S-3 XRD patterns. Sample a (left), left flank, A horizon, 10 cm depth. Sample C (right), beneath sample a, 1½ m depth.

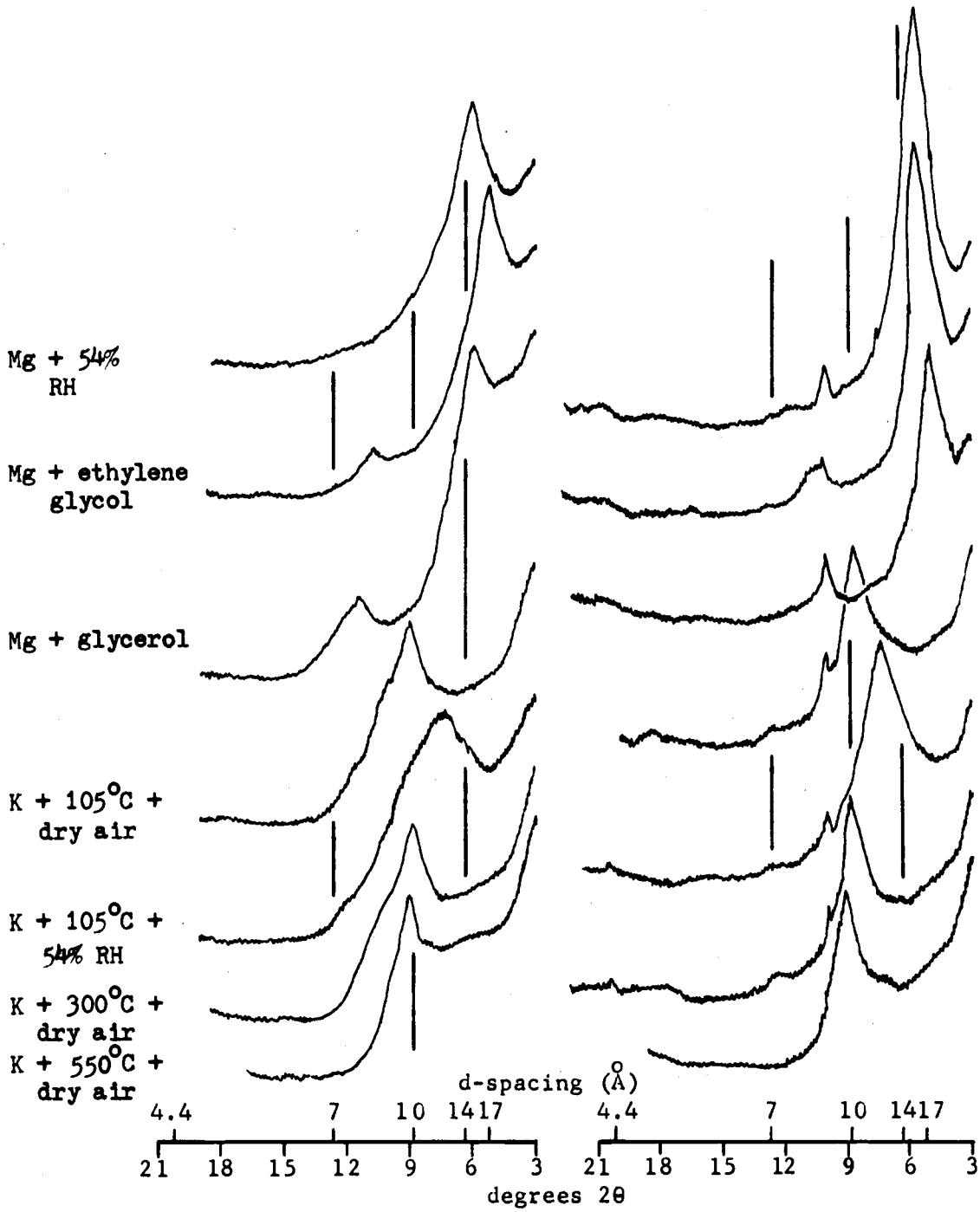

Figure 28. Site SS-S-3 XRD patterns. Sample d (left), beneath samples a and c in the left flank, 2 m depth. Sample f (right), gray glacial material of failure surface.

discernible amorphous material; however, the smectite is much stronger than in the upper zones, although it does show evidence of hydroxy interlayering. Finally, sample f, from the failure plane in the central portion of the failure, exhibits the strongest montmorillonite, with negligible evidence of hydroxy interlayering. Zeolite peaks are also evident here.

Rotational Slump

All landslide movements, including debris avalanches, have a rotational component. In the case of failures such as the debris avalanche, however, the rotational component may be ignored, as it is quite small and is apparent only in the relatively homogeneous surficial material, at the head of the failure. Landslides in homogeneous cohesive soil on the other hand occur only along failure surfaces which are relatively deep and which are concave upward. Furthermore, deep seated rotational slumps develop only in those soils which have a significant amount of cohesive clay. These phenomena are clearly explained by Carson and Kirkby (1972) and by Wu (1976).

A relatively small planar failure with progressive rotational components and a small resultant earthflow was investigated at site MFW-1. The soil profile at the failure's flank consists of a thin layer of basaltic colluvium over two to three thin layers of color-banded plastic clay above the slip surface, and mottled plastic clay beneath the slip surface. The XRD patterns of both samples show strong montmorillonite peaks, slight zeolite, weak, broad halloysite and no amorphous band (Figure 29). The halloysite is more distinctive, however, in the clay from above the failure surface than in that from below it, and the smectite may be slightly more hydroxy interlayered in the upper sample. These latter observations are similar to, but much weaker than, the relationships of halloysite above the montmorillonite failure surface in the debris flows described earlier.

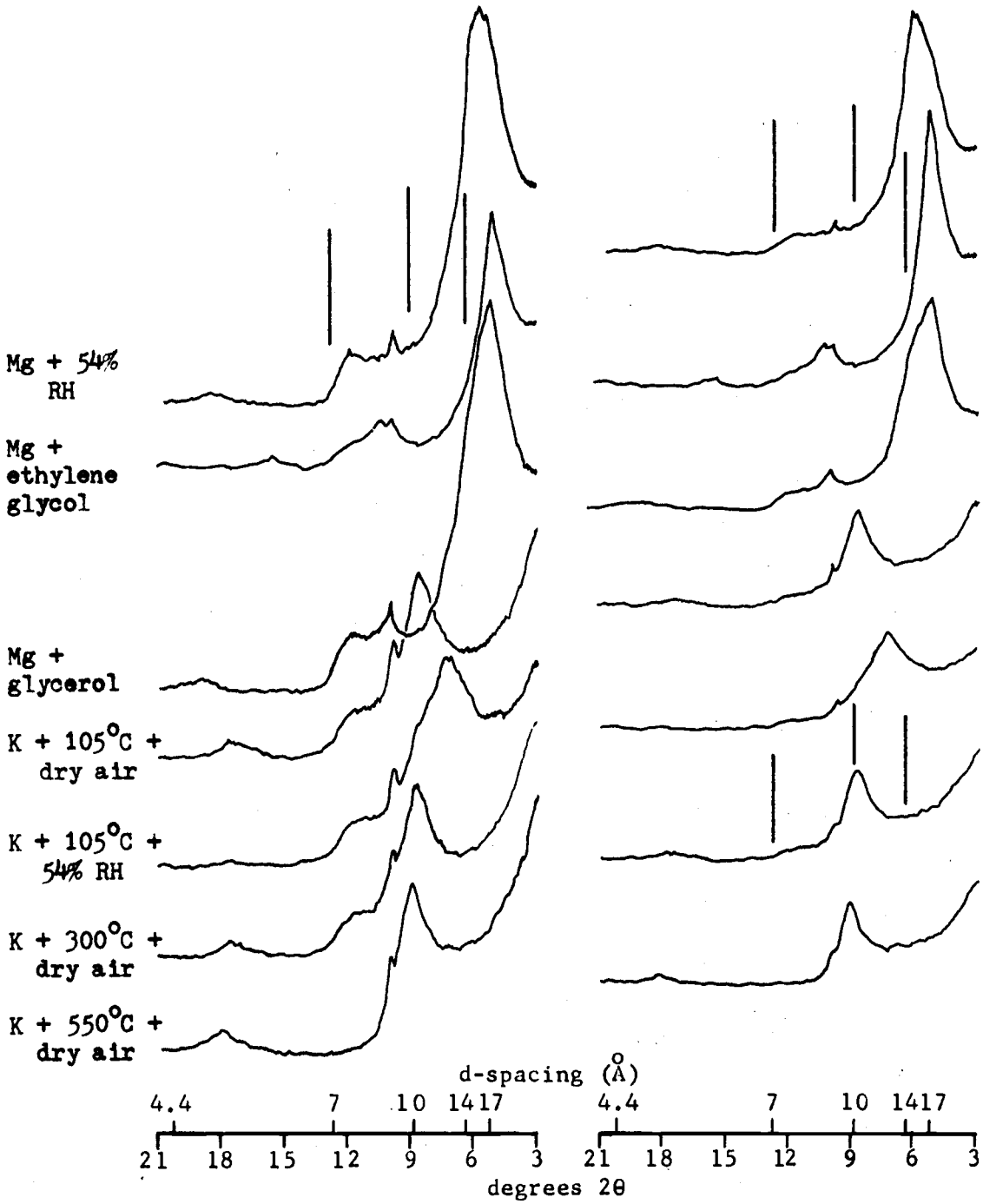

Figure 29. Site MFW-1 XRD patterns. Sample a (left), color banded clay above failure plane. Sample b (right), mottled clay beneath failure plane.

The failures at site MS-P-1, SS-SF-1, and R-CM-1, involve several processes, including deep seated rotational slumping. The major surfaces of rotational failure could not be identified at these sites due to the old age, large size and continued movement of the failures. Therefore, samples were collected from locations which, according to best judgement, were thought to duplicate the material of the failure zones.

At site MS-P-1 the clay material near the toe of the large slump unit was sampled where it had been uncovered by road construction. At site SS-SF-1 several locations were excavated and augered in order to sample clay from as near to the surface of rotational failure as possible. Site R-CM-1 was sampled at several points along the road which cut through the toe section of a large slump unit. Analyses of the clay fraction of each of these samples revealed smectite to be the strongest component of the XRD patterns (Figures 14, 20, 19, and Appendix III). It was therefore, inferred that smectite, and montmorillonite in particular, is the principal clay mineral involved in the deep failures of these sites.

Additional evidence of the importance of smectite to rotational failures is given by site MS-2 (Figure 16, right), the sample of which was taken from one of several rotational slump blocks in the Middle Santiam drainage. The XRD patterns of this sample are virtually identical to those of the clay in the large scarp at the head of Donaca Creek, across the drainage (site MS-D-1, Appendices II and III).

As discussed previously, the failure at site MK-D-1 consists of a well defined rotational slump block supporting soil derived from colluvium and volcanic ash, which is prone to debris flow failure. Again, due to limitations imposed by sampling techniques, it was not possible to sample the lower, rotational surface of rupture; however, an investigation of the lowest part of a lateral wall of the failure revealed very plastic smectite clay.

A small, fresh, well defined rotational failure surface in highly weathered greenish breccia in a road cut at site MS-B-1 was

sampled at two positions, both of which contained strong smectite in the clay fractions (Figure 30). The X-ray patterns of these samples also show an amorphous component and halloysite in various states of hydration, as indicated in the Mg-saturated treatment by the broad shoulder in the vicinity of 10 Å on the 15 Å peak, and by broad 7.5-8 Å peaks of the K-saturated heat treatments. It is very likely that the latter minerals are illuvial at these positions, as the weathered pyroclastic material is overlain by a shallow deposit of weathered basaltic colluvium. The deeper of the two samples (b) was taken from beneath the failure plane and shows a sharp zeolite peak at approximately 9 Å.

A third sample c was taken from deeper in the road cut, well below the plane of the small failure mentioned above. The patterns show very strong montmorillonite with some hydroxy interlayering, amorphous material, and perhaps a trace of halloysite (Figure 31). The small road cut slump occurs within a much larger slump block, with which this well developed montmorillonite is assumed to be involved.

A large, well defined rotational slump at site MS-H-1, which is very near site MS-B-1, was randomly sampled in a road bank which cuts through the slump block. Again, the materials are of pyroclastic origin and the clay fraction is nearly pure montmorillonite (Figures 31 and 34). The clay fraction of another small, distinct rotational surface of failure, site MFW-H-1, shows strong montmorillonite, kaolinite and some mica (Figure 32, sample a). The failure represented by this sample occurred at the top of a flank of a much larger, complex slump-earthflow. Additionally, the patterns of a random sample from the central portion of the earthflow, about 100 m downslope from the small failure show strong montmorillonite (Figure 32, sample b).

Finally, a large, distinct slump-earthflow failure is represented by the infamous Canyonville slide, site SU-C-1. The failure occurred entirely within a deep soil deposit overlying hard serpentine bedrock. XRD patterns of samples from five locations

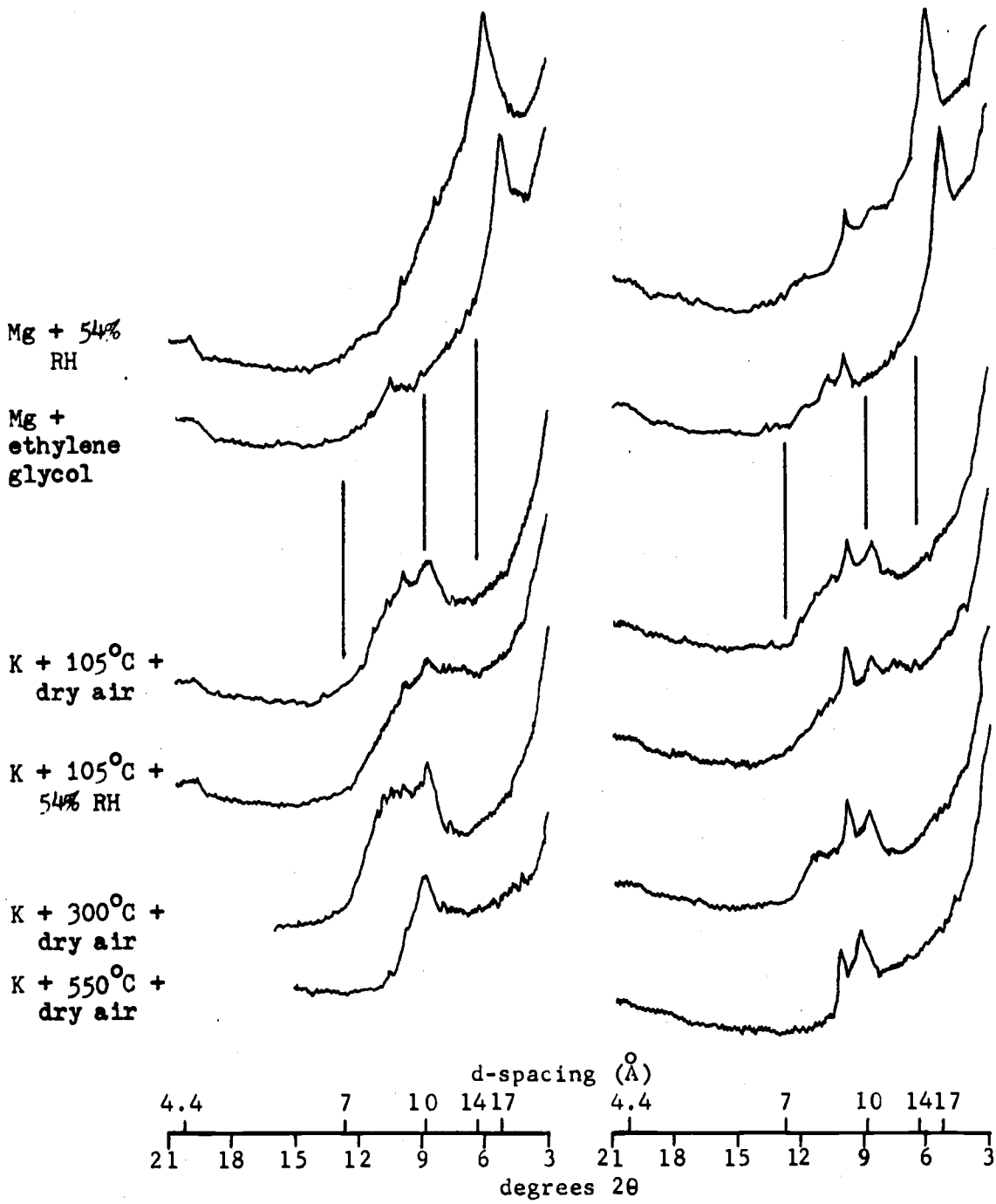

Figure 30. Site MS-B-1 XRD patterns. Sample a (left), failed material at failure surface. Sample b (right), beneath failure surface.

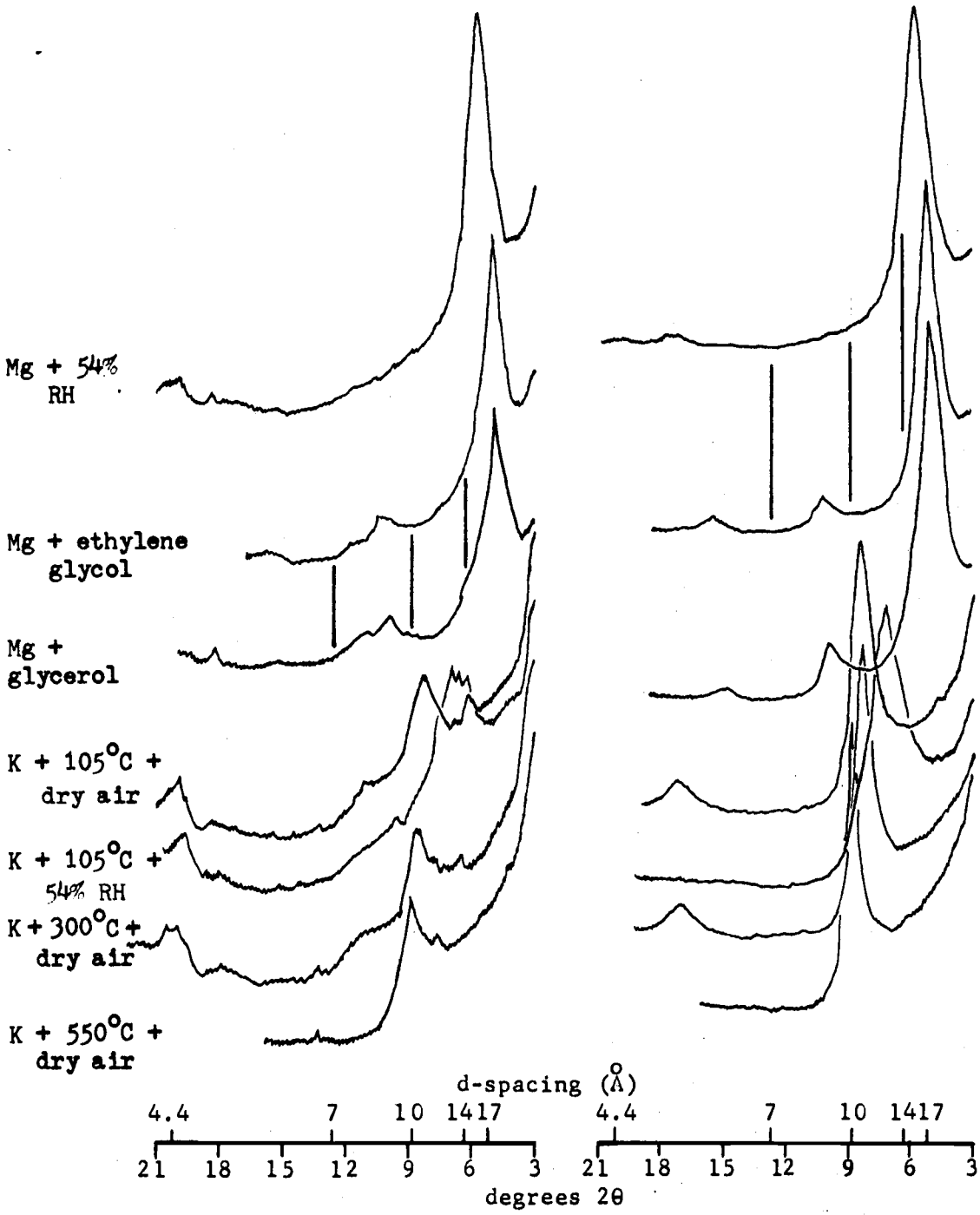

Figure 31. XRD paterns of clay from six meters depth, below the surface of rupture site MS-B-1c (left), and of random sample of slump block site MS-H-1b (right).

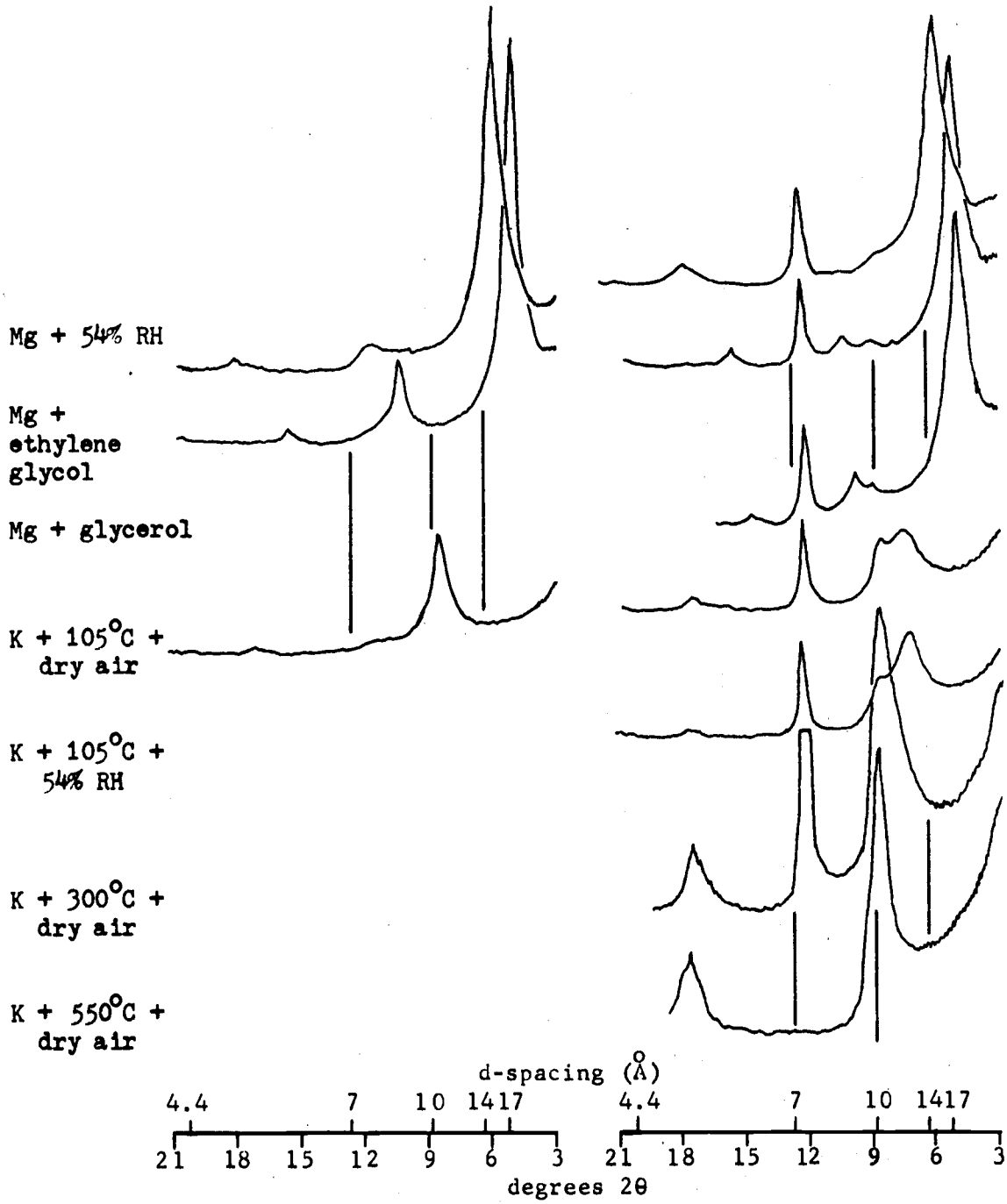

Figure 32. Site MFW-H-1 XRD patterns. Sample b (left), central portion of earthflow, 1 m depth. Sample a (right), flank of small rotational slump.

within the failure (headwall scarp, left and right flanks, central terrace, and toe) revealed the clay mineralogy to be relatively homogeneous throughout. Dehydrated halloysite is indicated in the XRD patterns (Figure 33) by the somewhat broad 7.3 Å peaks which disappear with heating at 550°C, and in the DTA pattern (Figure 34) by the two distinctive endotherms and exotherm. Chloritic intergrade and mica are also present.

The identity of the expandable 2:1 component is uncertain: its constant 14.3 Å spacing with Mg-saturation and organic solvations, and collapse to a constant 10 Å spacing with K-saturation and heating is suggestive of vermiculite; however, its plastic nature and apparent high shrink-swell capacity in the field suggest smectite. The DTA pattern gives no indication of vermiculite, but it does show a dehydration endotherm at 180°C in addition to the one for halloysite, and a small exotherm at 370°C which could be due to iron oxidation. The reddish yellow color of the soil in the field also suggests the presence of iron. It is possible for nontronite, an iron-rich smectite, to be confused with vermiculite in XRD given the characterization treatments used. Furthermore, although nontronite cannot be identified in the DTA pattern, it could nonetheless be present, with its intermediate temperature endotherm and high temperature exotherm masked by those of halloysite. Thus, on the basis of the evidence and the realization that there is a good possibility for its existance in the site locale, the mineral is inferred to be nontronite.

Earthflows

Rotational slumps frequently initiate earthflow movements, which are translational downslope "flow(s) of slow to very rapid velocity involving mostly plastic or fine-grained nonplastic material" (Varnes, 1958). They move over a discrete basal shear surface which is approximately parallel with the ground surface, and with increasing fluidity they grade into mudflows or debris flows

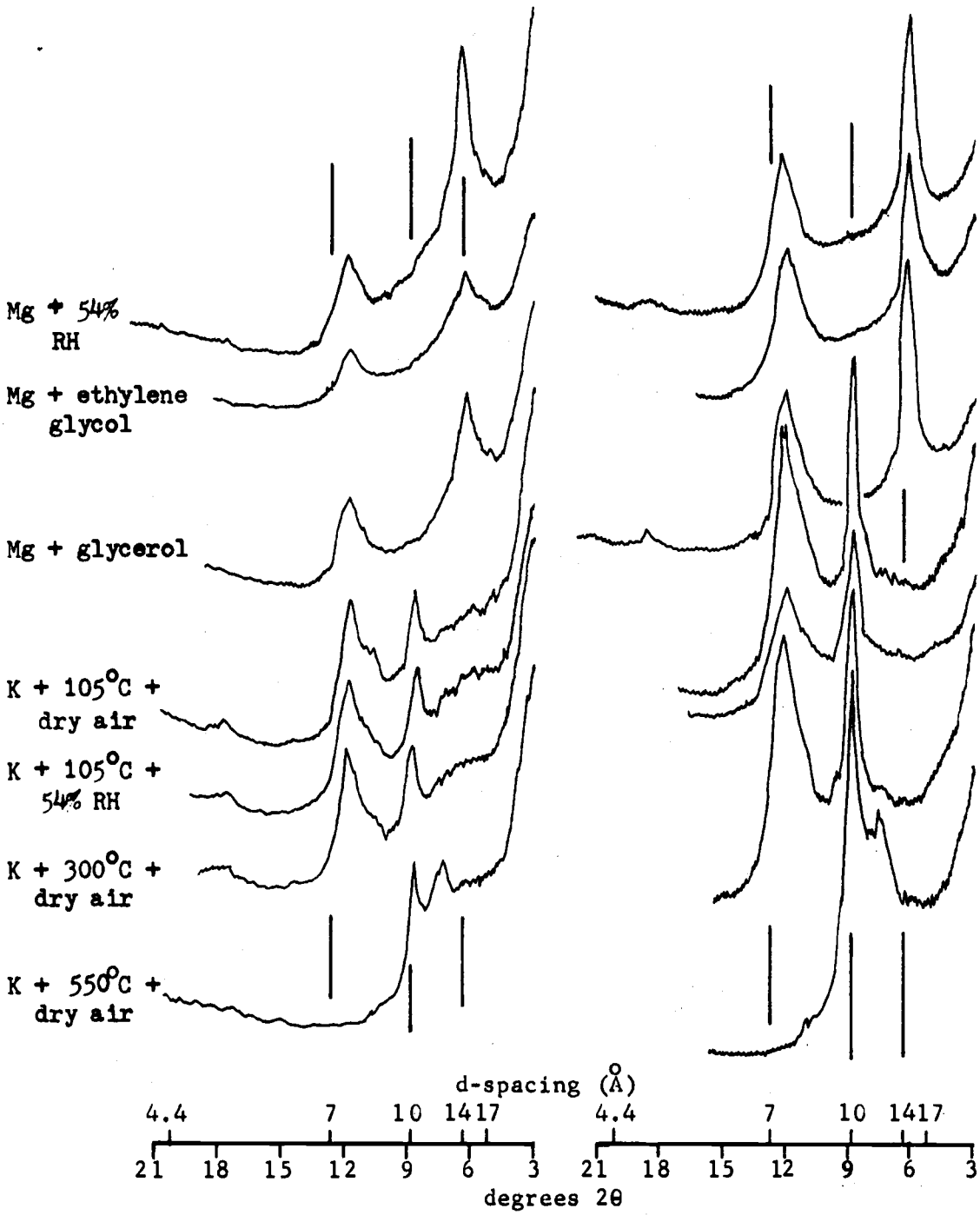

Figure 33. Site SU-C-1 XRD patterns. Sample c (left), right scarp wall, 2 m from original surface. Sample d (right), slump bench just above toe of failure.

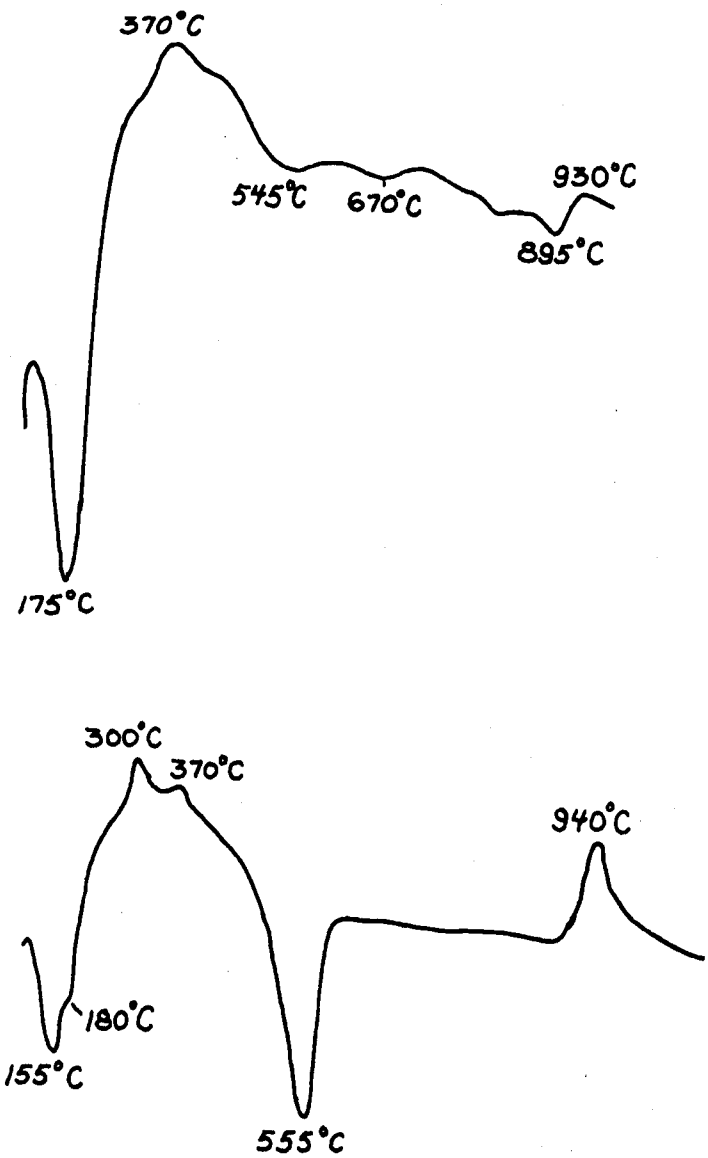

Figure 34. DTA patterns of samples MS-H-1b and SU-C-1b.

(American Geological Institute, 1972). Earthflows have been further described as "slow moving, deep seated, poorly drained features" which typically involve "deep, cohesive soils and clay-rich bedrock" (Swanston and Swanson, 1976). Hence, an arbitrarily chosen thin line often separates the earthflow process from those of debris flow and even deep seated soil creep.

For purposes here, earthflow landforms are identified by wet soils, large size (several hectares to several square kilometers in area), considerable depth (several meters), slow rate of movement (a few centimeters per year), low slope gradient (less than about 30%), old age (thousands of years?), and a number of distinctive features, including: tension cracks, pressure ridges, hummocky topography, displaced roads and stream channels, and jackstrawed trees.

The terms "plastic" and "cohesive", which are frequently used in discussions of earthflow materials, imply a dominance of smectite clays. However, of the four earthflows investigated in the Western Cascades, smectite was only occasionally observed. The clay samples of three of the earthflows contained significant amorphous components in the form of gel, imogolite strands, glass shards, and opal phytoliths. Kaolin (usually identified as halloysite) and chloritic intergrade also were commonly present. (Similar findings were made in an earthflow near the eastern edge of the Coast Range, discussed in Appendix I).

The XRD patterns of the clay fractions of two samples taken from near the surface of the earthflow on Quartzville Creek were presented in Figure 25 (site MS-Q-1). These samples, which originated from a debris flow failure within the larger earthflow, contained very strong evidence of hydrated halloysite and amorphous material. An additional shallow sample (not shown) taken from the base of the debris flow also contained strong hydrated halloysite and amorphous material and gave a pattern nearly identical to that of sample d.

The rates of movement of the three other earthflows sampled in the Western Cascades have been reported by Swanston and Swanson (1976). Lookout Creek (sites MK-L-2 and MK-L-3), Boone Creek (site SFMK-B-1), and Landes Creek (site MFW-L-1) earthflows have been moving at the rates of 7, 25, and 12 cm/yr, respectively.

Three samples collected from two areas within the Lookout Creek earthflow (sites MK-L-2 and MK-L-3) gave surprisingly similar XRD patterns (Figure 35 and Appendix III). These patterns show the major constituents to be amorphous material, halloysite with a range of hydration, and chloritic intergrade. The electron micrograph (Plate 17) also shows these components. The samples of Figure 35 were taken some distance apart at depths of up to three meters in wet soil with a very high content of basaltic colluvium. Field characteristics of additional soils at various locations in the earthflow were investigated and found to be very similar to those collected. The earthflow runs into Lookout Creek, which continually carries away soil from the tip of the lobe as it sloughs into the creek. A cursory examination of the soil on the opposite side of the creek suggested the presence of smectite clay, which in turn leads one to speculate that deeper sampling of the earthflow might reveal a smectite surface on which the flow is moving.

The Boone Creek earthflow (site SFMK-B-1) contains a mixture of lithic components consisting of colluvial cobbles of basaltic rock and weathered rhyolitic (?) porphyry generally overlying--but also well mixed with--greenish tuff breccia. Much of the soil of the earthflow has field characteristics which make it similar to the soil at Lookout Creek; however, there is greater color variation in the Boone Creek soil.

XRD patterns of five samples taken from a single location in the earthflow are given in Figures 36 and 37. Samples b, d, and c are subsamples of various colored materials collected within a few centimeters of each other. All samples display somewhat similar mineralogy, with the major components being amorphous material, halloysite and chloritic intergrade; however, for some unexplained

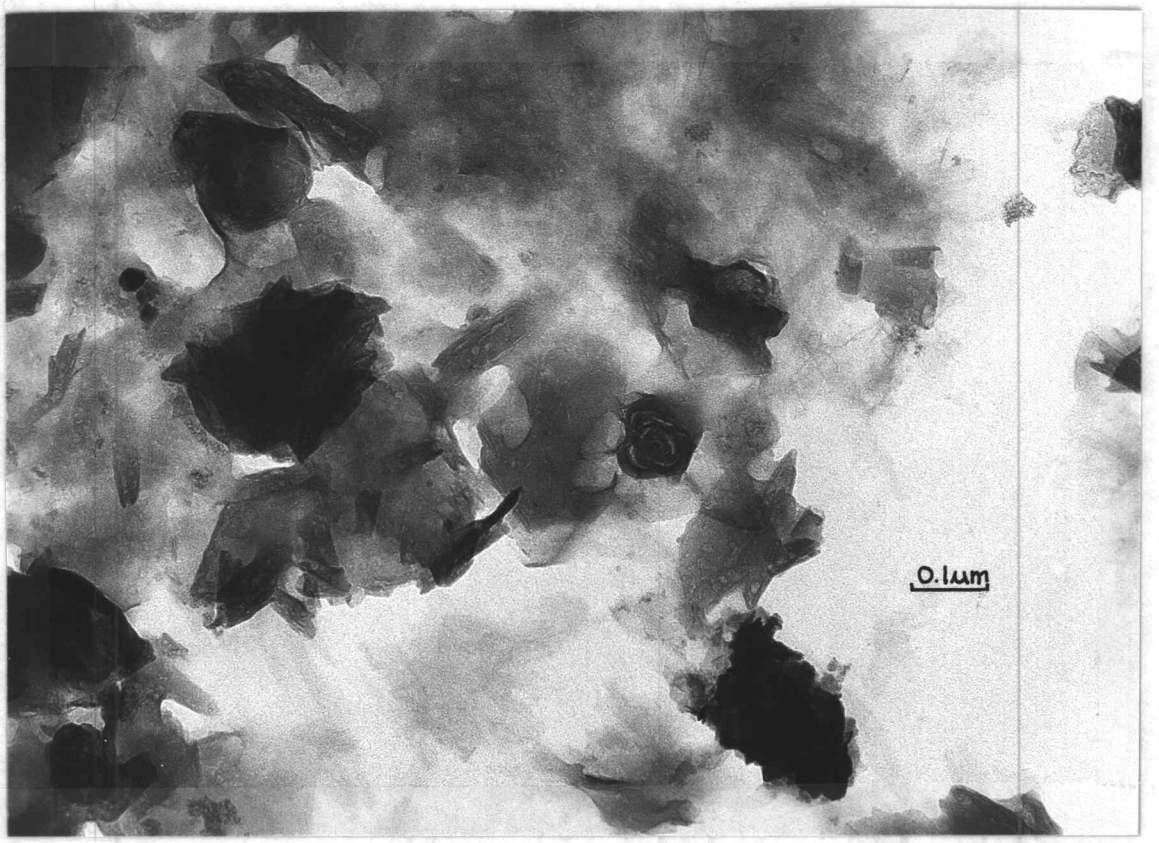

Plate 17. Electron micrograph of clay from site MK-L-3.

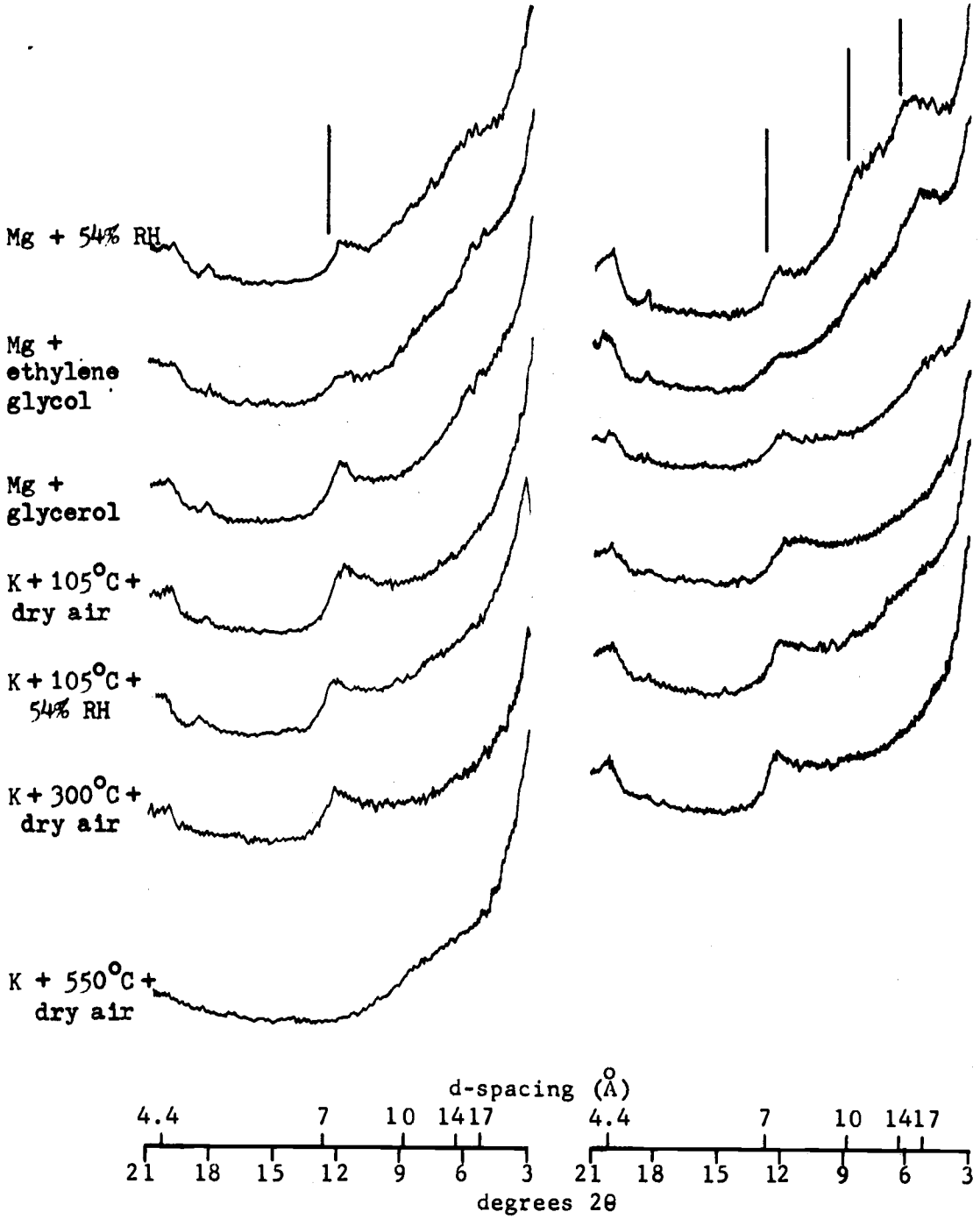

Figure 35. Sites MK-L-2b and MK-L-3 XRD patterns. Sample 2b (left), central retion of earthflow, 2 m depth. Sample 3 (right), toe of earthflow 3 m depth.

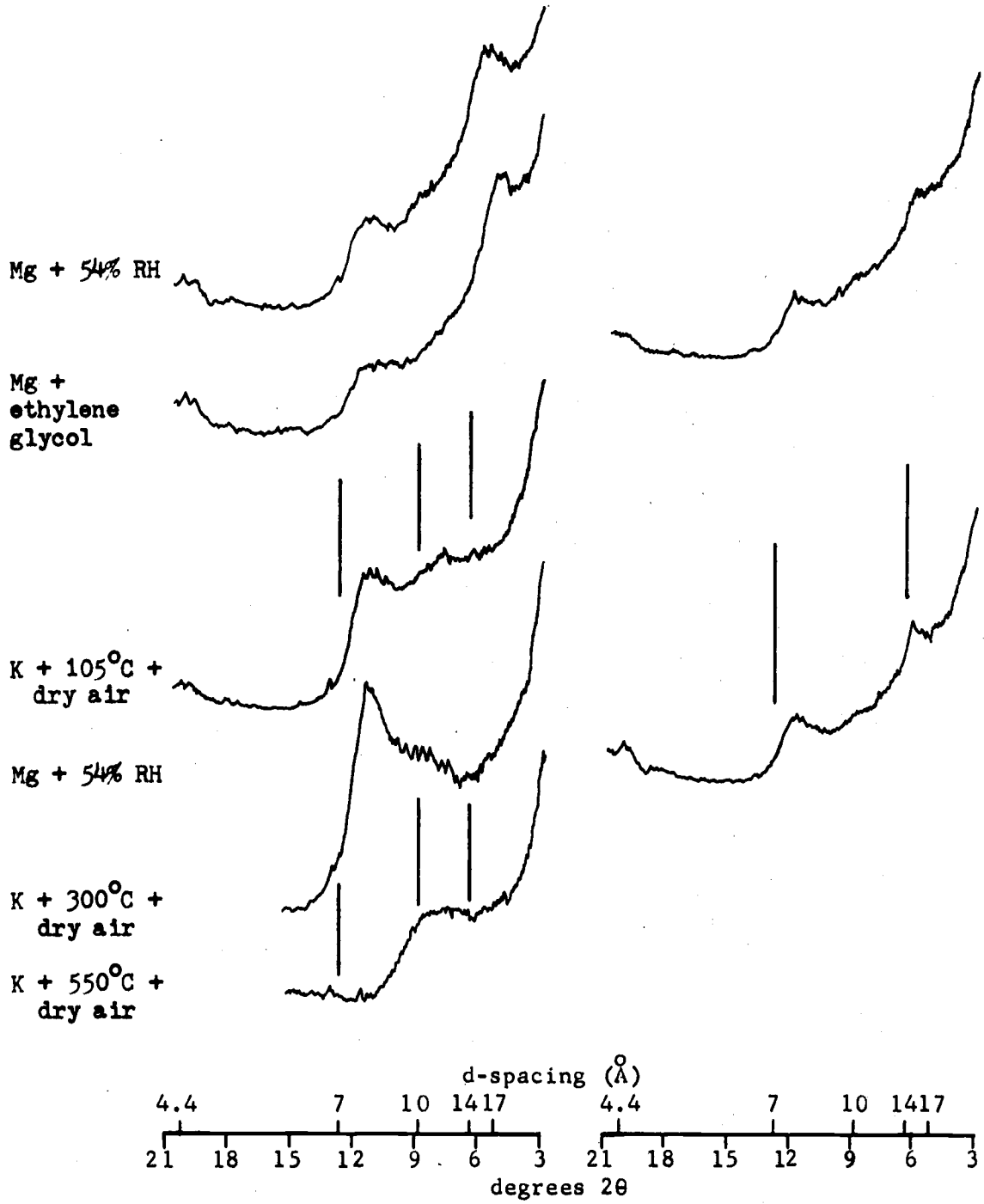

Figure 36. Site SFMK-B-1 XRD patterns. Sample b (left), gray subsample 1½ m depth. Sample a (right, top), homogeneous zone, 1 m depth. Sample d (right, bottom), maroon subsample 1½ m depth (Mg + 54% RH).

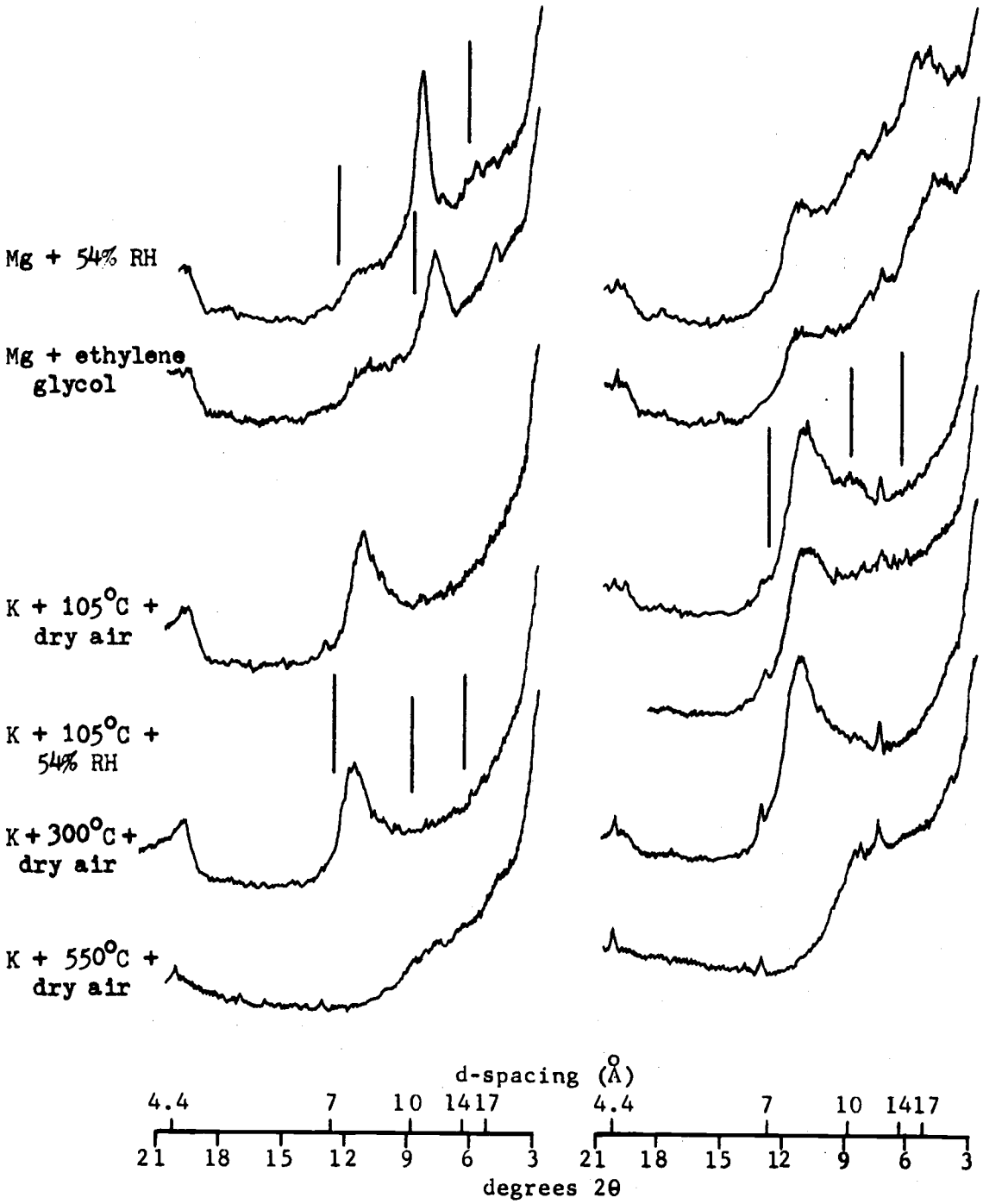

Figure 37. Site SFMK-B-1 XRD patterns. Sample c (left), reddish subsample, 1½ m depth. Sample e (right), 2 m depth.

reason the peak of the hydrated halloysite of the reddish subsample c is much sharper and stronger than those of any of the other samples. Based on field observations, sample e probably best represents the material of the earthflow in general. It is notable that, as in the Lookout Creek earthflow, there is little indication of well developed smectite in the moving material at this site.

The two clay samples from the Landes Creek earthflow have contrasting mineralogy (Figure 38). Sample a, from the central portion of the earthflow, contains amorphous material, halloysite and chloritic intergrade, as do the samples at Lookout and Boone Creeks. In addition, there are strong indications of hydroxy interlayered smectite. Sample b was taken from the top of a pressure ridge, the soil of which is considerably wetter than that of sample a. The ridge consists of highly weathered greenish breccia with some basaltic cobbles and lahar (?) rock. The soil's clay fraction is strikingly different from that of sample a in that it is composed largely of smectite, which may be either beidellite or hydroxy interlayered montmorillonite. The XRD patterns show no amorphous band, but they do show distinct, although weak, kaolin peaks and zeolite.

The relative positions on the landscape of the different materials of samples a and b, and the topographic features of the area suggest that the earthflow may be two-tiered--with an upper tier of amorphous material, halloysite and hydroxy interlayered smectite moving over a deeper tier consisting largely of smectite which is also moving and subject to buckling. It is notable in this regard that the pressure ridges at Landes Creek are the best developed of any of the earthflows investigated.

Creep

Soil creep in the deep seated, rheological sense refers to a time-dependent downslope deformation of the soil mantle under gravitational shearing stress. The rate of movement, which is controlled by the soil's viscous resistance, increases with plasticity, activity

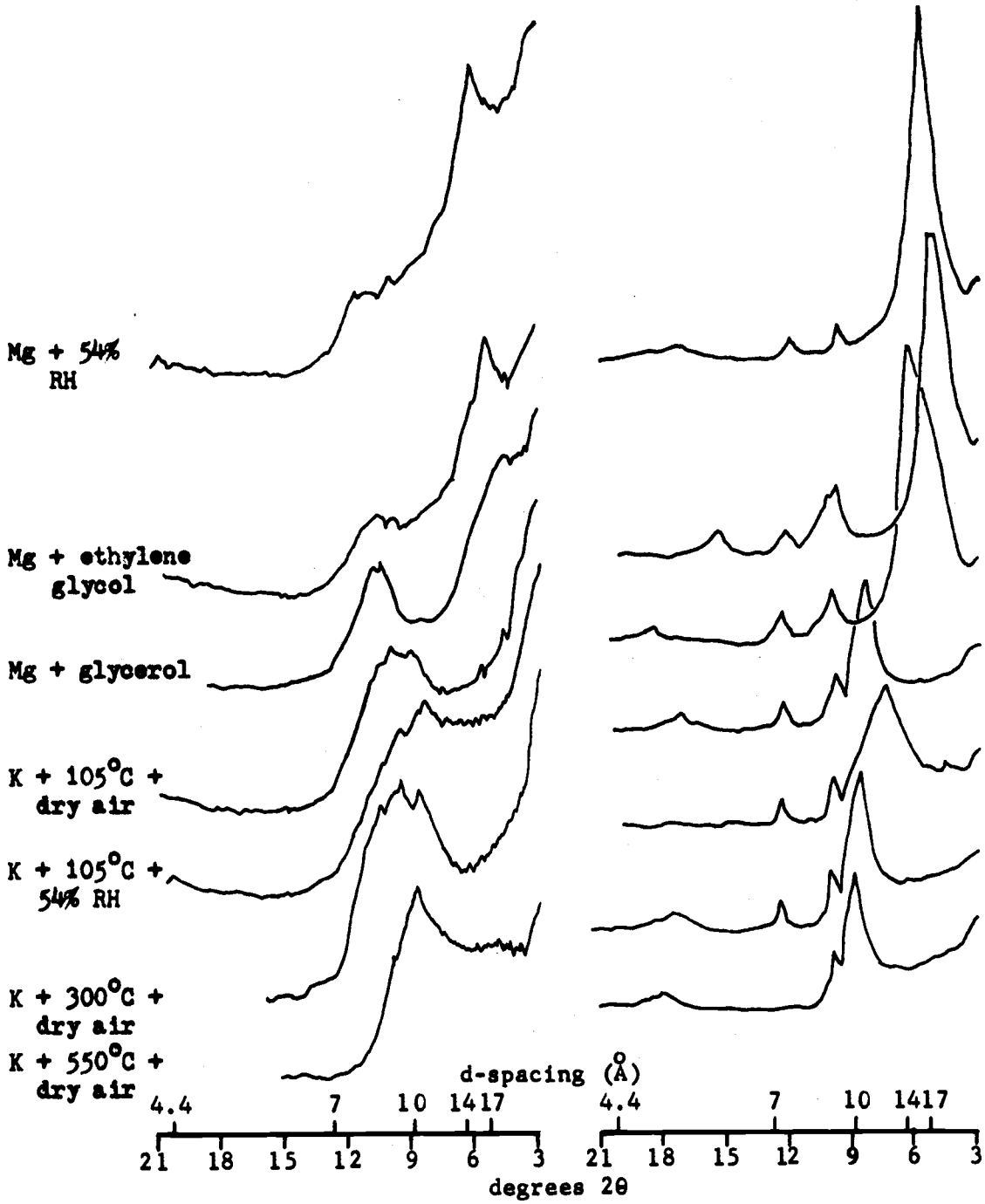

Figure 38. Site MFW-L-1 XRD patterns. Sample a (left), upper central portion of earthflow. Sample b (right), pressure ridge, 1 m depth.

and water content of the soil. Thus, creep movement is controlled to a great extent by the nature of the clay fraction (Mitchell, 1976).

The creep process causes a significant reduction in the shear strength of the soil; thereby making it more susceptible to failure by landslide processes. For this reason, rotational slumps are nearly always associated with creep to some degree. Furthermore, large earthflows are subject to creep, thus making it virtually impossible to distinguish slow flow from creep in many cases. In these cases, however, there is little point in trying to distinquish the two processes.

Several of the sites already discussed are undergoing deep soil creep. The most notable of these include sites MS-2 and MFW-L-1. The clay fractions of both of these sites consist primarily of well crystallized smectite (Figures 16 and 38).

Soil creep in the Western Cascades is most distinguishable in those regions where the landscapes have relatively little basaltic colluvium and volcanic ash, but which consist primarily of rock materials such as greenish breccia which have weathered to cohesive, smectite clays. Site SU-J-1, in the South Umpqua drainage, is a good example of this situation: the land surface here has the characteristic rumpled appearance; small rotational cutbank failures are common; trees exhibit considerable sweep; and the soil is high in saturated, very plastic clay. Two clay samples from this site are nearly pure montmorillonite except for slight evidence of zeolite and a poorly defined kaolin component (Figure 39). The field characteristics of the two are nearly identical except that sample a is somewhat drier and less mottled than sample b.

Stable

The most unstable soils in the Western Cascades lie between about 450 and 100 meters elevation, which roughly corresponds to the exposed distribution of pyroclastic tuffs and breccias, especially those of the Little Butte Volcanic Series (Peck et al., 1964). This

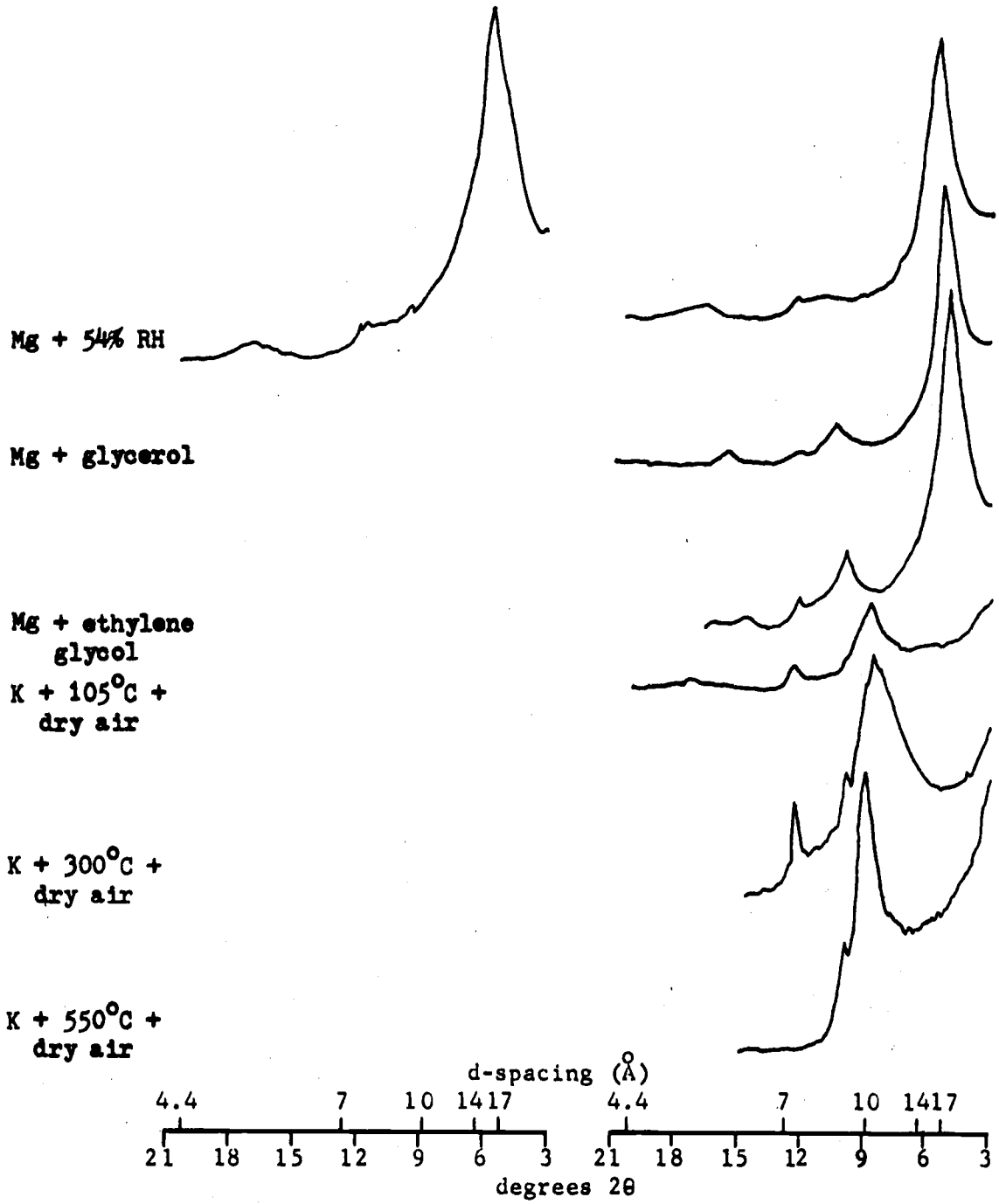

Figure 39. XRD patterns of smectite involved in deep seated soil creep, samples SU-J-1a and SU-J-1b.

observation is supported by the elevational distribution of the sampling sites, most of which lie between 400 and 1200 meters. Similar observations have been made by Dyrness (1967) and Swanson and James (1975).

A relatively small proportion of the Western Cascades can be considered as stable. Most of this land is above about 100 meters elevation. The higher elevation land is generally more stable because of greater bedrock control exerted by competent lava flow rock, and because of less advanced weathering, which maintains shallow soils with a very poorly developed clay fraction. These soils are generally drier and more permeable than the lower elevation soils, and they would be expected to have greater strength due to greater frictional resistance and better interlocking of soil grains.

The meager clay fractions of these sites give XRD patterns which are primarily amorphous bands, with a hint of chloritic intergrade, as noted in samples from sites MK-F-1 and MK-L-1 (Figure 40); the presence of gibbsite is also weakly indicated in MK-F-1. (Site MK-L-1 is located in the Lookout Creek drainage upslope from the earthflow reported in the previous section.) DTA patterns show similar components (Figure 41), as does electron microscopy (Plate 18).

Sample c of site NFMFW-C-1 was collected from relatively dry, shallow, coarse textured, stable soil at 1500 m elevation. The XRD patterns show strong, sharp gibbsite peaks, a significant amorphous band, and small indications of halloysite, chloritic intergrade and feldspar (Figure 42). Although this soil is generally stable it is subject to failure under conditions of a localized buildup of pore water pressures as occurred at the adjacent sample location, NFMFW-C-1a. Here, a spring emerging from a bedrock fissure just above the road cut caused a small planar failure of the soil over the surface of decomposing rhyodacite (?) porphyry.

A stable, relatively dry poorly developed soil at a lower elevation is represented by sample MS-P-1g. As mentioned previously,

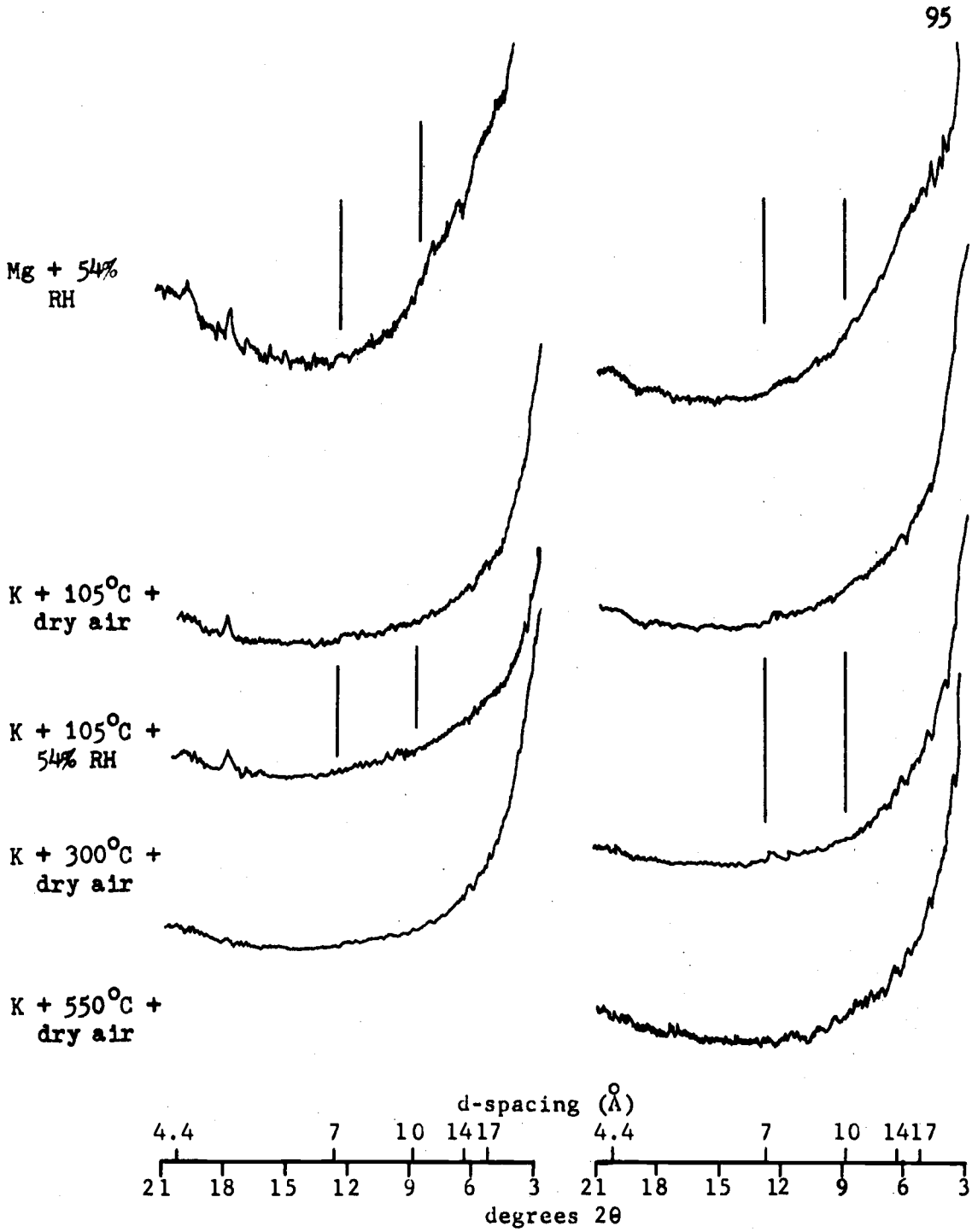

Figure 40. XRD patterns of coarse textured, stable soils MK-F-1 (left) and MK-L-1 (right).

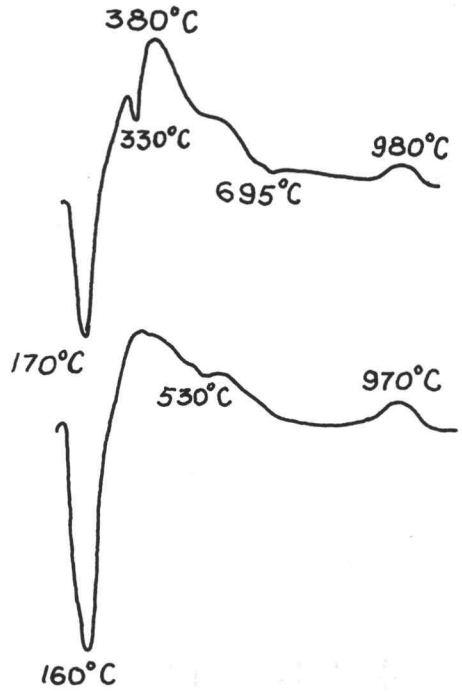

Figure 41. DTA patterns of clay from stable sites MK-F-1 and MK-L-1.

Plate 18. Electron micrograph of devitrified glass and other components, site MK-F-1.

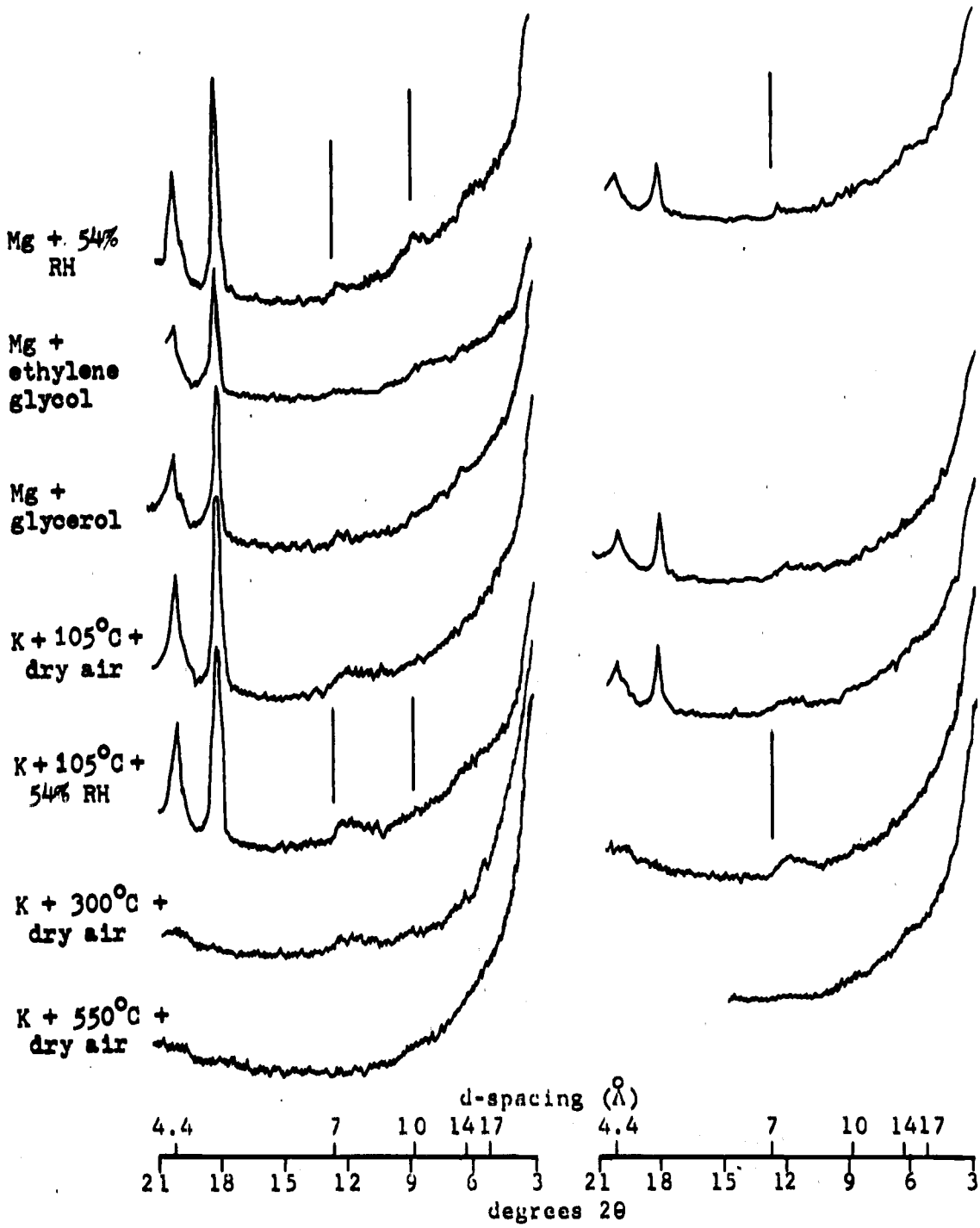

Figure 42. XRD patterns of clay fraction of shallow, stable soil at site NFMFW-C-1c (left) and adjacent failed soil at point of emerging water, NFMFW-C-1a (right).

this sample consists of chloritic intergrade, amorphous material and zeolite (Figure 15).

Other sites are unstable with respect to one type of mass movement but stable with respect to another. The best examples of this are the debris avalanche sites, which fail at relatively shallow discontinuities, but which are often stable at greater depths. Site R-SP-2 is near debris avalanche site R-SP-1 and has similar mineralogy, but is of gentler slope, and therefore more stable. The clay of these two sites contains chloritic intergrade and strong, sharp kaolinite (Figures 43 and 45).

Other examples involve the relatively shallow soils from the lower end of the Soda Fork drainage of the South Santiam. Site SS-SF-6 has suffered considerable abuse from improper timber harvesting and its related activities. The site has experienced a debris torrent and several small road related debris avalanches; nonetheless, it remains more stable than most of the sites investigated further up the drainage. The XRD patterns of the clay fraction of soil involved in the debris torrent indicate chloritic intergrade with some smectite character, halloysite, amorphous material, gibbsite, and kaolinite which is probably forming by alteration of the halloysite (Figure 44). The significant point here is that although the site contains clays that are normally associated with instability, it also contains clays which are more likely to be found on stable sites--namely, sharp 7 Å kaolinite, and halloysite that is largely dehydrated.

A site with still greater stability can be found down the drainage a short distance at site SS-SF-7. The clay fraction (Figures 44 and 45) is somewhat similar to that of site SS-SF-6 except that the chloritic intergrade has little if any smectitic character, and the kaolinite appears better developed. Electron micrographs (Plate 19) show tubular halloysite particles coalesced with amorphous material to form the beginnings of plate-like particles. The amorphous films appear to be generally thicker and stronger than those noted at previous, unstable, sites. The arrangement of tubular halloysite surrounding the amorphous material was noted frequently

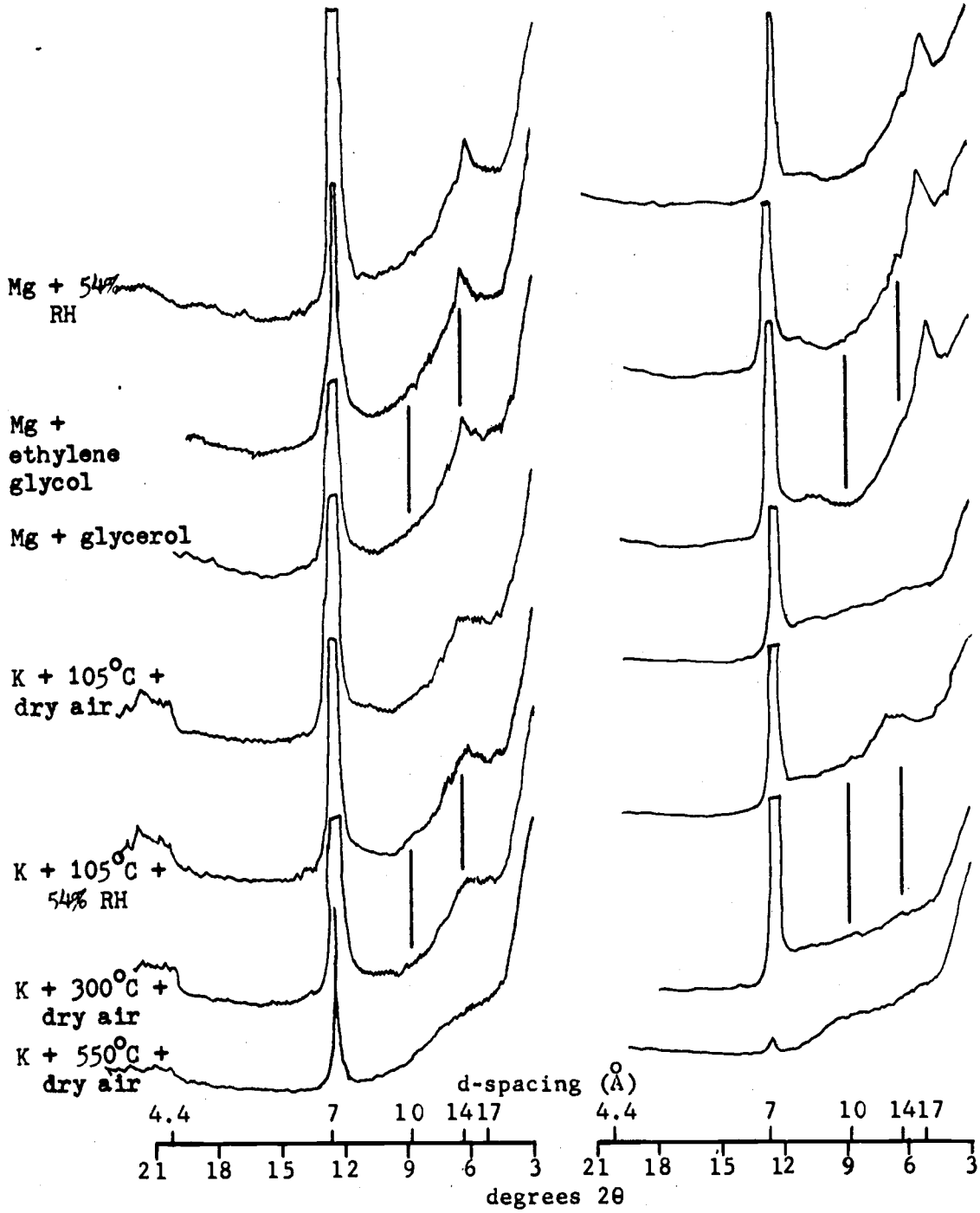

Figure 43. XRD patterns of clay of sites R-SP-2 (left) and R-SP-1 (right).

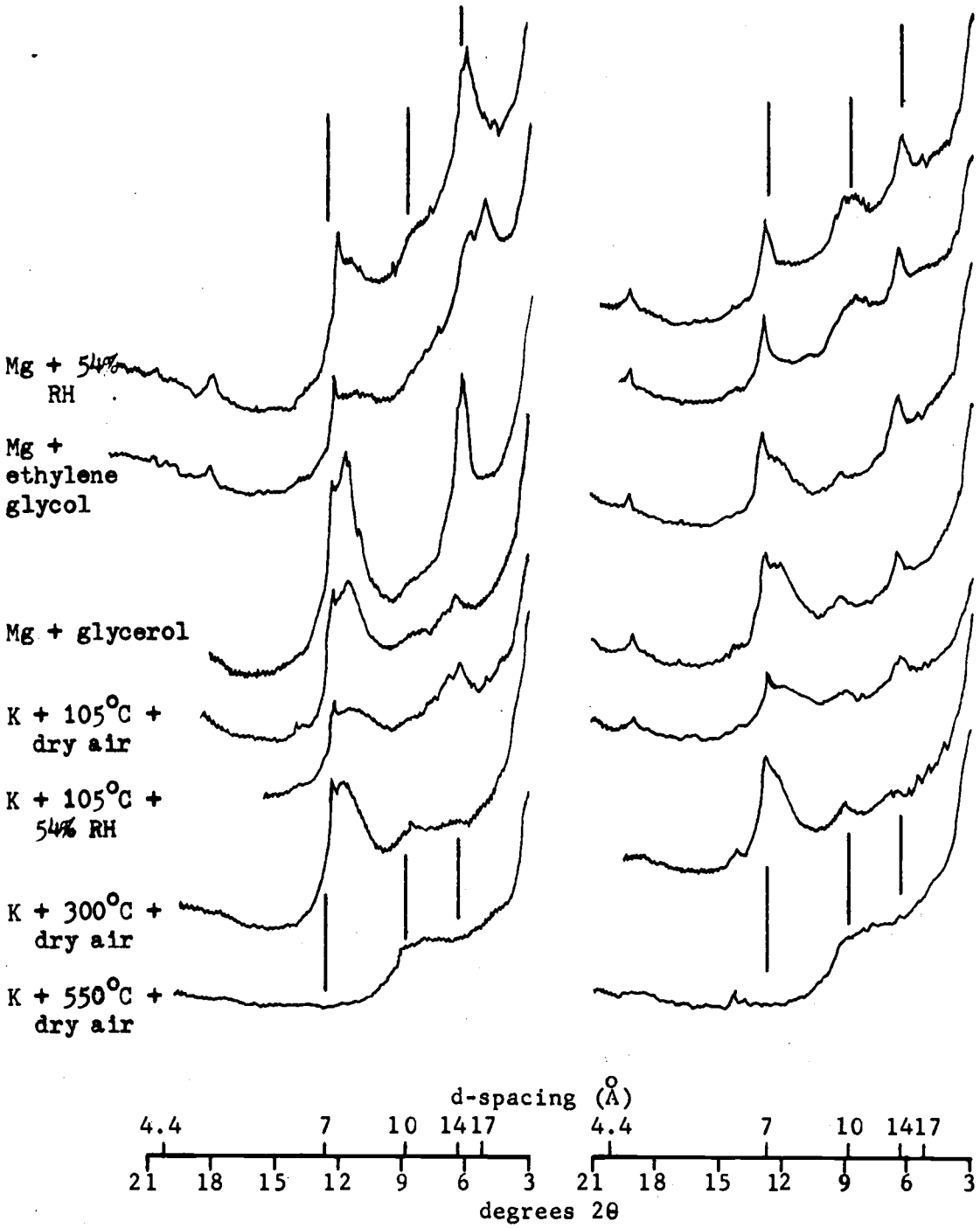

Figure 44. XRD patterns of clay from the relatively stable site SS-SF-6 (left) and the slightly more stable site SS-SF-7 (right).

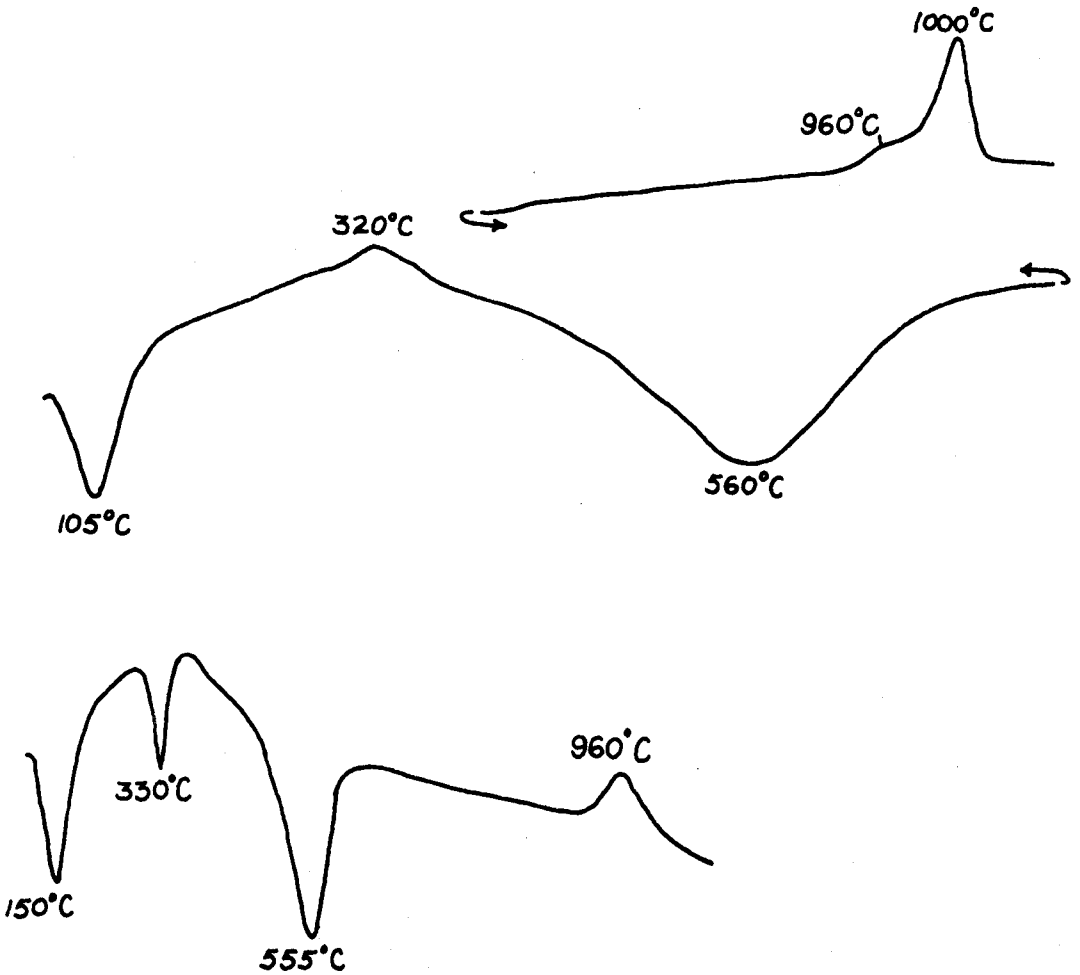

Figure 45. DTA patterns of clay samples R-SP-2 and SS-SF-7. (Note different scales.)

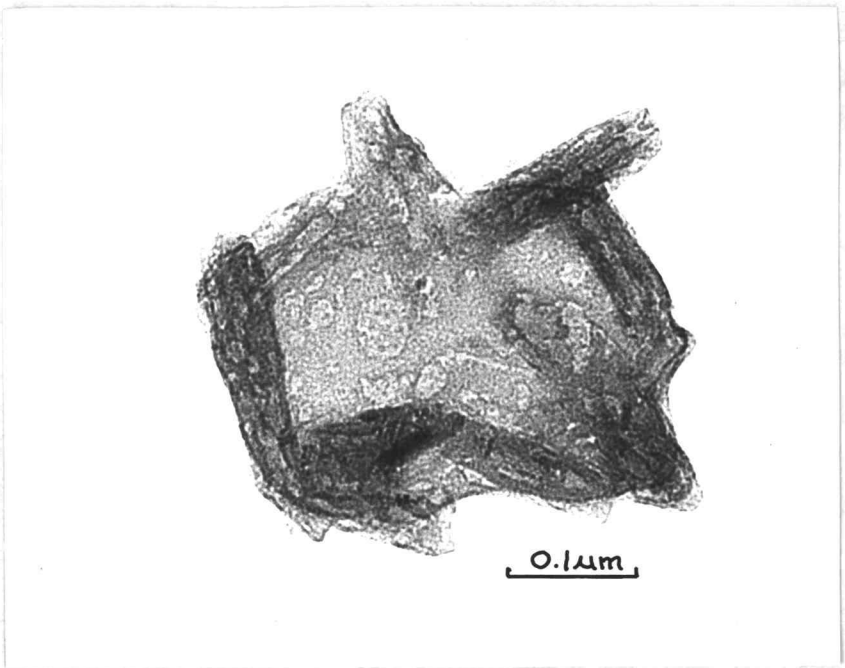

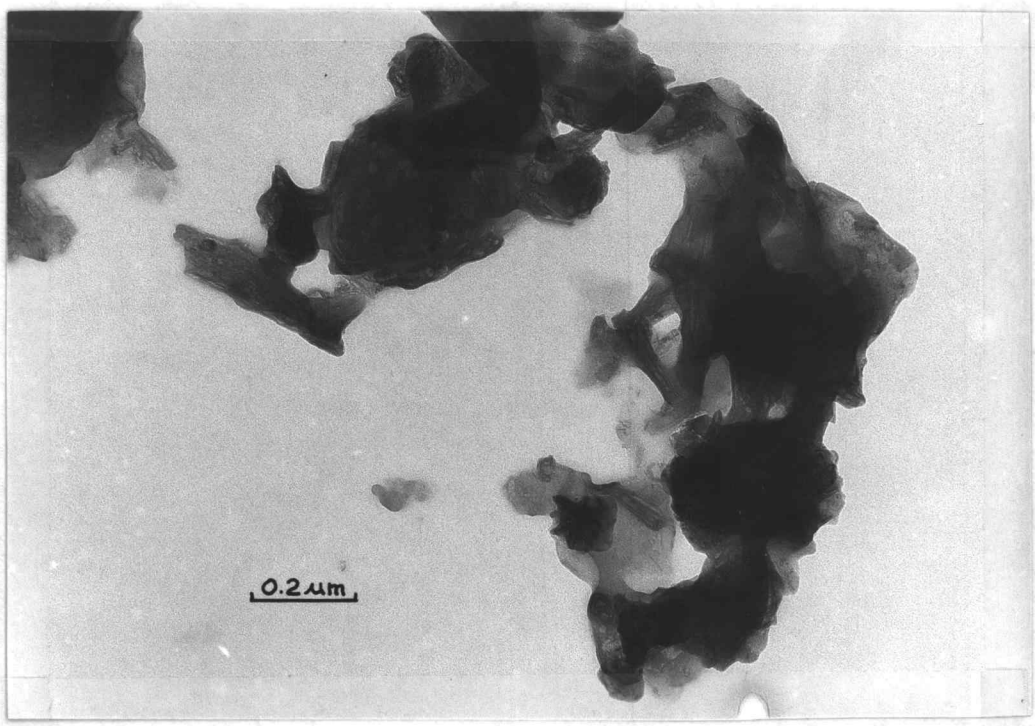

Plate 19. Electron micrographs of halloysite and amorphous material, site SS-SF-7.

under the electron microscope and appeared to be more distinctive (viz., ordered) in samples from the better drained sites which show indications of kaolinite in the XRD patterns. (An analogous arrangement of amorphous material within spheroidal halloysite was reported by Askenasy et al., 1973) Often the conjugated masses were seen to take on a shape which roughly resembles that of kaolinite--crystals of which were also noted. Unfortunately, the micrographs of the better formed of these masses and of kaolinite crystals are of very low quality, and are therefore, not included.

V. THE OVERALL SIGNIFICANCE OF CLAY MINERALOGY IN THE WESTERN CASCADES

Relationships to Landscape Development

Interpretations of aerial photographs and topographic maps, combined with on-site observations, suggest that the type of mass movement varies with stream drainage maturity or with position in the drainage. During geologic time watershed drainage patterns probably have developed by a series of successively receding rotational slumps and subsequent earthflows, with an occasional debris torrent, avalanche or flow.

Large, well defined rotational slumps seem to be most prevalent in the headwater regions where lava flow rock, which provides a substantial overburden pressure, overlied weathered ignimbrite (Figures 4 and 46). Downcutting of the stream channel proceeds with relatively little resistance in the pyroclastic material, thus creating stream banks the heights of which rapidly approach the critical value (Capper and Cassie, 1976; Terzaghi and Peck, 1967). Concurrently, the critical height value decreases due to a reduction in cohesive strength of the slope materials by weathering. The result, once the critical height is attained, is a large rotational slump. The process is especially notable along the contacts of the Sardine and Little Butte Formations--areas which appear to have experienced the most spectacular mass failures. These relationships have also been observed by other investigators (Swanson and James, 1975; Personal communications with F. J. Swanson, Geologist and D. N. Swanston, Principal Geologist, Pacific Northwest Forest and Range Experiment Station, U. S. Forest Service, Corvallis, Oregon).

The situation is exacerbated by the fact that pyroclastic rocks in the Western Cascades weather to clay which is predominately montmorillonite, which has long been recognized for its suceptibility to rotational slumping. The resultant soils, if they are deep and fairly homogeneous, posses cohesive strength sufficient to preclude abrupt

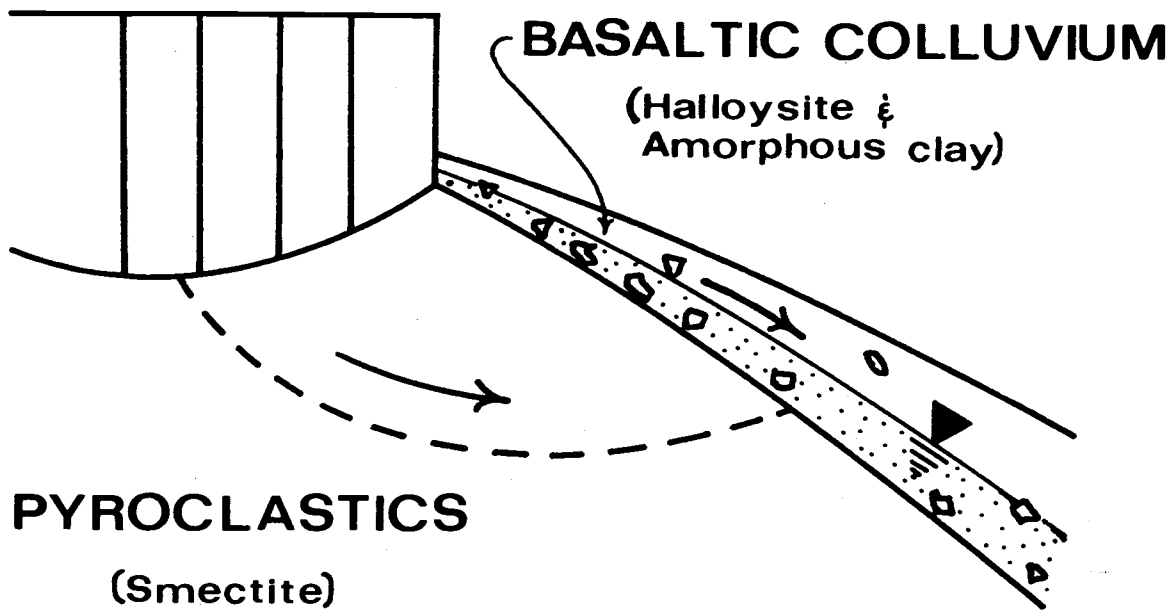

Figure 46. Rotational slump in smectite-rich, decomposed pyroclastic material capped by lava flow rock, and planar failure of basaltic colluvium containing halloysite and amorphous clays and a perched water table.

shallow failures of their mass. Instead, they are more likely to fail at a depth comparable to the lateral dimensions of the failure, because at that depth shear stress is sufficient to overcome shear strength. [Most of the shear strength in homogeneous plastic soils is due to the cohesive resistance, which is greatly reduced under the conditions of high pore water pressure.]

The andesitic or basaltic overburden gradually breaks into cobbles which move downslope, forming a layer of colluvium over the weathering pyroclastic material (Figure 46). Additionally, on many sites volcanic ash from more recent eruptions (e. g., Mt. Mazama) has become mixed with the colluvial deposits. The presence of the underlying montmorillonitic clay and plentiful water lead to the development of perched water tables in this soil. [The colluvial debris and ash weather to amorphous gel and hydrated halloysite, which in turn help to maintain the soil's relatively high water content throughout the year.] The combination of mineralogy, water and slope provides ideal conditions for the debris flows which commonly occur on top of the larger slump blocks.

Further downslope, the large saturated deposits of disintegrating slump blocks and colluvial debris grade into earthflows of mixed lithology. Several of the very large earthflows have soils whose clay fractions consist most importantly of amorphous gels and hydrated halloysite. It is inferred that these masses are slowly sliding and creeping downslope on a deposit of montmorillonite clay, which may also be moving. These large earthflows easily become dissected by deep V-shaped stream channels. The channels frequently develop along the flanks where they are downcut by waters draining from earthflows and from the lateral hillslopes with which they are in contact.

Debris avalanches contribute to further drainage development by scouring the steep hillslopes and sides of the deeply incised stream channels. The depth of these failures is determined by the presence of subsurface discontinuities, whereat failure is probably initiated by the development of abnormally high pore water pressures. The clay

fraction of the soil subject to avalanching consists primarily of amorphous material--mostly devitrified volcanic glass and fibers--and chloritic intergrade, often with associations of gibbsite, dehydrated halloysite, kaolinite, zeolite, or mica. Smectites in relatively small amounts at bedrock surface promote debris avalanching of overlying shallow soil, largely because their presence decreases the soil's frictional resistance and impedes water flow.

Limited observations suggest that the process may be somewhat different in those areas which are more distant from the fringes of contrasting rock layers, and where the geology is composed more uniformily of pyroclastic rock which has weathered to smectite. In these areas, such as the upper reaches of the Jackson Creek drainage of the South Umpqua, the rotational failures seem to be smaller and better defined than those which involve an overburden of competent lava rock. Earthflows, which may follow the slumping, also appear to be smaller in size and more easily delineated. Deep seated soil creep, which gradually produces a deformed, rumpled landscape, is a much more apparent process in these soils with a high proportion of the expandable, cohesive clays.

Summary of Important Clay Characteristics

Although it is well established that smectites are involved in mass movements throughout many parts of the world, the greatest mineralogical significance of this study lies in relating halloysite and amorphous materials, as well as smectites, to land failures in the volcanic deposits of the Western Cascades. The literature contains a considerable amount of seemingly contradictory information regarding the role played by halloysite and amorphous clay in soil erosion (Yong and Warkentin, 1975; Wesley, 1973; Robertson, 1963; Birrell 1962; Hill et al., 1975; Wallace, 1973; Pope and Anderson, 1960; Lumb, 1975; Fieldes, 1955; McKyes et al., 1974). Furthermore, although this study has shown that they may contribute significantly to slope failures, amorphous materials and halloysite may also be found on

stable sites. The reason for the seeming contradiction is that these soil components take on different forms and behavior under different sets of conditions. Therefore, the broad question of whether they contribute to stability or to instability is immaterial unless conditions are specified.

Water availability (current and historical) seems to be the most important factor controlling the form and behavior of halloysite and amorphous materials. Generally, it appears that in areas where these materials remain wet throughout the year they contribute very little to soil strength; hence, they promote soil instability. The reason lies in the fact that hydrated halloysite and amorphous gels and imogolite which have not been allowed to dry have a very high water holding capacity (Maeda and Warkentin, 1975; Warkentin and Maeda, 1974). The water is thought to be held between the separated layers in halloysite, and in voids between gel linkages and imogolite strands (Askenasy et al., 1973; Fieldes and Furkert, 1966). Electron micrographs produced in this study support these interpretations. However, they also prompt the suggestion that the amorphous gels form microscopic balloons which are filled with water and a random assortment of clay particles. (This theory can not be proven by electron microscope techniques, however, because any water which might normally be held in these balloons would be lost when the sample is placed in the vacuum of the microscope.)* Assuming that the water balloon theory is correct, it is easy to visualize these fragile containers imparting a huge water holding capacity to the soil, and upon disturbance releasing the stored water while at the same time allowing the particles to rearrange themselves into a configuration of lower strength. In support of this, Wells and Furkert (1972) have shown that significant changes in water retention of amorphous materials takes place upon remoulding of the soil.

Some sites the soils of which contain halloysite and amorphous clays tend to be relatively stable. These do not have perched water tables. They exist at higher elevations in environments wherein clay mineral development is minimal, or in areas in which the clays

might have dried irreversibly at some time in their history, or in lower elevation, relatively well drained areas. The soils of these sites would be expected to have high frictional resistance in addition to their high permeability. The clay fraction as seen under the electron microscope contains irregularly shaped microaggregates of clay particles which are tightly bound by an intricate net of partially dried amorphous gel and imogolite strands. It is reasonable to assume that a considerable portion of the silt fraction of these soils is also due to aggregates of this type. Each of these aggregates probably acts as a primary soil particle which can have a very high degree of interlocking with its neighbor.

In many soils tubular halloysite conjoins with the gelatinous amorphous component to form what appear to be incipient platelets, which may be precursors of kaolinite. These seem to be more prevalent in the lower elevation, well drained soils which give kaolinite peaks in X-ray diffraction; however, this relationship is not certain. (It is certain, however, that this form of amorphous material is far more stable than the "balloon" membranes under the electron beam.) These fused particles would be expected to contribute far more to soil shear strength than would the less organized arrangements of similar components on wetter sites.

VI. SUGGESTIONS FOR FURTHER STUDY

A number of questions concerning the relationships of clay mineralogy to landscape stability are yet to be answered. It has been shown that amorphous clays, halloysite and smectites are commonly involved in mass movements in the Western Cascades; however, the problem remains of quantifying the extent to which these materials influence slope stability, and, further, of developing a method for determining how much they control the stability of a given site. This information is needed in order to rate the importance of these materials for the development of stability prediction models.

The mechanical properties of these clays--especially of the amorphous clays and halloysite--should be established. Relatively simple determinations such as plastic and liquid limits, and activity ratios, combined with vane shear and penetration testing, could yield further valuable information regarding their behavior. This work might be followed by more complex, direct shear and sensitivity investigations (Skempton, 1953; Seed et al., 1964; Ingles, 1968; Terzaghi and Peck, 1967; Mitchell, 1976). These studies could be complemented by investigations of structure (i.e., macro- and microfabric) (Collins and McGown, 1974), and more definitive work on water relations.

Mechanisms and trends in the genesis and alteration of the various amorphous materials and halloysite are still uncertain. As was pointed out, there appears to be a relationship between the stages of development and alteration of these components and moisture conditions on the site--which in turn are related to soil stability. Furthermore, the questions relating to the effects of these clays on water quality (viz., suspended sediments and turbidity) are far from being answered. Additional suggestions include studies on the relationships of mineralogy to plant ecology and site productivity.

Finally, there is the problem of bringing together and evaluating knowledge of the various relationships in order to select the best alternatives for land management.

BIBLIOGRAPHY

American Geological Institute. 1972. Glossary of geology and related sciences. A.G.I. Washington, D.C.

Askenasy, P.E., J. B. Dixon and T. R. McKee. 1973. Spheroidal halloysite in a Guatemalan soil. Soil Sci. Soc. Amer. Proc. 37:799-803.

Baldwin, Ewart M. 1976. Geology of Oregon. Univ. of Oregon Cooperative Bookstore. Eugene, Oregon. 165 pp.

Beaulieu, J. D. 1971. Geologic formations of western Oregon. Oregon Dept. Geology and Mineral Industries Bull. 70.

Berry, Richard W. and Per Jorgensen. 1971. Grain size, mineralogy and chemistry of a quick-clay sample from the Ullensaker slide, Norway. Engng. Geol. 5(1):73-84.

Beutelspacher, H. and H. W. Van Der Marel. 1968. Atlas of electron microscopy of clay minerals and their admixtures. Elsevier Pubs. Co. Amsterdam. 333 pp.

Birrell, K. S. 1962. Physical properties of New Zealand volcanic ash soils. In: Grim, R. E. (ed.). Applied Clay Mineralogy. Conf. Shear Testing of Soils. Melbourne. pp. 30-34.

Borchardt, Glenn A. 1976. Clay mineralogy and slope stability. Special Rept. Calif. Div. Mines & Geology. 41 pp.

Booy, Emmy and Paul F. Kerr. 1973. Mineralogy of some "bentonites" involved in slope failures in Wyoming. 22nd Clay Minerals Conf. Banff, Alberta.

Brindley, G. W. 1961. Kaolin, serpentine and kindred minerals. In Brown, G. (ed.). The x-ray identification and crystal structures of clay minerals. Mineralogical Society, London. pp. 51-131.

Burroughs, Edward R. et al. 1976. Slope stability in road construction. Bureau Land Management, Portland, Oregon. 102 pp.

Capper, P. Leonard and W. Fisher Cassie. 1976. The mechanics of engineering soils. E. and F. N. Spon Ltd. London, and Halsted Press, John Wiley & Sons, Inc. New York. 376 pp.

Carson, M. A. and M. J. Kirkby. 1972. Hillslope form and process. Cambridge Univ. Press, London. 475 pp.

Collins, K. and A. McGown. 1974. The form and function of microfabric features in a variety of natural soils. Geotechnique. 24(2):223-254.

Crawford, C. B. 1968. Quick clays of eastern Canada. Engng. Geol. 2:239-265.

Crozier, M. J. 1969. Earthflow occurrence during high intensity rainfall in eastern Otago (New Zealand). Engng. Geol. 3(4):325-334.

Dingus, Delmar deLee. 1974. The nature and properties of amorphous colloids formed from Mazama tephra. Diss. Abst. 73-32755. Jan 74. 34(7):3037-B.

Dudas, M. J. and M. E. Harward. 1975. Weathering and authigenic halloysite in soil developed in Mazama ash. Soil Sci. Soc. Amer. Proc. 39(3):561-566.

Dyrness, C. T. 1967. Mass soil movements in the H. J. Andrews Experimental Forest. USDA Forest Service Research Paper PNW-42.

Fieldes, M. 1955. Clay mineralogy of New Zealand soils. Part II: Allophane and related mineral colloids. N.Z. Jour. Sci. and Tech. 37:336-350.

Fieldes, M. and R. J. Furkert. 1966. The nature of allophane in soils. N.Z. Jour. Sci. 9:608-622.

Fleming, Robert W. and Arvid M. Johnson. 1975. Rates of seasonal creep of silty clay soil. Q. Jour. Engng. Geol. 8(1):1-29.

Gard, J. A. (ed.). 1971. The electron-optical investigation of clays. Mineralogical Society. Monograph 3. London. 383 pp.

Gillott, Jack E. 1968. Clay in engineering geology. Elsevier Pub. Co. New York, Amsterdam. 196 pp.

Grim, Ralph E. 1962. Applied clay mineralogy. McGraw-Hill Book Co., Inc. New York. 422 pp.

Hill, D., A. Stamatopoulos, and P. Kotzias. 1975. Discussion of "Some basic engineering properties of halloysite and allophane clays in Java, Indonesia." Geotechnique. 25(2):417-423.

Ingles, O. G. 1968. Soil chemistry relevant to the engineering behavior of soils. In: Lee, I. K. (ed.). Soil Mechanics, Selected Topics. American Elsevier Pubs. Co. New York. pp. 1-57.

Jones, R. C. and G. Uehara. 1973. Amorphous coatings on mineral surfaces. Soil Sci. Soc. Amer. Proc. 37:792-798.

Kerr, Paul F. and Isabella Milling Drew. 1968. Quick-clay studies in the U.S.A. Engng. Geol. 2(4):215-238.

Klages, M. G. and Y.P. Hsieh. 1975. Suspended solids carried by the Gallatin River of southwestern Montana; II. Using mineralogy for inferring sources. J. Environ. Qual. 4(1):68-73.

Ladd, G. E. 1935. Landslides, subsidences and rockfalls. Am. Ry. Eng. Assoc. Proc. 36:1091-1162.

Lumb, Peter. 1975. Slope failures in Hong Kong. Q. Jour. Engng. Geol. 8(1):31-65.

Mackenzie, R. C. (ed.). 1957. The differential thermal investigation of clays. Mineralogical Society. London. 456 pp.

Mackenzie, R. C. 1970. Differential Thermal Analysis. Vol. 1. Fundamental Aspects. Academic Press. London. 775 pp.

Maeda, T. and B. P. Warkentin. 1975. Void changes in allophane soils determining water retention and transmission. Soil Sci. Soc. Amer. Proc. 39:398-403.

McKee, Bates. 1972. Cascadia. McGraw-Hill Book Co. New York. 394 pp.

McKyes, E., A. Sethi, and R. N. Yong. 1974. Amorphous coatings on particles of sensitive clay soils. Clays and Clay Min. 22:427-433.

Mitchell, J. K. 1976. Fundamentals of soil behavior. John Wiley. New York. 422 pp.

Paeth, R. C., M. E. Harward, E. G. Knox, and C. T. Dyrness. 1971. Factors affecting mass movement of four soils in the Western Cascades of Oregon. SSSAP 35:943-947

Parham, Walter E. 1969. Formation of halloysite from feldspar; Low temperature, artificial weathering versus natural weathering. Clays and Clay Min. 17(1):13-22.

Peck, D. L. et al. 1964. Geology of the central and northern parts of the Western Cascade Range in Oregon. U.S. Geol. Surv. Prof. Pap. 449, 56 p.

Pope, Robert J. and M. W. Anderson. 1960. Strength properties of clays derived from volcanic rocks. Am. Soc. Civ. Eng. Research Conf. on shear Strength of Cohesive Soils. Univ. of Colo. Boulder. p. 315-340.

Prior, D. B. and C. Ho. 1972. Coastal and mountain slope instability on the islands of St. Lucia and Barbados. Engng. Geol. 6(1):1-18.

Rai, Dhanpat and W. L. Lindsay. 1975. A thermodynamic model for predicting the formation, stability, and weathering of common soil minerals. Soil Sci. Soc. Amer. Proc. 39:991-996

Ramp, Len. 1972. Geology and mineral resources of Douglas County, Oregon. Oregon Dept. Geol. Min. Industries, Bull. 75. 106 pp.

Robertson, R. H. S. 1963. Allophanic soil from Trail Bridge, Oregon, with notes on mosaic growth in clay minerals. Clay Min. Bull. 5(29):237-247.

Rosenqvist, I. Th. 1966. Norwegian research into the properties of quick clay - a review. Engng. Geol. 1(6):445-450.

Seed, H. B., R. J. Woodward, and R. Lundgren. 1964. Clay mineralogical aspects of the Atterberg limits. Jour. Soil Mech. and Found. Div. Am. Soc. Civ. Engrs. 90(Sm 4):107-131.

Sharpe, C. F. S. 1938. Landslides and related phenomena. Columbia Univ. Press, New York. 137 pp.

Skempton, A. W. 1953. The colloidal activity of clay. Proc. Third Intl. Conf. on Soil Mech. and Found. Engng. 1:57-61.

Sudo, Toshio and Haruo Yotsumoto. 1977. The formation of halloysite tubes from spherulitic halloysite. Clays and Clay Min. 25:155-159.

Swanson, Frederick J. and Michael E. James. 1975. Geology and geomorphology of the H. J. Andrews Experimental Forest, western Cascades, Oregon. USDA For. Serv. Res. Pap. PNW-188, 14 p.

Swanston, D. N. 1969. Mass wasting in coastal Alaska. U.S. Department of Agriculture Forest Service Research Paper PNW-83, 15 pp.

Swanston, D. N. 1970. Principal mass movement processes influenced by logging, road building, and fire. In: Forest Land Uses and Steam Environment Symposium Proc. Ore. St. Univ.

Swanston, D. N. 1976. Erosion processes and control methods in North America. XVI IUFRO World Congress Proceedings, 251-275.

Swanston, D. N. and F. J. Swanson. 1976. Timber harvesting, mass erosion, and steepland forest geomorphology in the Pacific Northwest. In: Geomorphology and Engineering. D. R. Coates, ed. Dowden, Jutchinson & Ross, Inc. pp. 199-221.

Terzaghi, Karl. 1929. The mechanics of shear failures on clay slopes and the creep of retaining walls. Public Roads, 10.

Terzaghi, Karl. 1950. Mechanism of landslides. In: Application of Geology to Engineering Practice. Geol. Soc. America. 83-123.

Terzaghi, Karl and Ralph B. Peck. 1967. Soil mechanics in engineering practice. John Wiley & Sons, Inc. New York, London, Sydney. 729 pp.

U. S. Geol. Survey. 1955 (1963 revision). Topographic map of Medford Quadrangle, Oregon. 1:250,000 scale. Map No. NK 10-5.

U. S. Geol. Survey. 1958 (1970 revision). Topographic map of Roseburg Quadrangle, Oregon. 1:250,000 scale. Map No. NK 10-2.

U. S. Geol. Survey. 1960 (1967 revision). Topographic map of Salem Quadrangle, Oregon. 1:250,000 scale. Map No. ML 10-11.

Varnes, D. J. 1958. Landslide types and processes. In: Landslides and Engineering Practice. Highway Research Board. Spec. Rept. 29:20-47.

Wahlstrom, Ernest E. and T. C. Nichols, Jr. 1969. The morphology and chronology of a landslide near Dillon Dam, Dillon, Colorado. Engng. Geol. 3(2):149-174.

Walker, G. W. and P. B. King. 1969. Geologic map of Oregon. U.S. Geol. Surv. Misc. Geol. Inv. Map 1-595. In: Mineral and water resources of Oregon Dept. Geol. and Min. Indus. Bull. 64.

Wallace, K. B. 1973. Structural behavior of residual soils of the continually wet highlands of Papua, New Guinea. Geotechnique. 23:210-218.

Warkentin, B. P. and T. Maeda. 1974. Physical properties of allophane soils from the West Indies and Japan. Soil Sci. Soc. Amer. Proc. 38:372-377.

Wells, N. and R. J. Furkert. 1972. Bonding of water to allophane. Soil Science. 113:110-115.

Wells, F. G. and D. L. Peck. 1961. Geologic map of Oregon west of the 121st meridian. U. S. Geol. Survey Misc. Geol. Invest. Map 1-325, in coop. with Oregon Dept. Geol. and Min. Indust.

Wesley, L. D. 1973. Some basic engineering properties of halloysite and allophane clays in Java, Indonesia, Geotechnique 23(4): 471-494.

Wilding, L. P. and L. R. Drees. 1976. Biogenic opal in soils--morphology, physical and chemical properties. Amorphous and Poorly Crystalline Clays. Extended Abstracts of U.S.-Japan Seminar, Oregon State Univ., Corvallis. p. 9-13.

Winsler and Kelly Engineers. 1975. Redwood Creek - an integrated study. Winsler and Kelly Engineers Water Laboratory P. O. Box 1345. Eureka, Ca. 95501. 44 pp.

Wu, T. H. 1976. Soil mechanics. Allyn and Bacon, Inc. Boston. 440 pp.

Yong, Raymond N. and Benno P. Warkentin. 1975. Soil properties and behavior. Elsevier Scientific Pubs. Co. 449 pp.

Youngberg, C. T., M. E. Harward, G. H. Simonson, D. Rai, P. C. Klingeman, D. W. Larson, H. K. Phinney, and J. R. Bell. 1971. Hills Creek Reservoir turbidity study. Oregon State Univ. Water Resour. Res. Inst. WRRI-14. Corvallis, Ore.

Zaruba, Q. and V. Mencl. 1969. Landslides and their control. Elsevier Pubs. Co. Amsterdam. 205 pp.

APPENDICES

APPENDIX I

FAILURES OUTSIDE THE WESTERN CASCADES

Several sites outside of the Western Cascades were investigated in order to develop some feeling for conditions under different geologic and environmental settings. Most of the additional sites were examined in only a cursory manner, and all but two are located in the Klamath Mountains of southwestern Oregon, a region of great geologic diversity and complex mineralogy.

The most detailed mineralogical information was gathered from an earthflow at site W-S-1 in the Soap Creek drainage on the eastern edge of the Coast Range. The soil of the area contains a considerable amount of basaltic colluvial rock. Eight clay samples taken at various depths from about 1½ to 10 meters in a drill hole show a remarkable degree of homogeniety in the flow. All samples contain dehydrated halloysite and some hydrated halloysite, amorphous material, and chloritic intergrade or hydroxy interlayered smectite (Figures 47-50). Oddly, sample b, from the 2½ meter depth, and sample h, from the 10 meter depth, contain anolmalous mica. The mica may also be present in other samples, but in very small amounts and/or in a poorly crystallized form, and so is not readily apparent. The presence of the mica, however, raises the question of whether or not all of the material was developed from basaltic colluvium, as it could be evidence of mixing of the mass with sedimentary rock. Furthermore, the homogeneity of the materials with depth suggests that the drill hole did not reach the bottom of the earthflow as there is no evidence of a discontinuity.

The other additional site outside of the Klamath Mountains, JD-1, is located along the highway near the John Day River north of Mitchell, Oregon. It consists of a moderate sized rotational failure with a well defined scarp wall in multicolored, clayey soil. The soil here, which has formed from the pyroclastic debris of the John Day Formation, appears typical of much of the plastic, clayey soil of the John Day country which has experienced some tremendous slumps in the distant past. As expected, the clay fraction consists of nearly pure smectite, most of which is montmorillonite, but with perhaps a beidellite component as well (Figure 51).

The most notable of the Klamath Mountain sites (A-S-1) involves a large, slow moving slide of schistose soil into Squaw Creek, near the California border. The mass of the failure is also undergoing deep creep, and the toe has lost great sections into the creek by rapid sliding. Large tension cracks have developed along the periphery of the main failure, which is about 400 meters wide.

The XRD patterns of clay samples of this failure are quite complex (Figure 52). Sample a is from relatively stable material which is being rafted along within the large failure, and sample b is from the slip plane of one of the large toe slides at the creek. In both samples chlorite and mica are present as is probably vermiculite and kaolinite. Kaolinite typically is difficult to identify in the presence of chlorite due to possible confusion of the first order kaolinite line with that of second order chlorite (Brindley, 1961).

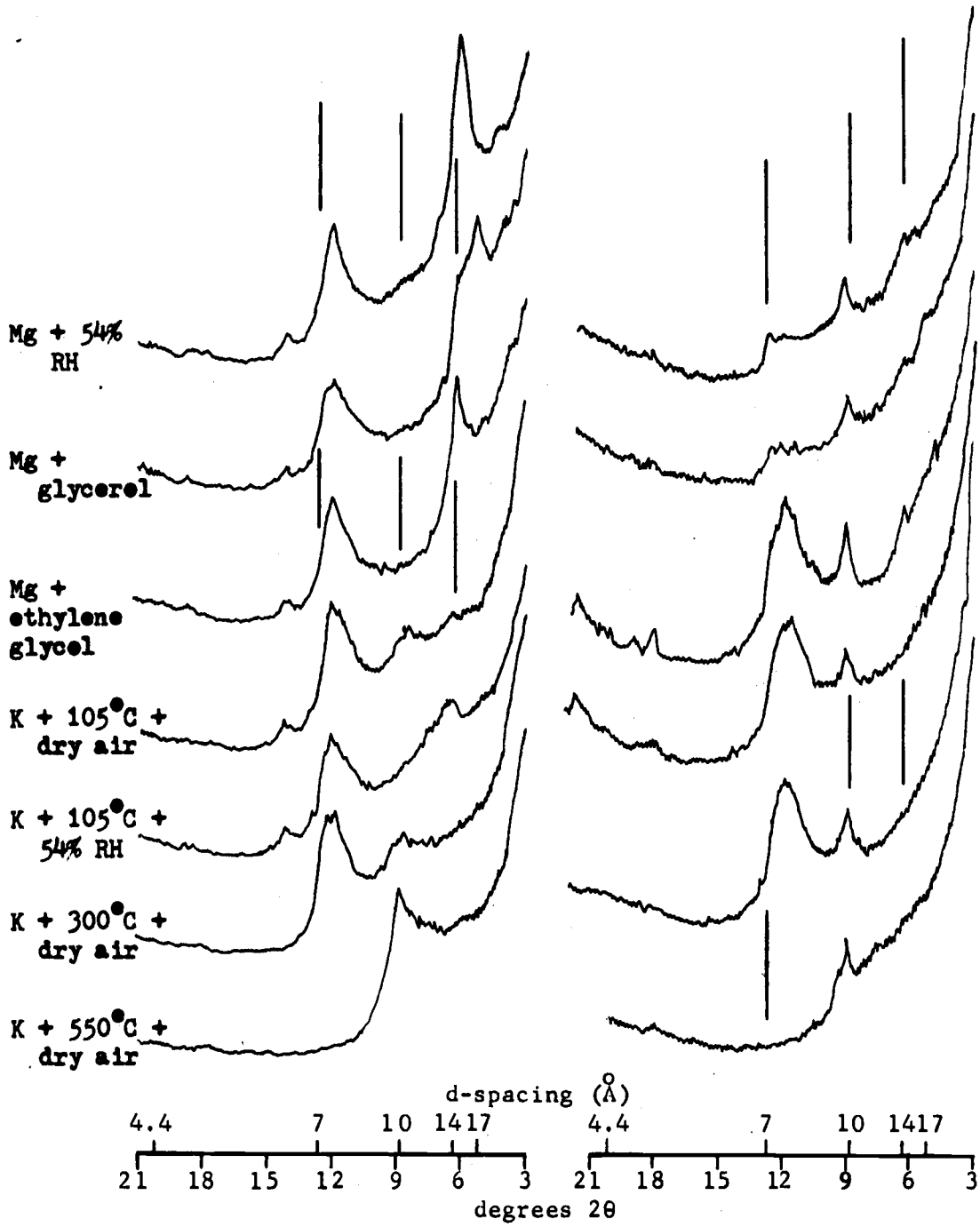

Figure 47. Site W-S-1 XRD patterns. Sample a (left), 1.5 m depth. Sample b (right), 2½ m depth.

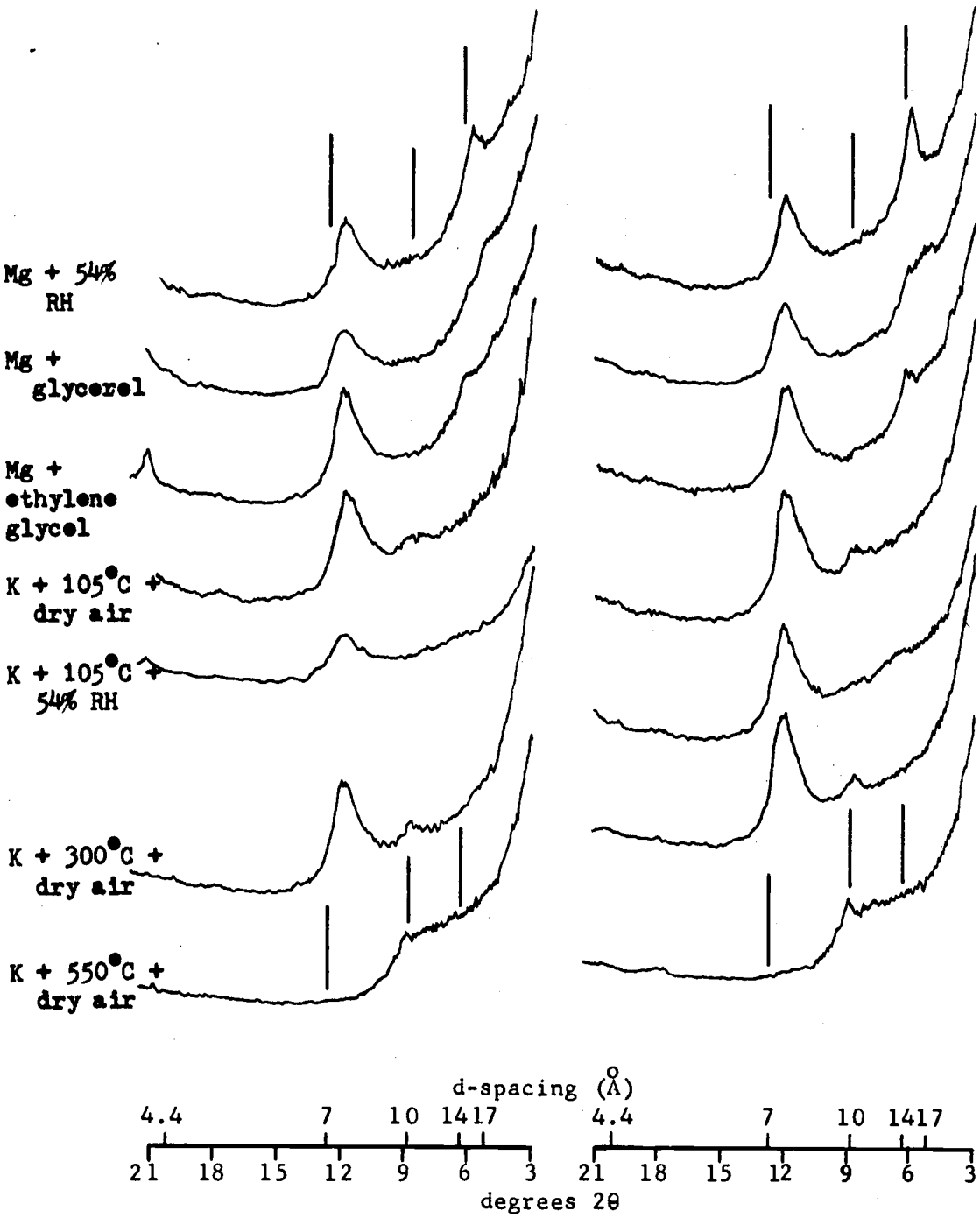

Figure 48. Site W-S-1 XRD patterns. Sample c (left), 3 m depth. Sample d (right) 4½ m depth.

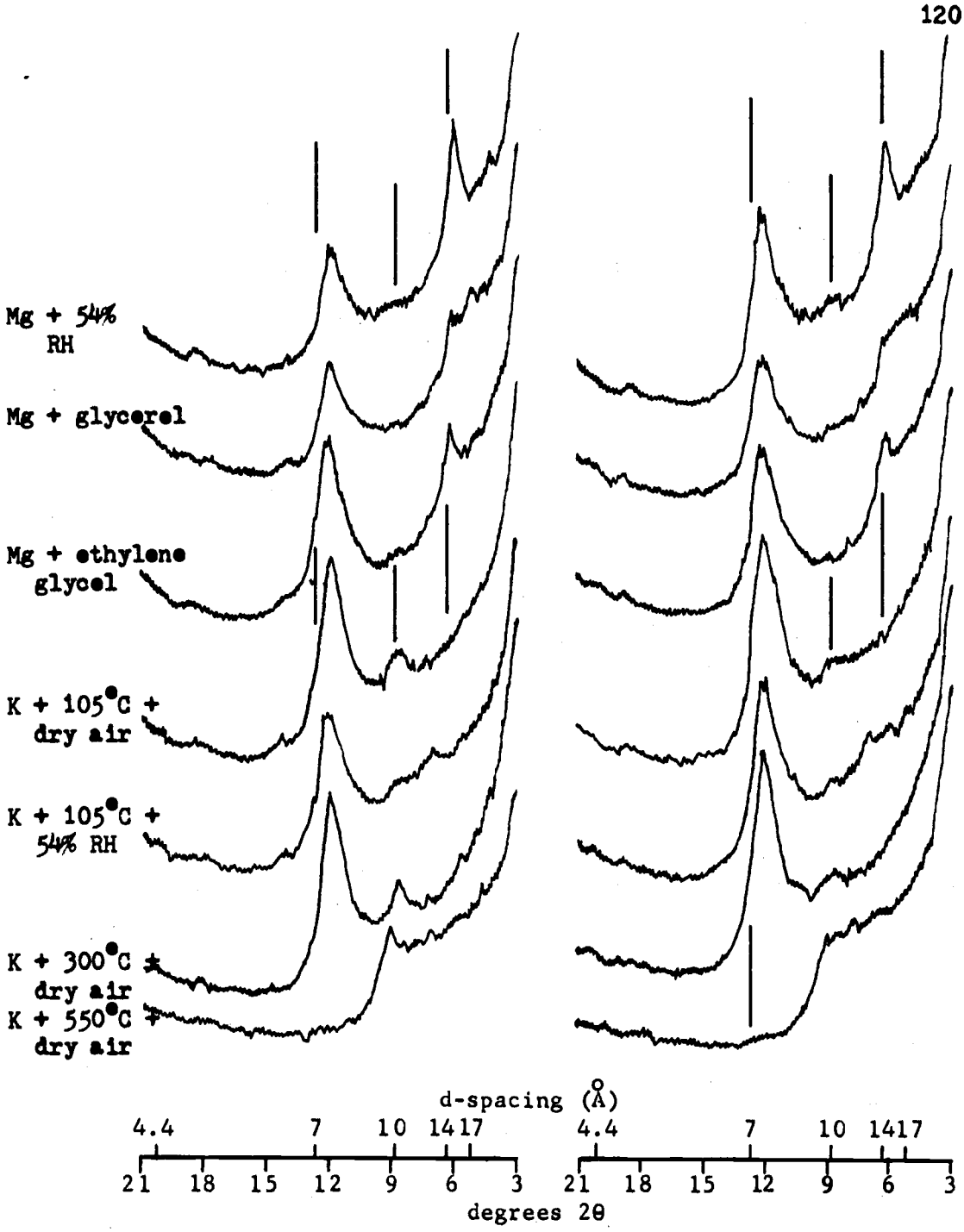

Figure 49. Site W-S-A XRD patterns. Sample 3 (left) 6 m depth. Sample f (right) 6 3/4 m depth.

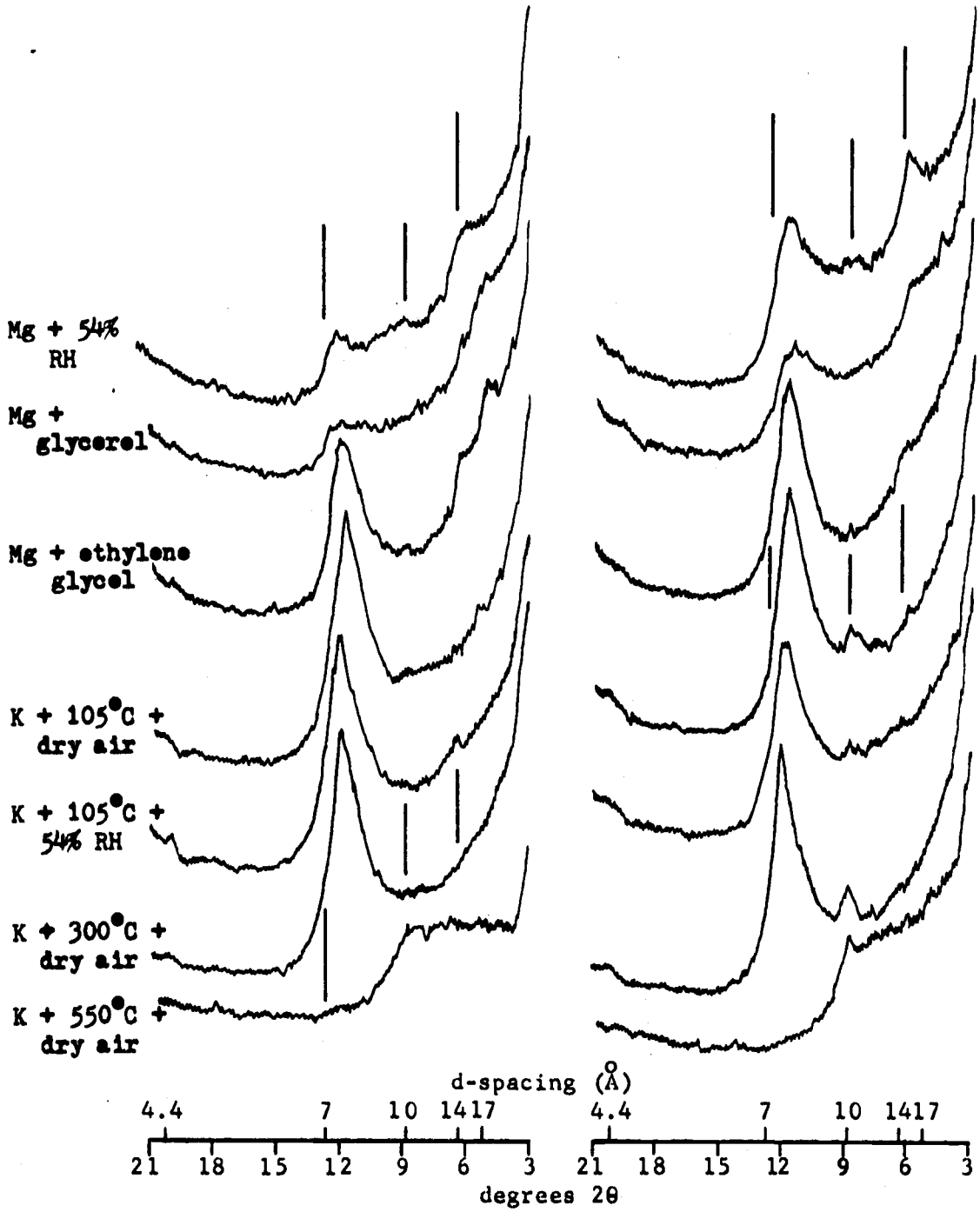

Figure 50. Site W-S-1 XRD patterns. Sample g (left), 8½ m depth. Sample h (right), 10 m depth.

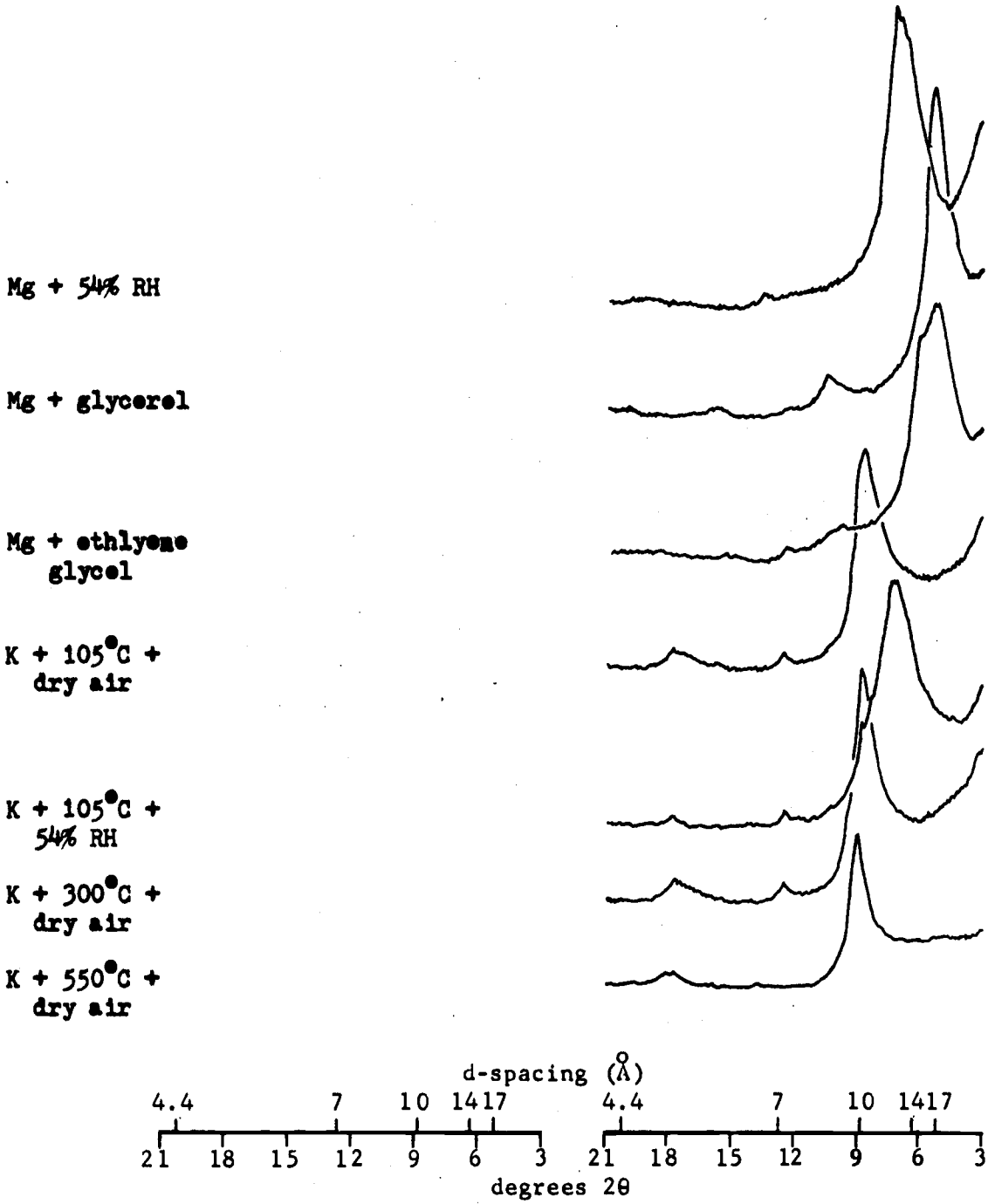

Figure 51. XRD patterns of montmorillonite clay from site JD-1, along the John Day River.

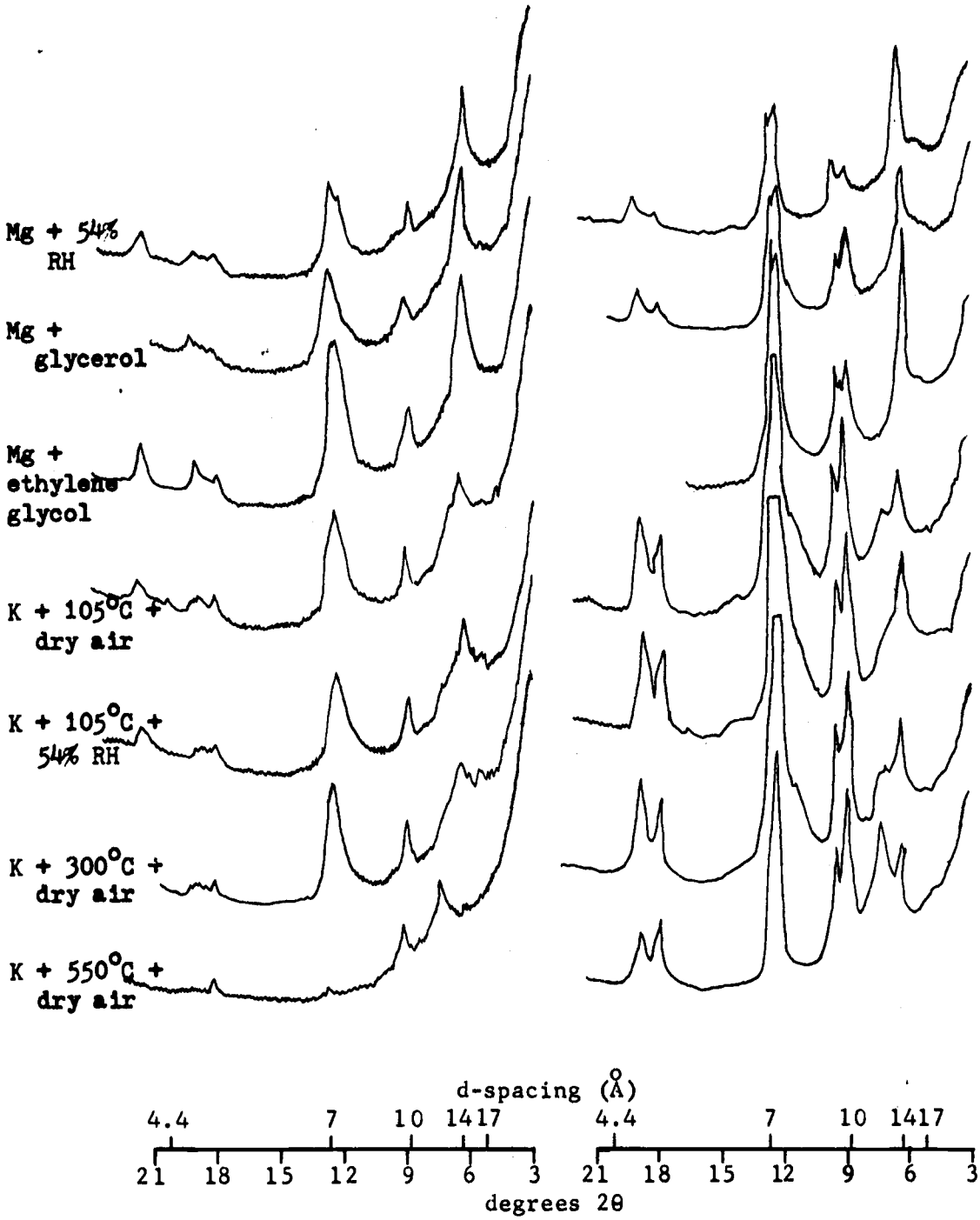

Figure 52. XRD patterns of clay in schistose material, site A-S-1a (left) and A-S-1b (right).

In this case, however, there is clearly a doublet (which is more obvious in the originalpatterns than in the reproductions) in the region of 7.1 Å which very likely indicates the two components. In addition there is a doublet in the patterns of sample b in the region of 10 Å, the lower spacing peak of which is interpreted as paragonite,

Similar mineralogy has been found in soils subject to failures of a similar type in Redwood Creek drainage of northern California. (Winsler and Kelly, 1975). It might be fruitful to investigate site A-S-1 further to determine whether or not there are any distinctive characteristics of the soil within the failure zone. The distribution of paragonite, for instance, may be significant.

A large failure in the Bigelow Creek drainage, site A-B-1, involved relatively complex and variable mineralogy. Samples c, d, e, and f are subsamples which represent materials of various colors at progressively greater depths within a 3/4 meter profile section of the failure surface; whereas sample b is a random sample of a nearby road cutbank. The XRD patterns indicate smectite (beidellite?). vermiculite, kaolin (disordered kaolinite?), mica, zeolite, some amorphous material, chloritic intergrade, and perhaps an interstratified component (Figures 53, 54, and 55). The complexity of the failure combined with the complexity and variability of the clays make it impossible to determine the relevance of the clay fraction to the failure process without further investigation. The main reason for presenting the data here is to point out the mineralogical variability of the area and to record the analyses for posterity.

Site R-WUR-1 is in an area of deep seated soil creep, rotational slumping and slow flowage in degraded schistose material with fragments of very hard argillite along the lower Rogue River. The soil's clay fraction, which is somewhat similar to that at Squaw Creek (A-S-1), consists of chlorite, mica, vermiculite, and a randomly interstratified component which is probably mica-vermiculite (Figure 55). Kaolinite may also be included, but its presence is unconfirmed.

Further down the Rogue, near Gold Beach, is an area of deep creep subject to slumping and earthflowing. The materials of the site, R-1, have undergone considerable mixing due to a long history of mass movement. The clays here are similar to those at site R-WUR-1 except for the presence of weakly displayed smectitic material (Figure 56). The samples were taken a few centimeters from each other in a moderate sized road bank failure; sample a represents the block of soil which has actually dropped away from the main bank, and sample b represents the soil of the bank failure surface. The patterns show much stronger 7 Å peaks in sample a than sample b. (It is not known whether the 7 Å peaks are due to kaolinite or second order chlorite.) They also show less evidence of chlorite in sample b than in a, and strong evidence of a randomly interstratified component in b. The significance, if any, that these differences may have to the stability of the site is undetermined.

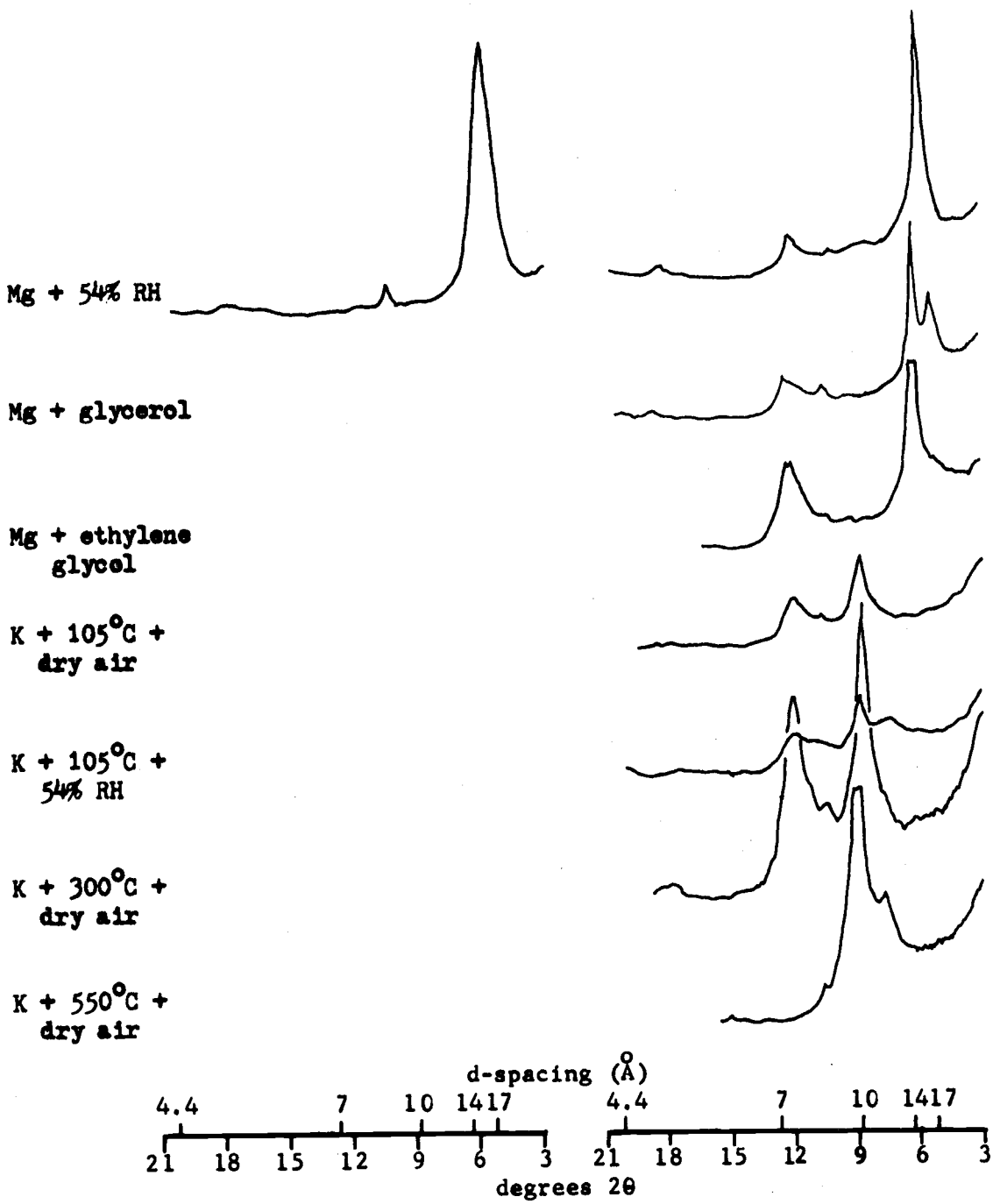

Figure 53. XRD patterns of greenish subsample c (left) and brown subsample d (right), site A-B-1.

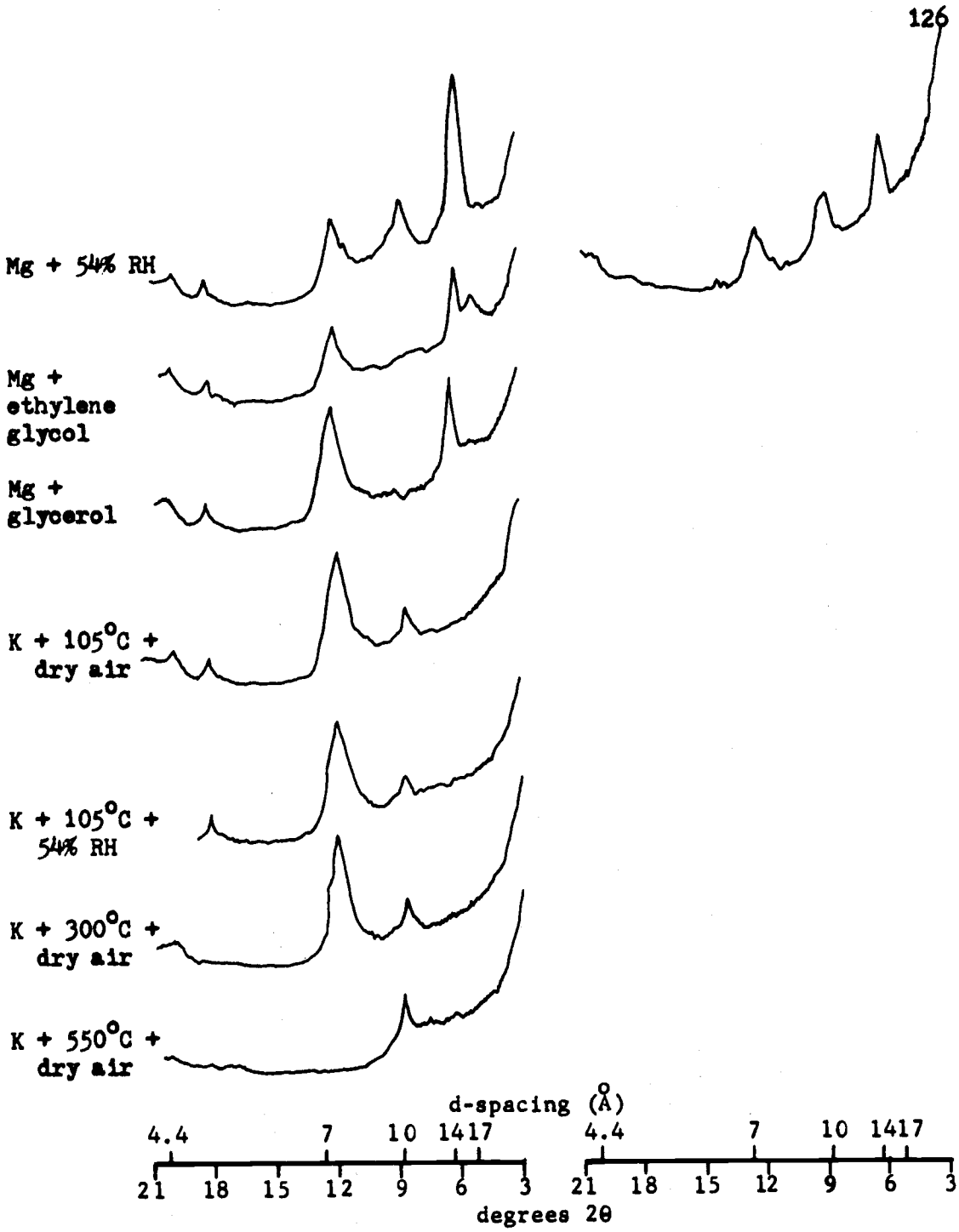

Figure 54. XRD patterns of orange-brown subsample e (left) and orange subsample f (right), site A-B-1.

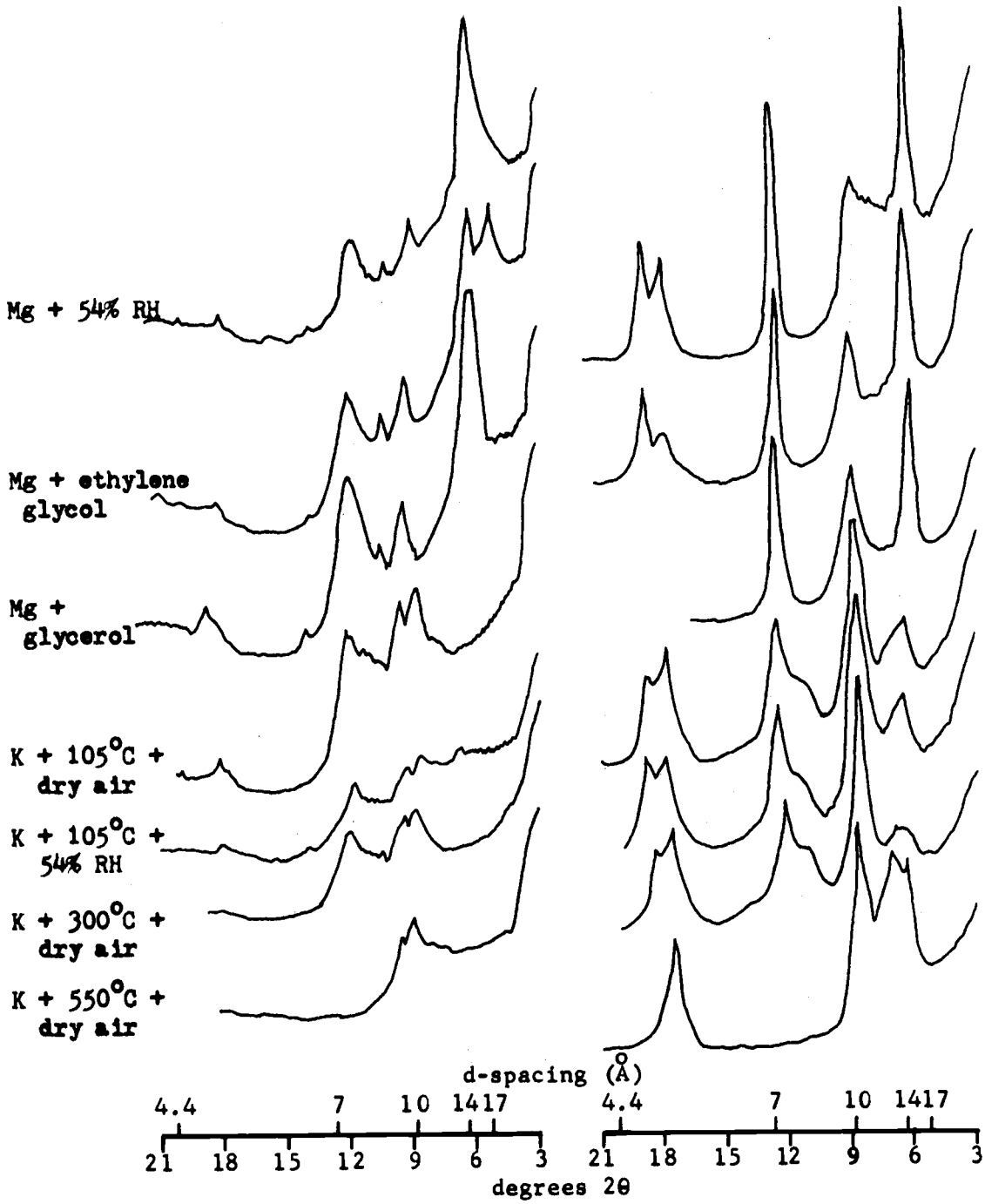

Figure 55. XRD patterns of clay sample A-B-1b (left) and R-WUR-1 (right).

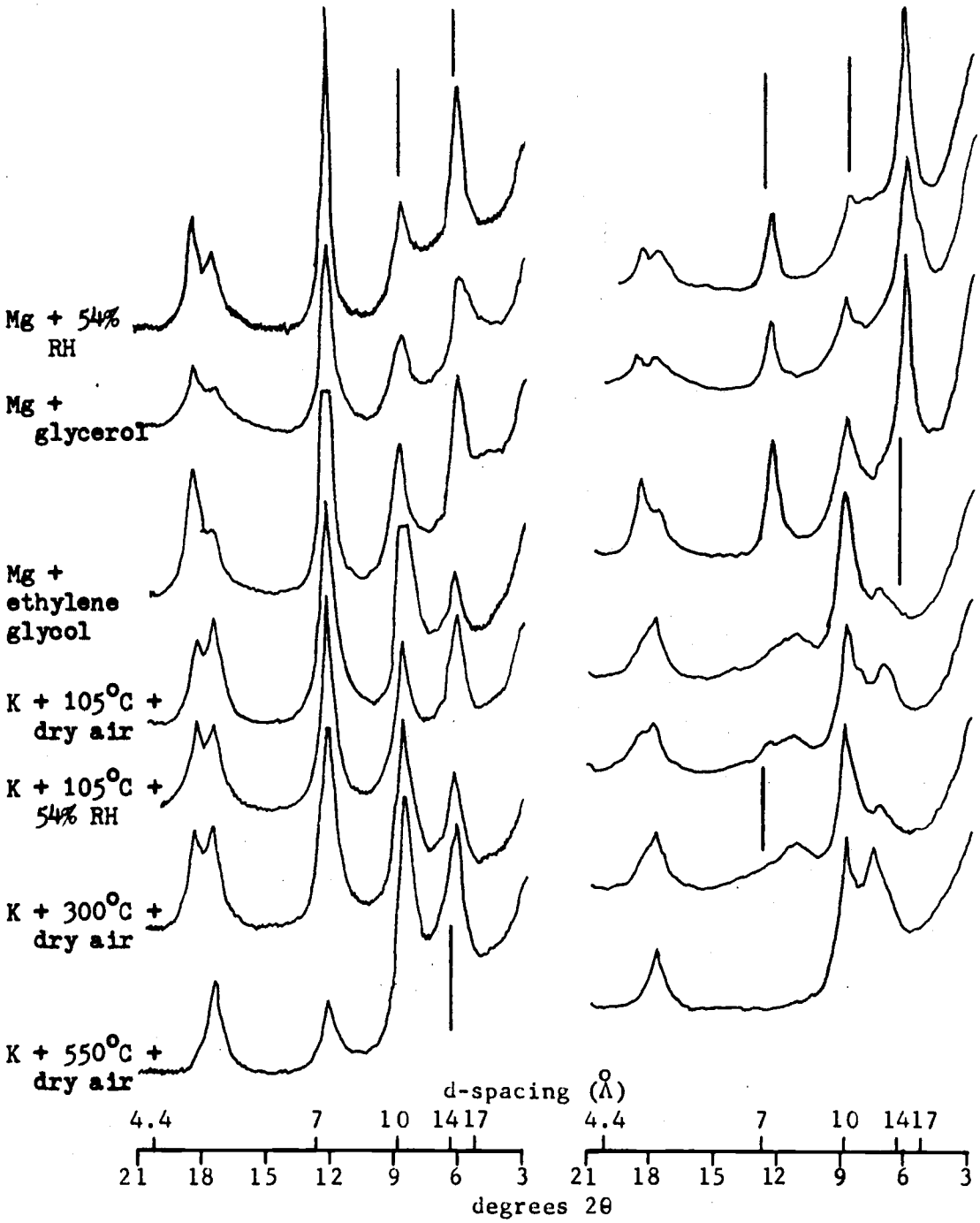

Figure 56. XRD patterns of failure material sample a (left) and failure surface sample b (right), site R-1.

Finally, soil of a sample from the Otter Point geologic formation along the Sixes River contains chlorite, mica and perhaps kaolinite as the major constituents; however, the strong presence of well crystallized montmorillonite is also indicated by the XRD patterns (Figure 57). The site is undergoing deep seated soil creep and is prone to small scale slumping. The instability of this part of southwestern Oregon is great enough to merit considerably more study.

Major differences noted between the Klamath Mountain sites and those of the Western Cascades are the apparent scarcity of perched water tables and the lack of amorphous and halloysite clays in the Klamaths. Overall, the clay minerals of the Klamath sites are much more distinct, better crystalline phyllosilicates which seem to be less prone to failure by debris flow.

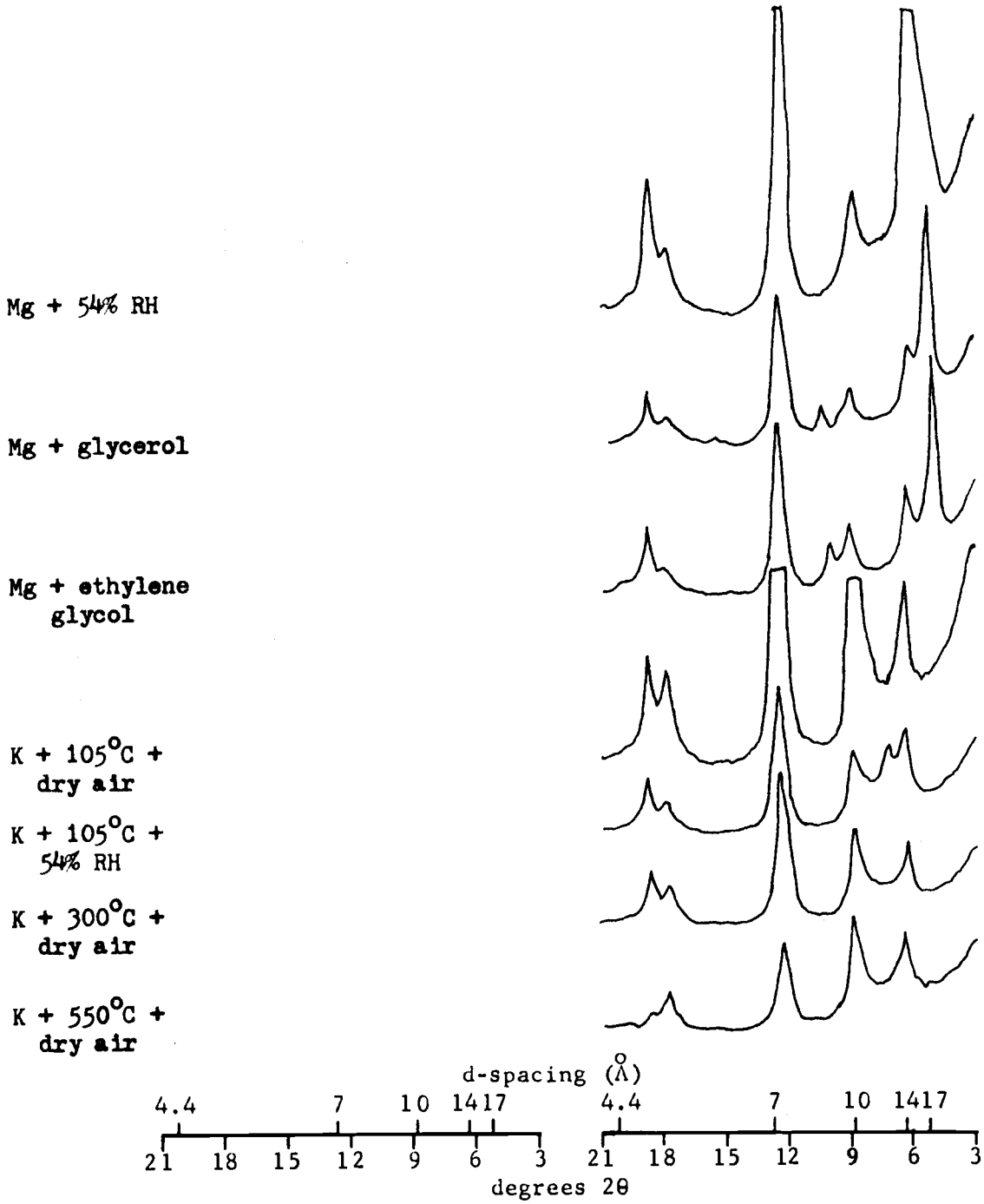

Figure 57. XRD patterns of clay from site S-1 along the Sixes River.

BIBLIOGRAPHY

Brindley, G. W. 1961. Kaolin, serpentine and kindred minerals. In Brown, G. (ed.). The x-ray identification and crystal structures of clay minerals. Mineralogical Society, London. pp. 51-131.

Bradley, W. F. and R. E. Grim. 1961. Mica clay minerals. In: Brown, G. (ed.). The x-ray identification and crystal structures of clay minerals. Mineralogical Society. London. pp. 208-241.

Winzler and Kelly Engineers. 1975. Redwood Creek - an integrated study. Winzler and Kelly Engineers Water Laboratory. P. O. Box 1345. Eureka, Ca. 95501. 44 pp.

APPENDIX II
FIELD DATA FORM AND FIELD DATA

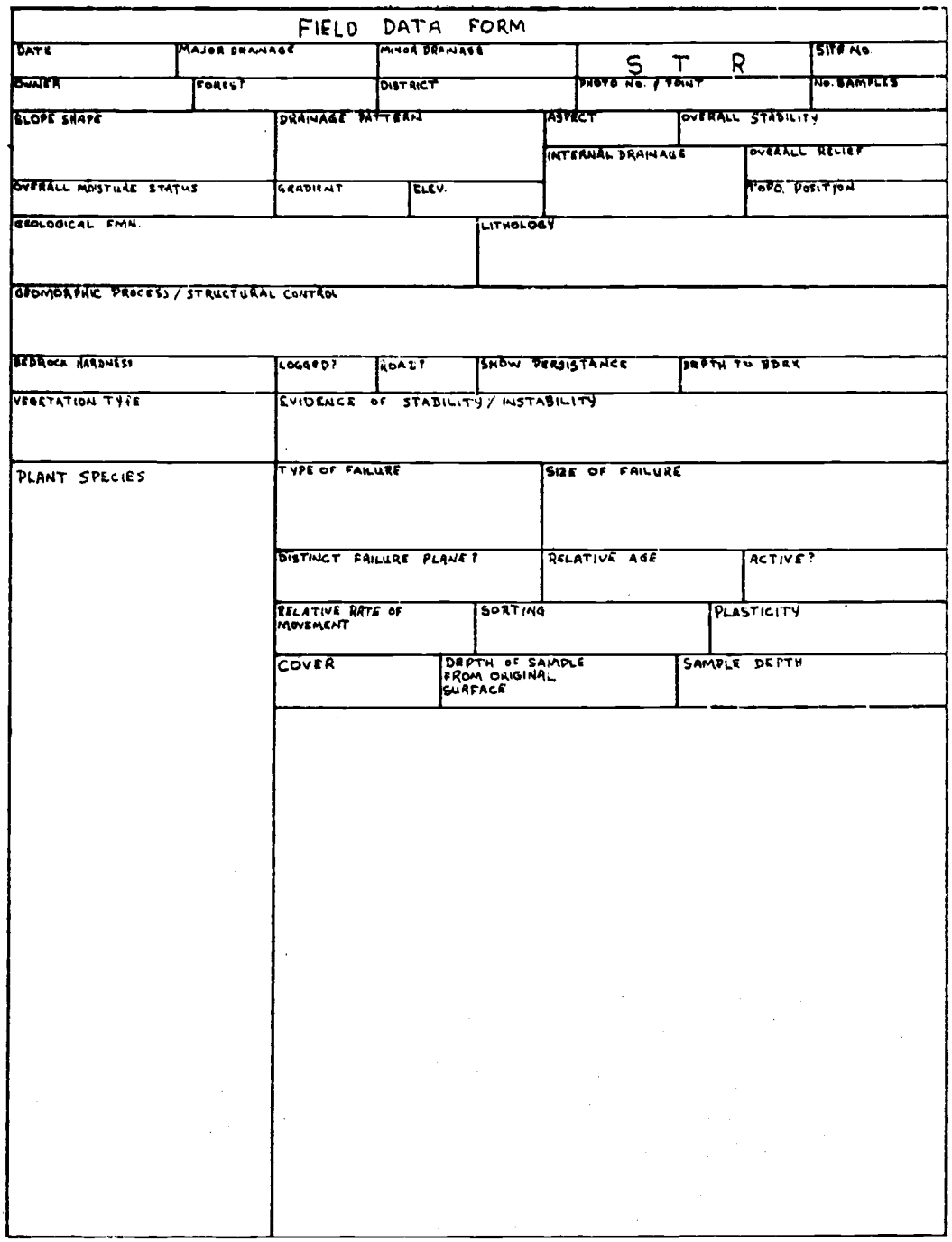

Figure 58. Field Data Form.

Site no.: NS-BC-1 No. samples: 6

Major drainage: North Santiam

Minor drainage: Box Canyon Creek

Overall stability: very unstable

Location: SWNW S15, T11S, R5E; below Rd. 1158H

Geologic formation: Sardine (Tsa), near contact with High Cascade Volcanics (QTv)

Lithology & soil: hard silicate rock (agate), basaltic colluvium & volcanic ash (?) overlying red & green plastic clay formed from reddish & greenish pyroclastic rock; quartz intrusions in the breccia; overlying soil has good drainage

Elevation: 1040 m Aspect: SW Gradient: 50%

Slope shape: overall convex with benches Logged: yes

Vegetation: Douglas-fir, rhododendron

Evidence of stability/instability: Fresh debris avalanches, benchy topography with old slump blocks, tension cracks in nearby road

Failure description: moderate sized, recent debris avalanche with distinct failure plane of cohesionless soil over plastic reddish & greenish clay; not road related

Sample locations & depths: sample a--surface soil (0-50 cm) above crown of failure; sample b--head of slide, 45 cm from top, surface material; sample c--crusty debris surface midslope in slide; sample d--reddish clay; sample e--yellowish material associated with reddish clay; sample f--greenish clay

Site no.: NS-BC-2 No. samples: 1

Major drainage: North Santiam

Minor drainage: Box Canyon Creek

Overall stability: very unstable

Location: NESW S15, T11S, R5E; cutbank Rd. 1158H

Geologic formation: Sardine (Tsa)

Lithology & Soil: basaltic (?) colluvium with reddish-brown, wet, soil, sleazy & slightly sticky; green breccia beneath

Elevation: 1150 m Aspect: W Gradient: 30%

Slope shape: rumpled, overall convex Logged: yes

Vegetation: Douglas-fir, rhododendron

Evidence of stability/instability: hummocky topography, water emerging from slope, small cutbank failures, tension cracks in road

Failure description: small road cut debris flow failure in large ancient rotational slump which occurred in deeper material

Sample location & depth: 30 cm deep into failing roadcut ¼ mi N of Rd. 1158 junction & approx. 50 m N of Creek

Site no.: MS-Q-1 No. samples: 4

Major drainage: Middle Santiam

Minor drainage: Quartzville Creek

Overall stability: unstable

Location: SENW S29, T11S, R5E

Geologic formation: Sardine (Tsa)

Lithology & Soil: basaltic colluvium (cobbles), some with dark green weathering surfaces; silty soil, sleazy, slightly sticky, holds much water, flows readily when disturbed

Elevation: 850 m Aspect: SSE Gradient: variable

Slope shape: convex to slightly concave Logged: yes

Vegetation: Douglas-fir, fireweed, alder, Equisetum, western hemlock, blackberry

Evidence of stability/instability: fresh failure surfaces, hummocky topography, jackstrawed trees, cracks in road, water emerging from fresh failure

Failure description: large active earthflow with several smaller recent debris flows with barren surfaces

Sample location & depth: sample a--composite of material which flowed from fresh failure; sample b--upper portion of set zone in fresh failure surface, very little clay in this; sample c--30 cm deep into soil near top of fresh failure surface immediately above wet zone; sample d--75 cm deep into soil near top of fresh failure surface and in wet zone

Site no.: MS-D-1 No. samples: 1

Major drainage: Middle Santiam

Minor drainage: Donaca Creek

Overall stability: very unstable

Location: NENE S10, T12S, R5E; Donaca Scarp

Geologic formation: Little Butte (Tlt) at contact with Sardine (Tsa)

Lithology & soil: greenish pyroclastic tuff & breccia

Elevation: 1150 m Aspect: S Gradient: 100%

Slope shape: slightly convex to concave Logged: no

Vegetation: Douglas-fir, alder, rhododendron

Evidence of stability/instability: large headwall scarps of ancient failures with lake & sink ponds below, large pressure ridges, jackstrawed trees

Failure description: very large ancient slump earthflow which is still active

Sample location & depth: approx 50 m down from top & at eastern edge of headwall scarp in large fissure

Site no: MS-P-1 No. samples: 10

Major drainage: Middle Santiam

Minor drainage: Pyramid Creek (Single Creek)

Overall stability: unstable

Location: SWNW S19, T12S, R6E; along Rd. 1234

Geologic formation: Little Butte (Tlt) near contact with High Cascade Volcanics (QTv)

Lithology & soil: subangular to subrounded basaltic or andesitic cobbles overlying decomposed igimbrite; soil well drained above crown of ancient slump, poorly drained in mid & lower portions where reddish-brown sleazy (i.e., slippery but not sticky) soil overlies heavier, plastic clay

Elevation: 1120 m Aspect: NW Gradient: 45-70%

Slope shape: concave in failure, convex laterally adjacent, little curvature above

Vegetation: large Douglas-fir, western red cedar, western hemlock, true fir, devil's club, rhododendron, alder, Equisetum, sword & bracken fern

Evidence of stability/instability: ancient slump blocks, reactivated by road construction resulting in recent debris flow

Failure description: large, ancient multiple rotational slump with small debris flow above toe triggered by road construction activity

Sample location & depths: sample a--15 m above crown of main ancient scarp in drier, more stable condition than that downslope, 15 cm depth; sample b--same location as sample a, 75 cm depth; sample c--wet slumpy region 75 m downslope from stable profile samples a & b and 30 m upslope from newly failed material, 5-10 cm depth; sample d--same profile as sample c, 15 cm depth; sample e--same profile as sample c, 45 cm depth; sample f--same profile as sample c, 75 cm depth; sample g--road cut bank left of left flank (southwest), 2 m from surface; sample h--middle portion of freshest, radially cracked failure area, 10 m above road, 60 cm depth; sample i--inside right flank; sample j--road cut bank, right of right flank

Comments: Site very wet and holds much water, even on steep (70%) slope

Site no.: MS-1 No. samples: 1

Major drainage: Middle Santiam

Minor drainage: same

Overall stability: very unstable

Location: NWNE S26, T12S, R5E

Geologic formation: Little Butte (Tlt)

Lithology & soil: moderately hard to moderately soft, highly altered andesitic rocks with mixed glacial (?) debris on surface; soil slightly sticky & sleazy, moderately high water retention

Elevation: 670 m Aspect: N Gradient: 60-80%

Slope shape: convex to concave Logged: yes

Vegetation: Douglas-fir, western red cedar, western hemlock

Evidence of stability/instability: large, ancient slumps common in area, numerous road cutbank failures, large tension cracks, jack-strawed & split trees, recent road fill failures

Failure description: large, translational road fill debris flow failure with distinct failure plane

Sample location & depth: 20 cm deep into road cut bank

Comments: Road has failed at least twice at this location, most recently in spring 1976, and will fail again; flow of material from earlier failure inundated trees at bottom of slope & is probably responsible for death of large western red cedars; site is on verge of failing again

Site no.: MS-2 No. samples: 1

Major drainage: Middle Santiam

Minor drainage: same

Overall stability: very unstable

Location: SWNE S27, T12S, R5E; along Rd. 1263

Geologic formation: Little Butte (Tlt)

Lithology & soil: moderately hard to hard porphyritic basaltic rock & mixed glacial debris with moderately well drained surface soil over wet clayey material

Elevation: 800 m Aspect: NE Gradient: 40%

Slope shape: convex overall Logged: yes

Vegetation: Douglas-fir, Equisetum

Evidence of stability/instability: hummocky ground, numerous small slumps, jackstrawed trees

Failure description: one of several small, poorly defined road cut slumps in a much larger, older slump

Sample location & depth: random sample, 50 cm deep into wet, exposed soil.

Site no.: MS-J-1 No. samples: 2

Major drainage: Middle Santiam

Minor drainage: Jude Creek

Overall stability: unstable

Location: SESE S33, T12S, R5E; along Rd, 1263G

Geologic formation: Sardine (Tsa) near contact with High Cascade Volcanics (QTv)

Lithology & soil: soft to moderately hard altered porphyritic andesitic rock with well drained soil

Elevation: 1150 m Aspect: ENE Gradient: 55%

Slope shape: slightly convex to slightly concave Logged: yes

Failure description: recent debris avalanche up to 3 m deep in road cut and fill with flow at toe

Sample locations & depths: Sample a--failed soil from above which dropped into road; sample b--random sample from remaining road cut bank

Site no.: MS-B-1 No. samples: 3

Major drainage: Middle Santiam

Minor drainage: Bachelor Creek

Overall stability: unstable

Location: NENE S3, T13S, R5E

Geologic formation: Sardine (Tsa)

Lithology & soil: subangular porphyritic basaltic cobbles in well drained soil 1 m deep overlying highly altered plastic, clayey greenish pyroclastic material with colorful greens, yellows, reds

Elevation: 1000 m Aspect: N Gradient: 50%

Slope shape: variable, convex at failure Logged: yes

Vegetation: Douglas-fir, western red cedar, western hemlock, rhododendron, alder, twinflower, prince's pine

Evidence of stability/instability: recent failure, hummocky topography, old slumps common, numerous road cut bank failures

Failure description: small, fresh, well defined rotational failure with distinct failure surface in weathered breccia & some planar sliding of basaltic material off the pyroclastic

Sample locations & depths: sample a--failed material at failure surface, 2¼ m from soil surface; sample b--below failure surface, 3 m from soil surface; sample c--random sample from roadcut bank in larger slump deeper into weathered pyroclastic, 6 m depth from soil surface

Comments: Most water in soil is in upper 30 cm of the weathered pyroclastic clay; tree roots are more abundant in the upper soil which has formed in the basaltic cobbles

Site no.: MS-H-1 No. samples: 2

Major drainage: Middle Santiam

Minor drainage: Holman Creek

Overall stability: very unstable

Location: SENW S2, T13S, R5E; along Rd. 1304

Geologic formation: Sardine (Tsa) near contact with Little Butte (Tlt)

Lithology & soil: basaltic flow rock approx. 5 m thick over reddish breccia with interlayered greenish breccia

Elevation: 1000 m Aspect: N

Slope shape: variable Logged: yes

Vegetation: Douglas-fir, rhododendron, western red cedar

Evidence of stability/instability: fresh rotational scarp, tilted trees, obvious slump block

Failure description: large rotational slump (75 m across) composed of several blocks with distinct failure plane near headwall, probably ancient failure which has reactivated several times

Sample locations & depths: sample a--small debris pile of failed material; sample b--road bank above debris pile

Site no.: SS-SF-1 No. samples: 12

Major drainage: South Santiam

Minor drainage: Soda Fork

Overall stability: unstable

Location: NWSE S5, T13S, R5E

Geologic formation: Sardine (Tsa)--Little Butte (Tlt) contact & near contact of High Cascade Volcanics (QTv)

Lithology & soil: wet, reddish-brown sleazy soil which flows when disturbed & containing angular cobbles of porphyritic basaltic colluvium overlying plastic, clayey highly weathered pyroclastic material of mottled yellowish to grayish color

Elevation: 1030 m Aspect: SE Gradient: 30-50%

Slope shape: convex to slightly concave Logged: no above failure

Vegetation: western red cedar, western hemlock, Douglas-fir, rhododendron, true fir

Evidence of stability/instability: fresh failure in road cut, water emerging, apparent large ancient slump block

Failure description: relatively small debris flow of reddish-brown soil over plastic clay; also a large ancient rotational slump with failure plane probably in the heavy clay

Sample locations & depths: sample a--unfailed surface horizon soil at edge of clearcut above failure, ½ m depth; sample b--same profile as sample a, 2½ m depth; sample c--downslope from samples a & b at base of ancient headwall scarp, 2½ m depth; sample d--downslope from sample c & upslope from fresh debris flow, 2½ m depth; sample e--wet, sensitive material at head of recent debris flow, 2 m depth; sample f--saturated sensitive soil at top of failure plane, 3 m depth; sample g--yellowish plastic saprolite beneath sample f, supports water table, 3½ m depth; sample h--yellowish saprolite beneath sample g, 4 m depth; sample i--left flank debris flow, reddish brown soil, 1 m depth; sample j--beneath sample i, 1½ m depth; sample k--stable cut bank to right of debris flow, 3¼ m depth; sample l--stable soil from road back SW of creek, 3 m depth.

Comments: perched water table on heavy plastic clay, reddish-brown soil remains wet year round and is much less stable than the heavy clay

Site no.: SS-SF-2 No. samples: 1

Major drainage: South Santiam

Minor drainage: Soda Fork

Overall stability: stable

Location: SWSE S5, T13S, R5E; 0.3 mi N of Rd. 1366-1263K jct.

Geologic formation: Sardine (Tsa) at contact with Little Butte (Tlt)

Lithology & soil: well drained shallow, hard soil to weathered pyroclastic (?) bedrock containing inclusions of highly weathered porphyritic andesitic rock

Elevation: 1020 m Aspect: SE Gradient: 35%

Slope shape: convex Logged: no

Vegetation: Douglas-fir, rhododendron

Evidence of stability/instability: smooth, stable road cutbanks, dry, no evidence of instability

Failure description: none

Sample location & depth: cut bank of small borrow pit at road pullout, 1½ m depth from soil surface

Comments: appears to be a dry stable ridge with wet, unstable areas on either side

Site no.: SS-SF-3 No. samples: 2

Major drainage: South Santiam

Minor drainage: Soda Fork

Overall stability: unstable

Location: SWSE S5, T13S, R5E; along Rd. 1366K

Geologic formation: Little Butte

Lithology & soil: sleazy, reddish-brown soil with subrounded basaltic cobbles overlying plastic, yellowish saprolite which appears to have originated from greenish pyroclastic rock; basaltic cobbles have worked their way into the upper meter of saprolite

Elevation: 960 m Aspect: SSW

Slope shape: slightly concave Logged: no

Vegetation: western red cedar, western hemlock, Douglas-fir rhododendron, salal

Evidence of stability/instability: fresh road cut failures

Failure description: recent road cut debris flow failure of reddish-brown soil sliding off the underlying saprolite & with a larger, much deeper ancient rotational failure probably in the saprolite

Sample locations & depths: sample a--reddish-brown material at upper boundary of yellowish saprolite, $2\frac{1}{2}$ m from soil surface; sample b--yellowish material beneath, 3 m depth from original soil surface

Comments: perched water table on saprolite; conditions here are similar to those at site SS-SF-1 and several other unsampled sites in the area

Site no.: SS-SF-4 No. samples: 3

Major drainage: South Santiam

Minor drainage: Soda Fork

Overall stability: moderately stable, locally unstable

Location: SESW S18, T13S, R5E; along Rd. 1366

Geologic formation: Little Butte (Tlt)

Lithology & soil: mixed lithology of moderately soft, highly weathered pyroclastic rock which failed, andesitic rock at the right flank and a layer of sandstone (large colluvial boulder?) 3 m from the original soil surface which apparently served as a conduit for water over the pyroclastic material; subangular, poorly sorted colluvial cobbles of porphyritic andesitic and rhyolitic rock are mixed in the weathered pyroclastic material; angular blocky, clayey soil of the scarp has poorly defined bands of reddish & yellowish color

Elevation: 600 m Aspect: SSW Gradient: 65%

Slope shape: convex Logged: no

Vegetation: Douglas-fir, western red cedar, western hemlock

Evidence of stability/instability: fresh road cut failure; soil adjacent to this site is very shallow to bedrock & hence more stable

Failure description: road cut failure approx. 15 m across & with distinct failure plane at head wall occurred spring 1975

Sample locations & depths: sample a--material that has actually failed & dropped approx. 1 m from above at left flank to 2½ m from original soil surface; sample b--material of the left flank scarp wall, suspected at the time of sampling to be same as sample a, 2½ m depth from original soil surface; sample c--multicolored, brown, red, yellow material of head wall scarp, 1 m below siltstone & 4 m below original soil surface

Site no.: SS-SF-5 No. samples: 4

Major drainage: South Santiam

Minor drainage: Soda Fork

Overall stability: moderately stable except that steep slopes are subject to debris avalanche when slope is undercut

Location: SWSW S18, T13S, R5E; along Rd. 1366

Geologic formation: Little Butte (Tlt)

Lithology & soil: shallow, highly permeable, nonplastic coarse textured soil with subangular porphyritic andesitic and rhyolitic (?) stones & cobbles overlying highly altered, moderately soft unidentifiable rock surface

Elevation: 600 m Aspect: WSW Gradient: 65-70%

Slope shape: slightly convex Logged: regenerated

Vegetation: Douglas-fir, western hemlock, western red cedar, alder, vine maple, sword fern, big leaf maple, salal

Evidence of stability/instability: shallow cut bank sloughing common, sweep & pistol butts on trees

Failure description: recent debris avalanche 2 m deep above road

Sample locations & depths: sample a--left flank, A horizon 10-15 cm depth; sample b--left flank, C horizon 75 cm depth; sample c--midslope slip plane in highly altered rock outcrop, 1½ m from original surface; sample d--midslope slip plane in clayey material adjacent to altered rock outcrop

Comments: area is very unstable with respect to the occurrence of shallow debris avalanche failures where the steep slope has been undercut; otherwise these materials couls be considered stable

Site no.: SS-SF-6 No. samples: 1

Major drainage: South Santiam

Minor drainage: Soda Fork

Overall stability: moderately stable

Location: NWNW S19, T13S, R5E

Geologic formation: Little Butte (Tlt)

Lithology & soil: reddish breccia

Elevation: 490 m Aspect: E Gradient: 50%

Slope shape: convex Logged: yes

Evidence of stability/instability: small debris torrent in stream channel subjected to poor quality timber harvesting operation, most erosion is surficial, otherwise relatively stable with steep slopes

Failure description: debris torrent which scoured tributary stream channel

Sample location & depth: random sample in stream bed in area of torrent

Site no.: SS-SF-7 No. samples: 1

Major drainage: South Santiam

Minor drainage: Soda Fork

Overall stability: moderately stable to stable

Location: SESE S24, T13S, R4E

Geologic formation: Little Butte (Tlt)

Lithology & soil: greenish to reddish moderately hard pyroclastic rock

Elevation: 475 m Aspect: ESE Gradient: 70%

Slope shape: convex Logged: no

Vegetation: Douglas-fir, western hemlock, vine maple, big leaf maple, fern

Evidence of stability/instability: road cut banks show little sloughing, smooth slopes, no evidence of significant instability

Failure description: none

Sample location & depth: road cut bank, 3 m down from top of bank

Site no.: SS-3-2 No. samples: 4

Major drainage: South Santiam

Minor drainage: Sheep Creek

Overall stability: very unstable

Location: SWNE S28, T13S, R5E; facing creek at Hwy 20 bridge

Geologic formation: Little Butte (Tlt)

Lithology & soil: very loose angular basaltic cobbles & gravels make up 40-50% of soil profile which is well drained above & moderately well drained below 1 m depth

Elevation: 670 m Aspect: E Gradient: 50%

Slope shape: convex Logged: no

Vegetation: Douglas-fir, western red cedar, western hemlock, rhododendron, salal, ferns

Evidence of stability/instability: fresh failures, jackstrawed trees, tension cracks, hummocky ground

Failure description: recent debris avalanche with failure plane distinct near the top but obscured by debris below

Sample locations & depths: sample a--top of head wall scarp in A horizon, 2-70 cm depth; sample b--B horizon, 70-100 cm depth; sample c--upper right flank 3 m horizontally south of a & b & 2 m depth, material here is relatively hard & blocky & appears stable due to its dryness

Site no.: SS-S-3 No. samples: 6

Major drainage: South Santiam

Minor drainage: Sheep Creek

Overall stability: very unstable

Location: NWSE S28, T13S, R5E; facing Hwy 20 at bridge

Geologic formation: Little Butte (Tlt)

Lithology & soil: brownish to multicolored colluvial soil, 1-2 m deep at crown of main scarp overlies deposit of brown subangular colluvial cobbles 4-6 m thick which overlies gray, glacially deposited subrounded cobbles & boulders of basaltic rock with quartz intrusions & clayey soil

Elevation: 680 m Aspect: S Gradient: 40%

Slope shape: convex to concave Logged: no

Vegetation: alder, Equisetum, Douglas-fir, western red cedar, western hemlock, rhododendron, salal, ferns, whortle berry, twinflower

Evidence of stability/instability: fresh failure surface, jackstrawed trees, hummocky ground, tension cracks

Failure description: rapid translational failure of brown colluvial material off the gray glacial deposit leaving distinct failure plane with somewhat rotational component in the colluvium

Sample locations & depths: sample a--left flnk, A horizon, 10 cm depth; sample b--left flank, 1 m depth; sample c--left flank 1½ m depth; sample d--left flank, 2 m depth; sample e--left flank 10 m downslope from a-d & 1 m depth; sample f--gray glacial material in main head scarp 10 m below crown

Comments: water emerging at contact of brown colluvium & gray glacial material; soil deposited on bench created on failure plane of glacial material is wet year around & has flowed here from above

Site no.: SS-1 No. samples: 1

Major drainage: South Santiam

Minor drainage: same

Overall stability: moderately stable to unstable

Location: NENE S36, T13S, R4E; along Hwy 20

Geologic formation: Little Butte (Tlt)

Lithology & soil: shallow coarse textured soil with 50-60% coarse fragments over moderately soft bedrock of greenish & some reddish pyroclastic material

Elevation: 470 m Aspect: SSW Gradient: 65%

Slope shape: convex Logged: no

Vegetation: Douglas-fir, bracken fern, madrone, salal, vine maple, alder

Evidence of stability/instability: freshly sloughed road cut & large failures where soil deposits have been undercut, otherwise stable due to bedrock control

Failure description: debris avalanche above Hwy 20

Sample location & depth: left flank 8-9 m from crown & 1½ m from original surface

Site no.: MK-D-1 No. samples: 3

Major drainage: McKenzie River

Minor drainage: Deer Creek (Cadenza Creek)

Overall stability: unstable

Location: NNW S28, T14S, R6E; south of wildcat Mtn.

Geologic formation: High Cascade Volcanics (QTv) above (?) contact with Sardine (Tsa)

Lithology & soil: porphyritic andesitic cobbles with few fragments of reddish vesicular rhyolite (?) & some volcanic ash overlying clayey weathered pyroclastic rock

Elevation: 1300 m Aspect: SW Gradient: 50%

Slope shape: slightly convex to concave Logged: yes

Vegetation: Ceanothus, pachistima, vine maple, thimbleberry, Ribes, wild rose, lupine, sword fern

Evidence of stability/instability: fresh failure, old slump scarps & benches

Failure description: ancient rotational slump, 40 m across with debris flow of material above saprolite

Sample locations & depths: sample a--left flank failure plane, $\frac{1}{2}$ m deep & 3 m from original surface; sample b--left flank, 1 m deep & 3-4 m from original surface, represents wetter material underlying material of sample a; sample c--right flank plastic clay in weathered pyroclastic rock

Site no.: MK-F-1 No. samples: 1

Major drainage: McKenzie

Minor drainage: Fritz Creek

Overall stability: stable

Location: NESE S33, T14S, R6E; near head of drainage

Geologic formation: High Cascade Volcanics (QTv)

Lithology & soil: moderately hard nonvesicular dacite (?) bedrock overlain (?) mostly by subangular vesicular andesite (?) and reddish rhyolite (?) colluvium & a few subrounded glacial remnants; soil gravelly & very porous with many pores several cm in diameter

Elevation: 1340 m Aspect: NE Gradient: 65%

Slope shape: flat to slightly convex Logged: yes

Vegetation: Douglas-fir, western hemlock, rhododendron, western red cedar

Evidence of stability/instability: long smooth slopes, no evidence of old failures, stable road cutbanks, pistol butted trees suggesting dry surficial creep

Failure description: none

Sample location & depth: road cutbank 1½ m from top, ½ m depth

Comments: appears typical of the few stable sites in the Western Cascades i.e., higher elevation, shallow soil over hard bedrock, dry, coarse textured soil

Site no.: MK-L-1 No. samples: 1

Major drainage: McKenzie River

Minor drainage: Lookout Creek

Overall stability: moderately stable

Location: ENW S19, T15S, R6E

Geologic formation: Sardine (Tsa)

Lithology & soil: cobbly, coarse textured, high porosity soil containing poorly sorted subangular basaltic cobbles & boulders

Elevation: 1160 m Aspect: S Gradient: 80%

Slope shape: convex to concave Logged: yes

Vegetation: Douglas-fir, chinkapin, fireweed, ceanothus, pachistima, vine maple, sambucus

Evidence of stability/instability: large road cutbank intact, trees straight, soil dry, surrounding area unstable

Failure description: none

Sample location & depth: road cutbank

Comments: surrounding area unstable & this site which is stable, is probably the scarp of a large, ancient slump

Site no.: MK-L-2 No. samples: 2

Major drainage: McKenzie River

Minor drainage: Lookout Creek

Overall stability: unstable

Location: SESW S19, T15S, R6E

Geologic formation: Sardine (Tsa)

Lithology & soil: porous, well drained, nonplastic soil with poorly sorted, subangular colluvial basaltic cobbles & boulders

Elevation: 975 m Aspect: S Gradient: 20%

Slope shape: slightly convex Logged: no

Vegetation: western red cedar, Douglas-fir, pachistima, western hemlock, Oregon grape, sword fern, beargrass

Evidence of stability/instability: jackstrawed trees, rumpled ground

Failure description: ancient, active earthflow

Sample locations & depths: middle portion of earthflow in bank of dry stream sample a--3 m vertically up from stream bottom, 1 m depth; sample b--½ m vertically up from stream bottom, 1 m depth

Comments: Although this is an active earthflow, this site appears fairly stable within the flow. Material apparently is being rafted along this flow. Earthworm found in this soil.

Site no.: MK-L-3 No. samples: 1

Major drainage: McKenzie

Minor drainage: Lookout Creek

Overall stability: very unstable

Location: W S30, T15S, R6E; same earthflow as site MK-L-2, near Swanston's inclinometer tube

Geologic formation: Sardine (Tsa)

Lithology & soil: soil is very cobbly & similar to that of site MK-L-2 but is wetter, very slightly sticky & more plastic; moderately poorly sorted subangular basaltic cobbles & boulders

Elevation: 880 m Aspect: S Gradient: 5-10%

Slope shape: slightly convex to concave Logged: no

Vegetation: Douglas-fir, western hemlock, Equisetum, fireweed, mosses, alder, western red cedar, willow, sword fern, vine maple, pearly everlasting

Evidence of stability/instability: jackstrawed trees, small fresh scarp at sample site, hummocky ground, tension cracks, pressure ridges

Failure description: large earthflow undergoing deep creep

Sample location & depth: lower end of flow along bank of Lookout Creek, 3 m down from top of bank & a m depth

Site no.: SFMK-B-1 No. samples: 5

Major drainage: S. Fork McKenzie River

Minor drainage: Boone Creek

Overall stability: unstable

Location: SESW S17, T17S, R5E

Geologic formation: Sardine (Tsa)

Lithology & soil: colluvial, subangular, basaltic cobbles and highly weathered rhyolitic (?) porphyry cobbles overlying & mixed with degraded multicolored, generally greenish breccia

Elevation: 610 m Aspect: E Gradient: 10-20%

Slope shape: slightly convex Logged: no

Vegetation: Equisetum, salal, alder, Douglas-fir, western red cedar, big leaf maple, sword fern, mosses, western hemlock

Evidence of stability/instability: jackstrawed trees, road displaced, wet, rumpled ground

Failure description: actively creeping earthflow

Sample locations & depths: left flank of earthflow along Boone Creek streambank sample a--highly weathered, homogeneous material, 1 m depth; sample b--gray subsample 1½ m depth; sample c--reddish subsample 1½ m depth; sample 3--maroon subsample 1½ m depth; sample e--probably the most representative, 2 m depth

Site no.: NFMFW-C-1 No. samples: 3

Major drainage: North Fork Middle Fork Willamette

Minor drainage: Christy Creek

Overall stability: stable, locally unstable

Location: NWNE S30, T18S, R5E; South Hardy Pass

Geologic formation: Sardine (Tsa)

Lithology & soil: moderately soft, dark gray to reddish rhyodacite (?) porphyry (similar to rock found at site MK-SF-1) with shallow, coarse textured, nonplastic, well drained soil

Elevation: 1500 m Aspect: W Gradient: 55%

Slope shape: slightly convex Logged: yes

Vegetation: alder, pearly everlasting, rush, noble fir, ceanothus, lupine, fireweed, white pine

Evidence of stability/instability: small, recent failure, otherwise long smooth slopes & little sign of instability

Failure description: planar flowage of soil (approx. 30 m across & 2-3 m deep) over decomposing bedrock

Sample locations & depths: sample a--surficial soil layer in failure, 75 cm thick, sampled at 50 cm depth; sample b--wet gravel layer 15 cm thick underlying surficial soil & overlying decomposing bedrock; sample c--dry road cut just north of failure, 1 m depth in shallow soil overlying reddish bedrock

Comments: water emerging from slope at failure site; gravel layer (sample b) acts as a water conduit

Site no.: MK-D-2 No. samples: 1

Major drainage: McKensie

Minor drainage: Deer Creek

Overall stability: unstable

Location: WSW S33, T14S, R6E

Geologic formation: Sardine (Tsa?)

Lithology & soil: moderately soft greenish pyroclastic rock overlain by basaltic colluvium of variable thickness

Elevation: 1000 m Aspect: WNW Gradient: 100% (?)

Slope shape: slightly convex Logged: no

Vegetation: Douglas-fir, western red cedar, fireweed, grand fir, Vaccinium, rhododendron, pachistima, sword fern, western hemlock, vine maple

Evidence of stability/instability: fresh failures, stream cuts through old slump block

Failure description: series of small (15 m across debris flow failures on much larger, ancient, slump

Sample location & depth: head region of planar failure near failure plane, approx. 1 m from original soil surface

Site no.: MFW-1 No. samples: 2

Major drainage: Middle Fork Willamette

Minor drainage: same

Overall stability: unstable

Location: NESE S11, T22S, R3E; just south of Modoc Creek

Geologic formation: Little Butte (Tlt)

Lithology & soil: colluvial subangular cobbles of weathered basaltic rock and some sandstone ½ m deep, overlying 30 cm of heavy, plastic dark brown to yellowish banded clay, overlying plastic, mottled dark brown and gray clay containing fragments of greenish breccia; soil generally is somewhat poorly drained

Elevation: 490 m Aspect: NW Gradient: 70%

Slope shape: convex Logged: no

Vegetation: Douglas-fir saplings, western red cedar, sugar pine seedlings, alder, bunchgrasses, madrone, salal, bracken fern

Evidence of stability/instability: numerous small planar failures which have moved only a few meters, tension cracks

Failure description: shallow (1 m deep) progressive planar failure with rotational components and small earthflow 10 m wide & 10 m long with distinct failure plane

Sample locations & depths: sample a--left flank in heavy, banded clay, 75 cm depth; sample b--left flank beneath sample a in mottled clay, 2 m depth

Comments: probably reactivated toe portion of ancient slump block; water draining out at toe, supporting cattails, rush, Equisetum

Site no.: MFW-L-1 No. samples: 2

Major drainage: Middle Fork Willamette

Minor drainage: Hills Creek (Landes Creek)

Overall stability: very unstable

Location: SENW S21, T22S, R4E

Geologic formation: Little Butte (Tlt)

Lithology & soil: mixed lithology of poorly sorted greenish breccia, basaltic cobbles & boulders & weadly cemented subrounded to rounded moderately sorted lahar (?) gravels & cobbles; silty clay, angular blocky mottled soil with much oxidized iron & clay pseudomorphs

Elevation: 730 m Aspect: ENE Gradient: 35%

Slope shape: slightly convex

Vegetation: Douglas-fir, western red cedar, black cottonwood, western hemlock, Equisetum, manzanita, salal, rush, rhododendron, alder, Vaccinium, thimbleberry

Evidence of stability/instability: pressure ridges, tension cracks, jackstrawed trees, hummocky ground, small slumps along creek banks

Failure description: large, active earthflow

Sample locations & depths: sample a--along creek bank in upper central portion of earthflow, 10 cm below surface; sample b--large pressure ridge crossed by road, 1 m depth

Comments: soil of pressure ridge appears to be much higher in plastic clay than does soil of central portion of earthflow

Site no.: MFW-BW-1 No. samples: 1

Major drainage: Middle Fork Willamette

Minor drainage: Big Willow Creek

Overall stability: moderately stable

Location: SW S24, T22S, R3E

Geologic formation: Little Butte (Tlt) below contact (?) with High Cascade Volcanics (QTv)

Lithology & soil: moderately hard rhyodacite (?) dike with shallow, coarse textured, relatively dry soil

Elevation: 800 m Aspect: SE Gradient: 50%

Slope shape: slightly convex to flat Logged: no

Vegetation: Douglas-fir, western red cedar, grand fir, bunchgrasses, salal

Evidence of stability/instability: no obvious evidence of failure, even slopes, mostly straight trees but a few have pistol butts, no water emerging

Failure description: none

Sample location & depth: roadcut 1½ m from surface, 15 cm depth at bedrock

Site no.: MFW-CP-1 No. samples: 3

Major drainage: Middle Fork Willamette

Minor drainage: Coffeepot Creek

Overall stability: unstable

Location: NWNE S12, T23S, R3E

Geologic formation: Little Butte (Tlt)

Lithology & soil: glacially deposited vesicular porphyritic andesitic cobbles & boulders (1 m thick) over reddish tuff (?) (5 m thick) over thin bed of sedimentary rock; soil slightly plastic, somewhat poorly drained

Elevation: 1080 m Aspect: NNE Gradient: 60%

Slope shape: convex to concave Logged: yes

Vegetation: willow, mosses, thimbleberry, vetch, fireweed, sword fern, Douglas-fir seedlings

Evidence of stability/instability: hummocky ground, fresh failure surfaces

Failure description: series of small interconnected planar failures 15-30 m wide in larger ancient rotational failure 75 m wide

Sample locations & depths: sample a--reddish material on surface of small planar failure; sample b--material at failure plane 75 cm beneath sample a & 3 m below original soil surface; sample c--soft, reddish rock below failure plane & which supports perched water table

Site no.: MFW-B-1 No. samples: 3

Major drainage: Middle Fork Willamette

Minor drainage: Buck Creek

Overall stability: very unstable

Location: NWNE S13, T23S, R3E

Geologic formation: Little Butte (Tlt)

Lithology & soil: highly weathered greenish lapilli tuff or breccia with poorly drained mottled, plastic clay supporting perched water table

Elevation: 1000 m Aspect: S Gradient: 80%

Slope shape: convex to concave

Vegetation: Equisetum, fireweed, twinflower, alder, rhododendron, western red cedar, Douglas-fir, salal, western white pine

Evidence of stability/instability: active planar slides common, jackstrawed trees, hummocky ground, tension cracks

Failure description: very large ancient slump dissected by stream and reactivated with numerous debris flow failures of varying size, and undergoing creep

Sample locations & depths: surficial failure along Buck Creek below old road and west of Powder Creek; samples--10 cm below surface in failure (probably at failure plane) in wet, yellowish clay containing much gravel; sample b--20 cm below surface in saturated blue, gravelly material which is the major zone of water flow; sample c--30-50 cm below surface in wet, blue, heavy, plastic clay with very few gravels and which appears to be highly weathered pyroclastic rock

Site no.: MFW-D-1 No. samples: 3

Major drainage: Middle Fork Willamette

Minor drainage: Dome Creek

Overall stability: very unstable

Location: NWNW S31, T24S, R4E

Geologic formation: Little Butte (Tlt) just below contact with High Cascade Volcanics (QTv)

Lithology & soil: vesicular porphyritic andesitic colluvial cobbles & boulders with reddish rhyolite (?) colluvium over greenish decomposed breccia with gravelly, nonplastic well drained soil

Elevation: 975 m Aspect: SSE

Slope shape: variable Logged: yes

Vegetation: Douglas-fir, vine maple, rhododendron, chinkapin, vetch, salal, alder

Evidence of stability/instability: fresh failures, jackstrawed trees, hummocky ground

Failure description: very large ancient failure, recently reactivated with several planar slide approx. 40 m wide

Sample locations & depths: sample a--scarp above landing above large, fresh debris flow east of road below Dome Rock, 2½ m depth; sample b--recent debris flow just east of that below sample a, upper right flank, 4 m from original surface, 1 m deep into failure surface; sample c--center portion of failure in wet zone approx. 6 m from original surface, 1 m deep into failure surface

Site No.: MFW-H-1 No. samples: 2

Major drainage: Middle Fork Willamette

Minor drainage: Hills Creek

Overall stability: unstable

Location: NWSE S36. T21S, R3E, across reservoir from C. T. Beach campground

Geologic formation: Little Butte (Tlt)

Lithology & soil: soft yellowish pyroclastic rock with plastic clayey soil along steep left flank of earthflow; central portion of earthflow is more heterogeneous & multilayered with dark brown clayey soil of variable thickness (e.g., 30 cm) overlying yellowish plastic layer (20-40 cm thick) of smectite clay apparently from greenish pyroclastic rock & supporting a perched water table; under this clay layer is dark brown sandier soil with basaltic cobbles at 1 m depth

Elevation: 550 m Aspect: E Gradient: 70% at flank

Slope shape: convex to concave Logged: yes

Vegetation: Douglas-fir seedlings, western red cedar seedlings, rhododendron, bracken fir, chickapin, bunchgrasses, Equisetum

Evidence of stability/instability: broadly hummocky ground, fresh failures

Failure description: earthflow with small rotational slumps at flanks

Sample locations & depths: sample a--right flank of small rotational slump at left flank of earthflow; sample b--random sample from central portion of earthflow, 1 m depth and in soil with basaltic colluvium below the clay layer which supports the perched water table

Comments: small rotational failures in the homogeneous material along the steep flanks of the earthflow; numerous, small, shallow planar failures in central portion of earthflow above perched water table

Site no.: NU-LR-B-1 No. samples: 1

Major drainage: North Umpqua

Minor drainage: Little River, Black Creek

Overall stability: stable

Location: NWSW S10, T28S, R1W; along Rd. 2719

Geologic formation: Little Butte (Tlt)

Lithology & soil: decomposed reddish breccia with outcrops of altered porphyritic andesitic rock

Elevation: 900 m Aspect: E Gradient: 40%

Slope shape: convex Logged: no

Vegetation: Douglas-fir, western hemlock, western red cedar, rhododendron, vine maple, bracken fern, willow

Evidence of stability/instability: ancient slump benches common but no evidence of recent slumping; trees straight road cut banks smooth and intact; no emerging water

Failure description: none

Sample locations & depths: road cut bank 2 m from top and 75 cm deep

Site no.: SU-S-1 No. samples: 2

Major drainage: South Umpqua

Minor drainage: Slick Creek

Overall stability: stable (?)

Location: SESW S23, T28S, R1W; along Rd. 2719

Geologic formation: Colestin-Fisher

Lithology & soil: decomposing yellowish pyroclastic rock with reddish plastic clay in cracks (most abundant in horizontal cracks); outcrops of porphyritic andesite (?) nearby

Elevation: 800 m Aspect: N Gradient: 50-60%

Slope shape: convex Logged: yes

Vegetation: Douglas-fir, western red cedar, western hemlock, rhododendron, fireweed, vine maple, ceanothus

Evidence of stability/instability: smooth slopes, cutbanks intact, trees straight

Failure description: none

Sample location & depth: sample a--random sample from road cutbank, 2 m from top, ½ m deep; sample b--red plastic clay from fissures

Site no.: SU-J-1 No. samples: 2

Major drainage: South Umpqua

Minor drainage: Jackson Creek

Overall stability: unstable

Location: NWNW S31, T29S, R2E; Jct Rds. 2930 & 2932

Geologic formation: Colestin (Tc) just below contact with Little Butte (Tlt)

Lithology & soil: subangular cobbles of highly altered porphyritic dacite (?) with wet highly plastic clayey soil

Elevation: 800 m Aspect: S Gradient: 25-30%

Slope shape: variable Logged: yes

Vegetation: sugar pine, ponderosa pine, incense cedar, Douglas-fir, madrone, rush, Equisetum

Evidence of stability/instability: benchy, hummocky topography, numerous cutbank failures along road, swept trees

Failure description: area of deep seated soil creep with numerous small slumps

Sample locations & depths: sample a--random sample of relatively dry, ungleyed soil in small rotational failure along road, 1 m depth; sample b--random sample of wet gleyed soil along creek, 2 m depth

Site no.: SU-1 No. samples: 2

Major drainage: South Umpqua

Minor drainage: same

Overall stability: unstable

Location: NENE S23, T29S, R1W

Geologic formation: Colestin-Fisher

Lithology & soil: reddish to yellowish highly altered pyroclastic rock with highly weathered angular porphyritic basaltic colluvial cobbles

Elevation: 450 m Aspect: E Gradient: 50%

Slope shape: convex to concave Logged: yes

Vegetation: western red cedar, Douglas-fir, Equisetum, western hemlock, sword fern, dogwood, mosses, alder, Oregon grape, chinkapin, twinflower

Evidence of stability/instability: fresh failure, hummocky ground

Failure description: road cutbank failure 30-40 m wide with numerous small planar block glides; failure has been seeded, drained and rocked to stabilized

Sample locations & depths: sample a--right portion of failure $\frac{1}{4}$ of the way down from the top, 1 m depth; sample b--left portion of failure near head 1 m depth

Site no.: SU-C-1 No. samples: 5

Major drainage: South Umpqua

Minor drainage: Canyon Creek

Overall stability: locally unstable

Location: SESE S2, T31S, R5W; along Interstate 5

Geologic formation: Jurassic volcanic rocks

Lithology & soil: highly decomposed unidentifiable rock with mud cracks, plastic clay; underlain by serpentine rock

Elevation: 365 m Aspect: WNW Gradient: 50%

Slope shape: original slope concave with hummocks and small terraces, convex above failure

Vegetation: Douglas-fir, ocean spray, madrone, blackberry

Evidence of stability/instability: fresh failure, small cutbank failures, several old slump benches

Failure description: fresh, moderately large rotational slump and small resultant earthflow

Sample locations and depths: sample a--from root wad of Douglas-fir tree which slid from failure crown approx. 1 m depth from original surface: sample b--west scarp wall (left flank), 4 m from ground surface; sample c--east scarp wall (right flank) just above gravel road which had crossed slide area, 2 m from surface, 1 m into wall; sample d--random sample from slump bench just above toe near middle of failure; sample e--random sample of cracked and layered plastic clay at toe of slide

Comments: Catastrophic failure, occurred January 1974 during intense rainstorm, no water emerging from site today

Site no.: R-CM-1 No. samples: 6

Major drainage: Rogue River

Minor drainage: Elk Creek, Coal Mine Creek

Overall stability: very unstable

Location: SENW S16, T31S, R1E

Geologic formation: Little Butte, Sardine

Lithology & soil: gravels and cobbles of basaltic colluvium overlying greenish pyroclastic material which has weathered to heavy, plastic, mottled clay supporting perched water table

Elevation: 1040 m Aspect: E Gradient: 40-50%

Slope shape: convex to concave Logged: no

Vegetation: incense cedar, western red cedar, sugar pine, Douglas-fir, Equisetum, western hemlock, grand fir, vine maple, Oregon grape, sword fern, chinkapin, alder, Vaccinium

Evidence of stability/instability: small road cut failures common, hummocky or benchy topography

Failure description: planar sliding (20 m wide) of orangish colored material with basaltic colluvium in road cutbank off of heavy plastic clay at perched water table; rotational component in headwall region

Sample locations & depths: sample a--headwall region of failure, 1 m from crown; sample b--dry crusty material covering failure surface, 2 m from crown; sample c--failure surface at level of emerging water, 2½ m from crown; sample d--relatively stable portion of road cut in heavy clay below failure, 4-5 m from original surface; sample e--random sample from road cutbank off left flank (north) of small failure in wet plastic clay, 1½ m depth; sample f--random sample from road cutbank in gleyed clay north of sample e, 2 m depth

Site no.: R-SP-1 No. samples: 1

Major drainage: Rogue River

Minor drainage: Elk Creek, Sugar Pine Creek

Overall stability: stable except that steep slopes are subject to debris avalanche

Location: NW S14, T32S, R1E; along Sugar Pine road, 1.2 mi north of of Elk Creek road jct.

Geologic formation: unknown

Lithology & soil: rhyolitic colluvium of subangular cobbles over rhyolitic breccia bedrock; soil dry, shallow, very coarse textured

Elevation: 600 m Aspect: E Gradient: 90%

Slope shape: slightly convex Logged: yes

Vegetation: Douglas-fir, vine maple, alder, oceanspray, bigleaf maple

Evidence of stability/instability: steep slopes with relatively little evidence of mass failure other than debris avalanching of shallow soil when undercut

Failure description: dry debris avalanche just north of larger debris avalanche in road cutbank, 2 m from top

Comment: Soil judged as stable with respect to deep mass movement as slopes are smooth, very steep, dry and soil is shallow over bedrock; soil is unstable if considered with respect to shallow debris avalanching

Site no.: R-SP-2 No. samples: 1

Major drainage: Rogue River

Minor drainage: Elk Creek, Sugar Pine Creek

Overall stability: stable

Location: NW S14, T32S, R1E; along Sugar Pine road 0.6 mi north of Elk Creek road jct.

Geologic formation: unknown

Lithology & soil: see site no. R-SP-1

Elevation: 600 m Aspect: E Gradient: 45%

Slope shape: slightly convex Logged: N.A.

Vegetation: grass, Douglas-fir, vine maple, bigleaf maple

Evidence of stability/instability: little evidence of failure, road cutbanks intact

Failure description: none

Sample location & depth: random sample from road cutbank, 1 m from top

Site no.: R-M-1 No. samples: 3

Major drainage: Rogue River

Minor drainage: Elk Creek, Morine Creek

Overall stability: moderately unstable

Location: NENE S15, T33S, R1W 1.1 mi. south of jct. with Rd. 3357

Geologic formation: Sardine (?)

Lithology & soil: altered porphyritic andesite (?)

Elevation: 975 m Aspect: E

Slope shape: convex to concave Logged: yes

Vegetation: Douglas-fir, sugar pine, incense cedar, madrone, thimbleberry, snowberry oceanspray, grand fir; in failure: rush, willow, Equisetum, cattail

Evidence of stability/instability: rumpled ground surface

Failure description: small earthflow approx. 30 m wide

Sample locations & depths: sample a--saturated soil which flowed from upslope; sample b--somewhat drier material along right flank of flow; sample c--soil from road cutbank to the right (east) of flowing material

Site no.: A-S-1 No. samples: 3

Major drainage: Applegate River

Minor drainage: Squaw Creek

Overall stability: very unstable

Location: NENW S2, T41S, R3W; below Squaw Lake dam

Geologic formation: Triassic Schist

Lithology & soil: bluish mica schist

Elevation: 950 m Aspect: NNW Gradient: 20%

Slope shape: slightly convex to slightly concave

Logged: no

Vegetation: Douglas-fir, madrone, Oregon ash, grand fir, vine maple, striped maple, snowberry

Evidence of stability/instability: tension cracks, sunken road, numerous old small failures, fresh failures

Failure description: slow moving planar failure approx. 400 m wide with well defined lateral tension cracks and rapid slipping of toe portions into Squaw Creek; two adjacent toe failures, 50 m wide and 100 m wide

Sample locations & depths: sample a--cutbank in road to dam and campground and which crosses slow moving failure area, 2 m from top, 1 m into bank; sample b--upper central region of larger rapid slide failure surface, yellowish to greenish material overlying sample c; sample c--upper center of fresh failure surface beneath sample b and at point of water emergence in decomposing bluish schistose material

Comment: chemical stabilization being attempted by Ion Tech Co.

Site no.: A-S-2 No. samples: 1

Major drainage: Applegate River

Minor drainage: Squaw Creek

Overall stability: moderately stable to locally unstable

Location: NENE S4, T41S, R3W; Dividend Bar

Geologic formation: Triassic Schist

Lithology & soil: schist

Elevation: 730 m Aspect: N

Slope shape: convex Logged: yes

Evidence of stability/instability: road cut failures common

Failure description: road cutbank failure approx. 30 m wide

Sample location & depth: headwall region of failure 1½ m from crown

Comments: chased off by belligerent landowner

Site no.: A-B-1 No. samples: 6

Major drainage: Applegate River

Minor drainage: Bigelow Creek

Overall stability: unstable

Location: ENE S16, T40S, R5W; along Rd. 3930A

Geologic formation: Applegate Group

Lithology & soil: subangular boulders of very hard granitic rock (diorite?)

Elevation: 1250 m Aspect: SE Gradient: 60%

Slope shape: convex to concave Logged: no

Vegetation: Douglas-fir, sugar pine, striped maple, true fir, western hemlock

Evidence of stability/instability: large fresh failure

Site no.: R-WUR-1 No. samples: 2

Major drainage: Rogue River

Minor drainage: Wake Up Rilea Creek

Overall stability: unstable

Location: SENE S 31, T35S, R12W

Geologic formation: Galice (?)

Lithology & soil: soft schist, very hard argillite

Elevation: Aspect: NNW Gradient: 40-50%

Slope shape: variable Logged: yes

Vegetation: madrone, chinkapin, Douglas-fir, western red cedar, alder, Equisetum, manzanita, maple

Evidence of stability/instability: benchy topography, leaning trees, numerous fresh road cutbank failures

Failure description: slump-earthflow (approx. 20 m wide) in area of deep seated soil creep

Sample locations & depths: sample a--east side of creek in central portion of failure, 20 cm depth; sample b--random sample from roadcut west side of creek

Site no.: R-1 No. samples: 2

Major drainage: Rogue River

Minor drainage: same

Overall stability: unstable

Location: SESE S30, T36S, R14W

Geologic formation: Days Creek

Lithology & soil: mixed metamorphic colluvium

Elevation: 30 m Aspect: N Gradient: 30-40%

Slope shape: variable Logged: yes

Vegetation: Equisetum, alder, pearly everlasting, sword fern, maple, willow, true fir, blackberry, weeds

Evidence of stability/instability: hummocky topography, leaning trees, fresh failure surfaces

Failure description: deep seated soil creep with small localised, well defined rotational slumps

Site no.: S-1 No. samples: 1

Major drainage: Sixes River

Minor drainage: same

Overall stability: unstable

Location: SESW S4, T32S, R14W; along Rd. 322

Geologic formation: Otter Point

Lithology & soil: serpentine rock

Elevation: Aspect: S Gradient: 30-40%

Slope shape: variable Logged: yes

Vegetation: Douglas-fir, western red cedar, Equisetum, alder

Failure description: deep seated soil creep

APPENDIX III

ADDITIONAL XRD PATTERNS OF CLAY SAMPLES FROM THE VARIOUS SITES.

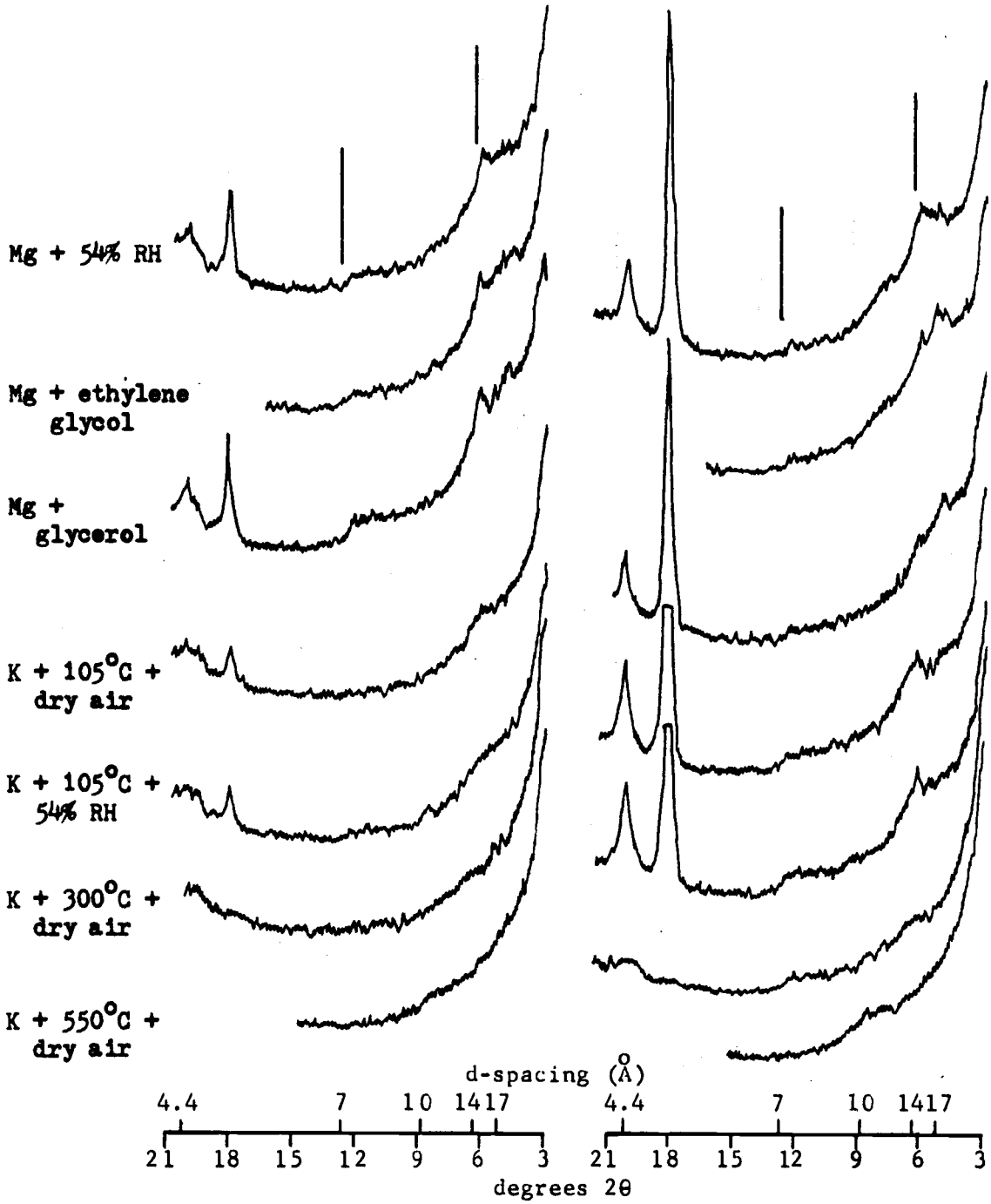

Figure 59. Site NS-BC-1 XRD patterns indicating amorphous material, gibbsite, chloritic intergrade and a trace of halloysite in samples a (left) and b (right).

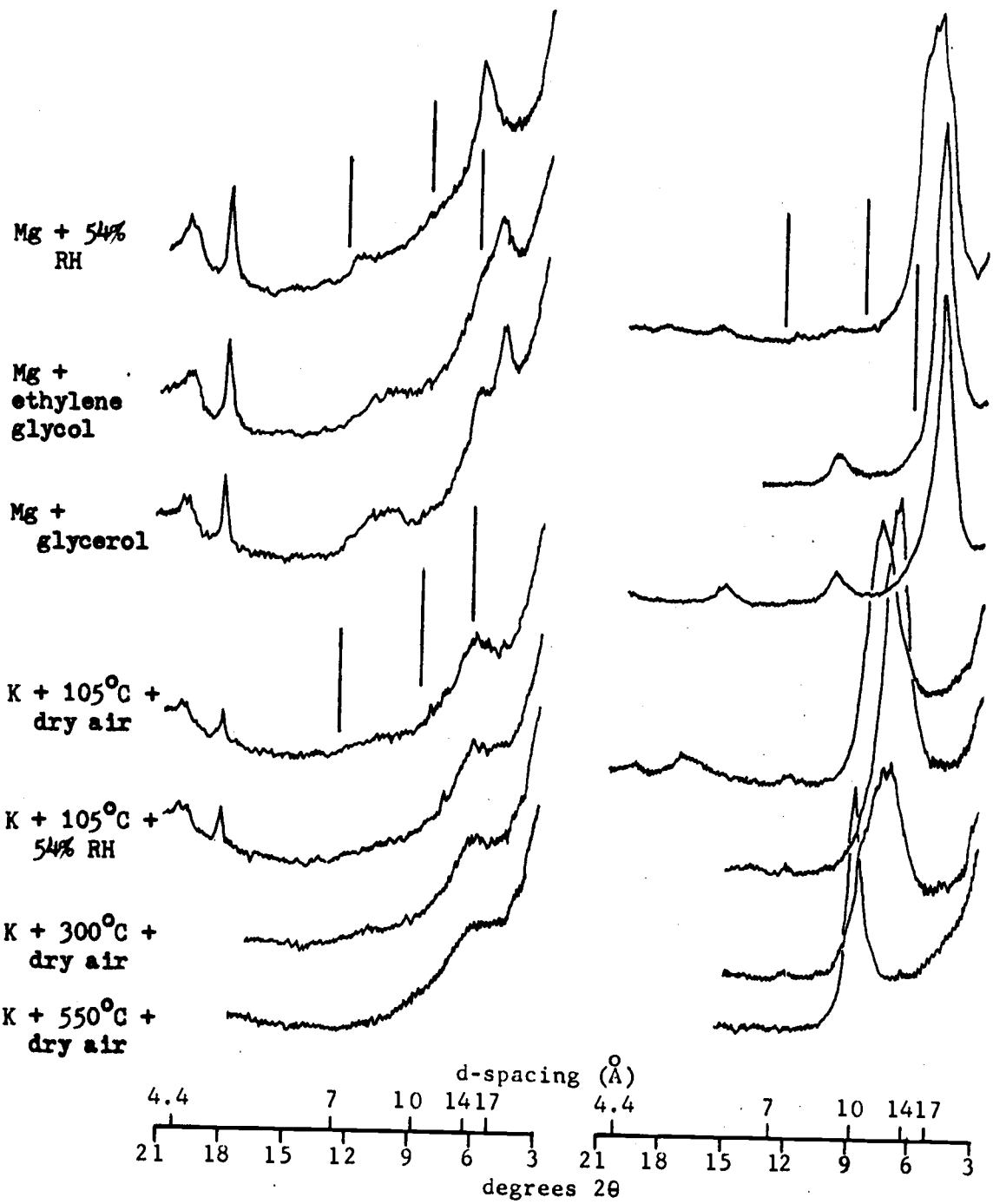

Figure 60. Site NS-BC-1 XRD patterns indicating chloritic intergrade, gibbsite, amorphous material and halloysite in sample c (left) and primarily montmorillonite in sample e (right).

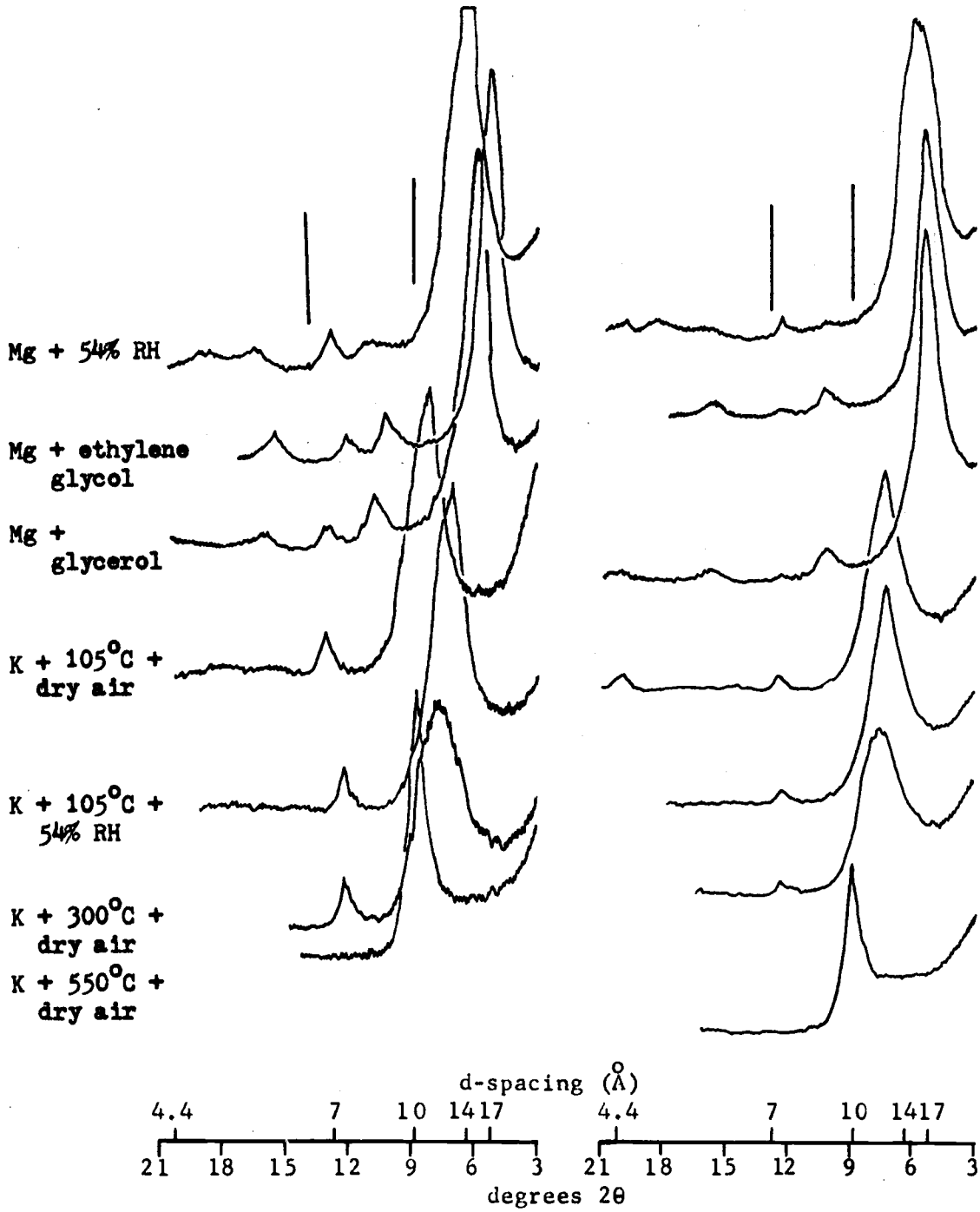

Figure 61. Site NS-BC-1 XRD patterns, indicating montmorillonite in samples d (left) and f (right).

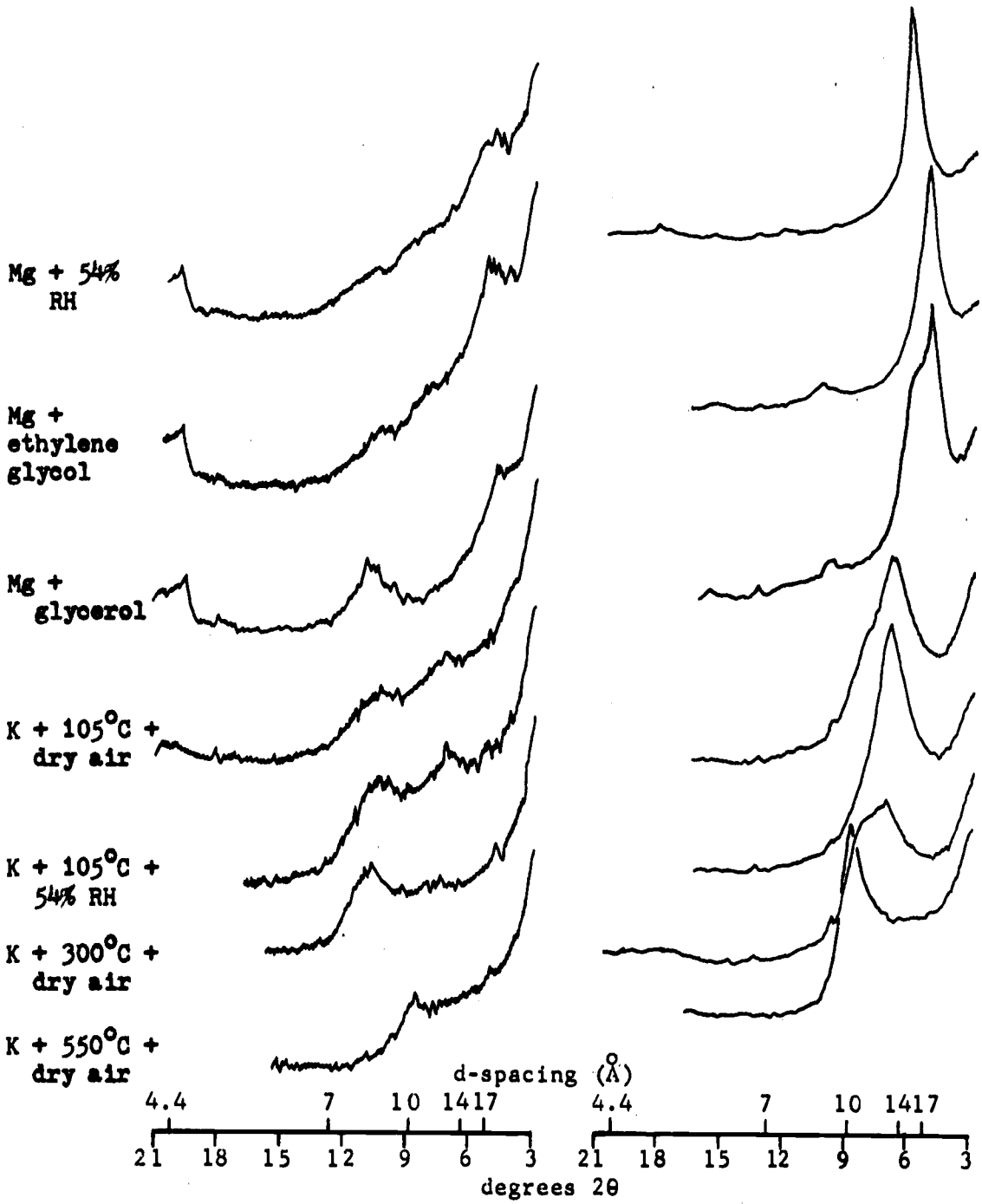

Figure 62. Site NS-BC-2 (left) debris flow soil and MS-D-1 (right) from Knob Rock scarp.

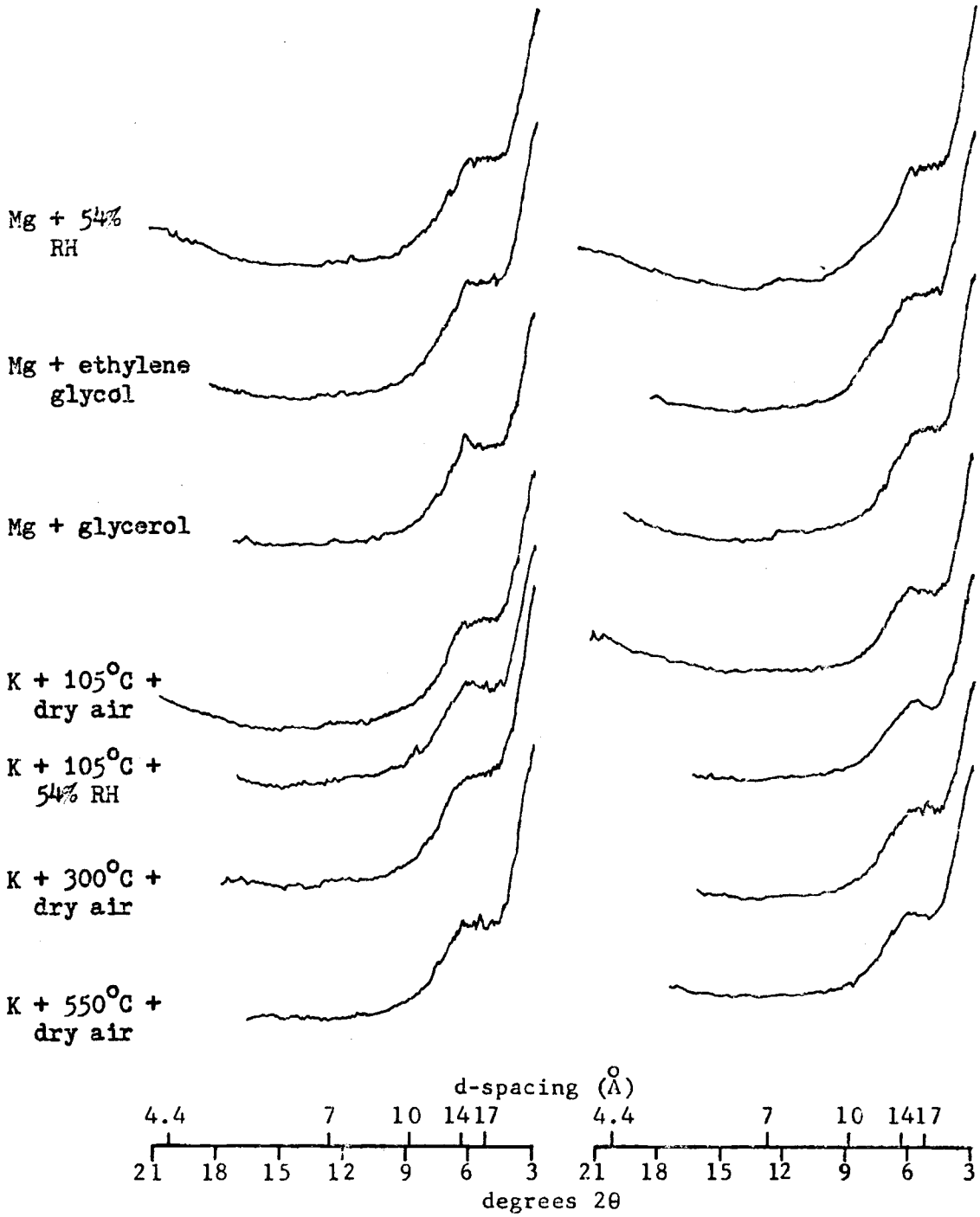

Figure 63. Site MS-P-1 XRD patterns indicating amorphous material, chloritic intergrade and a trace of halloysite in samples a (left) and b (right).

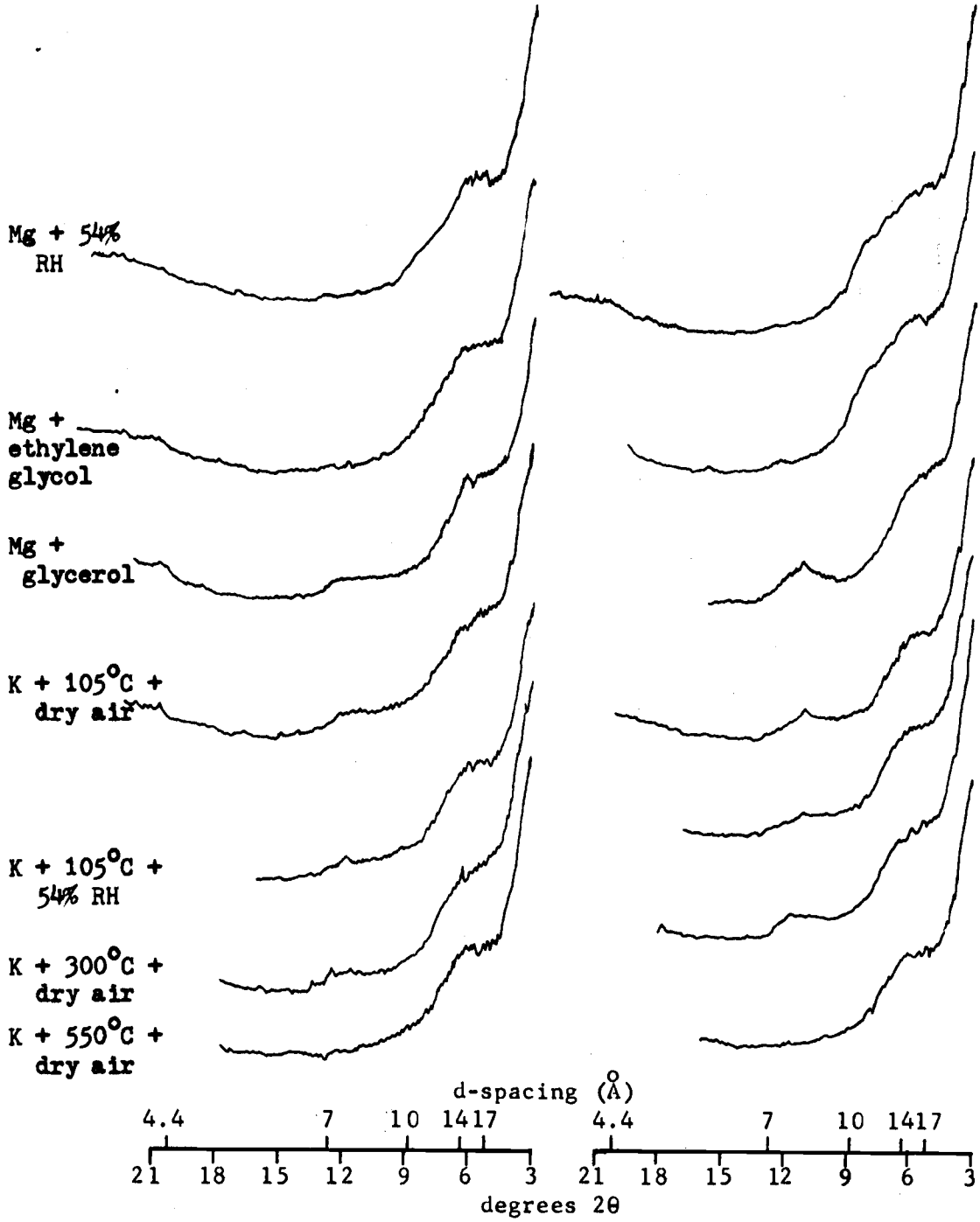

Figure 64. Site MS-P-1 XRD patterns, sample c (left) and sample d (right).

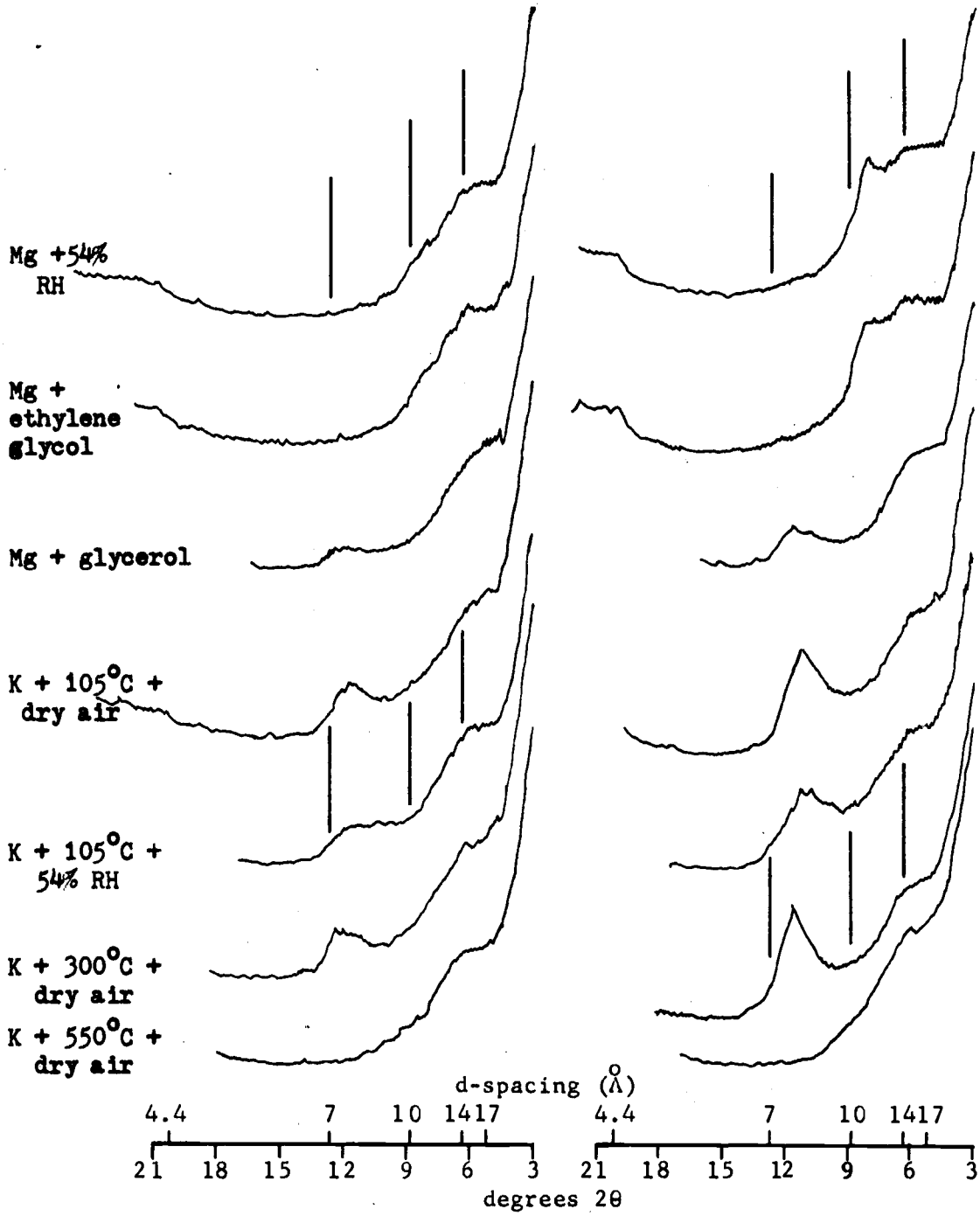

Figure 65. Site MS-P-1 XRD patterns, sample e (left) and sample f (right).

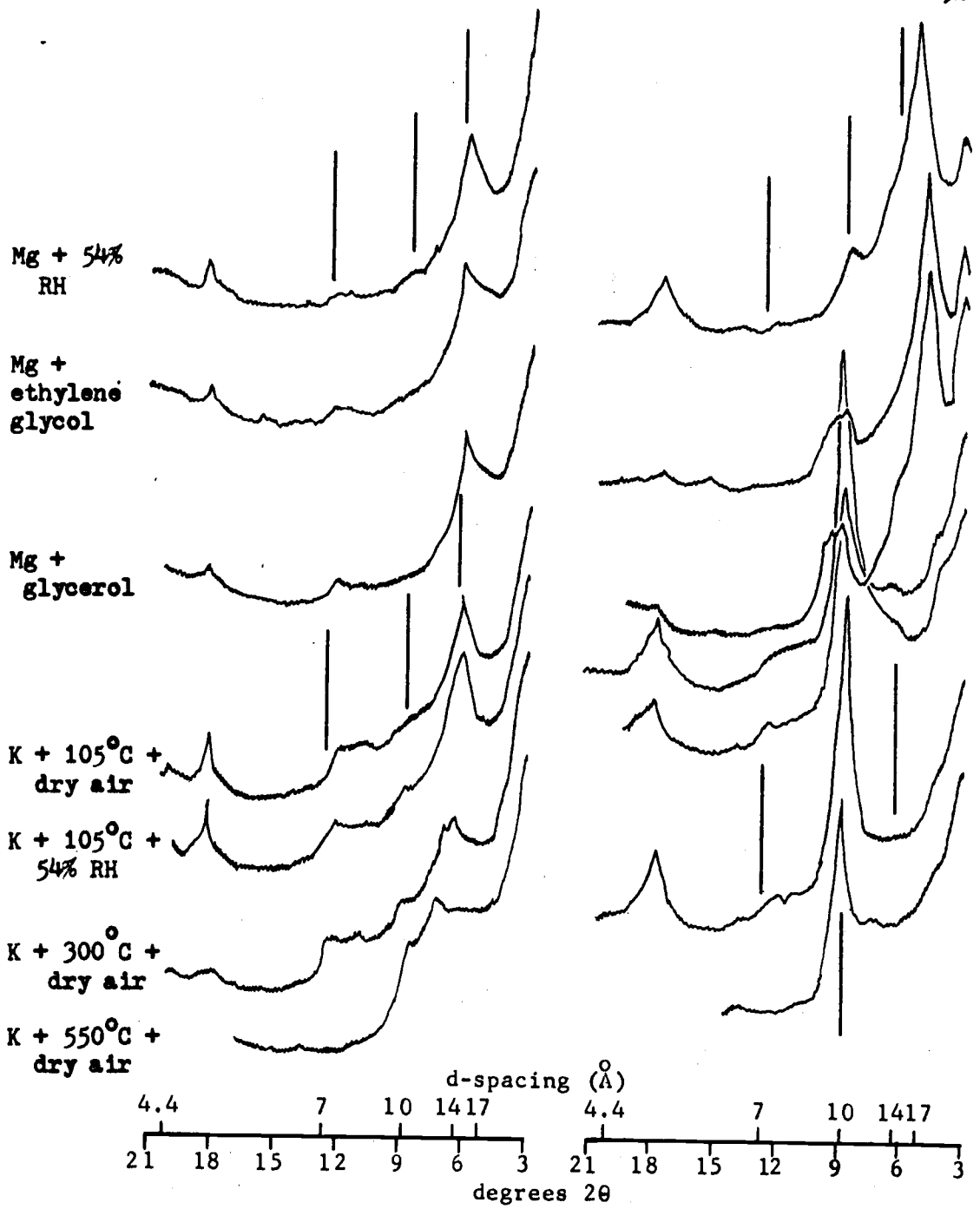

Figure 66. Site MS-J-1 XRD patterns, sample a (left) and sample b (right).

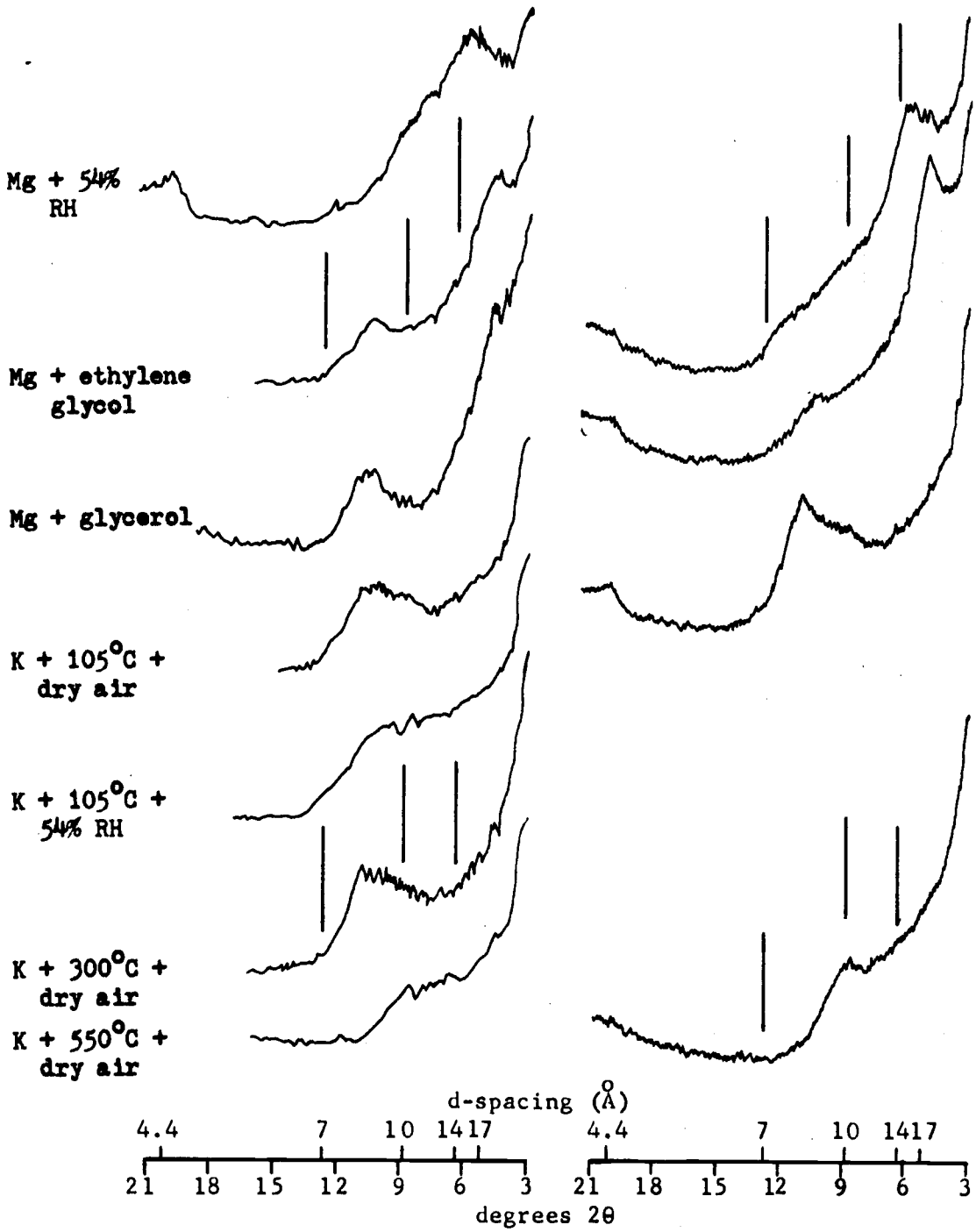

Figure 67. Site MS-3 XRD patterns of clay formed in reddish breccia, sample a (left) and sample b (right).

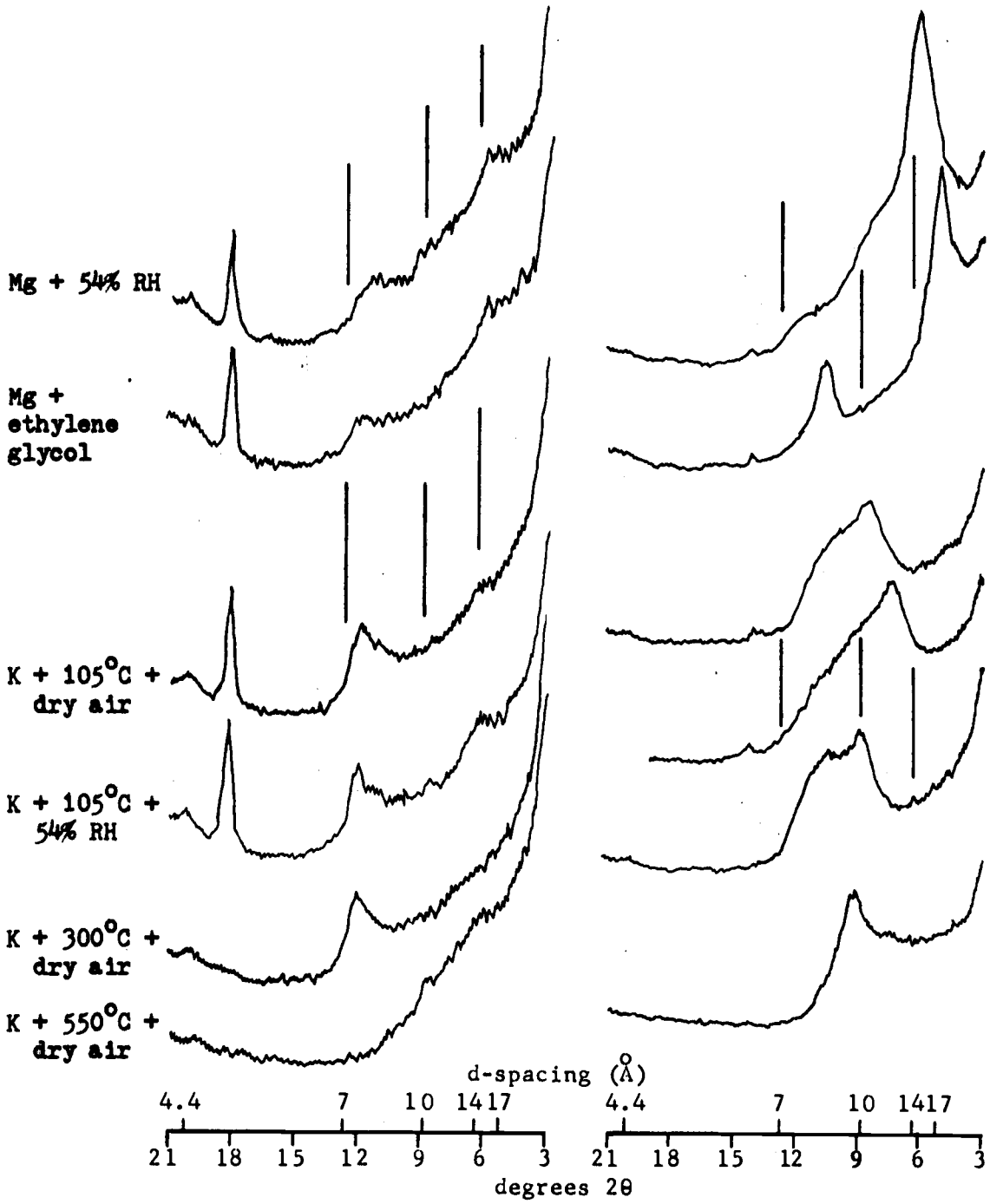

Figure 68. Site SS-SF-1 XRD patterns, sample a (left), sample b (right).

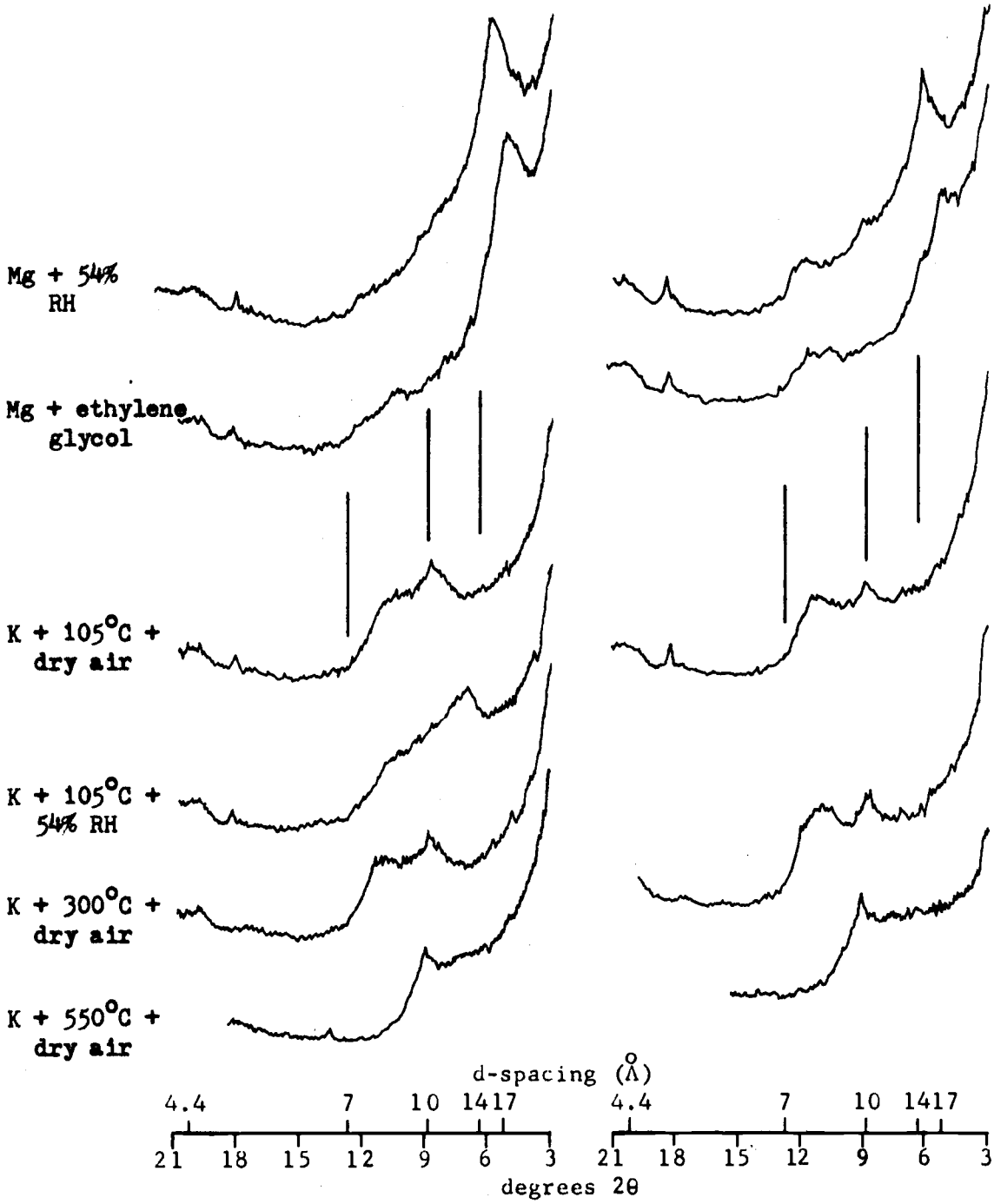

Figure 69. Site SS-SF-1 XRD patterns, sample c (left) and sample d (right).

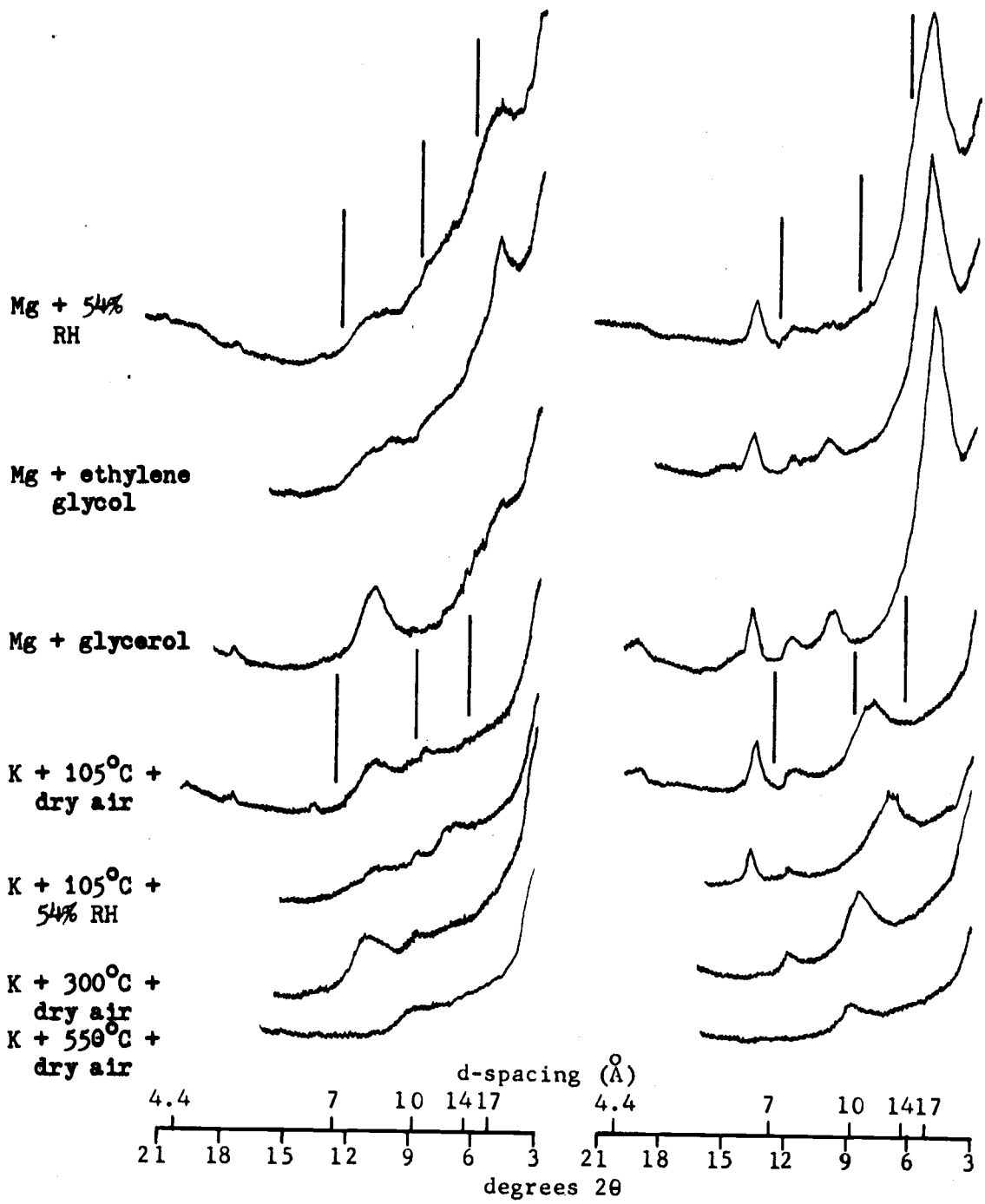

Figure 70. Site SS-SF-1 XRD patterns, sample f (left) and sample g (right).

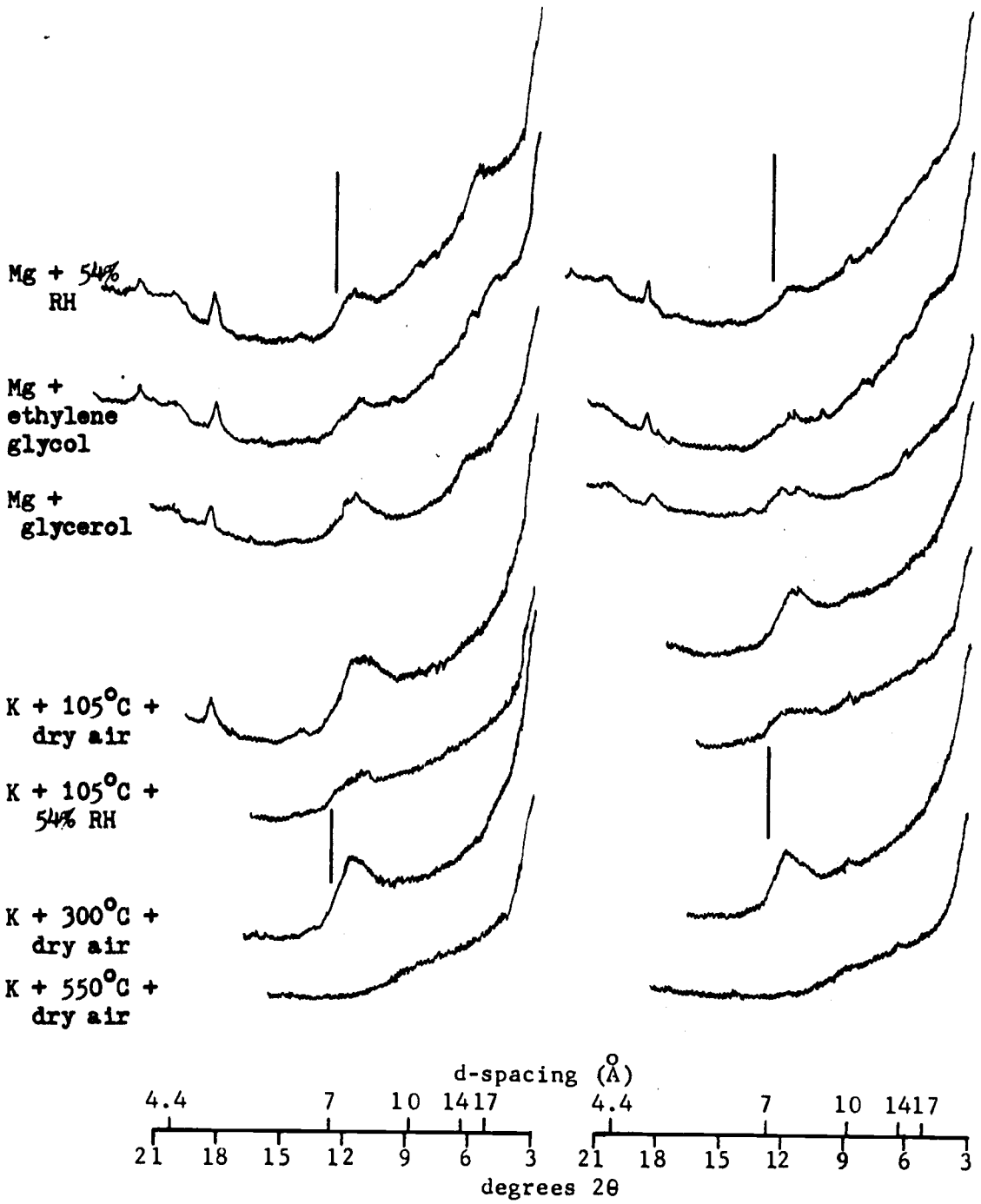

Figure 71. Site SS-SF-1 XRD patterns, sample i (left) and sample j (right).

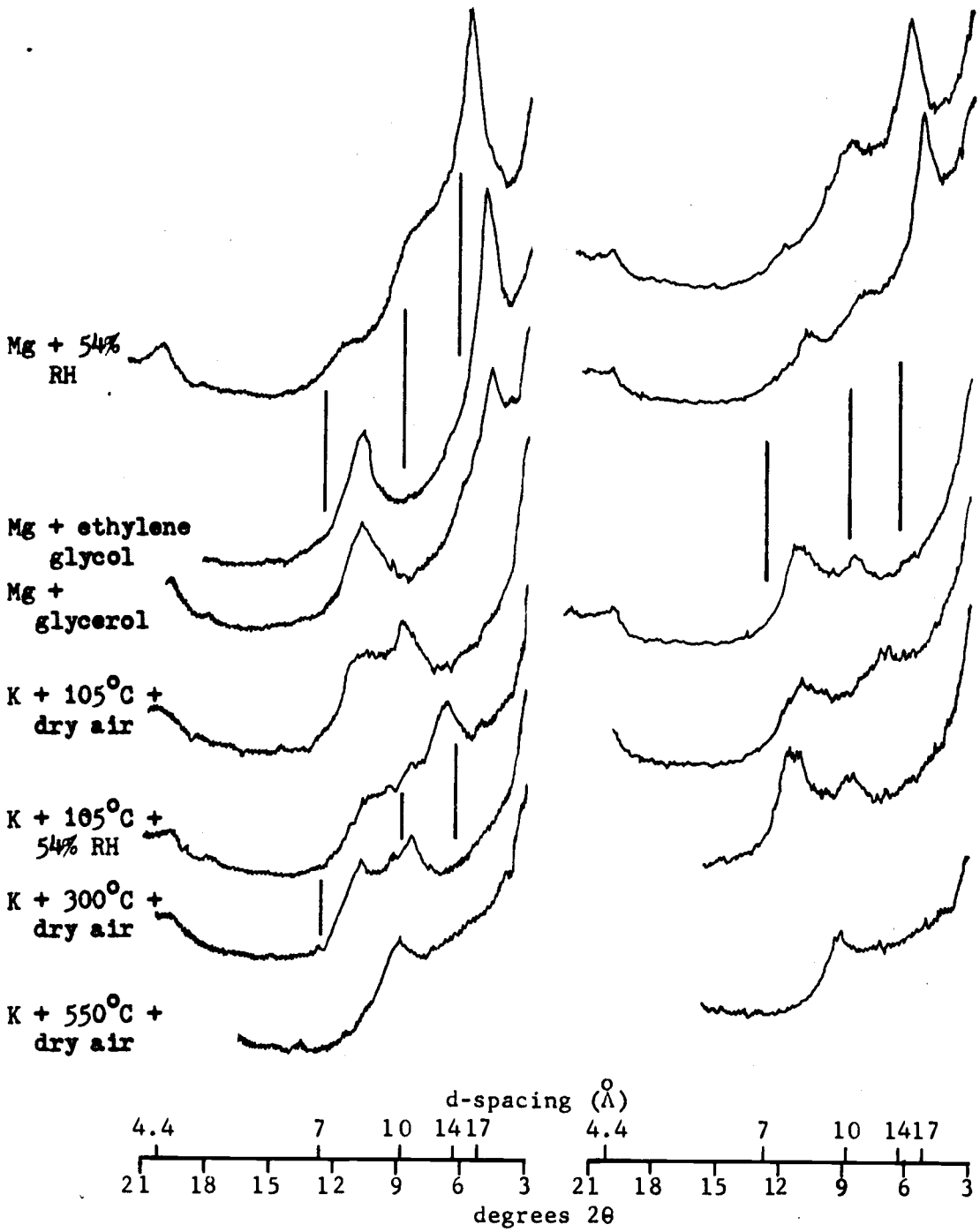

Figure 72. Sites SS-SF-2 (left) and SS-SF-11 (right), somewhat more stable soils in an overall unstable area.

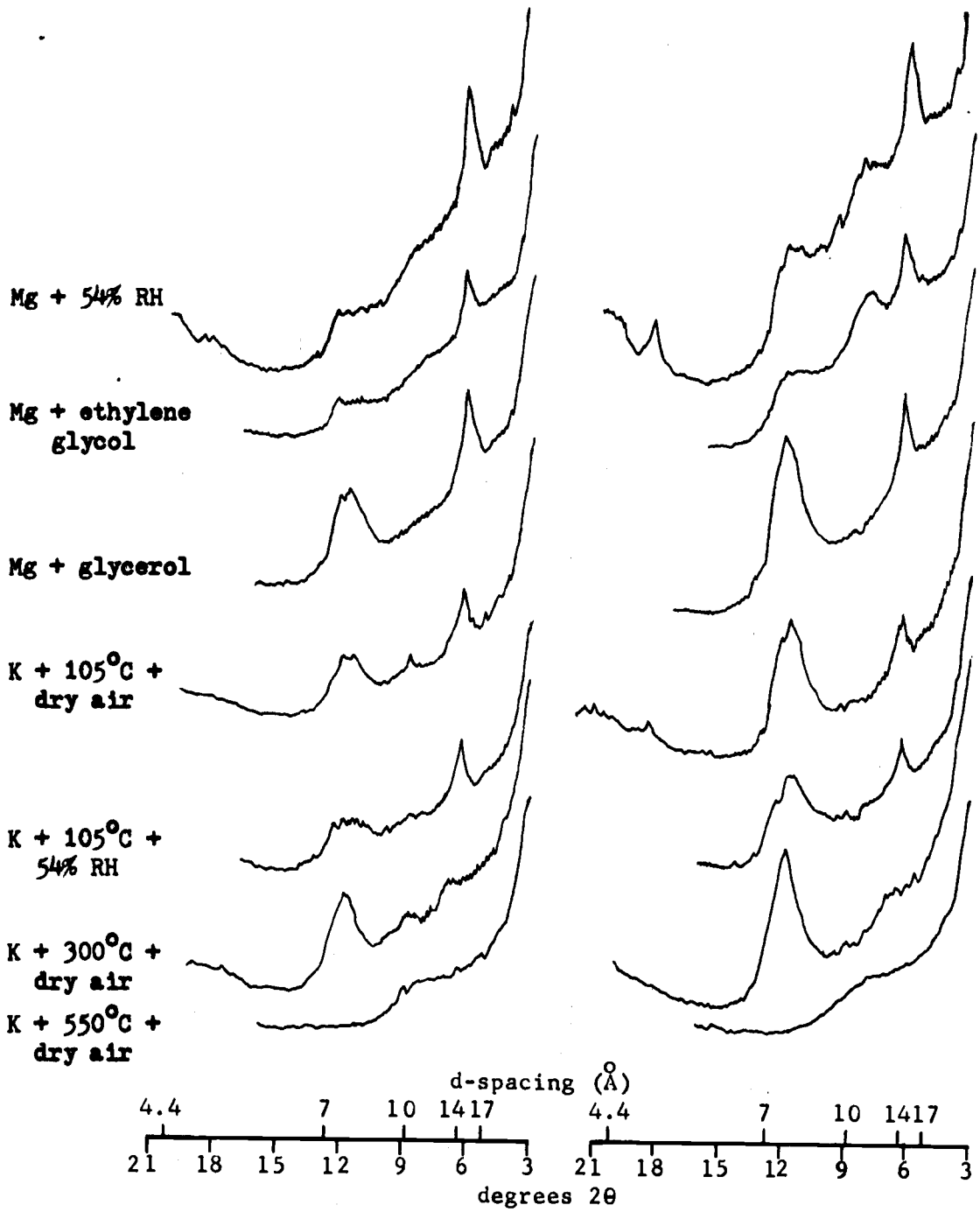

Figure 73. Site SS-SF-4 XRD patterns of soil block which split away (sample a, left) from scarp and of scarp wall (sample b, right).

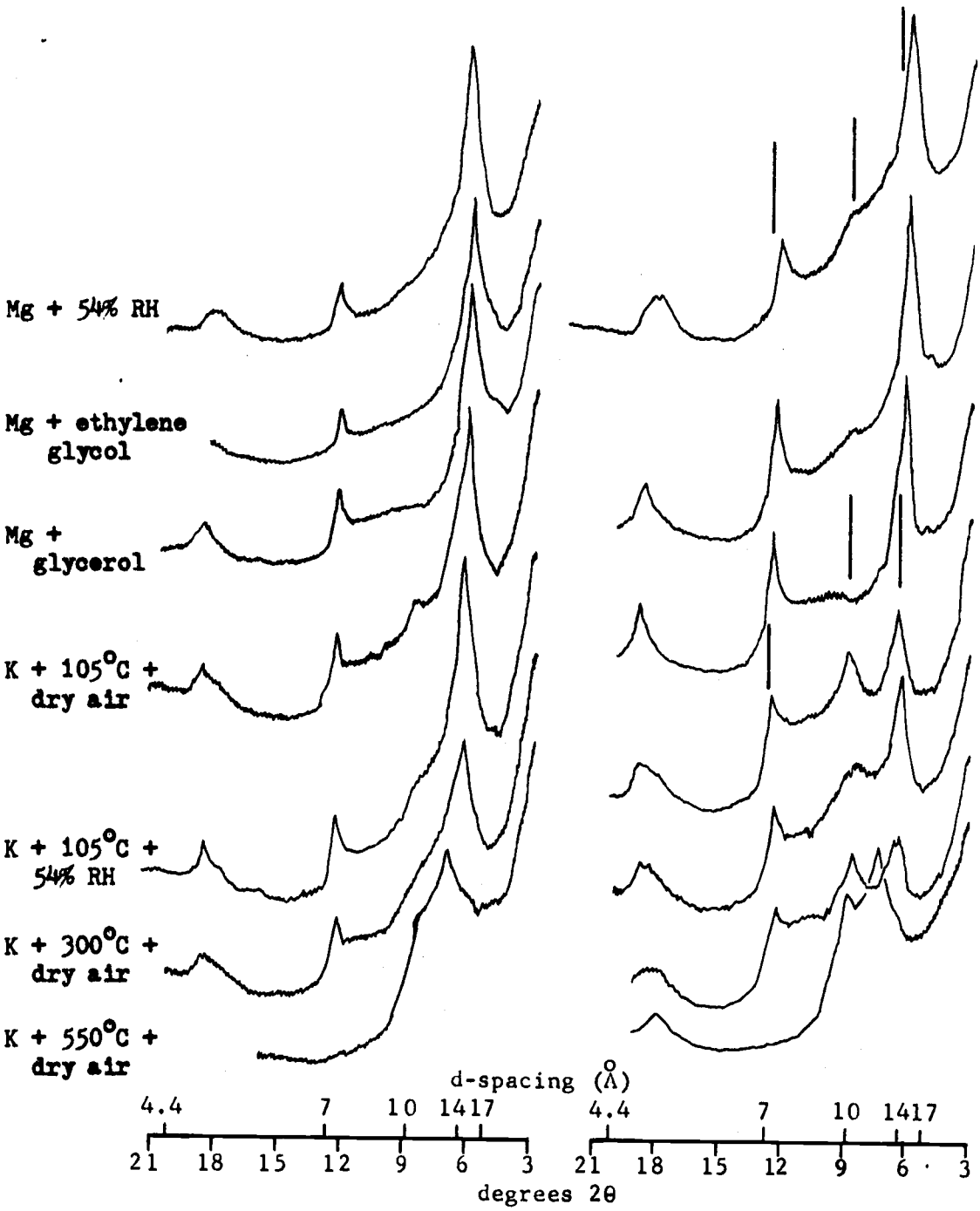

Figure 74. Debris avalanche site SS-SF-5 XRD patterns, sample a (left) and sample b (right).

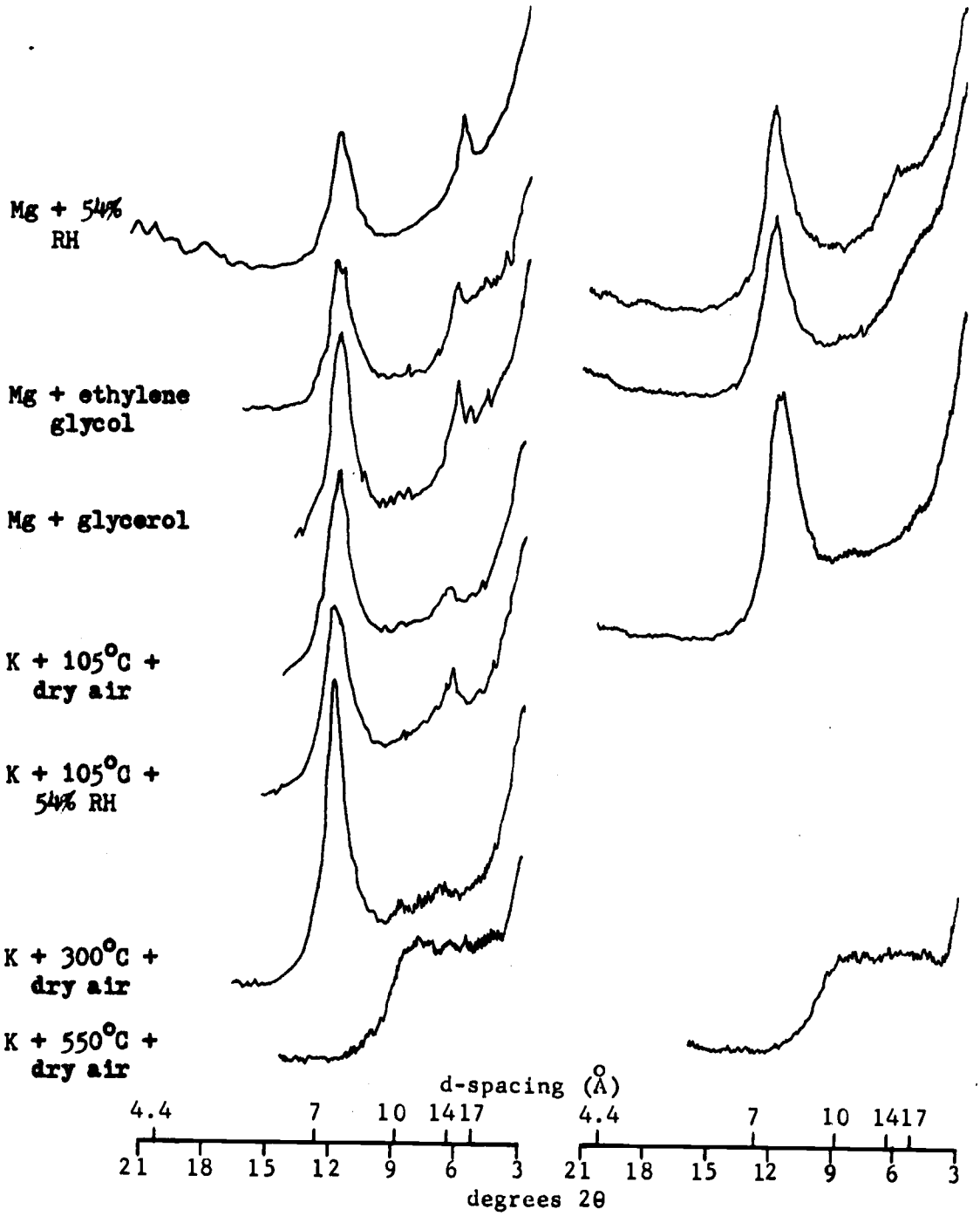

Figure 75. Site SS-2 at Foster scale station, sample a (left) and sample b (right).

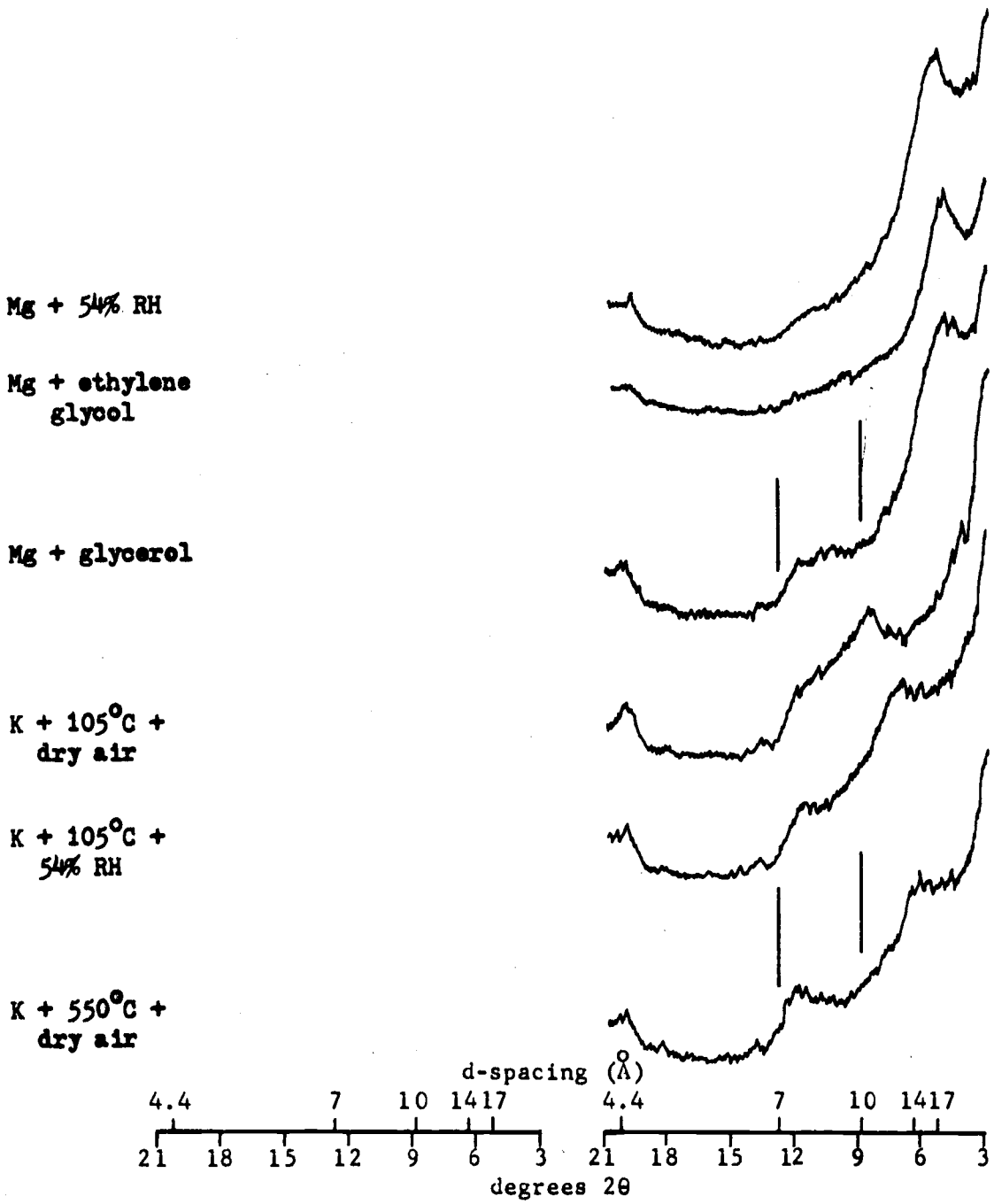

Figure 76. Site MK-D-2 XRD patterns indicating chloritic intergrade, amorphous material and halloysite which failed over smectite.

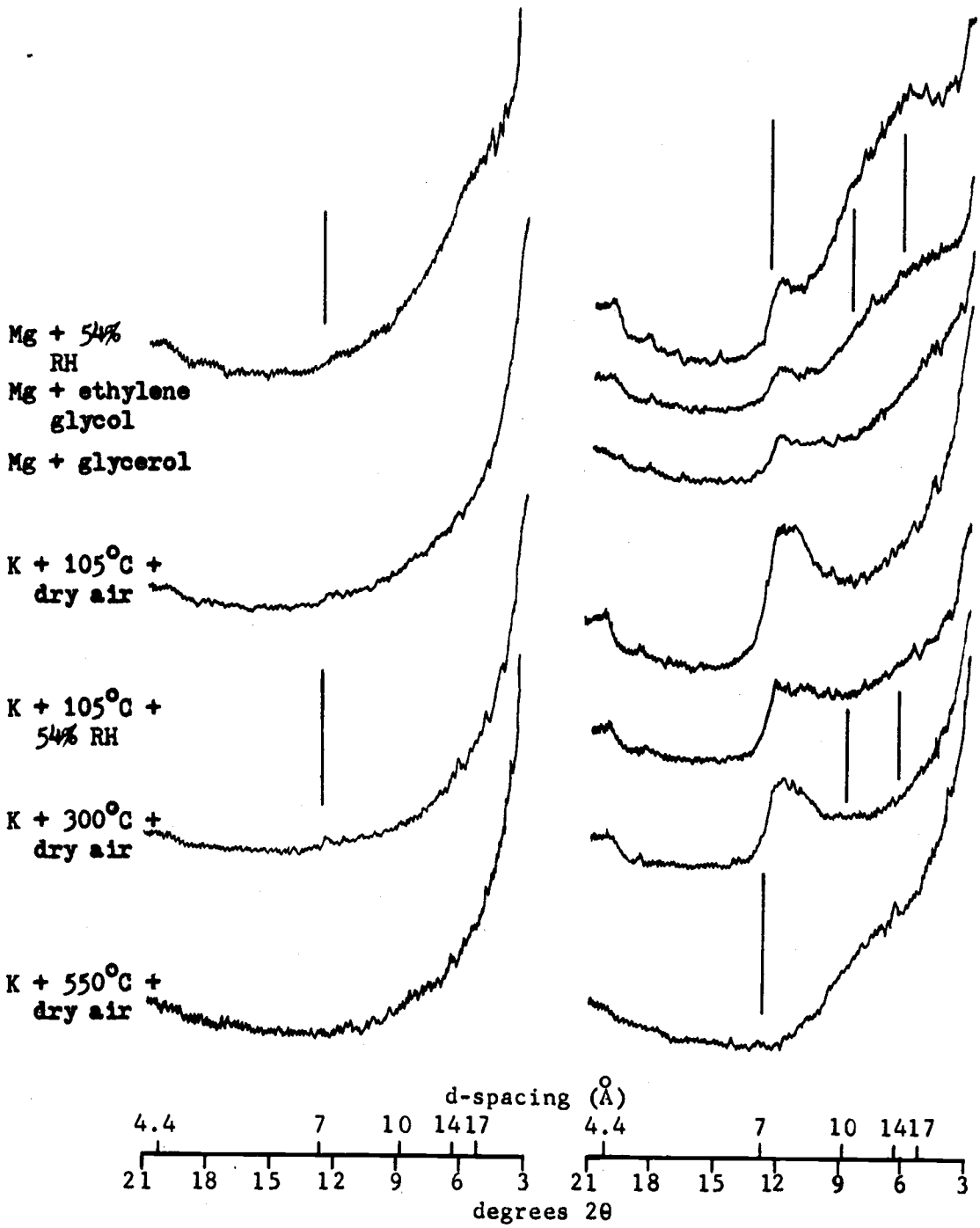

Figure 77. Site MK-L-1 (left) and MK-L-2a (right), stable and earthflor soils, respectively.

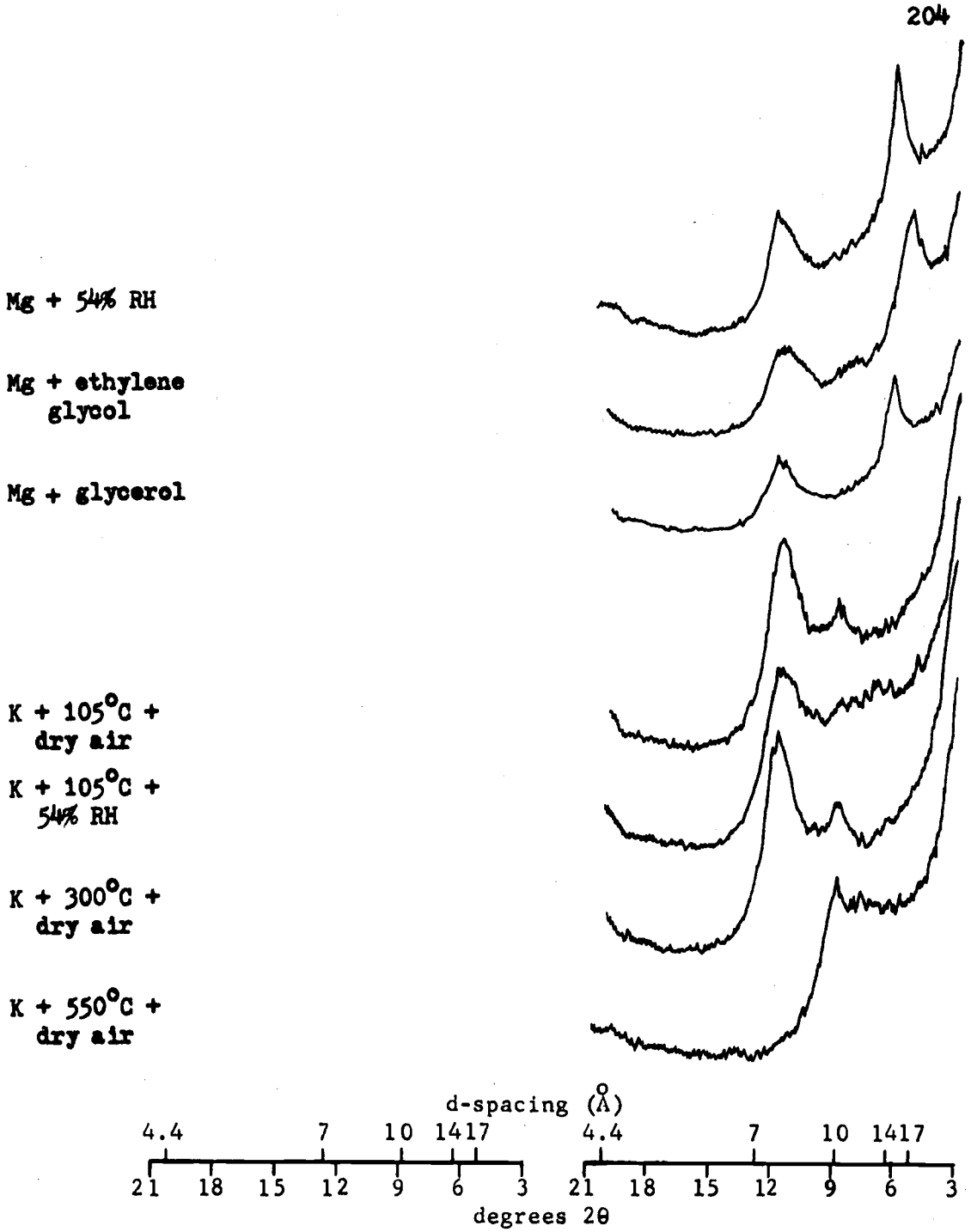

Figure 78. XRD patterns of the relatively stable site MFW-BW-1.

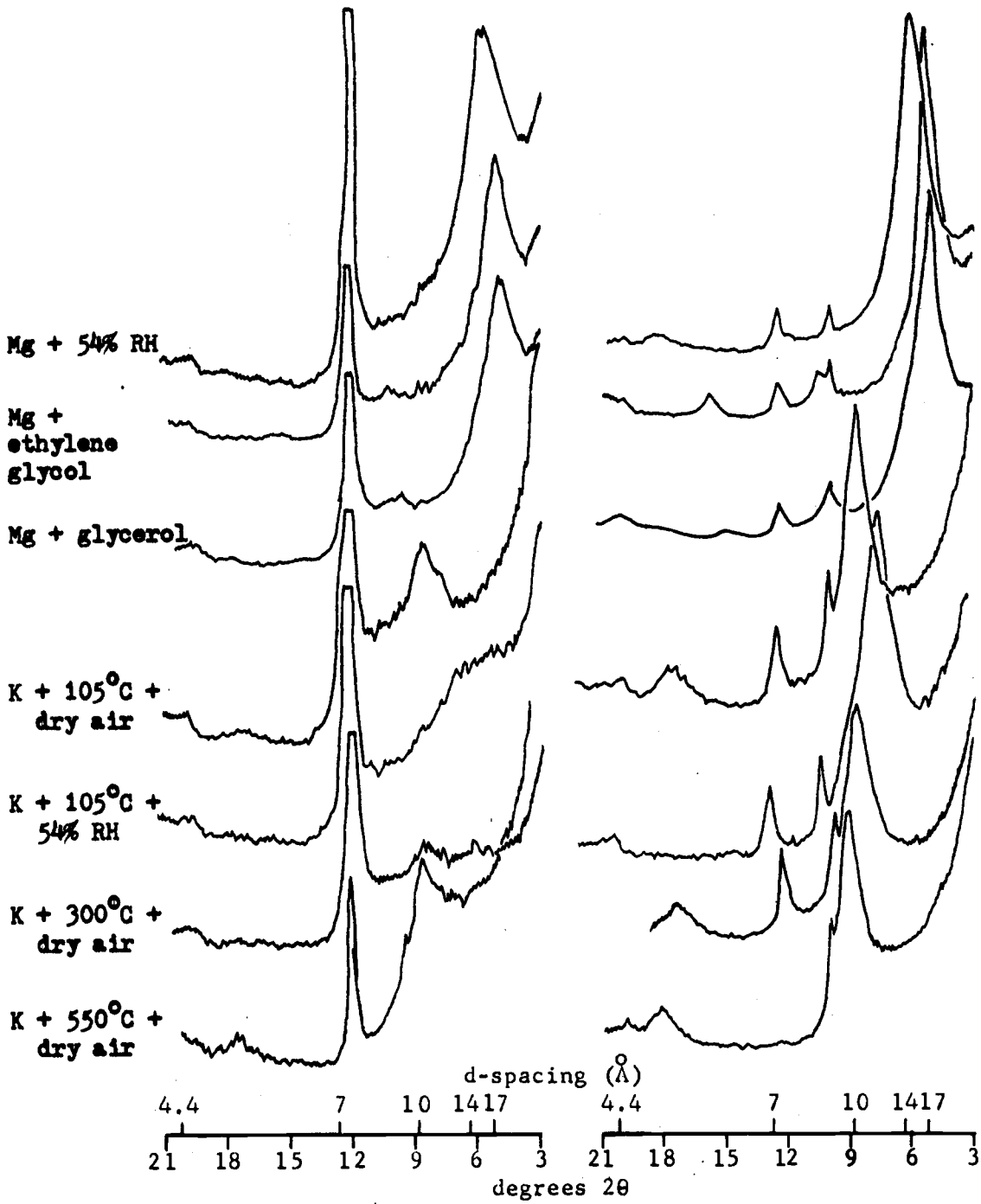

Figure 79. Site MFW-CP-1 XRD patterns, sample a (left) and sample b (right).

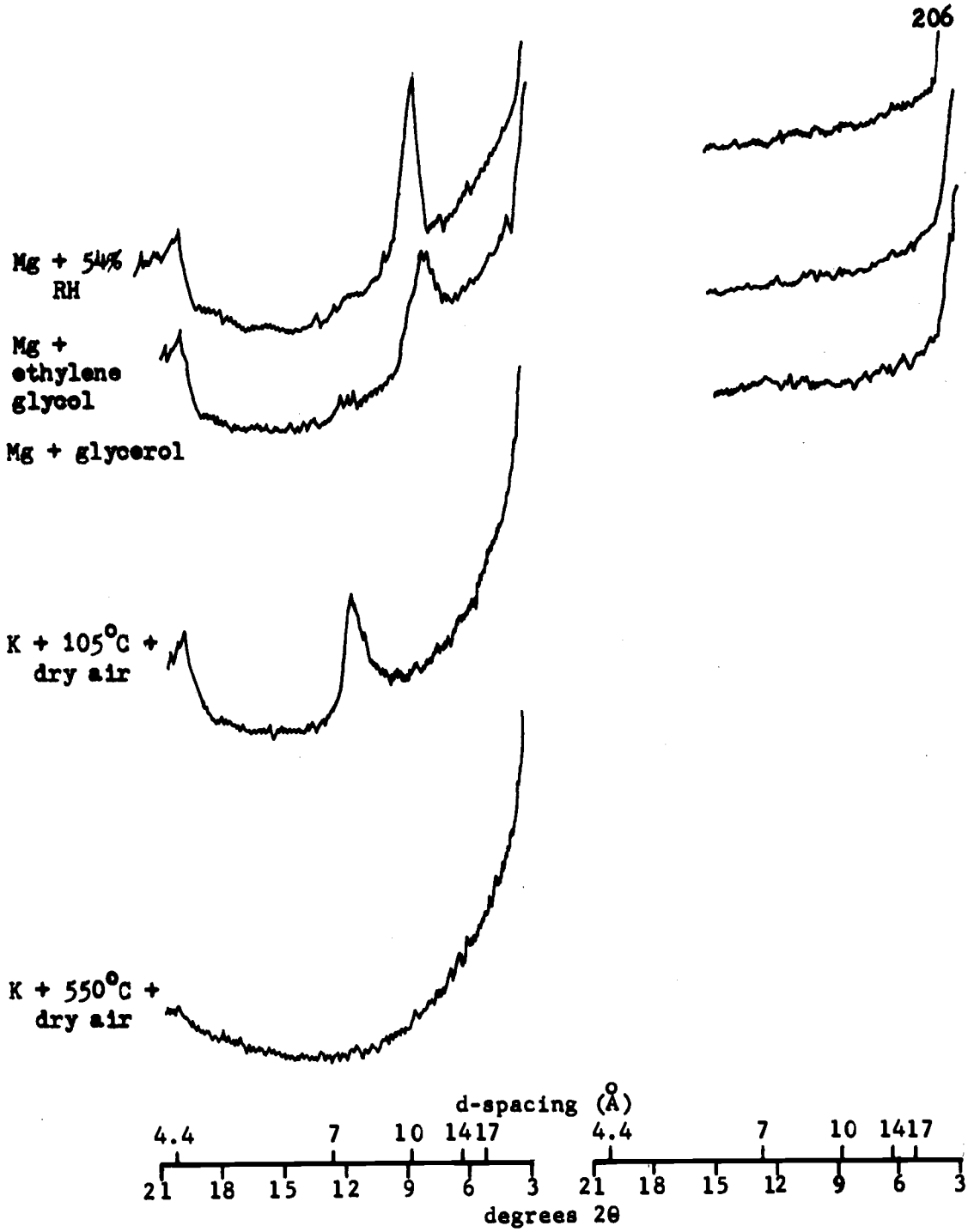

Figure 80. Site MFW-D-1c (left) and MFW-D-1 sample from Youngberg, et al. 1971, (right).

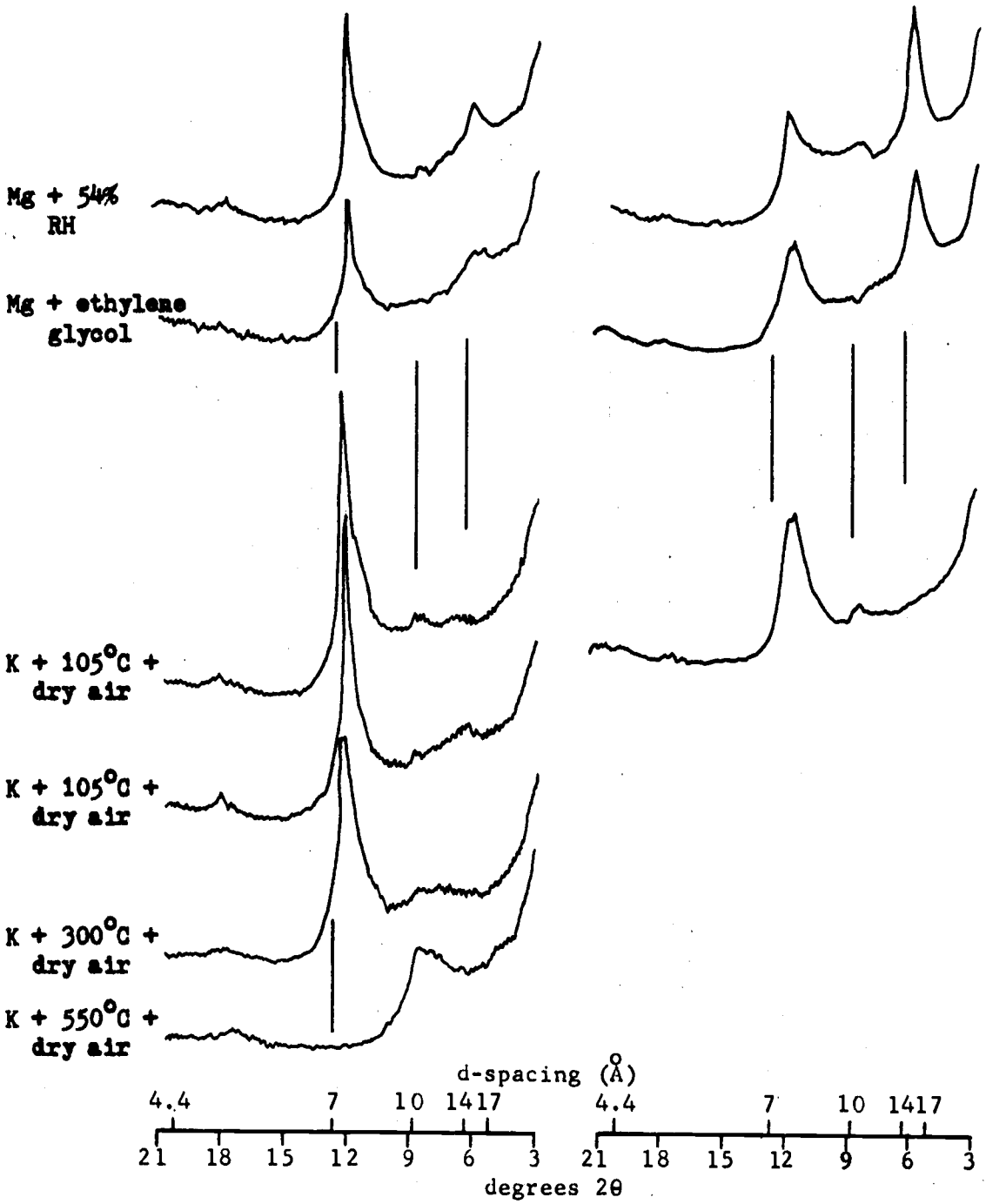

Figure 81. Site NU-LR-B-1 (left) and SU-S-1a (right), relatively stable soils.

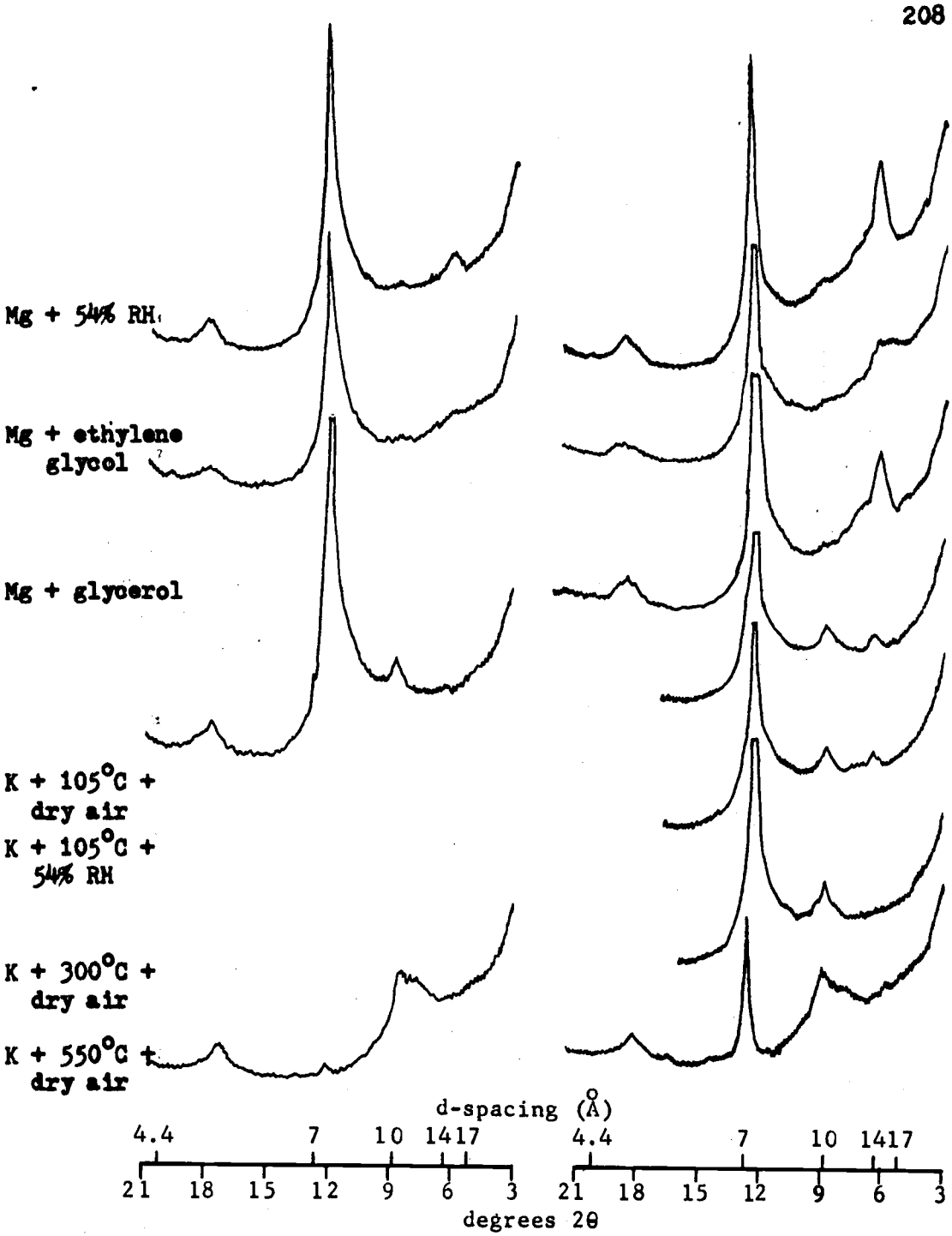

Figure 82. Site SU-1 XRD patterns, sample b (left) and sample a (right) indicating kaolinite as the dominant component in each.

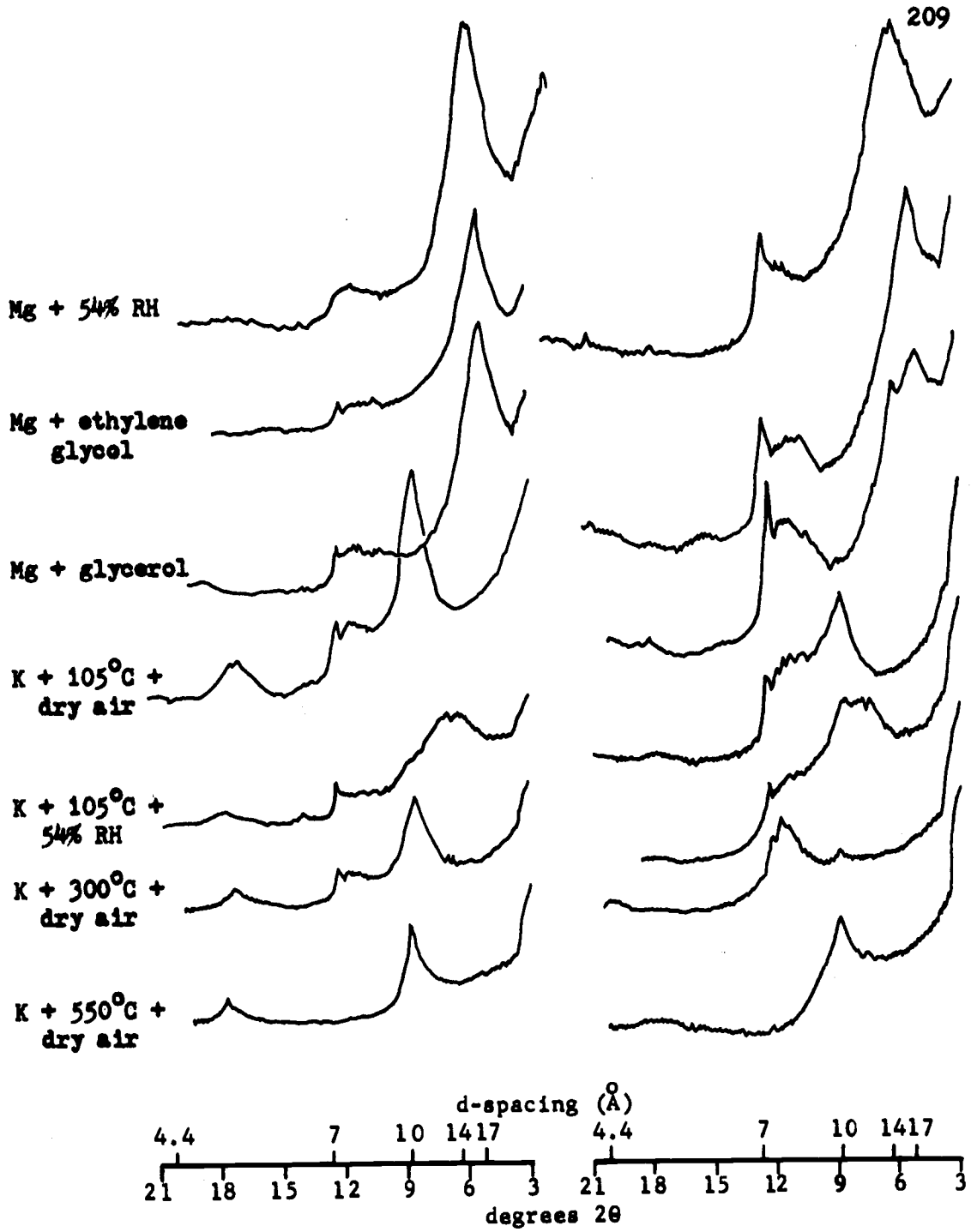

Figure 83. Site R-M-1 XRD patterns, sample c (left) and sample a (right).

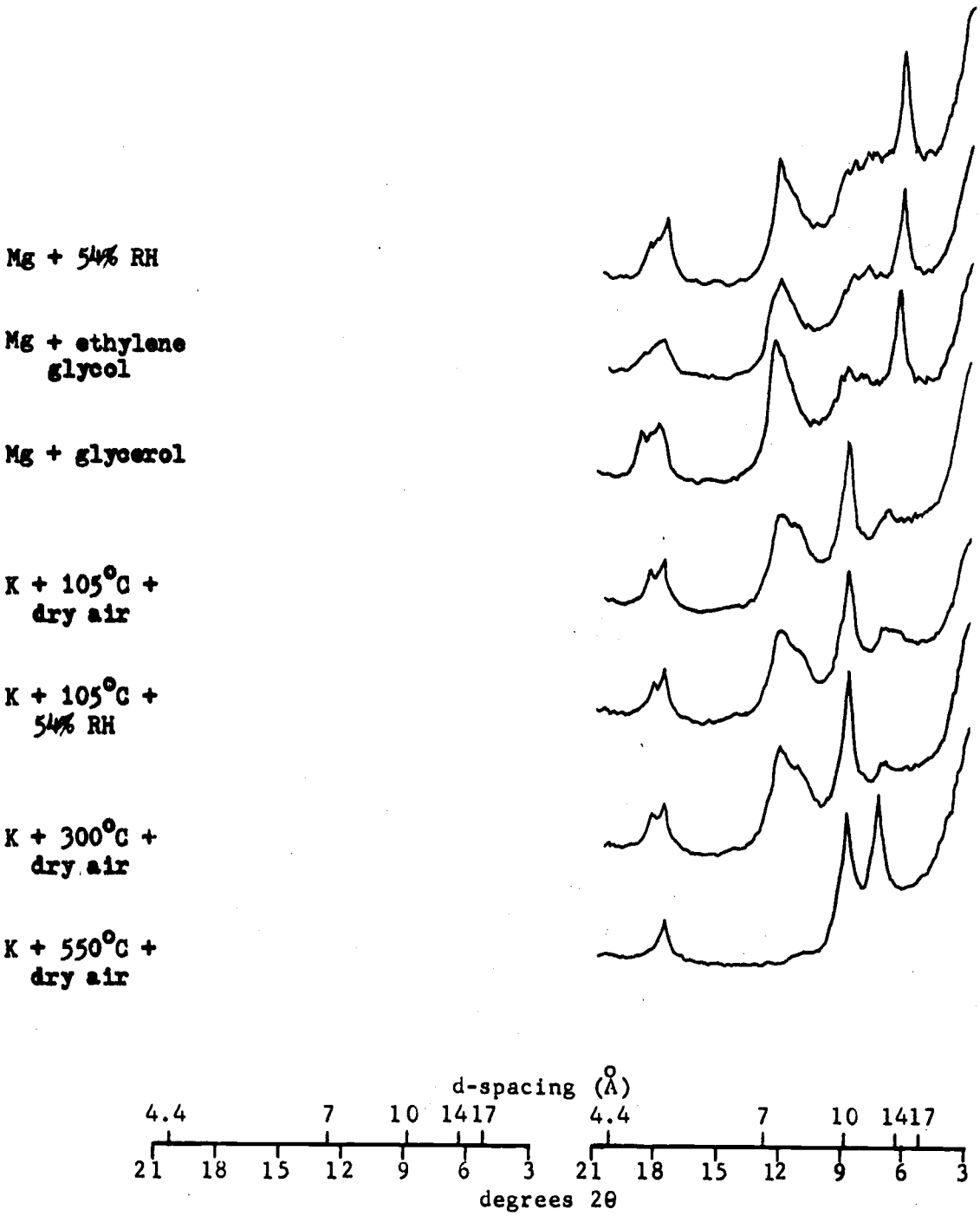

Figure 84. Site A-S-2 XRD patterns of soil from schistose parent material.

APPENDIX IV

PARTICLE SIZE ANALYSES

Table 2. Particle size analyses of selected soil samples by the Bouyoucos hydrometer method.

Site	% Sand	% Silt	% Clay
NS-BC-1d	56	25	19
NS-BC-2	46	38	16
MS-Q-1d	37	46	17
MS-P-1f	45	39	16
MS-P-1g	71	19	10
MS-1	38	40	22
MS-3-1b	16	45	39
MS-J-1b	66	19	15
MS-H-1b	68	21	11
SS-SF-1f	35	32	33
SS-SF-1g	42	25	33
SS-SF-1k	28	31	41
SS-SF-2	72	24	4
SS-SF-4b	28	32	40
SS-SF-5d	54	27	19
SS-SF-7	54	24	22
SS-S-3d	3	31	66
SS-S-3f	53	33	14
SS-2a	4	31	65
MK-D-1a	47	42	11
MK-D-1b	55	34	11
MK-D-2	43	38	19
MK-F-1	70	27	3
MK-L-1	1	94	5
MK-L-2a	35	28	37
SFMK-B-1e	17	36	47
NFMFW-C-1a	32	45	23
NFMFW-C-1b	39	37	24
MFW-H-1a	50	23	27

Site	% Sand	% Silt	% Clay
MFW-1b	21	30	49
MFW-L-1b	42	27	31
MFW-BW-1	60	27	13
MFW-CP-1b	50	25	25
MFW-B-1a	51	26	23
MFW-B-1b	27	36	37
MFW-B-1c	37	28	35
NU-LR-B-1	29	30	41
SU-S-1a	20	33	47
SU-J-1a	22	18	60
SU-J-1b	17	22	61
SU-1a	46	23	31
SU-C-1b	47	28	25
SU-C-1d	53	27	20
R-CM-1c	46	27	27
R-SP-1	34	24	42
R-SP-2	42	25	33
R-M-1a	36	25	39
R-M-1b	41	25	34
A-S-1c	68	26	6
A-S-2	39	22	39
R-WUR-1	51	30	19
S-1	35	29	36

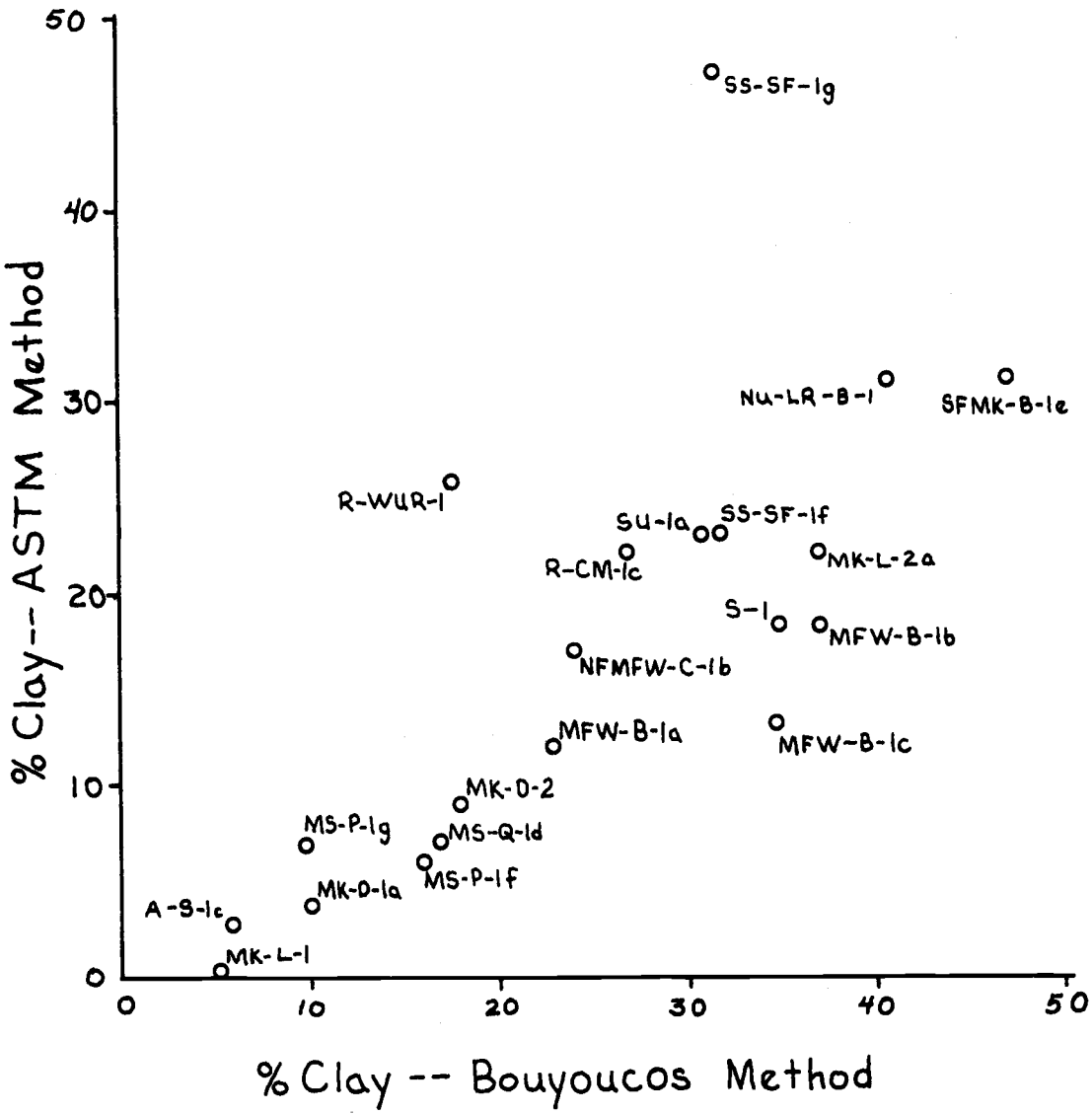

Figure 85. Comparison of clay percentages by ASTM and Bouyoucos hydrometer methods.

APPENDIX V

PREPARATION OF SOIL SAMPLES FOR CLAY MINERAL ANALYSIS BY X-RAY DIFFRACTION

PREPARATION OF SOIL SAMPLES FOR CLAY MINERAL ANALYSIS BY X-RAY DIFFRACTION

R. D. Taskey

M. E. Harward

1. Sample collection and handling

Less than one gram of clay is needed for identification of minerals by X-ray diffraction analysis. However, larger quantities are easier to process, so at least 100 g of total soil should be collected.

For most purposes do not dry the sample, as drying can alter the nature of some clay materials. Use doubled plastic bags and seal tightly. Refrigerate at approximately 5°C if the sample must be stored before preparation and analysis.

2. Separate the clay fraction (<2μm)

a) Remove coarse fragments either by picking them out by hand, or by wet sieving through a 2 mm (no. 10) screen, making sure to gently crush aggregates through the screen.

b) Disaggregate in distilled water by stirring on a milk shake blender equipped with a rubber policeman in place of the cutting blades, or by air jetting at 25 psi for three minutes. Some soils will not disaggregate in distilled water, so if necessary, suspend the sample in a solution of 2% Na_2CO_3 at room temperature and then stir or air jet. Alternatively, mild sonification may be used to disaggregate the sample, but this may destroy the integrity of some mineral particles.

c) Remove the sand-sized fraction by wet sieving through a 53 μm screen and collecting the silt and clay fractions which will pass the screen. Save the material which is retained in the screen, add water to it, and stir again to ensure that all aggregates are destroyed and all clay is washed from sand particle surfaces. Sieve through the 53 μm screen.

d) Separate the silt from the clay by centrifugation in distilled water (or dilute Na_2CO_3 as noted later) as per Stokes' Law. The following table applies to the International Centrifuge with head no. 242, and assumes a particle density of 2.65 gcm^{-3} and a 10 cm depth of suspension in 250 ml centrifuge bottles (the centrifugation schedule for separating materials at 5 µm is provided as additional information).

Water Temp °C	Time to settle>2 µm fraction at 900 rpm. (schedule for separation of silt from clay)	Time to settle>5 µm fraction at 300 rpm
22	3.7 min	5.4 min
24	3.6 "	5.2 "
27	3.5 "	5.0 "
28	3.3 "	4.8 "
30	3.2 "	4.6 "
32	3.0 "	4.4 "

Be sure to balance the bottles in pairs on a double pan balance, using distilled water to make up for weight differences between any two bottles in a pair, and place the members of a pair on opposite positions in the centrifuge.

After centrifuging, the silt will be deposited on the bottom of the container and the clay will be suspended in the supernatant liquid which may be poured off into a beaker. However, some of the clay will spin down with the silt, and so this material must be resuspended in distilled water, mixed and recentrifuged. (Note: some clays are difficult to disperse in distilled water. In those cases, it may be necessary to do this separation in dilute Na_2CO_3 (1 gm/9 liters or 1 gm/18 liters for amorphous materials) rather than distilled water.

c) Separate the clay from the water by centrifugation. Usually 15-20 minutes at 5000 rpm in the Sorval with the GSA (large) head is sufficient. However, if some clay remains in suspension it may be flocculated with sodium salt (0.5-1 N) and recentrifuged. (Do not flocculate with calcium salt if Na_2CO_3 was used above.)

3. Ion Saturations

a) The clay sample is now deposited on the bottom and side of the centrifuge bottle and is probably stratified. Mix it well with a spatula and transfer half to a small centrifuge tube (50 ml size) for saturation with K^+ and half to another tube for saturation with Mg^{2+}. Be sure to label the tubes! For a number of samples it is best to process the halves to be potassium saturated as a batch, separately from those to be magnesium saturated.

b) Fill the tubes containing the sample portions to be K saturated about 2/3 full with 1 N KCl. Do no more than eight tubes at a time, as this is all the centrifuge will hold.

c) Stir with a blender equipped with a rubber policeman. This can be done without losing a drop -- believe it or not! Hold the tube by its bottom and gently press the wall of the tube against the blending shaft with the shaft inserted nearly to the bottom of the tube. Operate the blender in short spurts while at the same time slowly rotating the tube. Note the diagram. Practice using a tube containing only water.

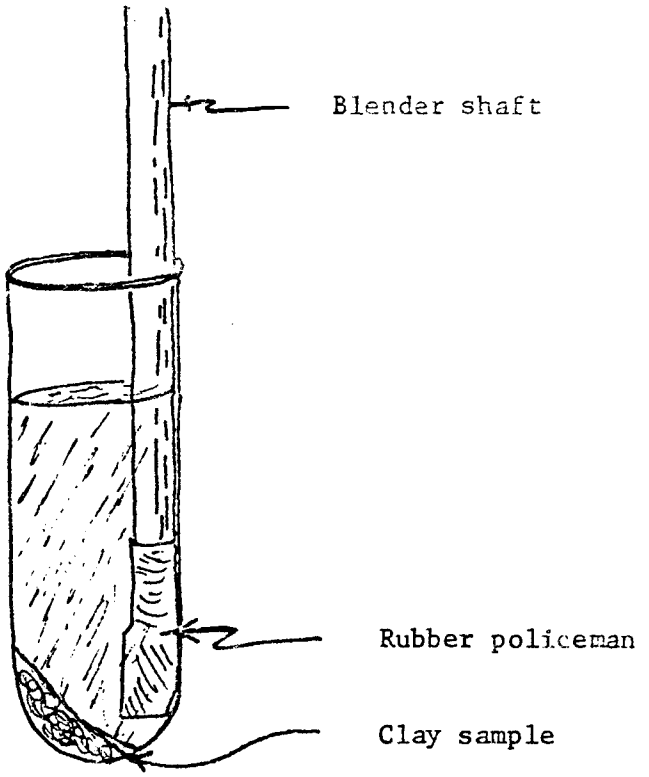

d) Balance the tubes and spin down the clay using the Sorval fitted with the SS-34 (small) head. Usually, 10 minutes at 10,000 rpm will do the job. Pour off the clear supernatant and repeat this saturation process two more times.

e) Now the sample must be washed with distilled water in order to remove the excess potassium chloride. Do this three times using the same procedure described above but with distilled water in place of the KCl.

f) Prepare the other half of the sample in the same manner, but saturating with 1 N $MgCl_2$ in place of the KCl. Remember, to wash three times after the third saturation.

4. Prepare Slides

You now have two 50 ml centrifuge tubes for each sample -- one tube containing the K-saturated portion and the other containing the Mg-saturated portion. There are several techniques of mounting

specimens for X-ray diffraction analysis, but the paste method of preparing an oriented sample is convenient and gives excellent results for most purposes.

a) The paste-like clay in each tube is probably stratified because of differences in densities and sizes of the constituents; therefore, mix it with a microspatula to ensure that a uniform, representative specimen will be analyzed.

b) Prepare one slide for the K-saturated portion of each sample and two slides for the Mg-saturated portion by placing a small dab of the clay paste near the center of a glass petrographic slide which has been labeled appropriately at one end. (A "Sharpie" pen works nicely for labeling, but caution, the ink will disappear on those slides which are heated to 550°C!) Smear the paste fairly evenly on the slide, making it just thick enough to be opaque, and being careful to not leave a berm at the edges. A small drop of water may be added if necessary to make spreading easier.

c) The K-saturated prepared slides may simply be placed on the lab bench as you work, however, the Mg-saturated prepared slides should not be allowed to dry. Therefore, place them immediately in a desiccator maintained at 54% relative humidity. The 54% R.H. is controlled by a saturated solution of $Mg(NO_3)_2$ in the bottom of the desiccator.

Heat the K-saturated slides at 105°C for two hours, then place them in a dry-air desiccator (i.e., one containing "Drie-Rite").

5. Characterization Treatments

Several different treatments are required to adequately characterize clay minerals, and especially to distinguish one from another in a complex sample. The following seven treatments normally will provide adequate information on the properties of the various phyllosilicates to allow identification. Samples should be treated and analyzed in sequence.

1) Mg-saturated, 54% RH.

2) Mg-saturated, ethylene glycol solvated, 54% RH.

To solvate using the vapor condensation technique, place the same slide as used in 1) horizontally, sample side up, in a desiccator containing ethylene glycol. With the vent hole in the lid open, place desiccator in a 65°C oven for two hours. Remove from oven, close the vent and allow 12 hrs for equilibration before analyzing.

3) Mg-saturated, glycerol solvated, 54% RH.

Solvate the other Mg saturated slide as above, but in a glycerol desiccator at 105°C for 2 hours. Again, equilibrate 12 hours before analyzing.

4) K-saturated, dried at 105°C, dry air.

5) K-saturated, 54% RH.

Allow sample to equilibrate 12 hours in a 54% RH desiccator before analyzing.

6) K-saturated, heated to 300°C for 2 hours, dry air.

7) K-saturated, heated to 550°C for 2 hours, dry air.

6. Mineral Identification

The attached table will facilitate identification of the more important phyllosilicates found in soils.

d (001) - Spacings (Å) of Clay Minerals Under Various Treatments

	Kaolinite	Halloysite	Mica	Vermiculite	Montmorillonite	Beidellite	Chlorite	Chloritic Intergrade
Mg-saturated								
54% RH:	7.15	7.3-10	10-10.5	14-14.5	15	14.5-15	14.2	14-15
ethylene glycol:	7.15	7.3-10	10-10.5	14-14.5	16.5-17	16.5-17	14.2	14-17
glycerol:	7.15	7.3-10	10-10.5	14-14.5	17.5	14.5	14.2	14-17
K-saturated								
105°C:	7.15	7.3-7.5	10	10-10.5	10-10.5	10-10.5	14	11-14
54% RH:	7.15	7.3-7.5	10	10-10.2	12	11.5-12	14	14
300°C:	7.15	7.3-7.5	10	10-10.2	9.9-10.4	10-10.5	14	11-14
550°C:	--	--	10	10	9.8-10.2	10	14	10-13

Note: Hydroxy interlayered smectites and chloritic intergrades may respond to solvation treatments in a manner similar to beidellite. Also, kalonite may not be recognized in the presence of chlorite (esp. Fe-rich chlorites).

REFERENCES

Brown, George. 1961. The X-ray identification and crystal structures of clay minerals. Mineralogical Society, London.

Brown, G., and R. Farrow. 1956. Introduction of glycerol into flake aggregates by vapor pressure. Clay Minerals Bull. 3:44-45.

Chu, T. Y., and D. T. Davidson. 1953. Simplified air jet dispersion apparatus for mechanical analysis of soils. Proc. Highway Research Board 32:541-547; and Engineering Report No. 21, Iowa Eng. Exp. Sta., Iowa State College, Ames, Iowa, 1954-1955.

Harward, M. E., and G. W. Brindley. 1965. Swelling properties of synthetic smectites in relation to lattice substitutions. Clays and Clay Minerals, Proceedings of 13th National Conf.:209-222.

Harward, M. E., D. D. Carstea, and A. H. Sayegh. 1969. Clays and Clay Minerals 16:437-447.

Jackson, M. L. 1956. Soil Chemical Analysis: Advanced Course. Univ. of Wisc., Madison. Published by the author.

Jackson, M. L., L. D. Whittig, and R. P. Pennington. 1950. Segregation procedure for the mineralogical analysis of soils. Soil Sci. Soc. Amer. Proc. 14:77-81.

Kunze, G. W. 1955. Anomalies in the ethylene glycol solvation technique used in X-ray diffraction. Clays and Clay Minerals, Proc. 3rd Nat'l Conf.:88-93.

Sayegh, A. H., M. E. Harward, and E. G. Knox. 1965. Humidity and temperature interaction with respect to K-saturated expanding clay minerals. American Mineralogist 50:490-495.

Singleton, P. C. 1966. Nature of interlayer materials in selected Oregon soils. Ph.D. Thesis. Oregon State Univ., Corvallis, 84 pp.

Theisen, A. A. and M. E. Harward. 1962. A paste method for preparation of slides for clay mineral identification by X-ray diffraction. Soil Sci. Soc. Amer. Proc. 26:90-91.